ITALIAN JOURNAL OF FOOD SCIENCE

Rivista italiana di scienza degli alimenti (www.itjfs.com)

Volume XXXIV
Number 1
(2022)

ITALIAN JOURNAL OF FOOD SCIENCE
(RIVISTA ITALIANA DI SCIENZA DEGLI ALIMENTI) 2nd series

Founded By Paolo Fantozzi under the aegis of the University of Perugia
Official Journal of the Italian Society of Food Science and Technology
Società Italiana di Scienze e Tecnologie Alimentari (S.I.S.T.Al)
Initially supported in part by the Italian Research Council (CNR) -Rome -Italy
Recognised as a "Journal of High Cultural Level"
by the Ministry of Cultural Heritage -Rome -Italy
(www.itjfs.com))

Publisher:
Codon Publications: email: admin@codonpublications.com, URL: www.codonpublications.com.

Aim:

The Italian Journal of Food Science is an international journal publishing original, basic and applied papers, reviews, short communications, surveys and opinions on food science and technology with specific reference to the Mediterranean Region. Its expanded scope includes food production, food engineering, food management, food quality, shelf-life, consumer acceptance of food stuffs. Food safety and nutrition, and environmental aspects of food processing. Reviews and surveys on specific topics relevant to the advance of the Mediterranean food industry are particularly welcome.

Upon request and free of charge, announcements of congresses, presentations of research institutes, books and proceedings may also be published in a special "News" section.

Review Policy:

The Co-Editors with the Editor-in-Chief will select submitted manuscripts in relationship to their innovative and original content. Referees will be selected from the Advisory Board and/or qualified Italian or foreign scientists. Acceptance of a paper rests with the referees.

Frequency:

Quarterly -One volume in four issues. Guide for Authors is published in each number and annual indices are published in number 4 of each volume.

Impact Factor:

0.875 published in 2020 Journal of Citation Reports, Scopus CiteScore 2020: 1.5. IJFS is abstracted/indexed in: Chemical Abstracts Service (USA); Foods Adlibra Publ. (USA); Gialine – Ensia (F); Institut Information Sci. Acad. Sciences (Russia); Institute for Scientific Information; CurrentContents®/AB&ES; SciSearch® (USA-GB); Int. Food Information Service - IFIS (D); Int. Food Information Service – IFIS (UK); UDL-Edge Citations Index (Malaysia); EBSCO Publishing; Index Copernicus Journal Master List (PL).

IJFS has a publication charge of USD 1100 each article.
Subscription Rate: IJFS is now an Open Access Journal and can be read and downloaded free of charge.

VOLUME XXXIV IJFS No. 1, 2022

CONTENTS

Italian Journal of Food Science, 2022; 34 (1): 1–12

Effects of drying methods and acidic strength on physicochemical properties of potassium caseinate

Fatma Maruddin[1]*, Wahyu Triputra Hasim[1], Nursida[1], Ratmawati Malaka[1], Hikmah Muhammad Ali[1], Muhammad Taufik[2], Syahriana Sabil[3]

[1]Department of Animal Production, Faculty of Animal Science, Hasanuddin University, Makassar, South Sulawesi, Indonesia; [2]Agricultural Development Polytechnic of Gowa, South Sulawesi, Indonesia; [3]Animal Science Study Program, Faculty of Agriculture, Animal Science and Forestry, Maros Moslem University, Maros, South Sulawesi, Indonesia

***Corresponding Author:** Fatma Maruddin, Department of Animal Production, Faculty of Animal Science, Hasanuddin University Perintis Kemerdekaan Street km 10, Makassar, South Sulawesi 90245, Indonesia. Email: fatma_maruddin@yahoo.co.id/fatma_maruddin@unhas.ac.id

Received: 22 January 2021; Accepted: 19 October 2021; Published 1 January 2022

PAPER

Abstract

The aims of the present study were to characterize physicochemical characteristics and chemical structures by Fourier Transform Infrared (FTIR), and mark dissolved protein content, microstructure, and moisture content of potassium caseinate prepared by drying methods and acid strength. The experiment was arranged according to factorial complete randomized design with triplicates, while data from FTIR and microstructure analysis was presented descriptively. The results demonstrated that acids and drying methods for preparing potassium caseinate could increase antioxidant activity, a* score (reddish) and b* score (yellowish). Specifically, freeze-drying method coupled with acid treatments accounted for reducing moisture content but improved viscosity and microstructural properties. Briefly, we could argue that drying techniques and acids established noticeable effects on the quality of potassium caseinate.

Keywords: acid; drying method; potassium caseinate; quality

Introduction

Potassium caseinate is derived from casein with aqueous potassium hydroxide (KOH) used to dissolve it (De Souza *et al.*, 2010). Casein itself is a milk protein and contains large amount of essential amino acids as commonly found in other types of casein products. The pH of potassium caseinate is close to neutral, which makes it favorable for food processing. Casein is widely employed in various foods such as cheese, ice cream, edible film, and health supplements (Badem and Ucar, 2017; Sarode *et al.*, 2016).

Chemical composition and functional properties of milk protein and peptides (casein and whey) could be altered rermarkably by processing conditions (Jimenez *et al.*, 2012). Quality of casein could be reduced by improper methods. A few changes in protein structure could be reponsible for release of other chemically bound molecules, but large changes may alter both quantity and quality of the protein. Degradation of protein chains is able to deactivate particular protein that acts as antioxidant (Pralea *et al.*, 2011; Winarno, 2008).

In processing of casein, precipitation is considered important since it accounts for separation of casein from milk. The techniques used may vary from chemical to physical approaches, using chemical agents and control over processing conditions such as temperature, pressure, agitation, and holding time, which influence pH of the

solvent, protein conformation, and properties of the final product (Jimenez *et al.*, 2012). Acid precipitation of casein could be a promising method, as commonly applied in food preparation by adding hydrochloric acid (HCl) and acetic acid (CH_3COOH), often recognized as strong and weak acids, respectively. Difference in acidity causes various effects to the extent that casein changes into a simple form of protein (Triyono, 2010; Vasbinder *et al.*, 2004).

Further, incredible stage in casein processing is dehydration (Djaeni *et al.*, 2015; Haque and Roos, 2006), which is a final step for producing potassium caseinate. In this case, drying is applied to induce mass transfer process, including removal of water present in the product (Sarode *et al.*, 2016). In addition, drying in the processing of potassium caseinate is further addessed to extend storability of the product, resulting in dry matter, which easily modifies its chemical components. However, it must be considered that product should be dehydrated without reducing the quality of end product. The drying process is often carried out using oven and freeze dryer. Even though oven-drying is less favorable for its undesired effects to color changes of the final product, it is affordable, easy to operate, and available comfortably. Oven-drying seems to be disadvantageous if applied to protein-rich foods, since it can incredibly reduce their quality (Liu *et al.*, 2008). As an alternative technique, freeze-drying is more favorable because it enables to minimize cellular damages because of heat. The main principle of freeze-drying is based on removal of ice from materials through the process of sublimation (Ciurzyńska and Lenart, 2011).

The use of acids and drying methods in isolation of casein inevitably affects its physical and chemical properties. Processing conditions allow to induce deformation of chemical bonds in functional groups of casein from other molecules. Casein is also an important source of peptides that are active biologically. Inactive peptides in protein chain can be turned into an active form and released through stimulation by using acid, enzyme, heating, mechanical treatments, and salts (Felix da Silva *et al.*, 2018; Winarno, 2008). However, the stimulating activities may cause some effects, such as changes in color and microscopic structure, shrinkage, porosity, and reduction of water-binding capacity as well as microscopic destruction. In addition, changes in chemical properties may also occur, such as antioxidative properties, protein content, and moisture content (Raikos, 2010; Witrowa-Rajchert and Lewicki, 2006).

The present study aimed to uncover the effects of acids and drying techniques on the physiochemical properties of potassium caseinate regarding antioxidant activity, content of crude and dissolved proteins, moisture as well as color (L*, a*, and b*) and chemical properties determined by Fourier Transform Infrared (FTIR) analysis.

Materials and Methods

Materials

The materials used were fresh milk, CH_3COOH pro-analysis grade, HCl pro-analysis grade, KOH pro-analysis grade, alcohol, and distilled water.

Experimental procedures

Skimming was performed by separating cream from fresh milk using cream separator. Then the skim was pasteurized at 85°C for 5 min. After being stored in refrigerator at 5°C for 24 h, the pasteurized skimmed milk was defatted under aseptic conditions. Casein was precipitated from the skimmed milk using HCl 1N and CH_3COOH 1N at 5% (w/v) and 10% (w/v) of the skimmed milk volume, respectively. Under these conditions, pH of casein was in the range of 4.4–4.6. Difference in concentration was due to difference in the acid strength of two acids. Subsequently, filtration was performed to collect casein curd while whey was discarded. The obtained casein curd was then washed thrice using distilled water with the similar volume of discarded whey. At the last washing, the curd was weighed and added to distilled water in 1:1 (w/w) ratio. The pH of casein was also measured and adjusted to 6–7 using KOH. Finally, casein curd was filtered and dried. The oven-drying (Ecocell SIS-B2V/EC111, D112457) was operated at 50°C for 48 h, while freeze-drying (Christ Freeze Dryer, type Alpha-2 LD) was performed at −40°C for 48 h, adopted from the methods described by Badem and Uçar (2017), Kumaresan *et al.* (2017), and Sarode *et al.* (2016).

Parameters

DPPH (1,1-diphenyl-2-picrylhydrazyl) Assay

Antioxidant activity was determined using DPPH assay (Pająk *et al.*, 2014). DPPH reagent (0.008 g) was mixed with methanol 50 mL. Sample (1 g) was dissolved in 9-mL distilled water, and the sample solution (1 mL) was mixed with 0.8-mL methanol. This sample solution was prepared in duplicate. Subsequently, 0.8 mL of each sample solution, 0.4-mL ethanol and 1.8-mL methanolic DPPH solution, was mixed. After 60 min, absorbance was measured at 515 nm using ultraviolet–visible spectroscopy (UV–VIS) spectrophotometer (Shimadzu IRP Prestige-21). The antioxidant activity was calculated using Eq. 1:

$$\text{DPPH}\,(\%) = \frac{(A_{DPPH} - A_{Sampel})}{A_{DPPH}} \times 100, \qquad (1)$$

where A_{DPPH} is the absorbance of DPPH solution, and A_{sample} is the absorbance of sample solution.

Determination of crude protein

Crude protein was quantified by using the method described by AOAC (2019). Briefly, casein (1 g) was transferred into Kjeldahl flask. Subsequently, 1-g copper sulfate ($CuSO_4$) and 2.5-mL concentrated sulfuric acid (H_2SO_4) were added to the flask, followed with thermal destruction at 100°C for 2 h. After destruction, the mixture was transferred into volumetric flask containing boiling chips. Afterward, 50-mL demineralized water and 15-mL sodium hydroxide (NaOH), 50% (w/v), were added prior to distillation. Then distillate was collected in Erlenmeyer containing 10-mL HCl, 0.02 N. Four drops of each methyl red and methyl blue were added to reach a total volume of 40 mL, then titrated with NaOH and standardized with oxalic acid ($H_2C_2O_4$), 0.02 N. Titration was stopped after purple color changed into green. The volume of NaOH used was recorded. Protein content was calculated using Eq. 2:

$$\text{crude protein (\%)} = \frac{(Vs - Vb) \times \text{N} \times 14.007 \times 6,25}{W} \times 100 \quad (2)$$

where *Vs* is the volume (mL) of the standardized acid used to titrate the sample,

Vb is the volume (mL) of the standardized acid used to titrate a reagent blank, and

W is weight (g) of sample portion of standard

Viscosity

Viscosity was measured according to the method described by Konstance and Strange (1991). Casein solution was prepared with 12% (w/v) casein powder blended with cold water using electric blender (Miyako BL-152 PF_AP) for 10 min. The solution was heated at 95°C for 5 min and left to cool for analysis. The cooled solution was transferred into a glass beaker, and the viscosity was determined using viscometer (with spindle 3) at a speed of 50 rpm. Viscosity was determined using Eq. 3:

$$Viscosity = value\ obtained\ in\ viscometer \times correction\ factor \quad (3)$$

Color

Digital color meter test (T135) was used to detect color, expressed as L* (0–100, dark to white), a* (–60–+60, green to red), and b* (–60–+60, blue to yellow). Prior to use, the color meter was callibrated to ensure its accuracy (Maruddin *et al.*, 2018).

FTIR analysis

Prior to FTIR analysis, casein (0.2 g) was dissolved in distilled water. The solution was dropped in calcium fluoride (CaF_2) window, coupled with another CaF_2 window, ensuring that the solution was thoroughly spread onto the surface of window. The CaF_2 window was then set in a holder. Analysis was performed using FTIR (Shimadzu IRP Prestige-21; Sari, 2011).

Determination of dissolved protein

Content of dissolved protein was calculated using the Lowry method (Wikandari *et al.*, 2011). Casein (1.5 g) was added in 7.5-mL distilled water and centrifuged for 15 min to collect supernatant. The supernatant was boiled on hotplate, centrifuged for 15 min to collect the final supernatant. The final supernant (2 mL) was added to 1-mL trichloroacetic acid (TCA) 10%, followed with centrifugation for 15 min. Then the sample (0.1 mL) was mixed with distilled water (1.9 mL) and Folin–Ciocalteu reagent (FCR; 2.5 mL), and incubated for 10 min at room temperature. Folin reagent (0.5 mL) was added again and incubated for 30 min till the color changes to blue. The absorbance was determined spectrophotometrically at 600 nm. Bovine Serum Albumine (BSA) was used as a standard solution. The level of dissolved protein was calculated using Eq. 4:

$$\text{Dissolved protein (\%)} = \frac{(A_{Sample} - A_{control})}{A_{Sample}} \times 100 \quad (4)$$

where A_{sample} is the absorbance of sampel solution and $A_{control}$ is the absorbance of BSA

Microstructure of casein

Microstructural feature of casein was observed using Scanning Electron Microscope (SEM; Hitachi SU 3500). Sample was set with a double adhesive tape, then coated with gold using Hitachi ion sputter MC 1000 in vacuum. Microstructural scanning was carried out in SEM at 20 kV. The image was recorded at different magnifications (20× to 2000×).

Determination of moisture content

Moisture content was determined using the method described by Kumesan *et al.* (2017). Porcelain was dried

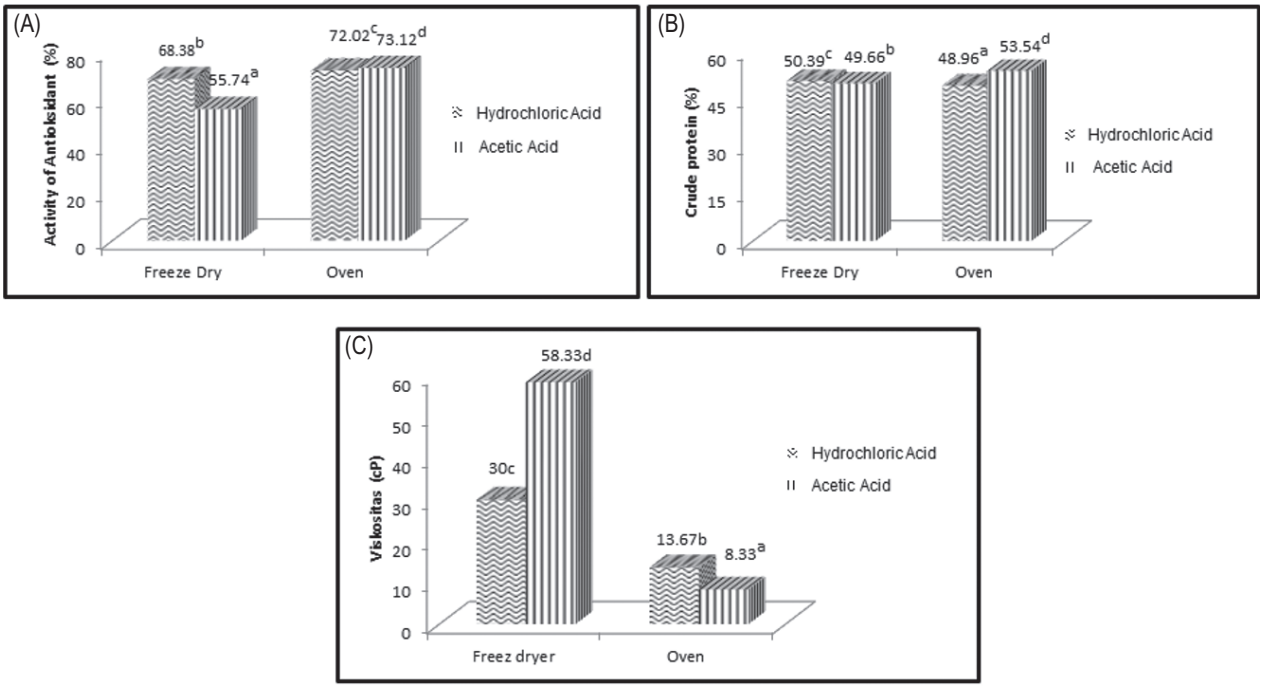

Figure 1. (a) Antioxidant activity of casein treated with acids and drying methods. Different superscripts above the bars depicted a significant difference ($p < 0.01$). (b) Content of crude protein in casein treated with acids and drying methods. Different superscripts above the bars depicted a significant difference ($p < 0.01$). (c) Viscosity of casein treated with acids and drying methods. Different superscripts above the bars showed a significant difference ($p < 0.01$).

in an oven for 15 min, desiccated and weighed (C). Casein (5 g) was transferred into porcelain and weighed (B). The sample was then dried in an oven at 105°C for 2 h, desiccated and weighed (A). Calculation of the moisture content was determined using Eq. 5:

$$\text{Moisture content (\%)} = \frac{(B-C)}{(B-A)} \times 100 \quad (5)$$

Results and Discussion

Antioxidant properties of casein

Antioxidant is a compound capable of alleviating oxidation reaction through scavenging of radicals and active molecules (Nahariah *et al.*, 2014; Pająk *et al.*, 2014; Winarsi, 2007). Figure 1a shows the antioxidant activity of casein ranging from 55.74% to 73.12%. This finding is in agreement with the previous result reported by Pralea *et al.* (2011) that antioxidant activity of casein added with sodium ranged from 45% to 95%.

Analysis of variance demonstrated that antioxidant activity was affected by interaction of acids and drying methods ($p < 0.01$). Additionally, statistical analysis demonstrated a significant difference between processes, that is, between: HCl + freeze-drying and HCl + oven-drying; and CH_3COOH + freeze-drying and CH_3COOH + oven. The highest antioxidant activity was attributed to CH_3COOH + oven-drying, while the lowest one was found in CH_3COOH + freeze-drying. The higher antioxidative activity represents stronger effect on free radical scavenging and *vice versa*. This suggests that sample contains a particular compound responsible for retardation of oxidation reaction. As explained by Simanjuntak *et al.* (2004), free radicals require electrons from adjacent electron pairs, thus donation of electron is needed to stabilize the radicals. Glab and Boratynski (2017) discussed that free radicals could be in the form of atom, molecule, or compound containing one or more unpaired electrons, which make them highly reactive and unstable.

The results demonstrated that average antioxidant activity of casein prepared from HCl was higher than CH_3COOH. It is well known that HCl serves as a strong acid, capable of breaking down peptide bonds. As previously explained by Felix da Silva *et al.* (2018) and Kusumaningtyas *et al.* (2015), peptides and amino acids resulted from protein degradation could exert antioxidative activities.

Interestingly, we also found that casein prepared from oven-drying showed a higher antioxidant activity in comparison to that prepared from freeze-drying. The

oven-drying could have a high antioxidant ability because of exposure of sample to high temperature, which converts protein into antioxidative peptides. Similarly, Pralea *et al.* (2011) reported that heating method could alter antioxidant properties of food. Exposure to heat could produce undesired effects on food quality, although some studies have revealed that antioxidant ability increases as more heat is provided. Morales and Babbel (2002) stated that correlation between antioxidant activities and heat level was due to formation of strong antioxidative components. Such components are able to scavenge free radicals resulted from chemical reaction during heating.

Crude protein

Protein is one of the macronutrients found in foods. In this work, the content of crude protein in casein ranged from 48.96% to 53.54%, as depicted in Figure 1b. This suggests that the range is much lower than standard set by Codex Alimentarius (2014), according to which the crude protein content must be at least 88.0%.

Statistical analysis established that interaction of acids and drying methods offered significant effects on the content of crude protein ($p < 0.01$). Additionally, average content of crude protein in casein prepared by oven-drying was higher than obtained by freeze-drying. This presumably relates to the ability of oven to remove water, which leads to increase in protein content of casein. Kusnandar (2011) argued that level of protein was influenced by coagulating properties of casein, which losses its ability to bind water molecules.

Statistical data exhibit a more satisfied content of crude protein in casein treated with oven-drying in comparison to freeze-drying, while the use of CH_3COOH + oven-drying is also more satisfied than CH_3COOH + freeze-drying regarding content of crude protein. Felix da Silva *et al.* (2018) and Sarode *et al.* (2016) reported that rate of denaturation and agglomeration of milk protein was noticeably controlled by heating and chemical conditions, that is, temperature and pH. These conditions must be emphasized in order to regulate rate of protein denaturation.

The application of HCl produced a completely ionized casein, resulting in the enhancement of crude protein content. Triyono (2010) found that HCl could ionize completely, thus able to degrade protein into smaller structures. As stated by Malaka (2014), precipitation of milk protein could be induced by acids, reaching the isoelectric points. Neutralization occurs if acid reacts with protein in milk, which in turn agglomerates to form a new complex. However, the use of HCl combined with high temperature (in oven-drying) promotes denaturation, which is the major cause of protein destruction and lower crude protein content compared to freeze-drying.

Viscosity

Viscosity constitutes a key parameter related to the characteristic of a fluid. This is noteworthy that viscosity may be incredibly influenced by several factors such as protein conformation, hydration properties, group of hydrophobicity, and distribution of charges.

As exhibited in Figure 1C, the viscosity ranged from 8.33 centipoise [cP] to 58.33 cP. Chairunnisa (1997) reported viscosity of other casein types, such as lactic casein (29.6 cP), co-precipitate casein (70.1 cP), and sodium caseinate (52.7 cP).

The results suggest that several significant factors affect the viscosity of casein, such as interaction of acids and methods of drying ($p < 001$). Statistical test revealed that types of acids used in freeze-drying showed a higher viscosity than those used in oven-drying. The viscosity tended to decrease due to change in temperature. However, the variability of viscosity in our experiment was considerably affected by acid types. High temperature (oven-drying) treatment can hydrolyze certain peptide bonds. The process changes the conformation of proteins by exposing hydrophobic proteins and resulting in decreased values of viscosity.

Broyard and Gaucheron (2015) asserted that proteolysis resulted in low secondary peptides. The peptides are closely related to a noticeable reduction in viscosity. In addition, casein proteolysis because of the use of acid and temperature during processing causes an increase in exposed fat molecules. As stated by Ting *et al.* (2016), viscosity was a result of internal friction between fat molecules present in a fluid. In general, the viscosity tends to decrease due to higher concentration of unsaturated fatty acids. Conversely, viscosity rises when the solution is hydrogenated. Raikos *et al.* (2009) investigated molecular weight of milk components with medium–high fat contents exposed to heat at 50, 95, and 125°C. Heating at >95°C leads to unfolding of protein chains, which promotes denaturation. As a consequence, hydrophobic components (such as fat) were more exposed, then aggregating to form larger molecules.

High temperature is responsible for alleviation of viscosity as it induces destruction of protein structure. We found that viscosity of casein dried using the freeze-drying process was higher than that of oven-drying process. This is in line with the process reported by Chairunnisa (1997) that heat treatment of milk protein isolates at 60°C reduces viscosity. Such condition is

Table 1. Color intensity.

Color parameters	Drying methods: Acids	Freeze-drying	Oven-drying	Average
L*	Hydrochloric acid	$90.92 \pm 0.34^{b,c}$	81.52 ± 3.68^{a}	86.22 ± 5.65^{A}
	Acetic acid	87.31 ± 0.52^{b}	91.57 ± 1.86^{c}	89.44 ± 2.63^{B}
Average		89.12 ± 2.01	86.55 ± 6.09	
a*	Hydrochloric acid	-3.41 ± 0.42^{a}	0.87 ± 0.42^{b}	-1.26 ± 2.37^{A}
	Acetic acid	0.54 ± 0.15^{b}	0.60 ± 0.20^{b}	0.57 ± 0.20^{B}
Average		-1.43 ± 2.18^{A}	0.73 ± 0.35^{B}	
b*	Hydrochloric acid	15.53 ± 0.42^{b}	20.93 ± 0.32^{d}	18.23 ± 2.97^{B}
	Acetic acid	12.82 ± 0.15^{a}	16.94 ± 0.04^{c}	14.88 ± 2.25^{A}
Average		14.17 ± 1.50^{A}	18.93 ± 2.19^{B}	

Note: Different superscripts (^{a,b,c,d}) following means in similar rows and columns showed significant difference ($p < 0.05$). Different superscripts (^{A,B}) following means in similar rows and columns showed significant difference ($p < 0.05$).

associated with thermal aggregation within casein isolates as well as degradation of protein hydrophobicity.

Color

The results revealed that the treatments (use of acids and drying techniques) significantly contributed to the color of casein, as presented in Table 1. L* (dark to white) was found to differ from 81.52 to 91.57. In general, the color of casein tends to be white, linked to its basic color. Regarding the base color of casein, Cheng *et al.* (2019) and Misawa *et al.* (2016) have argued that milk brightness is determined by the presence of nutritional components and the effect of processing.

Statistically, L* was significantly affected by interaction between acid types and drying methods ($p < 0.01$). Further, we found that L* of the casein treated with CH_3COOH + oven-drying was comparable with that treated with HCl + freeze-drying. Processing treatments could alter the whiteness degree of casein. The use of HCl (strong acid) seems to more incredibly affect changes in protein structure than CH_3COOH (weak acid). In terms of exposure to high temperature, oven-drying was able to reduce degree of whiteness, which could be linked to the Maillard reaction. The reaction promotes interaction between reducing sugars and amino acids, leading to reduction of white intensity of casein. Winarno (2008) explained that the Maillard reaction represents a browning activity triggered by high temperature, promoting reaction between reducing sugars and primary amino groups. Exposure to high temperature causes structural changes in protein, alleviating the intensity of white color.

Regarding a* color, the value was found in the range of –3.41–0.87, affected by the chemical composition of products and processing conditions. The range of a* was noticeably influenced by the chemical composition of products, using whey extract and casein isolate for fermented wine. The value of a* was –0.38–0.70 (greenish to reddish) in edible film made of dangke whey and carrageenan (Maruddin *et al.*, 2018), while casein-based edible film was reported to have an a* score of 4.59–5.20 (reddish; Wahyuni, 2017).

The results showed that the a* score of casein was affected by interaction between acids and drying methods. Furthermore, the a* score of casein treated with HCl + freeze-drying tends to be greenish. Meanwhile, the color of casein prepared with other processes was reddish.

In addition, the use of HCl for casein preparation enables to reform the structure of proteins, which displayed greenish color with presence of riboflavin. As discussed by Malaka (2014), one of pigments in milk is riboflavin, which is water-soluble and yellow-greenish in color.

High temperature in oven-drying during preparation of casein turned a* value into reddish. This is caused by interaction between reducing sugars and amino acids, known as the Maillard reaction, thus producing reddish color. Kusnandar (2011) explained that the Maillard reaction involved reaction of reducing sugars and amine groups that form simple proteins and release water molecules. Presence of water activity in casein escalates rate of reaction. This is in line with the use of high temperature, which could alter color intensity of casein into brownish-reddish.

Regarding b* color, the score ranges from 12.83 to 20.32 (yellowish), as presented in Table 1. The properties of b* are strongly linked to the characteristics of milk protein. In addition, the content of fat left from defatting process may also affect b* score. In general, the score of b* closely relates to carotenoid and riboflavin present in fat.

Casein is derived from skimmed milk. Although fat content in casein is low, addition of acids as coagulant could remarkably alter the color of casein. Skimmed milk originally appears bonewhite in color (Umaroh, 2018), which is due to low concentration of fat in skim. Meanwhile, presence of carotenoid and riboflavin in fat accounts for yellownish color of skim. Chairunnisa (1997) found that the b* score of milk protein modified by lactic acid was 12.8–16.4, displayed as a bright yellowish color.

Statistical analysis showed that b* color was affected by interaction of acids and drying methods ($p < 0.01$). We found that HCl + oven-drying process resulted in bright yellow b* color of casein, while other processes produced casein with a dark yellow color. CH_3COOH showed less destruction of protein than HCl. Winarno (2008) demonstrated that application of strong acid could drastically alter polypeptide chains and protein molecules. More the destruction of bonds, more the expansion of molecules. This changes configuration of proteins, leading to an increase in yellow intensity of casein.

The heat produced in oven-drying for casein preparation is able to unfold protein structures, thus uncovering fat molecules buried inside protein structures. This accounts for higher intensity of b* casein, displayed as bright yellow. Broyard and Gaucheron (2015) studied high temperature for hydrolyzing chemical chains of proteins, thereby inducing more intense hydrolytic activity of fats.

FTIR analysis of Casein

Spectroscopic analysis using FTIR is based on the characteristics of functional groups in proteins. The result is depicted in Figure 2. The HCl + freeze-drying process

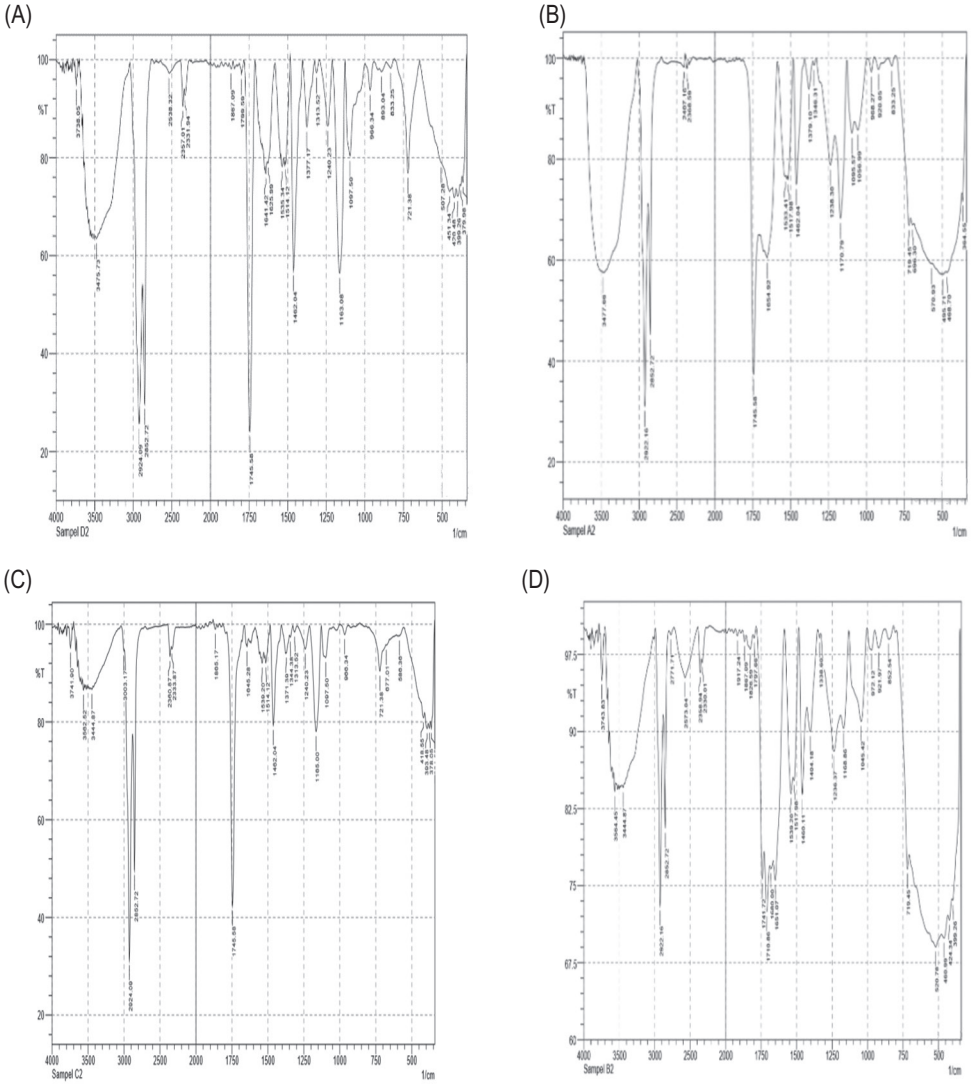

Figure 2. FTIR spectrum for casein prepared with: (a) HCl + freeze-drying; (b) HCl + oven-drying; (c) CH_3COOH + freeze-drying; (d) CH_3COOH + oven-drying.

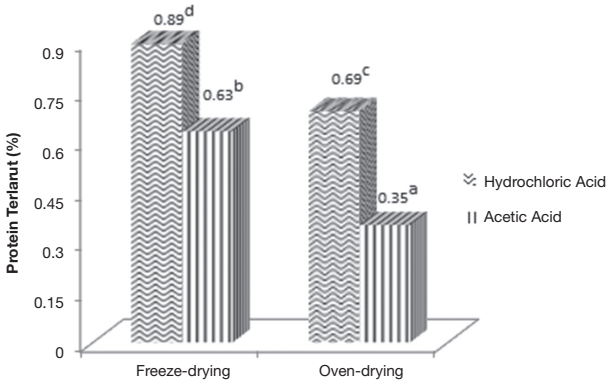

Figure 3. Contents of dissolved proteins after treatment with acids and freeze-drying methods. Different superscripts above the bars depicted a significant difference ($p < 0.01$).

(Figure 2a) resulted in seven regions of absorbance, with two specific peaks of 2924.09 cm^{-1} and 2852.72 cm^{-1}. The wave number of 3738.05 cm^{-1} refers to aromatic group (C-H). In addition, absorption peak of 2924.09 cm^{-1}–3475.73 cm^{-1} corresponds to methylene, while the peak range of 2538.32–2852.72 cm^{-1} refers to alkane (C-H bond). Furthermore, hydroxyl groups (O-H) were found in the wave number range of 2331.94–2357.01 cm^{-1}.

As depicted in Figure 2b, FTIR spectrum was detected in six regions of absorbance, with two specific peaks at wave numbers of 2922.16 cm^{-1} and 2852.72 cm^{-1}. The wave number of 3477.66 cm^{-1} corresponds to hydroxyl group (O-H), characterized by a wide region specific to the O-H group. Absorption peak range of 2852.72–2922.16 cm^{-1} refers to methylene, which is a asymetric stretch vibration of C-H bonds. Meanwhile, absorption peak range of 2368.59–2407.16 cm^{-1} is associated with hydroxyl group (O-H).

Figure 2c exhibits seven regions of absorbance with two sharp peaks, namely 2924.09 cm^{-1} and 2852.72 cm^{-1}. The absorption peaks of 3741.70 cm^{-1}, 3562.52 cm^{-1}, and 3444.67 cm^{-1} correspond to hydroxyl group (O-H), while the wave number range of 2852.72–2924.09 cm^{-1} represents methylene, referring to asymetric stretch vibration of C-H bonds. In addition, the wave number range of of 2333.87–2363.87 cm^{-1} demonstrates hydroxyl group (O-H).

Figure 2d depicts nine regions of absorbance with two sharp peaks. The wave numbers of 3743.83 cm^{-1}, 3564.45 cm^{-1}, and 3444.87 cm^{-1} correspond to hydroxyl group (O-H). In addition, peak at the wave number range of 2852.72–2922.16 cm^{-1} indicates presence of methylene group with asymetric stretch vibration of C-H bonds, while several peaks detected at wave numbers of 2771.71 cm^{-1}, 2573.04 cm^{-1} 2358.94 cm^{-1}, and 2330.91 cm^{-1} refer to hydroxyl group (O-H).

Dissolved proteins

Dissolved proteins refer to a group of simple proteins resulting from degradation of casein after treatment with acids and freeze-drying methods. The content of dissolved proteins in casein was found in the range of 0.35–0.89% (Figure 3), being slightly lower than that reported by Rahayu *et al.* (2013), reaching a range of 1.14–1.29% in casein treated with calcium chloride ($CaCl_2$).

Our experimental data statistically established that content of dissolved proteins was significantly affected by the given treatments ($p < 0.01$). Duncan statistical test revealed that the highest content of crude protein was attributed to HCl + freeze-drying process and next to HCl + oven-drying process. A strong acid such as HCl can iozine completely; consequently, this promotes the conversion of uncharged protein molecules into positive charged molecules. Thus, such condition increases the solubility of proteins. Winarno (2008) reported that treatment with a strong acid enhanced protein solubility because of changes in charge of proteins. Meanwhile, Kusumaningtyas *et al.* (2015) reported that acid treatment was also effective in destroying complex of protein molecules, converting them into simple parts such as peptides and amino acids.

Furthermore, difference in the formation of dissolved proteins is also linked to the drying techniques. As mentioned previously, HCl coupled with freeze-dyring produced higher quantity of dissolved proteins than HCl coupled with oven-drying. Previous studies (Felix da Silva *et al.*, 2018; Sarode *et al.*, 2016; Winarno, 2008) asserted that denaturation of proteins is achieved by using acid, alkali, heating, mechanical treatment, and salt. In this case, freeze-drying is considered as a mechanical treatment (low temperature) for casein, resulting in finer texture. For this reason, we could argue that each processing method caused different changes to protein features. Denaturation of protein is highly essential to consider as it causes loss of protein conformation because of structural changes (Deulgaonkar *et al.*, 2012).

Moreover, our experimental data established a higher content of dissolved protein in casein prepared by oven-drying. This is in accordance with the results of Felix da Silva *et al.* (2018), which demonstrated that higher temperature would bring greater changes to protein destruction, until reaching a constant level. As mentioned by Deulgaonkar *et al.* (2012), denaturation of protein could be induced by heat. In addition, Ciurzyńska and Lenart (2011) and Raikos (2010) reported that denaturation of protein induced by heat caused drammatical changes in the structural properties of protein, from strong double-structure to weak opened-structure.

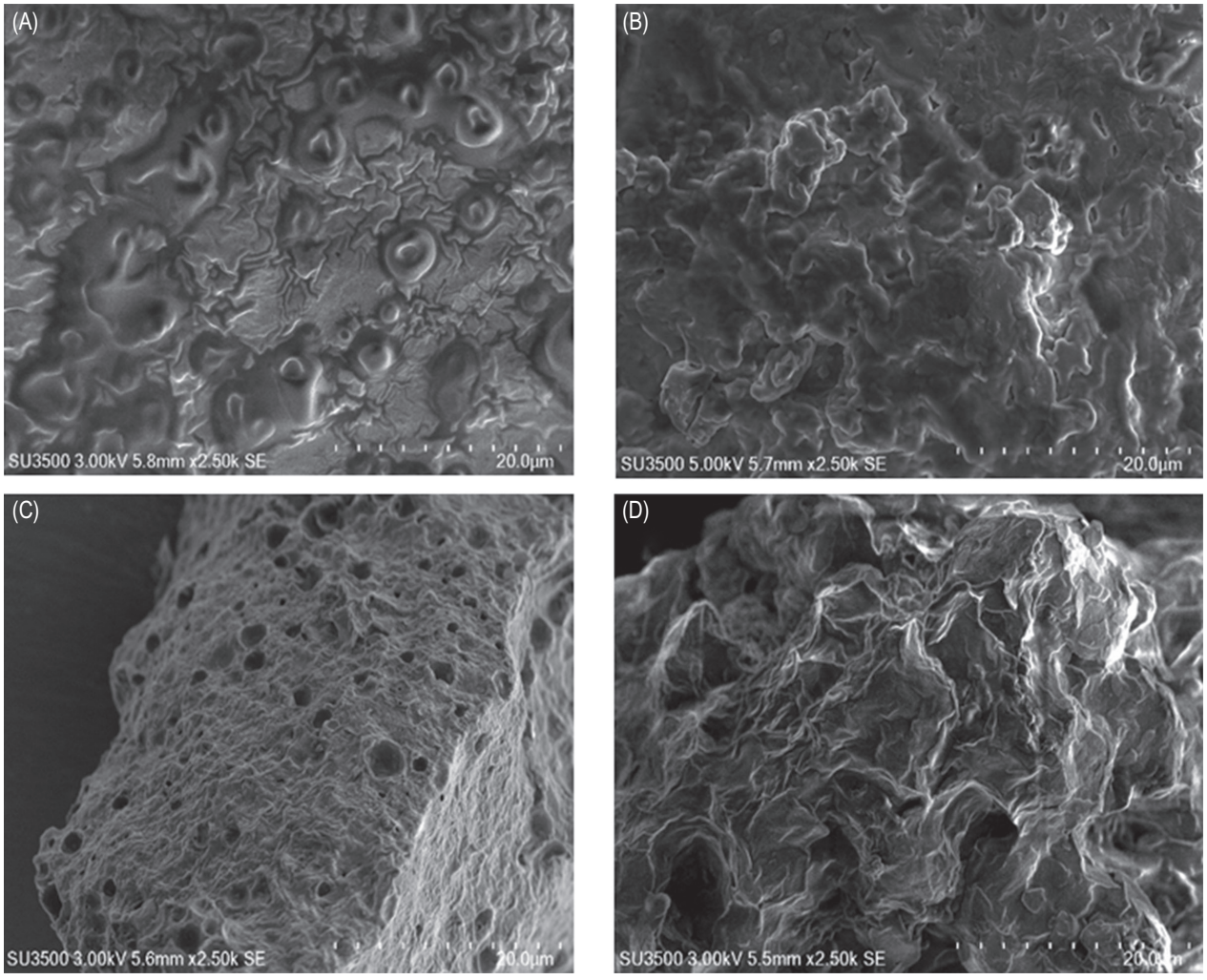

Figure 4. Potassium caseinate produced by different processes: (a) HCl + freeze-drying; (b) HCl + oven-drying; (c) CH_3COOH + freeze-drying; (d) HCl + oven-drying.

Microstructure

Microstructural analysis of casein by SEM is depicted in Figure 4. Images in Figure 4a seem to be solid, with absence of pores on their surfaces. Meanwhile, Figure 4c is found to have a more porous structure compared to Figures 4b and 4d. This suggested that combination of CH_3COOH and freeze-drying produced high porosity casein.

The moisture content of casein in HCl + freeze-drying process was 5.94%, which was higher than other processes. Dehydration process could be optimized through considering the factors retarding removal of water. These factors include amount and thickness of sample, drying temperature and time, and sample positioning in dryer. Deulgaonkar *et al.* (2012) stated that changes in food matrix occurred during dehydration, including shrinkage, browning, and case hardening.

Moisture content

Moisture content represents the quantity of water in foods. Kusnandar (2011) stated that chemical properties of water in food matrix differ remarkably, since water is bound in different manners. Water in food is often trapped in cells or bound with other chemical components of foods.

As depicted in Figure 5, mositure content of casein was found in the range of 5.29–5.94%. The range must be according to the standards set by Codex Alimentarius (2014), that is, maximum mositure of 8.0%. Statistical analysis revealed that acid types demonstrated a significant effect on moisture content ($p < 0.01$). The average moisture content in casein treated with HCl was higher than that treated with CH_3COOH. In short, acid used in this experiment enables to hydrolyze macromolecules,

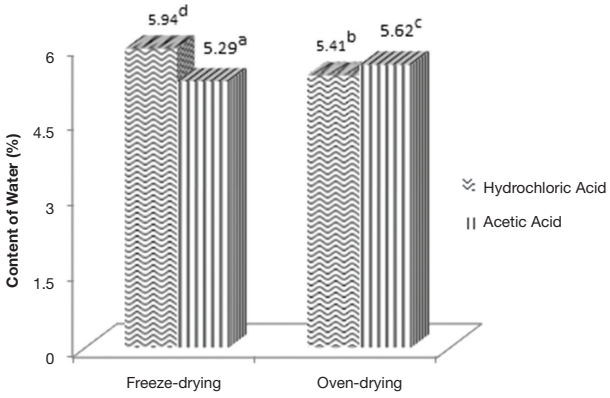

Figure 5. Moisture content of casein after treatments using acids and drying methods. Different superscripts above the bars depicted a significant difference ($p < 0.01$).

thus allowing to release more water. Broyard and Gaucheron (2015) and Felix da Silva *et al.* (2018) found that acid could alter moisture content. The more acid used would lead to increase in particle shrinkage to force more release of whey. As a consequence, more water is released. The highest moisture level was obsevred in HCl + freeze-drying process. However, there is a need to further investigate the use of drying methods for clarity.

Drying method requires a precise procedure ensuring that maximum water could be eliminated from foods. Regardless of food dimensions (amount, thickness, and area), drying techniques need to consider the capacity of instruments used and the period of drying. Previous studies conducted by Muchtadi and Sugiyono (2013) and Winangsih *et al.* (2013) reported that maximum drying rate could be achieved by considering the following factors: area of sample, temperature, air speed, humidity, air pressure, vacuum conditioning, evaporation, and period of drying process. Furthermore, Broyard and Gaucheron (2015) and Buckle *et al.* (1987) asserted several considerable factors of drying, including physical and chemical properties of sample, such as shape, quantity of sample, positioning, size, and initial water content. These factors are essential for controlling and obtaining the best performance of dehydration processes.

Conclusion

Our experimental data revealed that the use of oven-drying combined with either HCl or CH_3COOH enhanced antioxidant activity and a* (reddish) and b* (yellowish) scores. It being the fact that process of freezing-drying with acids alleviated moisture content but improved viscosity and microstructural properties. Combination of oven-drying and strong acid HCl was responsible for increase in L* (lightness) score and content of proteins and dissolved proteins as well as promoted changes in chemical features by FTIR analysis.

Acknowledgements

Authors would like to thank Ministry of Research, Technology, and Higher Education (KEMENRISTEKDIKTI), Republic of Indonesia, for funding this research under the scheme of STRANAS No. 123/SP2H/PTNBH/DPRM/2018. and scheme of Terapan 7/E1/KP/PTNBH/2021 We also express many thanks to LP2M, Hasanuddin University for valuable support in research regulations (No. SP-DIPA-042.06-1.401516/2018) and 752/UN4.22./PT.02.00/2021.

References

AOAC (Association of Official Analytical Chemists). 2019. Dairy Products. In: Robert L. Bradley, Jr. (Ed.), Official Methods of Analysis (21st Ed), AOAC international Suite 300 2275 research BLVD, Maryland, p.14.

Badem A. and Uçar G. 2017. Production of caseins and their usages. Int J Food Sci Nutr. 2(1): 4–9.

Broyard C. and Gaucheron F. 2015. Modifications of structures and functions of caseins: a scientific and technological challenge. Dairy Sci Technol. 95(6): 831–862. https://doi.org/10.1007/s13594-015-0220-y

Buckle K.A., Edwards R.A., Fleet G.H. and Wootton M. 1987. Food Science. UI Press, Jakarta, Indonesia.

Chairunnisa H. 1997. Isolasi dan Modifikasi Protein Susu Dalam Rangka Pemanfaatan Susu Sapi Substandard. PhD Dissertation, Bogor Agricultural University, Bogor, Java, Indonesia. Page 83–93. Available at: https://adoc.pub/pada-penelitian-ini-telah-diisolasi-protein-susu-dari-susu-s.html

Cheng N., Barbano D.M. and Drake M.A. 2019. Effect of pasteurization and fat, protein, casein to serum protein ratio, and milk temperature on milk beverage color and viscosity. J Dairy Sci. 102(3): 2022–2043. https://doi.org/10.3168/jds.2018-15739

Ciurzyńska A. and Lenart A. 2011. Freeze-drying-application in food processing and biotechnology – a review. Polish J Food Nutr Sci. 61(3): 165–171. https://doi.org/10.2478/v10222-011-0017-5

Codex Alimentarius. 2014. Standard for edible casein products: Codex STAN 290-1995. International Food Standards. Available at: http://www.fao.org/input/download/standards/185/CXS_290e.pdf.

De Souza P.M., Fernández A., López-Carballo G., Gavara R. and Hernández-Muñoz P. 2010. Modified sodium caseinate films as releasing carriers of lysozyme. Food Hydrocoll. 24(4): 300–306. https://doi.org/10.1016/j.foodhyd.2009.10.005

Deulgaonkar S.U., Ramteke L.P. and Thorat B.N. 2012. Filtration and drying characteristics of casein. Sep Purif Technol. 92: 50–56. https://doi.org/10.1016/j.seppur.2012.03.006

Djaeni M., Asiah N. and Sasongko S.B. 2015. Aplikasi Sistem Pengeringan Adsorpsi Untuk Bahan Pangan Dan Aditif. UNNESS Press, Semarang, Indonesia.

Felix da Silva D., Ahrné L., Ipsen R. and Hougaard A.B. 2018. Casein-based powders: characteristics and rehydration properties. Compr Rev Food Sci Food Saf. 17(1): 240–254. https://doi.org/10.1111/1541-4337.12319

Glab T.K. and Boratynski J. 2017. Potential of casein as a carrier for biologically active agents. Topics Curr. Chem. 375(71): 1–20. https://doi.org/10.1007/s41061-017-0158-z

Haque M.K. and Roos Y.H. 2006. Differences in the physical state and thermal behavior of spray-dried and freeze-dried lactose and lactose/protein mixtures. Innov Food Sci Emerg Technol (IFSET). 7(1–2): 62–73. https://doi.org/10.1016/j.ifset.2004.12.004

Jimenez X.T., Cuenca A.A., Jurado A.T., Corona A.A. and Urista C.R.M. 2012. Traditional method for whey protein isolation and concentration: effect on nutritional properties and biological activity. J Mex Chem Soc. 56(4): 369–377.

Konstance R.P. and Strange E.D. 1991. Solubility and viscous properties of casein and caseinates. J Food Sci. 56(2): 556–559. https://doi.org/10.1111/j.1365-2621.1991.tb05323.x

Kumaresan A., Selma C., Reshma N.V. and Jacinth N.A. 2017. Quantitative analysis of casein precipitation from the various milk samples. J Chem Pharm Res. 9(9): 113–115.

Kumesan E.C., Pandey E.V. and Lohoo H.J. 2017. Analisa total bakteri, kadar air dan pH pada rumput laut (*Kappaphycus alvarezii*) dengan dua metode pengeringan. Media Teknol Hasil Perikanan. 5(1): 30–35. https://doi.org/10.35800/mthp.5.1.2017.14911

Kusnandar F. 2011. Kimia Pangan: Komponen Makro. Dian Rakyat, Jakarta, Indonesia.

Kusumaningtyas E., Widiastuti R., Kusumaningrum H.D. and Suhartono M.T. 2015. Aktivitas antibakteri dan antioksidan hidrolisat hasil hidrolisis protein susu kambing dengan ekstrak kasar bromelin. J Teknol dan Indust Pangan. 26(2): 179–188. https://doi.org/10.6066/jtip.2015.26.2.179

Liu Y., Zhao Y. and Feng, X. 2008. Exergy analysis for a freeze-drying process. Appl Therm Eng. 28(7): 675–690. https://doi.org/10.1016/j.applthermaleng.2007.06.004

Malaka R. 2014. Teknologi Aplikatif Pengolahan Susu. Brilian Internasional, Jakarta, Indonesia.

Maruddin F., Ratmawati R., Fahrullah F. and Taufik M. 2018. Karakterisitik edible film berbahan whey dangke dengan penambahan karagenan. J. Veteriner. 19(2): 291–297. https://doi.org/10.19087/jveteriner.2018.19.2.291

Misawa N., Barbano D.M. and Drake M. 2016. Influence of casein as a percentage of true protein and protein level on color and texture of milks containing 1% and 2% fat. J Dairy Sci 99(7): 5284–5304. https://doi.org/10.3168/jds.2016-10846

Morales F.J. and Babbel M.B. 2002. Antiradical efficiency of Maillard reaction mixtures in a hydrophilic media. J Agric Food Chem. 50(10): 2788–2792. https://doi.org/10.1021/jf011449u

Muchtadi T.R. and Sugiyono. 2013. Prinsip Proses dan Teknologi Pangan. Alfabeta, Bandung, Indonesia.

Nahariah, Legowo A.M., Abustam E., Hintono A., Bintoro P. and Pramono Y.B. 2014. Endogeneous antioxidant activity in the egg whites of various types of local poultry eggs in South Sulawesi, Indonesia. Int J Poult Sci. 13(1): 21–25. https://doi.org/10.3923/ijps.2014.21.25

Pająk P., Socha R., Gałkowska D., Rożnowski J. and Fortuna T. 2014. Phenolic profile and antioxidant activity in selected seeds and sprouts. Food Chem. 143: 300–306. https://doi.org/10.1016/j.foodchem.2013.07.064

Pralea D., Dumitrascu L., Borda D. and Stanciuc N. 2011. Functional properties of sodium caseinate hydrolysates as affected by the extent of chy-motrypsinolysis. J Agroaliment Process Technol. 17(3): 308–314.

Rahayu P.P., Purwadi and Thohari I. 2013. Modifikasi Kasein Dengan $CaCl_2$ dan pH Yang Berbeda Ditinjau Dari Kelarutan Protein, Kelarutan Kalsium, Bobot Molekul dan Mikrostruktur. Postgraduate Thesis, University of Brawijaya, Malang, Indonesia.

Raikos V. 2010. Effect of heat treatment on milk protein functionality at emulsion interfaces. A review. Food Hydrocoll. 24(4): 259–265. https://doi.org/10.1016/j.foodhyd.2009.10.014

Raikos V., Kapolos J., Farmakis L., Koliadima A. and Karaiskakis G. 2009. The use of sedimentation field-flow fractionation in the size characterization of bovine milk fat globules as affected by heat treatment. Food Res Int. 42(5–6): 659–665. https://doi.org/10.1016/j.foodres.2009.02.001

Sari M. 2011. Identifikasi Protein Menggunakan Fourier Transform Infrared (FTIR). Undergraduate Thesis, Univerisity of Indonesia, Depok, Indonesia.

Sarode A.R., Sawale P.D., Khedkar C.D., Kalyankar S.D., and Pawshe R.D. 2016. Casein and caseinate: methods of manufacture. In: Caballero B, Finglas P. and Toldrá F (eds.), The Encyclopedia of Food and Health. Academic Press, London, pp. 676–682. https://doi.org/10.1016/B978-0-12-384947-2.00122-7

Simanjuntak P., Parwati T., Lenny L.E., Tamat S.R. and Murwani, R. 2004. Isolasi dan identifikasi senyawa antioksidan dari ekstrak benalu teh (*Scurrula oortiana* (Korth) Danser). J Ilmu Kefarmasian Indonesia. 2(1): 19–24.

Ting K., Liu Y.F., Tian-Li G. and Lu-Hua Z. 2016. Relationships between viscosity and the contents of macromolecular substances from milk with different storage styles. Food Sci Technol. 4(4): 49–56. https://doi.org/10.13189/fst.2016.040401

Triyono A. 2010. Mempelajari pengaruh penambahan beberapa asam pada proses isolasi protein terhadap tepung protein isolat kacang hijau (*Phaseolus radiatus* L.). Paper presented at Chemical and Process Engineering Seminar, University of Diponegoro Semarang, Semarang, Java, Indonesia, August 4–5.

Umaroh A. 2018. Pengaruh penambahan susu skim dan madu terhadap sifat organoleptik yoghurt kacang merah. J Tata Boga 7(2): 1–9.

Vasbinder A.J., van de Velde F. and de Kruif C.G. 2004. Gelation of casein-whey protein mixtures. J Dairy Sci. 87(5): 1167–1176. https://doi.org/10.3168/jds.S0022-0302(04)73265-8

Wahyuni T. 2017. Pengaruh Konsentrasi Kasein dan Volume Larutan Edible Yang Berbeda Terhadap Karakteristik Edible Film. Undergraduate Thesis, University of Hasanuddin, Makasar, Indonesia.

Wikandari P.R., Suparmo S., Marsono Y. and Rahayu E.S. 2011. Potensi bekasam bandeng (*Chanos chanos*) sebagai sumber angiotensin I converting enzyme inhibitor. Biota J Ilmiah Ilmu-Ilmu Hayati. 16(1): 145–152. https://doi.org/10.24002/biota.v16i1.69

Winangsih, Prihastanti E. and Parman S. 2013. Pengaruh metode pengeringan terhadap kualitas simplisia lempuyang wangi (*Zingiber aromaticum* L.). Bull Anat dan Fisiologi. 21(1): 19–25.

Winarno F.G. 2008. Kimia Pangan dan Gizi. M. Brio Press, Bogor, Indonesia.

Winarsi H. 2007. Antioksidan Alami dan Radikal Bebas. Kanisius, Yogyakarta, Indonesia.

Witrowa-Rajchert D. and Lewicki P.P. 2006. Rehydration properties of dried plant tissues. Int J Food Sci Technol. 41(9): 1040–1046. https://doi.org/10.1111/j.1365-2621.2006.01164.x

Italian Journal of Food Science, 2022; 34 (1): 13–23

Characteristics of non-gluten noodles from modified cocoyam (*Xanthosoma sagittifolium*) and porang (*Amorphophallus oncophyllus*)

Dedin Finatsiyatull Rosida*, Ulya Sarofa, Delbra Aliffauziah

Department of Food Technology, Universitas Pembangunan Nasional Veteran Surabaya, East Java, Indonesia

***Corresponding Author:** Dedin Finatsiyatull Rosida, Department of Food Technology, Universitas Pembangunan Nasional Veteran Surabaya, East Java, Indonesia. Email: dedin.tp@upnjatim.ac.id

Received: 30 May 2022; Accepted: 8 December 2021; Published: 26 January 2022

PAPER

Abstract

Foods product were developed after the discovery of gluten-free flour. This study aimed to determine the proper formulation of dry noodles from different proportions of modified cocoyam flour and porang flour. In addition, the use of egg was evaluated in terms of physicochemical and organoleptic properties. The first factor was the proportion of modified cocoyam flour and porang flour (90%:10%, 85%:15%, and 80%:20%). The second factor was the addition of eggs (5%, 10%, and 15%). The result showed that the best formulation according to chemical, physical, and organoleptic parameters was made with modified cocoyam flour and porang flour, 85%:15%, with 10% eggs. This non-gluten-based formulation of noodles showed both high dietary fibers content derived from glucomannan (60.14%) and high protein content (12.75%).

*Keywords***:** cocoyams tubers, eggs, modified flour, noodles, porang, soybean

Introduction

Noodles are long thin pieces of food made from flour, water, and eggs. Noodles usually cooked in soup or boiling water. Moreover, noodles are composed of wheat flour with a lot of gluten. Wheat flour should not be consumed by people who have certain digestive disorders. Hence, in this research, non-gluten flour was used. Non-gluten flour is obtained from tubers such as cocoyam (*Xanthosoma sagittifolium*). However, some limitations during production of noodles using non-gluten flour occurred. Therefore, other ingredients must be added to enhance the texture of noodles. Porang (*Amorphophallus oncophyllus*) flour is added to increase the texture elasticity of noodles.

Cocoyam is a commodity with an appreciable nutritional profile, high productivity, and better storability than other indigenous roots and tubers. In addition, cocoyam has the potential for sustainable food security. Cormels, flours, and starches could be explored in the snack and complimentary food industries by utilizing processing properties, ease of crop production, storability, and nutritional value (Boakye *et al*., 2018).

The utilization of cocoyam flour as a substitute for wheat flour in production of noodles has physical and sensory limitations such as dull color, too much stickiness when added with water, very low solubility and swelling strength, and soft texture. Therefore, modification of flour is required to enhance the physical and sensory properties of noodles. The physical and sensory properties of noodles can be improved in several ways. One of them is by fermenting the flour using lactic acid bacteria (LAB). Fast-growing microbes produce pectin lytic and cellulolytic enzymes. These enzymes can destroy the tuber cell wall allowing the liberation of starch granules (Subagio, 2008). These conditions change the characteristics of flour, including increased viscosity, gelation ability, rehydration, and dissolving ability.

The tuber flour modified by fermentation method resulted in lower water content, brighter flour color, and higher amylose content compared to the ordinary cocoyam flour. The increase of amylose content in cocoyam flour impacts production of dry noodles. Starch with high amylose content can absorb water due to amylase, which can form hydrogen bonds that are greater than amylopectin (Hidayat *et al.*, 2007). Additionally, amylose plays a role in increased firmness compared to amylopectin. Therefore, the higher amylose content reduces the stickiness of noodles (Supriyadi, 2012).

Noodles from 100% modified cocoyam flour have less elastic properties of dough. Thus, the need for additional ingredients plays an essential role in the chewy texture of noodles. A binder can be added to obtain the rubbery texture of noodles. Moreover, binder can trap water to form an elastic and springy texture (Saha and Bhattacharya, 2010). In this case, porang flour and eggs were used as a binder.

Tubers of porang (*Amorphophallus oncophyllus*), or often called "iles-iles" in Indonesia, from the *Araceae* family, grow in a warm subtropical climate such as in East Asia, South China, Japan, and Indonesia (Ambarwati *et al.*, 2000). Porang flour contains high content of glucomannan (15–64% on a dry basis) (Faridah *et al.*, 2012) Therefore, porang flour can absorb water, form a gel (gelling agent), and increases the elasticity of noodles (Wang *et al.*, 2012).

The addition of porang flour improves the texture, elasticity, and flexibility of noodles. Porang flour increases the thickness of noodles, thus can be used as a substitute for thickening chemicals in noodles. Therefore, porang flour can be a gelling agent (Retnaningsih and Hartayani, 2005). Formation of gel occurs when dispersed in water, as hydrocolloids and water molecules are trapped in the complex structures through hydrogen cross-linking. This condition leads to hydration process (Citra *et al.*, 2012). Glucomannan is a soluble dietary fiber with high water but low calorie contents (Yang *et al.*, 2006).

Nugraheni and Puspitaningrum (2013) examined the positive effect of porang tuber (*Amorphophallus konjac* K. Koch) on the liver. The results demonstrated that administering porang tuber flour to rats at a dosage of 2000 mg/kg alters the levels of serum glutamic oxaloacetic transaminase and serum glutamic pyruvic transaminase as well as the liver histopathology images of Wistar male rats induced by paracetamol.

The eggs added in production of noodles create more resilient dough so that the noodles will not break easily. Moreover, the noodles turbidity during boiling will be prevented. The function of egg yolk is to accelerate water hydration. The egg white protein forms a layer that is strong enough to cause a better binding of water to noodles and increase suppleness (Diniyah *et al.*, 2017).

The addition of eggs at low concentrations does not meet the Indonesian National Standard for dry noodles. Therefore, they must be supplemented with other ingredients with high protein content. Soybean is a food with a high nutritional content. It is the best source of protein among nuts. The addition of soybeans to the noodles production is expected to meet the protein quality standards of non-gluten dry noodles (Widaningrum and Soekarto, 2005), and produce a better texture and noodles taste. For this reason, a fixed proportion of soybean flour (15%) is added to the dry noodles composition. This study aimed to determine the exact proportion between the use of modified cocoyam flour, porang flour, and egg on the noodles quality.

Methods

Raw material properties

Cocoyam tuber, porang flour, and soda ash were used as raw materials to produce dry noodles. Cocoyam tubers and porang flour were obtained from Sleman, Indonesia. *Lactobacillus plantarum* FNCC 0027 strain (Agricultural Product Technology Laboratory, Gadjah Mada University, Indonesia) was used for the fermentation method. Hydrochloric acid (Sigma Aldrich), sodium hydroxide (Merck), Fehling A, Fehling B, sulfuric acid, De Man, Rogosa and Sharpe (MRS) broth (Oxoid Ltd.), bromocresol green, boric acid (HO_3BO_3), distilled water, 95% alcohol, isopropyl alcohol, and aluminum sulfate were used as analysis materials.

Modified cocoyam and porang flour

Cocoyam flour was made based on the method of Rosida *et al.*, 2020. Cocoyam tubers were peeled, washed, and sliced for 0.5-cm thickness. Sliced tubers were soaked in 7.5% NaCl solution for 1 h to remove calcium oxalate in the tuber tissue, which can cause itching (Rozali *et al.*, 2021). Sliced tubers were washed with tap water until clean and drained. These were dried using a cabinet dryer at 60°C for 12 h. Dried tubers were ground using a grinding machine. Finely knotted tubers were sifted using 80-mesh sieves.

A suspension of 2500-g cocoyam flour and 7500-mL distilled water was fermented using 7% *Lactobacillus plantarum* FNCC 0027 starter for 96 h at room temperature (25 ± 2°C). The fermented products were washed with distilled water at a neutral pH. Fermented flour

was dried at 60°C for 12 h. The modified cocoyam flour was analyzed for moisture, ash, protein (Association of Official Agricultural Chemists [AOAC], 2004), starch (Sudarmadji *et al.*, 1997), and amylose (International Rice Research Institute [IRRI], 1978). Cocoyam tubers and porang flour were obtained from Sleman, Indonesia. Similarly, porang flour was evaluated in terms of moisture, ash, protein (AOAC, 2004), starch (Sudarmadji *et al.*,1997), amylose (IRRI, 1978), and glucomannan (Widjanarko and Megawati, 2015).

Dry noodle production

Dry noodles were produced with the composition of modified cocoyam flour and porang flour (90%:10%, 85%:15%, or 80%:20%) and egg addition (5%, 10%, or 15%). Steps for dry noodles production are as follows: Modified cocoyam flour and porang flour (90%:10%, 85%:15%, or 80%:20%), soy flour (15%), soda ash (1%), and salt (2%) were mixed while adding water and egg (5%, 10%, or 15%) until it became an homogeneous dough. The dough was put into a noodle extruder machine. Noodles were steamed at 100°C for 5 min and dried using a cabinet dryer at 60°C for 7 h.

Experimental design

The experimental design was a completely randomized design with a factorial pattern that comprises two factors. Factor I comprised the three levels of the proportion of modified cocoyam flour and porang flour (90%:10%, 85%:15%, or 80%:20%), and factor II comprised the three levels of egg addition (5%, 10%, or 15%).

Dry noodles were analyzed for proximate composition such as moisture, ash content, protein content (AOAC, 2004), starch content (Sudarmadji *et al.*, 1997), rehydration (Ramlah, 1997), cooking loss (Subarna and Muhandri, 2013), elasticity (Ramlah, 1997), glucomannan level, and organoleptic properties (Wulandari *et al.*, 2008).

Dry noodles properties

Physical properties

Rehydration

The measurement of rehydration was conducted using the weighing method. Rehydration is the ability of noodles to absorb water after gelatinization. Measurements were made by (a) weighing 5 g of raw noodles, and (b) boiling for 4 min or until the noodles were completely gelatinized, and then weighing again. Rehydration was the percentage difference between (a) raw noodles and (b) gelatinized noodles.

Cooking loss test

Cooking loss was determined by boiling approximately 5 g of noodles in 150-mL water for 3 min and draining. Then noodles were dried at 100°C until their weight was constant. Other 5-g noodles were weighed for water content to calculate dry weight of the sample. The percentage of cooking loss was calculated based on the difference between dry weights of the sample before and after boiling divided by dry weight of the sample before boiling.

Elasticity

Elasticity was measured using a ruler. The cooked sample was placed on a ruler and measured (the initial length, P1); then it was pulled off until it broke and measured again (the final length, P2). Elasticity was calculated by the following formula: (P1 – P2/P1) × 100%.

Glucomannan levels using gravimetric method

The sample (25 g) and aluminum sulfate salt (2.5 g) were dissolved in 75-mL water 1:10 (w/v) with continuous stirring for 35 min. The precipitated samples were separated using a 2000-rpm centrifuge for 30 min. Supernatant was added with isopropyl alcohol in a ratio of 1:1 (v/v) with stirring until lumps were formed (Rhim and Wang, 2013; Yan *et al.*, 2012).

The lumps were filtered using a filter paper and dried at 60°C for 24 h and weighed. Glucomannan content was the percentage of the dry weight to the initial weight of the sample.

Organoleptic test

Food quality can be measured by three properties: chemical, physical, and sensory. Consumer acceptance is primarily determined by quality factors, especially organoleptic (Agustia *et al.*, 2019; Akonor *et al.*, 2017). Organoleptic properties are determined using the human senses: sight, smell, and taste (Chauhan *et al.*, 2018). The organoleptic properties of the dry noodle products tested in this study were color, taste, texture, and aroma. According to Friedman's test performed for the color, taste, and texture of non-gluten dry noodle products, there were significant differences ($X_{2count} \geq X_{2table}$). Panelists (n = 25) gave an assessment of color, taste, and aroma using the following evaluating scale: 5 = liked extremely, 4 = liked moderately, 3 = liked slightly, 2 = disliked moderately, and 1 = disliked extremely.

Data analysis

Data from all test parameters (except for ash content) were obtained and processed for variance analysis. Variance analysis was used to determine the interaction between each composition. Further tests were performed

using Duncan's multiple range test (5%) if there were significant differences.

Results and Discussion

Raw material properties

Table 1 shows the characteristics of modified cocoyam flour (Rosida *et al*., 2020) and porang flour compared to the previous research (Arifin, 2001; Aryanti and Abidin, 2015; Kumoro *et al.*, 2018; dan Widjanarko, 2015). The differences between the raw materials in this study and previous studies were harvesting period, tuberose varieties, and flour production method. According to Table 1, porang flour based on the data of previous studies contained 12.32% of water, 3.9% of ash (Aryanti and Abidin, 2015), 24.6% of starch, 18.2% of amylose (Kilara, 1994), 3.42% of protein (Kumoro *et al.*, 1994), and 63.49% of glucomannan (Widjanarko and Megawati 2015).

Dry noodles' proximate properties

Water and ash contents of dry noodles

The water content of dry noodles ranged from 6.05% to 7.49%. The lowest water content was 6.05 % in dry noodles. This result was obtained with the modified cocoyam flour 90%, porang flour 10%, and 5% egg yolk. In contrast, the formulation of modified cocoyam flour of 90%, porang flour of 15%, and the addition of 15% egg yolk produced the highest water content (7.49%). Table 2 shows the relationship of the proportions of modified cocoyam flour, porang flour as well as the addition of eggs to the water content of noodles.

In addition, as shown in Table 2, the water content of noodles increases with the lower composition of modified cocoyam flour, the higher composition of porang flour, and more addition of egg yolk. This condition is caused by the presence of glucomannan, which is a water-soluble fiber. Similarly, more addition of eggs increases the water level of noodles. Eggs contain hydrophilic proteins. The absorption of water by proteins is related to the side-chain polar groups such as carbonyl, hydroxyl, amino, carboxyl, and sulfhydryl groups. This condition causes hydrophilic proteins to form hydrogen bonds with water (Kilara, 1994). These proteins bind water molecules by the formation of hydrogen bonds (Sari, 2017).

Glucomannan absorbs maximum water compared to other food fibers (Charoenrein *et al*., 2011). A previous study (Chan, 2011) confirmed this property, reporting that porang flour contains glucomannan and absorbs up to 200 times of water. If more porang flour is added, the holding capacity of water becomes greater, resulting in higher water content of dry noodles. Regarding the quality of dry noodles, Indonesia National Standard (SNI) stated that the maximum water content is 10%. In the present study, dry noodles in each category satisfied this standard (SNI No. 01-2974-1996).

Ash levels of dry noodles were found in the range 1.68–1.84%. The smaller modified cocoyam flour resulted in the higher porang flour proportion and ash content. The ash content of porang flour was 3.33%. It was higher than the modified cocoyam flour raw material, which was 1.08%. The higher the ash content, the higher the minerals contained in a food ingredient. It is because the ash content from mineral elements and chemical composition does not evaporate during the drying process.

The addition of eggs further increases the ash content in noodles. It is due to the mineral content of eggs (Juanda and Cahyono, 2000). A total of 1% of ash content is found in eggs (Muchtadi *et al.*, 2010). Egg yolk contains several minerals, especially phosphorus (P), manganese (Mn), iron (Fe), iodine (I), copper (Cu), calcium (Ca) and a small portion of zinc (Zn), which are more than those found in egg white. Maximum mineral component found in egg yolk is P, which binds phospholipids, especially lecithin. More than 60% of P in egg yolk is found in lecithin. On the other hand, egg white contains minerals such as chlorine (Cl), magnesium (Mg), potassium (K), sodium (Na), and sulfur (S) in higher proportion than found in egg yolk (Andriani *et al.*, 2015).

Table 1. Raw material properties according to previous studies.

Component	Modified cocoyam flour	Modified cocoyam flour data in the literature	Porang flour
Water content (%)	8.92 ± 0.023	8.28	11.10 ± 0.030
Ash (%)	1.076 ± 0.021	1.05	3.33 ± 0.171
Starch (%)	63.31 ± 0.247	76.74	24.82 ± 0.182
Amylose (%)	22.77 ± 0.164	26.28	19.74 ± 0.158
Protein (%)	3.09 ± 0.008	–	3.47 ± 0.005
Glucomannan (%)	–	–	60.14 ± 0.192

Table 2. Water content, protein, starch, and amylose level of each composition of modified cocoyam flour and porang flour with addition of egg.

Formula composition					
Modified cocoyam flour and porang flour (%)	Egg (%)	Water content (%)	Protein (%)	Starch (%)	Amylose (%)
	5	$6.05^{a} \pm 0.10$	$12.23^{a} \pm 0.01$	$65.32^{e} \pm 0.84$	$23.50^{f} \pm 0.05$
90:10	10	$6.35^{a,b} \pm 0.22$	$12.93^{b} \pm 0.02$	$64.45^{d} \pm 0.76$	$23.14^{e} \pm 0.11$
	15	$7.14^{d} \pm 0.12$	$13.65^{c} \pm 0.01$	$64.03^{d} \pm 0.24$	$22.79^{c,d} \pm 0.12$
	5	$6.57^{b,c} \pm 0.19$	$12.55^{c} \pm 0.03$	$64.13^{d} \pm 0.07$	$23.14^{e} \pm 0.04$
85:15	10	$6.78^{c} \pm 0.19$	$13.22^{d} \pm 0.02$	$63.16^{b,c} \pm 0.10$	$22.67^{c} \pm 0.08$
	15	$6.71^{b,c} \pm 0.34$	$14.19^{e} \pm 0.08$	$62.59^{b} \pm 0.16$	$22.14^{b} \pm 0.18$
	5	$6.77^{c} \pm 0.24$	$12.87^{f} \pm 0.07$	$63.86^{c,d} \pm 0.63$	$22.91^{d} \pm 0.04$
80:20	10	$7.16^{d} \pm 0.13$	$13.53^{g} \pm 0.02$	$62.76^{b} \pm 0.10$	$22.26^{b} \pm 0.14$
	15	$7.49^{d} \pm 0.20$	$14.49^{h} \pm 0.01$	$60.98^{a} \pm 0.27$	$21.45^{a} \pm 0.16$

Products from animals contain high ash content because it contains several minerals such as Ca, Fe, and P. The heating process also affects the amount of ash content in the product produced. The drying process causes the decomposition of water molecular bonding components. Moreover, drying process increases sugar, fat, and minerals, thereby increasing ash content. The ash content should be only 3% according to the quality standard of dry noodles. In the present study, dry noodles in each category satisfied this standard (SNI No. 01-2974-1996).

Protein content

The protein content of dry noodles was 12.23–14.49%. The proportions of modified cocoyam flour of 90% and porang flour of 10% with an egg addition of 5% produced the lowest protein content (12.23%) whereas the proportions of modified flour of 80% and porang flour of 20% with an egg addition of 15% produced the highest protein content (14.49%). Table 2 shows the relationship of the proportions of modified cocoyam flour, porang flour as well as the addition of egg to the protein content of noodles.

Moreover, the smaller proportion of modified cocoyam flour, the higher proportion of porang flour, and the addition of eggs increased the protein content of dry noodles (Table 2). It was due to the higher protein content in porang flour than in modified cocoyam flour, thereby increasing the protein content of dry noodles. The protein content of raw material in porang flour was higher (3.47%) than the protein content of modified cocoyam flour (3.09%).

Similarly, the addition of more eggs increased protein level in dry noodles. According to Muchtadi *et al.* (2010), eggs have 12.7% of protein.

The egg added in the manufacture of dry noodles improves the quality of noodle protein and creates a more resilient dough (Astawan, 2008). Moreover, addition of soy flour to dry noodles increases protein content because soybean is a good source of protein. A total of 41.7% of protein is found in soybean. According to the quality standard of dry noodles, the standard protein content must be at a minimum of 8%. In this study, the dry noodles in each category satisfied this standard (SNI number 01-2974-1996).

Starch content

The starch content of dry noodles ranged from 60.98% to 65.32%. The proportions of modified cocoyam flour of 80% and porang flour of 20% with an egg addition of 15% produced minimum starch content (60.98%) whereas the proportions of modified cocoyam flour of 90% and porang flour of 10% with an egg addition of 5% produced maximum starch content (65.32%). Table 2 shows the relationship of the proportions of modified cocoyam flour, porang flour as well as the addition of eggs to the starch content of dry noodles.

Furthermore, the smaller proportion of modified cocoyam flour, the higher proportion of porang flour, and the addition of eggs decreased starch level in noodles (Table 2). This was because the starch level in porang flour was less than that in modified cocoyam flour. The starch level of dry noodles decreased by increasing the proportion of porang flour. Similarly, more eggs decreased starch levels in dry noodle products because eggs did not contain starch.

The starch content in modified cocoyam flour was 63.31%. It was higher than in porang flour (24.82%); hence, the lower proportion of modified cocoyam flour in noodle production reduced its starch content.

Amylose content

Amylose levels of dry noodles ranged from 21.45% to 23.50%. The proportions of modified flour of 80% and porang flour of 20% with an egg addition of 15% produced the lowest amylose content (21.45%) whereas the proportions of modified cocoyam flour of 90% and porang flour of 10% with an egg addition of 5% produced the highest amylose content (23.50%). Table 2 shows the relationship of the proportions of modified cocoyam flour, porang flour as well as the addition of eggs to the amylose content of noodles. These results indicated that the smaller proportion of modified cocoyam flour, the higher proportion of porang flour, and the addition of eggs resulted in the lower level of amylose in noodles.

This was because the amylose content in porang flour was less than that in the modified cocoyam flour. Therefore, the amylose content of dry noodles decreased by increasing the proportion of porang flour. Similarly, the addition of more eggs decreased the amylose levels of dry noodles.

The amylose content of modified cocoyam flour was 22.77%. It was higher than that of porang flour (19.74%). The high content of amylose in modified flakes was due to the activity of enzymes produced during fermentation. Therefore, the breakdown of amylopectin branch chain in α-1,6 glycosidic bonds caused the formation of new amylose.

The LAB has amylolytic properties that produce amylase and pullulanase enzymes. These enzymes hydrolyze starch. The release of amylopectin by pullulanase enzyme produces a straight-chain glucose polymer, which is amylose with a smaller degree of polymerization (Asha *et al.*, 2013). This pullulanase enzyme can be used to degrade glycosidic α-1,6 branch bonds to amylopectin and produce high amylose (Chen *et al.*, 2010).Microbes that produce pullulanase enzyme can break down high amounts of amylopectin into simple sugars, resulting in higher amylose concentrations of flour (Akbar and Yunianta, 2014).

Low amylose content in porang flour and high protein content in eggs cause the gel structure to form weakly. Additionally, these conditions cause higher dissolved solids, stickiness, and inelasticity in dry noodles. Amylose plays an important role in the gelatinization process and the character of starch paste (Rahim, 2007).

Physical properties

Rehydration

The rehydration of noodles ranged from 114.56% to 120.46%. The proportions of modified cocoyam flour of 90% and porang flour of 10% with the egg addition of 5% produced the lowest rehydration (114.56%) whereas the proportions of modified cocoyam flour of 80% and porang flour of 20% with the egg addition of 15% produced the highest rehydration (120.46%). The relationship of the proportions of modified cocoyam flour, porang flour as well as the addition of eggs to the rehydration of dry noodles is presented in Table 3.

The less proportion of modified cocoyam flour, the more proportion of porang flour, and the addition of eggs increased the rehydration of noodles (Table 3). These conditions show that porang flour contains glucomannan, which has high water absorption properties. Similarly, the addition of more eggs increased rehydration. It is indicated by lecithin in egg yolks that are hydrophilic. Moreover, the addition of eggs causes higher water absorption.

Lambrecht *et al*. (2014) reported that lecithin in egg yolks have polar and nonpolar groups. The polar group contains phosphate ester, which is hydrophilic and tends to dissolve in water. The nonpolar group contains fatty acid ester, which is lipophilic and tends to dissolve in fat or oil. It is supported by a previous study (Winarno, 2004) that reported that the use of eggs for non-gluten noodles accelerate hydration time. The presence of polar and nonpolar groups of egg yolk determines the water absorption rate and noodles' elasticity.

A previous study (Chan, 2011) revealed that porang flour has a high content of glucomannan. It absorbs up to 200 times of water and inhibits syneresis. Water-soluble polysaccharides increase the water absorption capacity of the product. Therefore, increased proportion of porang flour increases the rehydration of noodles (Faridah and Widjanarko, 2014). Glucomannan comprises monomer α,β-1,4-mannose and α-glucose. Glucomannan in ilesiles tubers strengthens the gel, improves texture, and increases thickness (Sande *et al.*, 2009).

The rehydration of dry noodles with cocoyam flour and the addition of mung bean flour ranged from 138.26% to 145.01% (Kartini and Widya, 2018). Difference in the rehydration of dry noodles is caused by different starch content, protein content, and processing activities.

Cooking loss

The cooking loss value ranged from 8.22% to 9.58%. The proportions of modified cocoyam flour of 90% and porang flour of 10% with the egg addition of 15% produced the lowest cooking loss value (8.22%) whereas the proportions of modified cocoyam flour of 90% and porang flour of 10% with the egg addition of 5% produced the highest cooking loss value (9.58%). The relationship

Table 3. Rehydration, cooking loss, and elasticity of each composition of modified cocoyam flour and porang flour with addition of egg.

Formula composition				
Modified cocoyam flour and porang flour (%)	Egg (%)	Rehydration (%)	Cooking loss (%)	Elasticity (%)
90:10	5	$114.56^{a} \pm 0.11$	$9.35^{a} \pm 0.04$	$9.30^{a} \pm 0.11$
	10	$115.29^{b} \pm 0.18$	$8.72^{b} \pm 0.02$	$10.47^{b} \pm 0.12$
	15	$115.86^{c} \pm 0.07$	$8.22^{b} \pm 0.02$	$11.50^{c} \pm 0.35$
85:15	5	$116.38^{d} \pm 0.15$	$9.47^{c} \pm 0.11$	$10.43^{b} \pm 0.14$
	10	$117.64^{e} \pm 0.14$	$8.75^{c} \pm 0.01$	$11.67^{c} \pm 0.08$
	15	$117.91^{f} \pm 0.08$	$8.39^{c} \pm 0.02$	$12.70^{d} \pm 0.30$
80:20	5	$118.35^{g} \pm 0.13$	$9.58^{d} \pm 0.03$	$13.74^{e} \pm 0.18$
	10	$119.44^{h} \pm 0.20$	$8.76^{e} \pm 0.01$	$13.85^{e} \pm 0.09$
	15	$120.46^{i} \pm 0.07$	$8.43^{f} \pm 0.01$	$14.66^{f} \pm 0.25$

of the proportions of modified cocoyam flour, porang flour as well as the addition of eggs to the cooking loss of noodles is presented in Table 3.

Our results demonstrated that the less proportion of modified cocoyam flour, the more proportion of porang flour, and the addition of eggs increased the value of cooking loss. It was due to less amount of amylose in porang flour. However, addition of more egg decreased the cooking loss value. It was due to the presence of protein in eggs that made dough more compact.

Porang flour has lower amylose content (19.74%) than modified cocoyam flour (22.77%). Setyani *et al.* (2017) stated that the loss of solids because of cooking loss in noodles is influenced by the presence amylose content in the raw materials used. The higher the amylose content, the stronger the gel structure formed. Therefore, the smaller total loss of solids happens in noodle strands during the cooking process.

Owing to the addition of eggs, the higher value of cooking loss decreased in non-gluten dry noodles. It was due to egg protein enhancing the noodle mixture compact and reducing water turbidity during cooking. Reza *et al*. (2008) stated that the higher the level of egg concentration added, the less the cooking loss in dried noodles, because eggs make the dough compact. If the noodle mixture is more compact, less solid is lost during cooking. Eggs use in gluten-free products reduces cooking loss (Jayadi, 2019). Egg protein (albumin) produces a thin and strong layer on the surface of noodles. The coating is effective in reducing water turbidity during cooking. The higher cooking loss resulted in more undesirable dry noodle products. A higher cooking loss causes water turbidity during cooking and the noodles leave a feeling of stickiness in the mouth (Uba'idillah, 2015).

Elasticity

The elasticity of noodles ranged from 9.30% to 14.66%. The proportions of modified cocoyam flour of 90% and porang flour 10% with the egg addition of 5% produced the lowest elasticity value (9.30%) whereas the proportions of modified cocoyam flour of 80% and porang flour of 20% with the egg addition of 15% produced the highest elasticity value (14.66%). Table 3 presents the relationship of the proportions of modified cocoyam flour, porang flour as well as the addition of eggs to the noodles elasticity.

Our results showed that the less proportion of modified cocoyam flour, the more proportion of porang flour, and the addition of eggs increased noodles' elasticity (Table 3). Porang flour contains glucomannan compounds, which form an elastic gel to hold water strongly. Similarly, the addition of eggs increased noodles' elasticity. Egg white forms a strong layer or strong adhesion and enhances the texture of dry noodles.

Moreover, the less proportion of modified cocoyam flour the more proportion of porang flour result in the higher elasticity of noodles. This is because porang flour contains glucomannan compounds, which form an elastic gel and hold water. The formation of hydrocolloid gel occurs due to the formation of a mesh or a three-dimensional gel matrix network by a primary molecule. The primary molecule extends to the entire volume of gel formed by trapping an amount of water, thus making noodles' texture more elastic (Winarno, 2004). The gel in porang flour contains 99.90% water and has special properties such as solidity and especially elasticity.

The elasticity of noodles prepared from kimpul flour, tapioca, and tempeh flour ranged from 20.00% to 43.33% (Kustanti *et al*., 2013). The difference in the elasticity

value of dry noodles was due to the content of amylose, amylopectin, and binder in different flours. Additionally, different processing activities cause differences in elasticity.

Organoleptic test

Table 4 shows the mean organoleptic value of dry noodle products. Our results showed that the proportion of modified cocoyam flour and porang flour (90%:10%) with the egg addition of 10% produced dry noodles with the highest level of color preference (brown). Additionally, the proportion of modified cocoyam flour and porang flour (90%:10%) with the egg addition of 15% produced dry noodles with the lowest level of color preference (blackish brown).

The color of dry noodles was brown to blackish brown, obtained from the modified cocoyam flour and porang flour. The color of cocoyam flour was white whereas the porang flour was brown. An increase in the proportion of porang flour decreased the level of panelist acceptance of color in dry noodles. The color change in dry noodles occurred because of the addition of porang flour; hence, if more proportion of porang flour was added, then the color of the dry noodles produced increasingly turned brown. Porang flour color tends to be brown, and if applied to the product, a darker color is produced (Sumarwoto, 2007). Hence, the addition of more porang flour produced less liked colors.

Table 4 shows that the panelists liked the aroma of noodles prepared with the modified cocoyam flour and porang flour formulation (90%:10%) with the egg addition of 5%. Owing to the 15% addition of egg, the aroma of noodles produced with the modified cocoyam flour and porang flour formulation (80%:20%) was similar to that of porang. Porang flour is light brown with a distinctive odor like that of a fish; hence, with a higher proportion of porang flour, the noodles smell fishier (Sumarwoto, 2005).

Moreover, the panelists' preference for the taste of noodles tended to be high in the proportion of modified cocoyam flour and porang flour (90%:10%) with the egg addition of 5%, which was 153.5% (Table 4). The taste of dry noodles tended to decrease with the addition of more eggs (Biyumma *et al.*, 2017). The use of eggs caused a savory taste to noodles due to the presence of lecithin in egg yolk, but the panelists did not like the excessive use of eggs because it made noodles too rancid (a fishy smell).

As shown in Table 4, the level of texture preference for dry noodles was obtained from the proportion of modified cocoyam flour and porang flour (85%:15%). Moreover, the egg addition of 5% was the most preferred composition to meet the preference of consumers. The higher proportion of porang flour and eggs decreased the preference level of panelists for the texture of dry noodles.

Starch has a high amylose content and hydrogen bond strength because of the large number of straight chains in granules. Therefore, it requires more energy for gelatinization and making the noodles chewier (Smith, 1982). Since porang flour has a low amylose content (19.7%), its addition to dry noodles reduces the texture value. Additionally, the more the proportion of porang flour and eggs used, the higher the softness of noodles that have been rehydrated.

The level of softness of dry noodles is determined by the presence of glucomannan hydrocolloids in porang flour. It absorbs up to 200 times water of its weight. An increase in porang flour increases the noodle water content and produces softer noodles (Citra *et al.*, 2012).

Egg yolk causes more water absorption. Additionally, egg white has crystallization control power because of albumin. It prevents water evaporation and makes the dough softer

Table 4. Organoleptic values.

Formula composition		Score			
Proportion of modified cocoyam flour and porang flour (%)	Egg addition (%)	Color	Aroma	Taste	Texture
90:10	5	3.28	3.08	3.12	3.16
	10	3.28	3.00	2.96	3.04
	15	3.04	2.64	2.72	2.68
85:15	5	3.20	3.04	3.04	3.12
	10	3.20	2.96	3.00	3.04
	15	2.76	2.60	2.52	2.72
80:20	5	3.00	3.00	2.88	2.88
	10	2.96	2.88	2.68	2.76
	15	2.48	2.48	2.56	2.52

with higher moisture (Risti and Arintina, 2013). Both of these properties might lead to the usage of additional eggs, resulting in softer dry noodles, which the panelists disliked.

Conclusion

The proportion of modified cocoyam flour to porang flour determined the texture of non-gluten noodles. The high content of amylose induced a degrading enzyme activity during fermentation. It led to the breakdown of the amylopectin branch chain in α-1,6 glycosidic bond, resulting in new amylose and noodles texture. The best chemical, physical, and organoleptic parameters were obtained for noodles produced with 85:15 modified cocoyam flour and porang flour formulation with 10% egg addition. This formulation was chosen based on the organoleptic tests which were quite good (most preferred) than all other compositions.

Acknowledgments

The authors sincerely thank the Ministry of Research, Technology and Higher Education, the Republic of Indonesia through the competency-based research programs and Research and Community Service Institutions, Universitas Pembangunan Nasional Veteran East Java, Surabaya, Indonesia

References

Agustia F.C., Subardjo Y.P., and Ramadhan G.R. 2019. Development of mocaf-wheat noodle product with the addition of catfish and egg-white flours as an alternative for high-animal-protein noodles. J Aplikasi Teknologi Pangan. 8(2):47–51. https://doi.org/10.17728/jatp.2714

Akbar M.R. and Yunianta. 2014. Effect of $Na_2S_2O_5$ soaking time and yeast fermentation tape on physical properties of corn flour chemical. J Food Agro Ind. 2(2):91–102.

Akonor P.T., Tortoe C., Buckman E.S., and Hagan L. 2017. Proximate composition and sensory evaluation of root and tuber composite flour noodles. Cogent Food Agr. 3(1):1–7. https://doi.org/10.1080/23311932.2017.1292586

Ambarwati E., Murti R.H., Haryadi, Basyir A., and Widodo S. 2000. Exploration and characterization of Iles-iles research report LP Gadjah Mada University in collaboration with PAATP Balitbangtan Yogyakarta. Yogyakarta, Indonesia.

Andriani T., Djaelani M.A., and Saraswati T.R. 2015. Proximate levels of Pengging duck eggs, Tegal ducks, Magelang ducks in Balai Pembibitan dan Budidaya Ternak Non Ruminansia (BPBTNR), Ambarawa. J Biol. 4(3):8–15.

Arifin M.A. 2001. Mechanical drying of iles-iles tubers to improve the quality of iles-iles chips. Thesis, Bogor Agriculture Institute, Bogor, Indonesia.

Aryanti N. and Abidin K.Y. 2015. Glucomannan extraction from local porang (*Amorphophallus oncophyllus* and *Amorphophallus muerelli* Blume). Metana. 11(1):21–30.

Asha R., Niyonzima F.N., and Sunil S.M. 2013. Purification and properties of vpullulanase from Bacillushalodurans. Int Res J Biol Sci. 2:35–43.

Association of Official Agricultural Chemists (AOAC). 2004. Official method of analysis, 12th ed. AOAC, Washington, DC.

Astawan M. 2008. Instant noodle making technology. Gramedia, Jakarta, Indonesia.

Biyumma U.L., Wiwik S.W., and Nurud D. 2017. Characteristics of dry noodles made from breadfruit flour (*artocarpus altilis*) and egg addition. J Agrotechnol. 11(1):23–34.

Boakye A.A., Wireko-Manu F.D., Oduro I., Ellis W.O., Gudjónsdóttir M., and Chronakis I.S. 2018. Utilizing cocoyam (*Xanthosoma sagittifolium*) for food and nutrition security: a review. Food Sci Nutr. 6(4):1–11. https://doi.org/10.1002/fsn3.602

Chan A.P.N. 2011. Konjac part I: cultivation to commercialization of components. The World of Food Science, IFT Foundation and IUFoST Organisation Ontario, Canada.

Charoenrein S., Tatirat O., Rengsutthi K., and Thongngam M. 2011. Effect of konjac glucomannan on syneresis, textural properties and the microstructure of frozen rice starch gels. Carbohyd Polym. 83:291–296. https://doi.org/10.1016/j.carbpol.2010.07.056

Chauhan D., Kumar K., Kumar S., and Kumar H. 2018. Effect of incorporation of oat flour on nutritional and organoleptic characteristics of bread and noodles. Cur Res Nutr Food Sci. 6(1):148–156. https://doi.org/10.12944/CRNFSJ.6.1.17

Chen L., Zan Q., Mingguang L., Shen J., and Liao W. 2010. Litter dynamics and forest structure of the introduced sonneratia caseolaris mangrove forest in Shenzhen, China. Estuar Coast Shelf Sci. 85(2):241–246. https://doi.org/10.1016/j.ecss.2009.08.007

Citra P.U., Sukma A., and Haryani K. 2012. Utilization of Iles (*Amorphophallus ochophyllus*) as a chewing agent in tofu making. J chem Technol Ind. 1(1):78–85.

Diniyah N., Denik S., Wiwik S.W., and Achmad S. 2017. Characteristics of mojang noodles (mocaf-corn) with different types and concentrations of binding materials. J Agr Postharv Res. 14(2):98–107. https://doi.org/10.21082/jpasca.v14n2.2017.98-107

Faridah A. and Widjanarko S.B. 2014. Addition of porang flour to noodle making with mocaf flour substitution (modified cassava flour). J Food Technol Ind. 25(1):98–105. https://doi.org/10.6066/jtip.2014.25.1.98

Faridah A., Wijanarko S.B., Sutrisno A., and Susilo B. 2012. Optimization of porang flour production mechanically from chip porang with response surface methods. J Ind Eng. 13(2):158–166. https://doi.org/10.22219/JTIUMM.Vol13.No2.158-166

Hidayat N., Padaga M.C., and Suhartini S. 2007. Industrial microbiology. Atmajaya University, Yogyakarta, Indonesia.

International Rice Research Institute (IRRI). 1978. Standard evaluation system for rice. IRRI, Los Banos, the Philippines.

Jayadi A.R. 2019. Physical quality characteristics of corn noodles by adding emulsifiers and eggs. Thesis, Bogor Agriculture Institute, Bogor, Indonesia.

Kartini A.Z. and Widya D.R.P. 2018. Effect of concentration of eggs and carboxymethyl cellulose on physical, chemical and

organoleptic characteristics of fermented dry noodles of jali flour (Coix Lacrymal Jobi-L). J Food Agro Ind. 6(2):52–62. https://doi.org/10.21776/ub.jpa.2018.006.02.6

Kilara A. 1994. Whey protein functionally in food systems. Marcel Dekker, New York.

Kumoro A., Yuganta T., Retnowati D., and Ratnawati R. 2018. Acid hydrolysis and ethanol precipitation for glucomannan extraction from crude porang (*Amorphophallus onchophyllus*). Tuber Flour Chem Chem Technol. 12(1):101–108. https://doi.org/10.23939/chcht12.01.101

Kustanti I.H., Astutik P., Sulistiastutik, and Theresia P. 2013. Substitution of belitung taro paste, soy tempe flour and tapioca flour in making wet noodles for patients with diabetes mellitus. Department of Health, Nutrition Polytechnic, Kemenkes Malang, Malang, Indonesia.

Lambrecht M.A., Rombouts I., Nivelle M.A., and Delcour J. A. 2017. The role of wheat and egg constituents in the formation of a covalent and non-covalent protein network in fresh and cooked egg noodles. J Food Sci. 82(1):2435. https://doi.org/10.1111/1750-3841.13558

Muchtadi T., Sugiyono, and Fitriyono A. 2010. Food science. CV Alfabeta, Bandung, Indonesia.

Nugraheni B. and Puspitaningrum I. 2013. Potential bulbs porang (*Amorphophallus konjac* k. Koch.) as nutrasetikal against hepatoprotective effects and histopathological picture liver male rats wistar strain induced by paracetamol. Research Report, STIFAR Semarang, Indonesia.

Pratama I.A. and Fithri C.N. 2014. Dry noodle formulation with cocoyam flour substitution (*Xanthosoma sagittifolium*) and addition of green bean flour (Phaseolus radiatus L.). J Food Agro Ind. 2(4):101–112.

Prayitno S.A., Agustini M., and Wulandari U. 2020. The socialization of yam noodles making without food preservatives at the health pioneer in Nganjuk district. Kontribusia. 3(1):xxx. https://doi.org/10.30587/kontribusia.v3i1.1059

Rahim A. 2007. Effect of method of processing instant starch noodle from aren starch on physical and sensory properties. Thesis, Gadjah Mada University, Yogyakarta, Indonesia.

Ramlah. 1997. Physical properties of noodle dough and several types of wheat with the addition of kansui, eggs and cassava. Thesis, Gajah Mada University, Yogyakarta, Indonesia.

Retnaningsih C.H. and Hartayani L. 2005. Application of Iles-iles flour (*Amorphophallus konjac*) as a substitute for the chemical thickening of wet noodles: judging from the physical and chemical properties of sensors beginner research program. Research Report, Faculty of Agricultural Technology, Soegijapranata Catholic University Semarang, Semarang, Indonesia.

Reza G.M., Yanti M.L., and Yuliani A. 2018. Making dried noodles from taro flour (*Xanthosoma sagittifolium*) with the addition of carrageenan and eggs. Unsyiah Agr Student Sci J. 3(1).

Rhim J.W. and Wang L.F. 2013. Mechanical and water barrier properties of agar/κ-carrageenan/konjac glucomannan ternary blend biohydrogel films. Carbohyd Polym. 96(1):71–81. https://doi.org/10.1016/j.carbpol.2013.03.083

Risti Y. and Arintina R. 2013. Effect of egg addition on protein, fiber levels, hardness and acceptance of gluten-free wet noodles made from composite flour (composite mocaf, tapioca and meizena flour). J Nutr College. 2(4):696–703. https://doi.org/10.14710/jnc.v2i4.3833

Rosida D.F., Angeline S.Y.C., Happyanto D.C., and Hapsari N. 2020. The effect of fermentation on physicochemical properties of Cocoyam (Xanthosoma sagittifolium) flour using L. plantarum bacteria. Eurasia J Biosci. 14(2):3951–3955. http://www.ejobios.org/article/the-effect-of-fermentation-on-physicochemical-properties-of-cocoyam-xanthosoma-sagittifolium-flour-8032

Rozali Z.F., Zulmalisa Z., Sulaiman I., Lubis Y.M., Noviasari S., Eriani K., and Asrizal C.W. 2021. Decreased of calcium oxalate levels in the purple taro flour (*Colocasia esculenta*) from Aceh Province, Indonesia using three immersion methods. IOP Conf. Ser Earth Environ Sci. 711:1–17. https://doi.org/10.1088/1755-1315/711/1/012022

Saha D. and Bhattacharya S. 2010. Hydrocolloids as thickening and gelling agents in food: a critical review. J Food Sci Technol. 47(6):587–597. https://doi.org/10.1007/s13197-010-0162-6

Sande M., Teijeiro-Osorio D., Remuñán-López C., and Alonso M.J. 2009. Glucomannan, a promising polysaccharides for biopharmaceutical purposes. Eur J Pharm Biophar. 72(2):453–462. https://doi.org/10.1016/j.ejpb.2008.02.005

Sari M.C. 2017. Characteristics of gluten-free cookies and casein (study of the proportion of corn flour: pedada flour and egg yolk addition). Thesis, UPN Veteran Jawa Timur Surabaya, Surabaya, Inodonesia.

Setyani S., Sussi A., and Florentina. 2017. Substitution of corn tempe flour in making wet noodles. J Ind Technol Agri Prod. 22(1):1–10.

Smith P.S. 1982. Starch derivatives and their uses in foods. In: Lineback dan D.R. and Inglett G.E. (eds.), Food carbohydrate. AVI, Westport, CT.

Subagio A. 2008. Industrialization of modified cassava flour (MOCAF) as food industry raw materials to support national food diversification. Thesis, University of Jember, Jember, Indonesia.

Subarna and Muhandri T. 2013. Corn noodle processing using calendaring method. J Tech Food Ind. 24(1):xxx. https://doi.org/10.6066/jtip.2013.24.1.75

Sudarmadji S., Haryono B., and Suhardi. 1997. Analysis procedures for food and agriculture materials liberty. Yogyakarta, Indonesia

Sumarwoto S. 2005. Iles-iles (*Amorphophallus muelleri* Blume) description and other properties. Biodiversity. 6(3):185–190. https://doi.org/10.13057/biodiv/d060310

Sumarwoto S. **2007.** Review: Constituen of mannan of iles-iles (Amorphophallus muelleri Blume.) Asian J Trop Biotechnol. 4(1):28–32. https://doi.org/10.13057/biotek/c040105

Supriyadi D. 2012. Study of the effect of amylose-amylopectin ratio and moisture on crackiness and hardness of fried products model. Thesis, Bogor Agriculture Institute, Bogor, Indonesia.

Uba'idillah A. 2015. Chemical physical characteristics of dry noodles from wheat flour in the modified gadung flour substitution. Thesis, Jember University, Jember, Indonesia.

Wang C., Xu M., Lv W.P., Qiu P., Gong Y., and Li S. 2012. Study on rheological behaviour of Konjac glucomannan. J Phy Procedia. 33:25–30. https://doi.org/10.1016/j.phpro.2012.05.026

Widaningrum W.S. and Soekarto S.T. 2005. Enrichment of soybean flour in making wet noodles with raw materials substituted by Garut flour. J Pascapanen. 2(1):41–48.

Widjanarko S.B. and Megawati J. 2015. Analysis of the colorimetric and gravimetric methods of measuring glucomannan levels in Konjac (*Amorphophallus konjac*). J Food Agro Ind. 3(4):1584–1588.

Winarno F.G. 2004. Food chemistry and nutrition. Gramedia, Jakarta, Indonesia.

Wulandari N., Kusnandar F., Nuraida L., Koswara S., Faridah D.N., and Kusumaningrum H.D. 2008. Guidance for integrated practicum for food processing: roasting technology. Department of Food Science and Technology of Bogor Agriculture Institute, Bogor, Indonesia.

Yan H., Cai B., Cheng Y., Guo G., Li D., Yao X., Ni X., Phillips G.O., Fang Y., and Jiang F. 2012. Mechanism of lowering water activity of konjac glucomannan and its derivatives. Food Hydrocol. 26(2):383–388. https://doi.org/10.1016/j.foodhyd.2011.02.018

Yang X.H., Zhu W.L., and Yan J.F. 2006. A time temperature rheological study of konjac glucomannan hydrocolloid. J Biomater Sci. 17(1–2):53–59. https://doi.org/10.1163/156856206774879063

Italian Journal of Food Science, 2022; 34 (1): 24–32

Effect of extraction process and storage time on the quality attributes of pomegranate juice of two local pomegranate varieties

Amal N. Alkuraieef, Amani AlJahani*

Department of Physical Sport Science, College of Education, Princess Nourah bint Abdulrahman University, Riyadh, Saudi Arabia

***Corresponding Author**: Amani Al-Juhani, Department of Physical Sport Science, College of Education, Princess Nourah bint Abdulrahman University, P.O. Box 84428, Riyadh 11671, Saudi Arabia. Email: ahaljahani@pnu.edu.sa

Received: 8 November 2021; Accepted: 30 December 2021; Published: 28 January 2022

PAPER

Abstract

This study investigates the impact of two extraction processes (squeezing the whole fruit and centrifuging the seeds) of pomegranate juice and storage on sweet and sour pomegranate quality attributes. The pH, acidity, and levels of organic acids, sugars and anthocyanin differed in both varieties and changed during the storage period. Fructose and glucose were the primary sugars, and citric acid was the dominant organic acid in the juice of both cultivars. A high level of established anthocyanin content was 15.40, 18.53, 18.03, 16.92, 16,68 and 15.47 mg/L when the storage period was 0, 5, 15, 32, 48 and 72 h, respectively, in the juice of sweet fruits obtained by squeezing the whole fruit. The juice prepared from the sweet fruits by squeezing method outscored, in all sensory quality attributes, the juice prepared by centrifuging process.

Keywords: anthocyanin; centrifugation of seeds; organic acids; sensory attributes; squeezing whole fruit

Introduction

Pomegranate (*Punica granatum*) fruit is known as 'miracle fruit' because of its vast food and pharmaceutical applications. The seeds are wrapped with juicy edible pulp and are consumed as food, pressed for juice production, and used as functional foods (Coronado-Reyes *et al.*, 2021; Hegazi *et al.*, 2021). Pomegranate fruit, peel, seeds and juice have high medicinal applications for treating and preventing various diseases such as inflammation, diabetes, diarrhea, obesity, dysentery, dental plaque and malaria (Ismail *et al.*, 2012). In addition, parts of pomegranate fruit are also used as food additives, functional food materials and active ingredients in nutraceutical products (Akhtar *et al.*, 2015). Pomegranate juice is a primary commercial product of pomegranate fruit with high consumer preferences because of its comprehensive nutritional and phytochemical components. It contains substantial amount of dietary polyphenols, tannins, anthocyanins and flavonoids with high potential antioxidant activities (Fahmy *et al.*, 2020). Topalović *et al.* (2021) identified among 97 phenolic compounds, 23 anthocyanins and their derivatives, 33 ellagitannins and derivatives of ellagic acid, 12 flavonols, 4 flavonol glycosides, 1 flavone, 17 hydroxybenzoic acids and 7 hydroxycinnamic acids and their derivatives. Cyanidin-3,5-diglucoside and cyanidin-3-glucoside are reported as primary anthocyanins in pomegranates (Kostka *et al.*, 2020). In addition, it was found that juice is a rich source of flavan-3-ols (2,650–9,820 mg/L), ellagitannins (2,010–6,420 mg/L) and hydroxybenzoic acids (720–3,390 mg/L) (Topalović *et al.*, 2021).

Therefore, pomegranate juice is favored as a healthy juice with great applications for treating and preventing obesity, diabetes, blood pressure and inflammation (Hegazi *et al.*, 2021). Factors such as cultivars, maturity stage, harvest season, climatic and agronomical conditions, post-harvest processing and juice extraction processes greatly affect the nutritional and phytochemical composition of pomegranate juice (Hegazi *et al.*, 2021; Mphahlele *et al.*, 2014).

ISSN 1120-1770 online, DOI 10.15586/ijfs.v34i1.2109

Optimization of these conditions is highly important to produce pomegranate juice with good quality attributes. Juice extraction is one of the critical steps that affect its functional properties, and this step is influenced by fruit genotype and other factors (Hegazi *et al.*, 2021; Mena *et al.*, 2014).

Generally, optimal time for fruit harvest and preparation process is the factor that plays an important role in the taste acceptability of consumers. In addition, the composition of organic acids and sugars in fruit juice plays a key role in flavor and sensory characteristics, such as pH, total acidity and sweetness (Ikegaya *et al.*, 2019). To date, several extraction processes have been used such as pressing the whole fruit or fruit halves by hand presser or squeezer, peeling off the fruit and extraction of juice using pressing and centrifugation, crushing the seeds and arils using the juice blender, and quartered cut fruit and pressing using rack and cloth (Hegazi *et al.*, 2021). Of these processes, the hand pressing of fruit halves gave the highest yield of phenolic contents, anthocyanins and antioxidant activity (Mphahlele *et al.*, 2016). Crushing the whole fruit or fruit halves resulted in a bitter taste because of the extraction of more tannins in the juice (Miguel *et al.*, 2004). In addition to the extraction process, fruit type (sweet, sweet–sour and sour) affected pomegranate juice's nutritional and sensory quality attributes (Hegazi *et al.*, 2021; Mphahlele *et al.*, 2014).

In Saudi Arabia, great interest has been found in recent years in producing and consuming pomegranate juice.

Consequently, cultivation of pomegranate has increased greatly, and several genotypes are cultivated throughout the country. Sweet (*Taifi*) and sour (*Bidah*) genotypes are the primary pomegranate cultivars produced in western and southern Saudi Arabia. Today, studies on production of juice from these cultivars are scarce. Therefore, the present study was conducted to investigate the effect of juice extraction process (squeezing or centrifugation) and storage period (up to 3 days) on the quality attributes of pomegranate juice of *Taifi* and *Bidah* cultivars.

Material and Methods

Materials

The samples of sweet and sour pomegranate fruits were obtained from two different locations in Saudi Arabia. Sweet pomegranate fruits were obtained from a farm of Taif city located in western Saudi Arabia whereas sour fruits were obtained from Bidah village of southern Saudi Arabia. The samples were transferred to laboratory on the same day of harvesting under controlled conditions. After sorting of samples by removing damaged fruits and selecting the same size and maturity stage fruits, they were washed thoroughly with tap water and rinsed thrice in distilled water before extraction of juice by the two processes.

Extraction of pomegranate juice

The two processes used for the extraction of pomegranate juice from both sweet and sour fruits were as follows:

1. Peels of the fruits (10 fruits of each type) were removed manually, and the seeds were separated. The juice was extracted from the seeds using an electric centrifuge (Philips Electric HR2738/01 Citrus Press Juicer, France).
2. The fruits (10 fruits of each type) were cut with knives into two halves and squeezed using juice maker (Philips Viva Collection Juicer-HR1863, France) to obtain the juice.

The extraction processes were repeated for six times, and the resulting juice was transferred into sterilized bottles and stored in the dark at 4°C for 72 h. The samples were collected at intervals of 0, 5, 15, 32, 48 and 72 h for analyzing physicochemical properties.

Determination of acidity and pH

The acidity was measured by titrating 10-mL juice against 0.1-N NaOH, and the results were expressed as percentage of citric acid (Association of Official Analytical Chemists [AOAC], 2000). The pH was measured using digital pH meter.

Determination of organic acids

Organic acids (tartaric, citric, malic and oxalic acids) of pomegranate juice samples were analyzed using the High-performance liquid chromatography (HPLC) method as described in the AOAC (2000) standard methods with some modifications. Briefly, 10-g juice sample was centrifuged at 6,000 relative centrifugal force (RCF) for 20 min, and the supernatant was collected and filtered using 0.45-µm filters (Millipore). Then, 20-µL supernatant was injected into reverse phase (RP) column (250 × 4.6 mm) and processed using 50-mM potassium phosphate buffer and 70% methanol at a flow rate of 1 mL/min. The peaks were detected at 210 nm, identified and quantified by comparing their retention time with the authentic standards of tartaric, citric, malic and oxalic acids.

Determination of sugars

The sugar contents of pomegranate juice were analyzed using the Shimadzu HPLC system (LC-10ADVP, Shimadzu,

Kyoto, Japan) equipped with a Spherisorb 5 NH2 column (30 × 0.65 cm) and a 1530 refractive index detector (RID) (Shimadzu). Before analysis, 1-mL juice sample was centrifuged at 13,000 rpm for 20 min. The supernatant was collected and filtered using 0.45-µm Millipore filters. Then, 10-µL sample was injected into the column having a temperature of 35°C and separated using 75% acetonitrile as mobile phase at a flow rate of 1 mL/min. The sugars were identified by comparing their retention time with authentic standards run under the same conditions, and the concentration was calculated using the standard curves of sugars.

Determination of anthocyanin contents

The anthocyanin contents of pomegranate juice samples were determined using the HPLC system described in the AOAC (2000) standard method. Briefly, 1-mL juice sample was centrifuged (3,000 RCF, 20 min), and the supernatant was filtered using 0.45-µm Millipore filters. The filtrate (20 µL) was injected into a 100-RP 10 LiChroCart® column and separated using a linear gradient of 5% formic acid (A) and methanol from 15% to 35% (B) for 15 min, followed isocratic application to a total run time of 20 min. The flow rate was 1 mL/min, and the anthocyanin peaks were detected at 510 nm. The anthocyanin content of the samples was detected by comparing their retention time with that of *authentic* standard anthocyanins quantified from the standard curves generated using 0-, 0.01-, 0.02-, 0.04- and 0.08-mg/L of authentic standard.

Sensory analysis

The sensory analysis of pomegranate juice samples of sweet and sour fruits extracted by above-mentioned two processes was conducted using 20-point scaling method (0–4: unacceptable, 5–8: acceptable, 9–12: good, 13–16: very good and 17–20: excellent; Chen *et al.*, 1991). A panel comprising 30 trained staff of the College of Home Economics, Princess Nourahbint Abdulrahman University, Saudi Arabia, evaluated the color, smell, taste, texture and overall acceptance of pomegranate juice samples. The data were collected and subjected to statistical analysis.

Statistical analysis

The data of three experiments were collected and analyzed using One-Way Analysis of Variance (ANOVA). The mean was calculated using Student's *t*-test, and $p < 0.05$ was considered as statistically significant (Roscoe, 1975).

Results and Discussion

Effect of storage and extraction process on the pH and acidity of pomegranate juice

The pH and acidity values of pomegranate juice of sweet and sour varieties as affected by extraction processes and storage period are shown in Table 1.

Table 1. Effect of storage and juice production method on the pH and acidity of local sweet (*Taif*) and sour (*Bidah*) pomegranate juice.

	Storage (hours)					
Parameters	**0**	**5**	**15**	**32**	**48**	**72**
pH						
Squeezing sweet pomegranate fruit	$4.26 \pm 0.03^{a,A}$	$4.20 \pm 0.02^{a,A}$	$4.26 \pm 0.02^{a,A}$	$4.20 \pm 0.05^{a,A}$	$4.12 \pm 0.08^{a,B}$	$3.87 \pm 0.04^{a,C}$
Centrifuging sweet pomegranate seeds	$3.90 \pm 0.01^{b,A}$	$4.01 \pm 0.09^{b,A}$	$3.96 \pm 0.09^{b,A}$	$3.87 \pm 0.10^{b,A}$	$3.05 \pm 0.15^{b,C}$	$3.63 \pm 0.20^{b,B}$
Squeezing sour pomegranate fruit	$3.80 \pm 0.03^{c,A}$	$3.84 \pm 0.03^{c,A}$	$3.86 \pm 0.09^{b,A}$	$3.88 \pm 0.08^{b,A}$	$3.60 \pm 0.15^{b,B}$	$3.68 \pm 0.11^{c,B}$
Centrifuging sour pomegranate seeds	$3.60 \pm 0.06^{d,A}$	$3.66 \pm 0.05^{d,A}$	$3.60 \pm 0.05^{c,A}$	$3.67 \pm 0.029^{c,A}$	$3.44 \pm 0.05^{b,B}$	$3.50 \pm 0.07^{c,B}$
Total acidity (mg/100 mL)						
Squeezing sweet pomegranate fruit	$288.1 \pm 5.98^{c,B}$	$289.8 \pm 7.78^{c,B}$	$302.1 \pm 5.97^{c,A}$	$296.0 \pm 3.50^{c,A,B}$	$294.2 \pm 0.00^{d,A,B}$	$294.2 \pm 0.00^{d,A,B}$
Centrifuging sweet pomegranate seeds	$394.1 \pm 29.21^{b,A}$	$381.8 \pm 36.41^{b,A}$	$404.6 \pm 26.42^{b,A}$	$385.3 \pm 0.00^{b,A}$	$385.3 \pm 0.00^{c,A}$	$378.3 \pm 9.89^{c,A}$
Squeezing sour pomegranate fruit	$394.1 \pm 29.21^{b,B,C}$	$381.8 \pm 36.41^{b,B,C}$	$404.6 \pm 26.42^{b,A,B,C}$	$448.3 \pm 55.29^{a,A,B}$	$453.6 \pm 8.80^{b,A}$	$444.3 \pm 4.04^{b,A,B}$
Centrifuging sour pomegranate seeds	$449.2 \pm 16.26^{a,A}$	$453.6 \pm 23.99^{a,A}$	$452.7 \pm 24.81^{a,A}$	$458.8 \pm 4.041^{a,A}$	$462.3 \pm 5.7^{a,A}$	$462.3 \pm 13.78^{a,A}$

Means ± SD of 10 samples followed by different superscript letters are significantly different at $p < 0.05$. The small letters indicate differences in the treatments (columns), while the capital letter indicate differences in the storage time (rows).

Comparing the pomegranate types demonstrated that sweet pomegranate juice had a higher pH than that of sour juice. Similarly, a previous report indicated that sweet pomegranate varieties have higher pH values than sour varieties (Fadavi *et al.*, 2005). The pH of juice was significantly affected by the extraction process and pomegranate variety, and high pH was determined in the juice prepared by squeezed method of sweet fruit seeds, followed by that of centrifuged sweet fruit seeds, whereas the least pH was found in the juice prepared from the centrifuged sour fruit seeds ($p < 0.05$). The storage period of up to 32 h did not affect the pH of juice; however, as the storage period increased to 48 h and 72 h, the pH of both types of pomegranate juice was decreased. The change in pH during extended storage period of pomegranate fruit juice was likely due to the formation of acids because of enzymatic and microbial activities during storage. The acidity was also higher ($p < 0.05$) in juice prepared from sour pomegranate fruits than that of sweet fruits, which agreed with the previous report of the juice prepared from 10 pomegranate varieties (Fadavi *et al.*, 2005). The highest acidity and the lowest pH of pomegranate juice of sour fruit types could be due to high acid content of sour varieties (Fadavi *et al.*, 2005). In this study, the extraction process greatly influenced the acidity of juice, with the highest values being found in the juice prepared from centrifuged sour fruit seeds, followed by that of squeezed sour fruit seeds, whereas the least acidity was observed in juice prepared from squeezed sweet fruits. Again, the storage did not affect the acidity of the juice extracted by both processes of pomegranate fruits. It has been reported that the acidity of pomegranate juice obtained by centrifuging the seeds decreased after 32 h of storage whereas decrease in acidity of the juice obtained by squeezing method was less noticeable (Miguel *et al.*, 2004). Difference between the results of these studies could be due to variation in the genetic background of used pomegranate fruits.

Effect of storage and extraction process on the content of organic acids of pomegranate juice

The content of organic acids in the pomegranate juice prepared from two types of fruits and extraction processes during 72 h of storage at 4°C is presented in Table 2. Both fruit types (sweet and sour) and extraction processes (squeezing the fruit or centrifuging the seeds) affected the content of organic acids in different manners ($p < 0.05$) whereas the effect of storage period on content of organic acids was limited. Citric acid is the major organic acid in pomegranate juice. Its level was higher in the juice prepared from sour fruits than that prepared from sweet variety regardless of the extraction method, suggesting that the fruit type influenced the content of citric acid found in pomegranate juice ($p < 0.05$). Similarly, citric acid was the primary organic acid found in the juice of various pomegranate varieties, and its content was affected by these varieties as reported by other studies (Aarabi *et al.*, 2008; Türkyılmaz, 2013). Moreover, citric acid was found higher in sour cultivars than sweet ones (Ghaderi-Ghahfarokhi *et al.*, 2016). The citric acid content in sour fruit juice remained unchanged for 72 h of storage, while it was reduced to minimum values at 15 h of storage in sweet fruit juice but increased again with the progress of storage period ($p < 0.05$). Changes in citric acid during 60 days of storage differed due to variation in the fruit type, chemical changes and extraction processes used, as reported previously for various pomegranate cultivars (Aarabi *et al.*, 2008). Tartaric acid and malic acid are the second major organic acids found in pomegranate juice of different varieties, as reported by previous studies (Aarabi *et al.*, 2008). Content of tartaric acid was affected more by the extraction process than the fruit type. The highest values were observed in the juice prepared by squeezing of sweet and sour fruits ($p < 0.05$). The increased tartaric acid in the juice obtained by squeezing the whole fruits could be due to the fact that some amount of acid is found in the peels of the fruit and peeling off could lead to releasing of this amount. The storage period did not affect the tartaric acid content found in both types of pomegranate juices.

The fruit type and the extraction process also affected the content of malic acid in pomegranate juice, and a pronounced effect was observed in sour fruit juice. The highest level of malic acid was found in the juice prepared by squeezing the whole sour fruits, while the least value was found in the juice prepared from the centrifugation of sour pomegranate fruit seeds ($p < 0.05$). Variation in the content of malic acid was reported in the juice prepared from different pomegranate cultivars, suggesting the influence of cultivar on malic acid (Aarabi *et al.*, 2008; Gundogdu and Yilmaz, 2012; Türkyılmaz, 2013). Malic acid levels were gradually reduced with the storage time of the juice prepared by centrifuging the seeds of sour fruits. Decrease in malic acid during storage was likely due to its metabolism by indigenous microflora present in the juice. Decrease in the content of organic acids after pressing step was observed in pomegranate juice (Akyıldız *et al.*, 2020).

The level of oxalic acid also varied between fruit types and extraction processes of the juice, with the highest value found in the juice prepared by squeezing whole sweet pomegranate fruits, and the lowest value found in the juice prepared by centrifugation of sour fruit seeds ($p < 0.05$). Similarly, different levels of oxalic acid were reported in pomegranate juice obtained from different cultivars and by various extraction processes (Aarabi *et al.*, 2008; Gundogdu and Yilmaz, 2012; Türkyılmaz,

Table 2. Effect of storage and juice production method on the organic acids of local sweet (*Taif*) and sour (*Bidah*) pomegranate juice.

	Storage (hours)					
Parameters	**0**	**5**	**15**	**32**	**48**	**72**
Citric acid (mg/100 mL)						
Squeezing sweet pomegranate fruit	357.88 ± 65.76^{b,A,B}	354.14 ± 11.15^{b,B}	261.73 ± 9.98^{b,C}	367.57 ± 4.66^{b,A,B}	374.17 ± 9.67^{b,A}	379.32 ± 7.12^{b,A}
Centrifuging sweet pomegranate seeds	344.63 ± 6.40^{b,B}	435.10 ± 45.87^{b,A}	292.87 ± 57.08^{b,C}	369.49 ± 15.17^{b,B}	373.21 ± 20.83^{b,B}	374.31 ± 25.82^{b,B}
Squeezing sour pomegranate fruit	471.13 ± 51.66^{a,A}	476.84 ± 2.27^{a,A}	474.53 ± 3.43^{a,A}	481.34 ± 4.92^{a,A}	487.07 ± 1.363^{a,A}	484.98 ± 6.04^{a,A}
Centrifuging sour pomegranate seeds	469.36 ± 1.81^{a,A}	472.48 ± 1.45^{a,A}	477.14 ± 9.39^{a,A}	479.58 ± 7.73^{a,A}	479.48 ± 3.62^{a,A}	476.98 ± 1.40^{a,A}
Tartaric acid (mg/100 mL)						
Squeezing sweet pomegranate fruit	159.30 ± 6.69^{a,A}	185.98 ± 6.86^{a,A}	156.99 ± 7.38^{a,A}	155.11 ± 8.04^{a,A}	155.05 ± 7.13^{a,A}	154.15 ± 7.42^{a,A}
Centrifuging sweet pomegranate seeds	135.64 ± 6.12^{b,A}	134.76 ± 5.67^{b,A}	133.34 ± 6.09^{b,A}	131.93 ± 6.2^{b,A}	131.31 ± 6.02^{b,A}	129.62 ± 6.46^{b,A}
Squeezing sour pomegranate fruit	157.30 ± 0.38^{a,A}	158.79 ± 13.61^{a,A}	158.81 ± 13.58^{a,A}	152.28 ± 4.47^{a,A}	147.24 ± 0.147^{a,B}	155.32 ± 10.03^{a,A}
Centrifuging sour pomegranate seeds	133.91 ± .0.17^{b,A}	135.16 ± 0.12^{b,B}	134.87 ± 0.45^{b,B}	125.05 ± 0.28^{b,C}	124.66 ± 0.26^{b,C}	123.10 ± .0.91^{b,D}
Malic acid (mg/100 mL)						
Squeezing sweet pomegranate fruit	116.38 ± 2.16^{b,A}	116.59 ± 5.29^{a,A}	108.66 ± 11.56^{b,A}	109.34 ± 8.69^{a,A}	104.81 ± 7.87^{a,b,A}	104.75 ± 7.05^{b,A}
Centrifuging sweet pomegranate seeds	104.86 ± 10.54^{b,A}	102.35 ± 11.39^{b,A}	100.22 ± 10.95^{b,A}	97.11 ± 11.30^{b,A}	97.42 ± 9.95^{b,A}	95.28 ± 11.58^{c,A}
Squeezing sour pomegranate fruit	123.33 ± 0.57^{a,A}	122.66 ± 1.54^{a,A}	116.77 ± 0.71^{a,A}	112.61 ± 0.56^{a,B}	112.77 ± 7.24^{a,B}	123.44 ± 9.12^{a,A}
Centrifuging sour pomegranate seeds	92.77 ± 0.68^{c,A}	87.87 ± 0.46^{c,B}	88.12 ± 0.58^{c,B}	85.67 ± 0.64^{c,C}	85.15 ± 0.29^{c,C}	85.44 ± 0.81^{d,C}
Oxalic acid (mg/100 mL)						
Squeezing sweet pomegranate fruit	20.62 ± 2.61^{a,A}	20.36 ± 2.75^{a,A}	18.61 ± 2.78^{a,A}	21.91 ± 2.26^{a,A}	19.97 ± 2.25^{a,A}	20.02 ± 2.59^{a,A}
Centrifuging sweet pomegranate seeds	11.19 ± 1.41^{b,A,B}	10.61 ± 1.21^{b,A,B}	9.83 ± 0.80^{b,B}	12.06 ± 1.25^{b,A}	11.19 ± 1.08^{b,A,B}	11.47 ± 0.91^{b,A,B}
Squeezing sour pomegranate fruit	11.73 ± 0.42^{b,A,B}	11.30 ± 0.20^{b,A,B}	10.90 ± 0.86^{b,B,C}	10.64 ± 0.43^{b,C}	10.41 ± 0.59^{b,C}	12.57 ± 1.35^{b,A}
Centrifuging sour pomegranate seeds	4.33 ± 1.54^{c,C}	5.72 ± 1.61^{c,A,B}	6.45 ± 0.69^{c,A,B}	6.37 ± 0.61^{c,A,B}	5.80 ± 0.45^{c,B,C}	8.15 ± 0.54^{a,A}
Total organic acids (mg/100 mL)						
Squeezing sweet pomegranate fruit	654.18 ± 4.78^{c,A}	650.07 ± 10.81^{c,A}	454.98 ± 15.58^{c,B}	653.92 ± 4.11^{c,A}	654.00 ± 11.77^{c,A}	658.24 ± 6.6^{c,A}
Centrifuging sweet pomegranate seeds	596.32 ± 59.53^{dA}	592.81 ± 54.79^{dA}	536.25 ± 65.42$^{c\,A}$	610.59 ± 24.58^{dA}	613.13 ± 29.28^{dA}	610.68 ± 35.03^{dA}
Squeezing sour pomegranate fruit	763.49 ± 2.29^{aA}	769.60 ± 11.60^{aA}	761.00 ± 16.49^{aA}	756.87 ± 3.74^{bA}	757.48 ± 7.16^{aA}	776.30 ± 12.47^{aA}
Centrifuging sour pomegranate seeds	700.37 ± 2.48^{bB}	701.23 ± 0.69^{bB}	706.58 ± 9.04^{bB}	969.68 ± 7.62^{aA}	695.09 ± 3.33^{bB}	693.67 ± 2.34^{bB}

Means ± SD of 10 samples followed by different superscript letters are significantly different at $p < 0.05$. The small letters indicate differences in the treatments (columns), while the capital letters indicate differences in the storage time (rows).

2013). During cold storage, the oxalic acid content fluctuated except in the case of juice prepared from the whole sweet pomegranate fruits, which demonstrated no change during storage.

The highest total organic acids content was found in the juice prepared by squeezing the whole sour fruits whereas the lowest organic acids content was found in the juice obtained by centrifuging the seeds of sweet fruits.

Similarly, a higher level of organic acids was reported in the juice obtained from sour pomegranate fruits than that obtained from sweet fruits (Ghaderi-Ghahfarokhi *et al.*, 2016). Among the fruit types, the highest values of organic acids were found in the juice prepared from whole fruit, indicating that removal of peels reduced total organic acids. The content of total organic acids in pomegranate juice was not influenced by storage, except in the case of the juice prepared from whole sweet fruits, which demonstrated decrease at 15 h and then increased to the same level, and the juice prepared from sour fruit seeds, which increased to the maximum at 32 h and thereafter decreased to the initial level with progression in storage time ($p < 0.05$). The changes, i.e., increasing and decreasing trends, in the level of organic acids during storage were likely due to occurrence of different chemical and enzymatic reactions. Content of organic acids fluctuated during storage, indicating decrease in the first 15 h of storage followed by an increment with progress in storage time (Aarabi *et al.*, 2008). Variations in the levels of organic acids in pomegranate juice of different varieties and prepared by various processes have been reported in numerous studies (Aarabi *et al.*, 2008; Gundogdu and Yilmaz, 2012; Türkyılmaz, 2013). The differences in the level of organic acids of pomegranate juice among these studies were likely due to variations in the genetic makeup, growing region and conditions, season and maturity stage, cultural and post-harvest practices, processes of preparing juice, and analysis of organic acids.

Effect of storage and extraction process on the content of sugars in pomegranate juice

The content of sugars in pomegranate juice prepared from sweet and sour fruits using two extraction processes as affected by storage time is shown in Table 3. Fructose and glucose were the primary sugars found in pomegranate juice, and content of both was affected by fruit type and extraction and processing processes. Previous studies have also indicated fructose and glucose as dominant carbohydrates in pomegranate juice (Aarabi *et al.*, 2008; Fadavi *et al.*, 2005; Hasnaoui *et al.*, 2011). On 0 day of storage, the highest ($p < 0.05$) level of fructose was found in the juice prepared from seeds of sweet pomegranate fruit by centrifugation extraction, whereas the least value was observed in the juice prepared by squeezing whole sweet fruit, suggesting the influence of extraction method on the fructose content of juice. The fructose content in the juice was also affected ($p < 0.05$) by the storage time in a fluctuated manner, reaching the highest level at 15 h (juice from the seeds of sweet fruits), 32 h (juice from whole sour fruits) and 48 h (juice from whole sweet fruits and seeds of sour fruits). The increase in the content of fructose during storage could be due enzymatic hydrolysis of disaccharides and polysaccharides present in the juice. However, as the storage period extended to 72 h, chemical complexing reactions and microbial metabolism might occur, which reduced the extractability of fructose and thereby its concentration.

The content of glucose was highest in the juice obtained by centrifugation of seeds of sweet fruits ($p < 0.05$). Storage greatly affected the glucose content of the juice of both types of fruits and extraction processes. Glucose content generally increased to the maximum at 15 h (juice obtained by centrifugation process of sweet fruit seeds) and 48 h (juice of whole sweet and sour fruits and the seeds of sour fruits). The fruit type and the extraction process did not affect the total sugar level on 0 day of storage. However, as the storage time progressed, significant changes were observed in juice depending on the fruit types and extraction processes, especially at 72 h of storage, suggesting the combined effects of fruit type, extraction process and extraction time on the total sugar contents of pomegranate juice. Previous reports have also indicated that sugar content in pomegranate juice decreased at 5 h of storage and then increased as the storage time progressed to the maximum at 48 h, and reduced again by the end of storage period (Aarabi *et al.*, 2008). This was attributed to decrease in carbohydrates because of the *de novo* synthesis of anthocyanin (Aarabi *et al.*, 2008). This might be the same reason for changes in the content of sugars during storage of pomegranate juice in the present study.

Effect of storage and extraction process on the anthocyanin content of pomegranate juice

The anthocyanin content of pomegranate juice of two fruit types (sweet and sour) and two extraction processes (squeezing whole fruit and centrifuging of seeds) as affected by the storage time of the juice is shown in Table 4. The level of anthocyanin in pomegranate juice was affected by fruit type, extraction process and storage time ($p < 0.05$). The highest anthocyanin level was observed in the juice prepared from whole sweet fruits, followed by that from whole sour fruits. The least level of anthocyanin was found in the juice prepared by centrifuging of seeds of both fruit types. This could be attributed to the fact that anthocyanin is found in pomegranate fruit peels, and removing the peels reduced its content in the juice. Compared the fruit types, the highest anthocyanin content was observed in the juice prepared from whole sweet fruits than that from the whole sour ones. During storage, the anthocyanin content of the juice prepared from sweet fruits increased to the maximum at 5 h (whole fruit juice) and 15 h (seed juice). Although the anthocyanin content decreased with increase in storage time, it decreased concomitantly in the case of sour fruits with increase of storage time ($p < 0.05$). The increase in anthocyanin content

Table 3. Effect of storage and juice production method on the sugar contents of local sweet (*Taif*) and sour (*Bidah*) pomegranate juice.

	Storage (hours)					
Parameters	**0**	**5**	**15**	**32**	**48**	**72**
Fructose (g/100 mL)						
Squeezing sweet pomegranate fruit	7.22 ± 0.34^{c,C}	7.56 ± 0.58^{a,B}	7.67 ± 0.32^{b,B}	6.57 ± 1.44^{d,D}	8.82 ± 2.55^{a,A}	7.65 ± 0.34^{a,b,B}
Centrifuging sweet pomegranate seeds	7.86 ± 0.12^{a,A,B}	7.95 ± 0.08^{a,A,B}	8.10 ± 0.24^{a,A}	7.73 ± .010^{c,B,C}	7.50 ± 0.39^{a,C}	7.73 ± 0.19^{a,B,C}
Squeezing sour pomegranate fruit	7.71 ± 0.01^{b,A}	7.82 ± 0.04^{a,A}	7.94 ± 0.04^{a,b,A}	8.05 ± 0.03^{a,A}	7.88 ± 0.12^{a,A}	6.98 ± 0.81^{b,B}
Centrifuging sour pomegranate seeds	7.69 ± 0.00^{b,B}	7.68 ± 0.02^{a,B}	7.81 ± 0.02^{a,b,A,B}	7.84 ± 0.03^{b,A,B}	7.89 ± 0.04^{a,A}	7.81 ± 0.08^{a,A,B}
Glucose (g/100 mL)						
Squeezing sweet pomegranate fruit	6.93 ± 0.21^{b,A,B}	7.12 ± 0.45^{a,b,A,B}	7.37 ± 0.41^{b,A,B}	6.25 ± 1.19^{d,B}	8.66 ± 2.45^{a,A}	7.36 ± 0..20^{a,A,B}
Centrifuging sweet pomegranate seeds	7.45 ± 0.17^{a,B}	7.56 ± 0.31^{a,B}	7.98 ± 0.03^{a,A}	7.55 ± 0.09^{a,B}	7.47 ± 0.29^{a,B}	7.62 ± 0.25^{a,B}
Squeezing sour pomegranate fruit	7.07 ± 0.01^{b,C}	7.16 ± 0.03^{a,b,B}	7.32 ± 0.01^{b,A}	7.35 ± 0.03^{b,A}	7.38 ± 0.05^{a,A}	6.67 ± 0.73^{b,D}
Centrifuging sour pomegranate seeds	6.89 ± 0.01^{b,D}	6.99 ± 0.03^{b,C}	7.13 ± 0.03^{c,B}	7.16 ± 0.02^{c,B}	7.26 ± 0.03^{a,A}	7.24 ± 0.05^{a,b,A}
Total sugars (Brix)						
Squeezing sweet pomegranate fruit	16.0 ± 0.00^{a,C}	16.8 ± 0.00^{b,A}	16.5 ± 0.00 ^{b,B}	16.0 ± 0.00^{c,C}	15.0 ± 0.00^{b,D}	8.5 ± 0.00 ^{c,E}
Centrifuging sweet pomegranate seeds	16.0 ± 0.00^{a,B}	17.3 ± 0.50^{a,A}	17.0 ± 0.00^{a,A,B}	17.3 ± 0.29^{a,A}	16.5 ± 0.58^{a,A,B}	17.3 ± 0.50^{a,A}
Squeezing sour pomegranate fruit	16.0 ± 0.00^{a,B}	16.0 ± 0.50^{b,A,B}	16.0 ± 0.00^{b,B}	16.5 ± 0.00^{b,A}	16.0 ± 0.41^{a,B}	9.3 ± 1.50 ^{c,C}
Centrifuging sour pomegranate seeds	16.0 ± 0.00^{a,A}	16.0 ± 0.00^{b,A}	16.0 ± 0.00^{b,A}	16.6 ± 0.25^{b,A}	15.8 ± 0.29^{b,B}	13.1 ± 0.85^{b,C}

Means ± SD of 10 samples followed by different superscript letters are significantly different at $p < 0.05$. The small letters indicate differences in the treatments (columns), while the capital letters indicate differences in the storage time (rows).

Table 4. Effect of storage and juice production method on the anthocyanin contents of local sweet (*Taif*) and sour (*Bidah*) pomegranate juice.

	Storage (hours)					
Parameters	**0**	**5**	**15**	**32**	**48**	**72**
Alkali treatment						
Squeezing sweet pomegranate fruit	15.40 ± 0.49^{a,C}	18.53 ± 0.43^{a,A}	18.03 ± 0.20^{a,A}	16.92 ± 0.44^{a,B}	16.68 ± 0.035^{a,B}	15.47 ± 6.86^{a,C}
Centrifuging sweet pomegranate seeds	11.07 ± 1.65^{c,C}	14.32 ± 2.81^{b,A}	14.92 ± 0.07^{b,A}	14.12 ± 0.53^{b,A,B}	13.55 ± 0.68^{b,B}	12.15 ± 0.58^{a,C}
Squeezing sour pomegranate fruit	14.74 ± 0.77^{b,A}	12.79 ± 0.09^{c,B}	12.47 ± 0.08^{c,B}	11.99 ± 0.11^{c,C}	11.70 ± 0.12^{c,D}	11.11 ± 0.36^{a,E}
Centrifuging sour pomegranate seeds	9.78 ± 0.82^{c,A}	9.48 ± 1.00^{d,A}	9.15 ± 1.09^{d,A}	8.64 ± 1.14^{d,A,B}	8.32 ± 1.13^{d,A,B}	7.19 ± 0.87^{bB}
Acid treatment						
Squeezing sweet pomegranate fruit	0.56 ± 0.02^{a,B}	0.76 ± 0.11^{a,A}	0.75 ± 0.14^{a,A}	0.71 ± 0.00^{a,A}	0.70 ± 0.01^{a,A}	0.68 ± 0.01^{a,A}
Centrifuging sweet pomegranate seeds	0.34 ± 0.06^{c,B}	0.50 ± 0.00^{b,A}	0.54 ± 0.25^{b,A}	0.53 ± 0.00^{b,A}	0.54 ± 0.03^{b,A}	0.51 ± 0.05^{b,A}
Squeezing sour pomegranate fruit	0.47 ± 0.00^{b,A}	0.46 ± 0.12^{b,A}	0.45 ± 0.00^{b,A}	0.43 ± 0.00^{c,A}	0.43 ± 0.00^{c,A}	0.42 ± 0.01^{c,A}
Centrifuging sour pomegranate seeds	0.30 ± 0.00^{c,A}	0.30 ± 0.05^{c,A}	0.29 ± 0.02 ^{c,A}	0.28 ± 0.01^{d,A,B}	0.27 ± 0.01^{d,B}	0.26 ± 0.01^{d,B}

Means ± SD of 10 samples followed by different superscript letters are significantly different at $p < 0.05$. The small letters indicate differences in the treatments (columns), while the capital letters indicate differences in the storage time (rows).

at the beginning of storage (5 h and 15 h) could be due to the *de novo* synthesis of anthocyanin from carbohydrates (Aarabi *et al.*, 2008) whereas decrease in its concentration with increase in storage time could be likely due to chemical reactions and microbial metabolism. Previous studies have also demonstrated the varying levels of anthocyanin in pomegranate juice of different origins such as Tunisian (Hasnaoui *et al.*, 2011), Iranian (Alighourchi *et al.*, 2008) and Turkey (Türkyılmaz, 2013) varieties. These studies established the influence of genotypes, environmental conditions, maturity stage, post-harvest processing and juice extraction processes on the levels of anthocyanin found in pomegranate juice. In addition, similar changing trend during storage of pomegranate juice extracted by two processes (squeezing and centrifugation) was also reported by Aarabi *et al.* (2008).

Sensory attributes of pomegranate juice

The sensory attributes of pomegranate juice prepared from two local varieties (sweet and sour) using two

Table 5. Sensory attributes of local sweet (*Taif*) and sour (*Bidah*) pomegranate juice produced by two different methods and from two different types of local verities.

Treatments	Sensory attributes					
	Stability	Color	Flavor	Texture	Smell	Overall acceptance
Squeezing sweet pomegranate fruit	17.7 ± 2.78^{a}	17.5 ± 2.92^{a}	17.76 ± 2.82^{a}	17.00 ± 3.83^{a}	17.66 ± 3.06^{a}	17.96 ± 2.39^{a}
Centrifuging sweet pomegranate seeds	15.93 ± 3.03^{ab}	15.76 ± 3.6^{ab}	16.70 ± 3.14^{ab}	14.93 ± 4.20^{ab}	16.86 ± 3.54^{a}	16.26 ± 2.80^{a}
Squeezing sour pomegranate fruit	15.16 ± 3.75^{b}	14.36 ± 4.24^{b}	15.20 ± 4.12^{ab}	13.70 ± 5.03^{ab}	16.63 ± 2.97^{a}	15.26 ± 2.91^{a}
Centrifuging sour pomegranate seeds	13.50 ± 4.99^{ab}	14.53 ± 5.42^{ab}	14.13 ± 5.09^{b}	13.16± 5.65^{b}	16.36 ± 3.66^{a}	14.20 ± 4.72^{a}

Means ± SD of 10 samples followed by different superscript letters are significantly different at $p < 0.05$.

extraction processes are shown in Table 5. Generally, the juice prepared from sweet fruits outscores the one prepared from sour fruits in all sensory attributes. This is due to the above-mentioned results, which indicated the superiority of sweet pomegranate juice over sour variety considering the levels of chemical components, namely sugars, organic acids and anthocyanins. Similarly, it has been reported that the juice prepared from sweet pomegranate fruits received higher preferences than that prepared from sweet–sour and sour fruits (Mayuoni-Kirshinbaum *et al.*, 2013). The scores of overall acceptability and all sensory attributes of all juice types were higher than 13, suggesting that the panelists ranked all juice types as very good and excellent, with the highest preference to the juice prepared from whole sweet fruits and the least preference for the juice prepared from the seeds of peeled off fruits. Previous studies have demonstrated that the sensory attributes of pomegranate juice depended on the factors such as genotype, maturity, season, agronomical practices, climatic conditions and processing methods (Borochov-Neori *et al.*, 2009; Mayuoni-Kirshinbaum *et al.*, 2013; Vázquez-Araújo *et al.*, 2014). Overall, the produced juices could have high consumer acceptability regardless of the fruit type and the extraction process.

Conclusion

This study investigated the production of pomegranate juice from local varieties using two different extraction processes (squeezing whole fruit, and centrifuging fruit seeds after removal of fruit peels). The results established that the quality attributes of the produced juice were affected by genotype, extraction method and storage period at different magnitudes. The juice prepared from the sweet variety had higher pH and sensory acceptability, and lower acidity and anthocyanin level than the juice prepared from sour fruits. Concerning the processing methods, the juice prepared by squeezing the whole fruit outscore, in most of quality attributes, the juice prepared by centrifuging the seeds after removal of fruit peels. Storage duration affected the quality attributes in a fluctuated manner. Overall, squeezing unpeeled pomegranate fruit is the most economical and easy process to produce acceptable and stable juice, especially from sweet pomegranate fruits. The future studies must specifically address the effect of sterilization and long storage conditions on the quality attributes of pomegranate juice.

Acknowledgments

This research was funded by Princess Nourah bint Abdulrahman University Researchers Supporting Project Number PNURSP2022R249, Princess Nourah bint Abdulrahman University, Riyadh, Saudi Arabia.

References

Aarabi A., Barzegar M., and Azizi M.H. 2008. Effect of cultivar and cold storage of pomegranate (*Punica granatum* L.) juices on organic acid composition. ASEAN Food J. 15(15): 45–55.

Akhtar S., Ismail T., Fraternale D., and Sestili P. 2015. Pomegranate peel and peel extracts: chemistry and food features. Food Chem. 174: 417–425. https://doi.org/10.1016/j.foodchem.2014.11.035

Akyıldız A., Karaca E., Ağçam E., Dündar B., and Çınkır N.I. 2020. Changes in quality attributes during production steps and frozen-storage of pomegranate juice concentrate. J Food Compos Anal. 92: 103548. https://doi.org/10.1016/j.jfca.2020.103548

Alighourchi H., Barzegar M., and Abbasi S. 2008. Anthocyanins characterization of 15 Iranian pomegranate (*Punica granatum* L.) varieties and their variation after cold storage and pasteurization. Eur Food Res Technol. 227: 881–887. https://doi.org/10.1007/s00217-007-0799-1

Association of Official Analytical Chemists (AOAC). 2000. Official methods of analysis. 17th ed. AOAC, Gaithersburg, MD.

Borochov-Neori H., Judeinstein S., Tripler E., Harari M., Greenberg A., Shomer I., and Holland D. 2009. Seasonal and cultivar variations in antioxidant and sensory quality of pomegranate (*Punica granatum* L.) fruit. J Food Compos Anal. 22: 189–195. https://doi.org/10.1016/j.jfca.2008.10.011

Chen J., Serafin F.L., Pandya R.N., and Daun H. 1991. Effects of extrusion conditions on sensory properties of corn meal extrudates. J Food Sci. 56: 84–89. https://doi.org/10.1111/j.1365–2621.1991.tb07981.x

Coronado-Reyes J.A., Cortés-Penagos C.D.J., and González-Hernández J.C. 2021. Chemical composition and great applications to the fruit of the pomegranate (*Punica granatum*): a review. Food Sci Technol. 2021: 1–8. https://doi.org/10.1590/fst.29420

Fadavi A., Barzegar M., Azizi M.H., and Bayat M. 2005. Note. Physicochemical composition of ten pomegranate cultivars (*Punica granatum* L.) grown in Iran. Food Sci Technol Int. 11: 113–119. https://doi.org/10.1177/1082013205052765

Fahmy H., Hegazi N., El-Shamy S., and Farag M.A. 2020. Pomegranate juice as a functional food: a comprehensive review of its polyphenols, therapeutic merits, and recent patents. Food Funct. 11: 5768–5781. https://doi.org/10.1039/d0fo01251c

Ghaderi-Ghahfarokhi M., Barzegar M., and Nabil M. 2016. Geographical discrimination of Iranian pomegranate cultivars based on organic acids composition and multivariate analysis. J Agr Sci Tech. 18: 1221–1232. http://hdl.handle.net/123456789/3788

Gundogdu M. and Yilmaz H. 2012. Organic acid, phenolic profile and antioxidant capacities of pomegranate (*Punica granatum* L.) cultivars and selected genotypes. Sci Hortic. 143 38–42. https://doi.org/10.1016/j.scienta.2012.05.029

Hasnaoui N., Jbir R., Mars M., Trifi M., Kamal-Eldin A., Melgarejo P., and Hernandez F. 2011. Organic acids, sugars, and anthocyanins contents in juices of Tunisian pomegranate fruits. Int J Food Prop. 14: 741–757. https://doi.org/10.1080/10942910903383438

Hegazi N.M., El-Shamy S., Fahmy H., and Farag M.A. 2021. Pomegranate juice as a super-food: a comprehensive review of its extraction, analysis, and quality assessment approaches. J Food Compos. Anal. 97: 103773. https://doi.org/doi: 10.1016/j.jfca.2020.103773

Ikegaya A., Toyoizumi T., Ohba S., Nakajima T., Kawata T., Ito S., and Arai E. 2019. Effects of distribution of sugars and organic acids on the taste of strawberries. Food Sci. Nutr. 7: 2419–2426. https://doi.org/10.1002/fsn3.1109

Ismail T., Sestili P., and Akhtar S. 2012. Pomegranate peel and fruit extracts: a review of potential anti-inflammatory and anti-infective effects. J Ethnopharmacol. 143: 397–405. https://doi.org/10.1016/j.jep.2012.07.004

Kostka T., Ostberg-Potthoff J.J., Briviba K., Matsugo S., Winterhalter P., and Esatbeyoglu T. 2020. Pomegranate (*Punica granatum* L.) extract and Its anthocyanin and copigment fractions-free radical scavenging activity and influence on cellular oxidative stress. Foods. 9: 1617. https://doi.org/10.3390/foods9111617

Mayuoni-Kirshenbaum L., Bar-Ya'akov I., Hatib K., Holland D., and Porat, R. 2013. Genetic diversity and sensory preference in pomegranate fruits. Fruits. 68: 517–524. https://doi.org/10.1051/fruits/2013090

Mena P., Martí N., and García-Viguera C. 2014. Chapter 18 - The impact of processing and storage on the (poly)phenolic fraction of pomegranate (*Punica granatum* L.) juices. In Processing and impact on antioxidants in beverages, Editor(s): Victor Preedy. Academic Press, San Diego, pp. 173–184.

Miguel G., Dandlen S., Antunes D., Neves A., and Martins D. 2004. The effect of two methods of pomegranate (*Punica granatum* L) juice extraction on quality during storage at 4°C. J Biomed Biotechnol. 2004: 332–337. https://doi.org/10.1155/S1110724304403064

Mphahlele R.R., Fawole O.A., Mokwena L.M., and Opara U.L. 2016. Effect of extraction method on chemical, volatile composition and antioxidant properties of pomegranate juice. S Afr J Bot. 103: 135–144. https://doi.org/10.1016/j.sajb.2015.09.015

Mphahlele R.R., Fawole O.A., Stander M.A., and Opara, U.L. 2014. Preharvest and post-harvest factors influencing bioactive compounds in pomegranate (*Punica granatum* L.)—a review. Sci Hortic. 178: 114–123. https://doi.org/10.1016/j.scienta.2014.08.010

Roscoe J.T. 1975. Fundamental research statistics for the behavioral sciences. Holt, Rinehart and Winston, New York, NY.

Topalović A., Knežević M., Gačnik S., and Mikulic-Petkovsek M. 2020. Detailed chemical composition of juice from autochthonous pomegranate genotypes (*Punica granatum* L.) grown in different locations in Montenegro. Food Chem. 330: 127261. https://doi.org/10.1016/j.foodchem.2020.127261

Topalović A., Knežević M., Ivanović L., Gačnik S., and Mikulic-Petkovsek M. 2021. Phytochemical screening of wild pomegranate (*Punica granatum* L.) juices from the market. J. Food Compost. Anal. 100: 103933. https://doi.org/10.1016/j.jfca.2021.103933

Türkyılmaz M. 2013. Anthocyanin and organic acid profiles of pomegranate (*Punica granatum* L.) juices from registered varieties in Turkey. Int J Food Sci Technol. 48: 2086–2095. https://doi.org/10.1111/ijfs.12190

Vázquez-Araújo L., Nuncio-Jáuregui P.N., Cherdchu P., Hernández F., Chambers IV, E, and Carbonell-Barrachina Á.A. 2014. Physicochemical and descriptive sensory characterization of Spanish pomegranates: aptitudes for processing and fresh consumption. Int J Food Sci Technol. 49: 1663–1672. https://doi.org/10.1111/ijfs.12472

The behavior of apricot kernel oil body and proteins during *in vitro* gastric and intestinal digestion

Aslı Kancabas Kilinc, Sibel Karakaya*

Food Engineering Department, Faculty of Engineering, Ege University, Izmir, Turkey

***Corresponding Author:** Sibel Karakaya, Food Engineering Department, Faculty of Engineering, Ege University, Izmir, Turkey. Email: sibel.karakaya@ege.edu.tr

Received: 7 October 2021; Accepted: 13 December 2021; Published: 25 January 2022

PAPER

Abstract

In this study, an apricot kernel milk suspension was prepared, for which Hacıhaliloğlu-type raw and roasted apricot kernels were used. Protein, total lipid, and ash contents of apricot kernels and apricot kernel milk were determined. Palmitic acid, oleic acid, and linoleic acid were considered as major fatty acids according to gas chromatography. During *in vitro* gastrointestinal digestion, the proteins of raw and roasted apricot kernel milk were hydrolyzed and pepsin-resistant proteins were determined. No difference was recorded between the pancreatic lipase penetration in the oil–water interface of oil bodies of both milk types.

Keywords: fatty acids; oil body; protein hydrolysis; vegetable milk; vegetable protein; waste by-products

Introduction

Currently, owing to the increasing global population and rising environmental concerns, demand for the sustainability of food and agriculture systems has been intensifying. The global consumption of meat and dairy products is projected to increase by ~173% and 158%, respectively, from 2010 to 2050 (Food and Agriculture Organization of the United Nations [FAO], 2011). In particular, considerable concerns for the production and consumption of animal protein in terms of environmental effects, such as increasing greenhouse emissions and water consumption, have caused increased interest in producing alternate sources of proteins, such as vegetable proteins, which are already present in the human diet (Fasolin *et al.*, 2019). Moreover, the current intention of consumers to include additional plant-based proteins in their daily diet requires greater knowledge about using alternative protein sources and their impact on the human health. The by-products of alternative protein sources and food wastes have considerable potential to be included in the human diet, especially those rich in protein, vitamins, minerals, fibers, oils, and bioactive compounds (Coman *et al.*, 2019; Morais *et al.*, 2015).

Apricot (*Prunus armeniaca* L.) kernels, a valuable by-product obtained from the processing of apricot plants, can have the potential to be used as a functional food ingredient to increase product differentiation and accomplishment of consumer requirements. The total production of apricots in the world is 4.3 million tons per year, and Turkey itself produces ~985,000 tons (Turkey Ministry of Agricultural and Forestry, 2020). Turkey produces 10–12% of fresh apricot and 60–65% of dried apricot in the world; moreover, ~10–20% of fresh apricot and 80–85% of dried apricot are exported throughout the world (Sığırcı *et al.*, 2015). Moreover, the apricot kernel is rich in phytochemicals, vitamins, minerals, unsaturated fatty acids (oleic acid and linoleic acid), α-, γ-, δ-tocopherols, and fibers (Al Juhaimi *et al.*, 2018; Fratianni *et al.*, 2018). Lipids found in apricot kernel are in the form of oil body, in which triglyceride particles are

coated with a stabilizing layer of phospholipids and proteins (Gallier *et al.*, 2017). The oil body is a lipid-storage compartment in plant seeds and its structure is similar to that of emulsions. In most oil seeds, oil bodies have a diameter of 0.6–2 μm, while it could be 10–20 μm in some fruits (Dave *et al.*, 2019). Owing to easy extraction, high recovery yield, and safe use in food products, plant-derived oil bodies have received considerable attention (Abdullah and Zhang, 2020). Several studies related to oil bodies from different sources have focused on their physicochemical characteristics such as droplet size, zeta (ζ) potential, emulsifying properties, and their microstructures (Dave *et al.*, 2019; Ishii *et al.*, 2017; Yan *et al.*, 2016). However, few studies have investigated the behavior of oil bodies from different sources, including almond oil bodies, bovine milk fat globules, and sunflower oilseed bodies during *in vitro* digestion (Gallier *et al.*, 2012, 2013; Mandalari *et al.*, 2008; Wang *et al.*, 2020; White *et al.*, 2008). Certain studies have focused on the occurrence, structure, and allergenicity of oil bodies (Barre *et al.*, 2018), the possibility of oil bodies derived from a plant source with unique facilities that could be used as an alternative to milk fat globules (Mantzouridou *et al.*, 2019), the extraction, isolation, and characterization of oil bodies (Zderic *et al.*, 2016), and the effects of food processing, such as roasting, sterilization, and high-pressure homogenization, on oil bodies (Yan *et al.*, 2016; Zaaboul *et al.*, 2019).

Protein contents determined in various types of apricot kernels are reported as 15.1–24.2% (Gezer *et al.*, 2011). Moreover, proteins determined in apricot kernels contain high levels of tyrosine, cysteine, methionine, aspartic acid, glutamic acid, serine, proline, and alanine (Elkot *et al.*, 2017). Owing to this valuable composition, especially protein and fat contents, the apricot kernel could be considered as a functional food or functional food ingredient. However, for the food industry, only a small amount of apricot kernel is consumed as nuts and a large amount is a waste by-product. Therefore, in spite of having a considerable industrial potential, lack of systematic collection and utilization has led to the lack of exploitation of this valuable product. The primary concern is amygdalin, a cyanogenic glycoside, contained in the kernels and seeds of apples, apricots, almonds, cherries, plums, and peaches (Mirzaei and Razei, 2019). Karsavuran *et al.* (2015) reported that the amount of amygdalin in sweet Hacıhaliloğlu-type apricot seeds was 0.25 mg/g and the predicted amount of hydrogen cyanide was 0.014 mg/g. With this amygdalin level, approximately 800-g seed would have to be ingested to cause poisoning of a child weighing 20 kg. However, this amount that causes poisoning in a child weighing 20 kg was very low for bitter apricot seeds (i.e., for Paviot-type, 4.48-g seeds; for Alyanak-type, 6.29-g seeds; and for Ninfa-type apricot, 12.87-g seeds).

In recent years, rather than dairy products, plant-based food alternatives, such as vegetable milk extracted from soy, almond, rice, and oats, have increased. The beverage obtained from apricot kernel could be a good alternative. Generally, studies related to apricot kernel as a functional food ingredient were based on foods added with apricot kernel. Elkot *et al.* (2017) produced stirred yogurt supplemented with apricot kernel powder and reported an increase in the protein content of yogurt. Eyidemir and Hayta (2009) incorporated apricot kernel flour into the noodle and indicated the increased contents of protein, lipid, and ash in the noodle.

To our knowledge, the possibility of extracting vegetable milk from apricot kernel has not been studied to date. In addition, the physicochemical characteristics of oil bodies and proteins of apricot kernel and their behavior during *in vitro* gastrointestinal digestion have not been explored. As most apricot kernels are waste by-products, converting them into value-added products would be beneficial in terms of both waste utilization and human health. Therefore, in order to explore certain physicochemical properties of oil bodies and proteins, protein profile and protein hydrolysis during *in vitro* gastrointestinal digestion are substantial.

The objectives of this study are to: characterize certain physicochemical properties of oil bodies and proteins of apricot kernel milk, understand their behavior during *in vitro* gastrointestinal digestion, evaluate the effect of microstructure on the physicochemical properties of oil bodies, evaluate it as an alternative vegetable protein source, and, finally, investigate the effect of roasting on all these properties.

Materials and Methods

Samples and reagents

Apricot kernels (Hacıhaliloğlu-type) were supplied by Apricot Research and Application Centre, Inonu University, Malatya, Turkey.

Following chemicals were purchased from Sigma Aldrich Corporation (St. Louis, MO, USA): Bradford reactive (B6916), bile acid (B8631), pepsin (P7000), pancreatin (P7545), glycine (G8898), bromphenol blue (B0126), Coomassie brilliant blue R (27816), sodium dodecyl sulfate (L4390), marker for sodium dodecyl sulfate–polyacrylamide gel electrophoresis (SDS-PAGE; S8445), and fatty acids methyl esters standard (47885-U). Mini-PROTEAN TGX precast gels (12%) were purchased from Bio-Rad (New York, USA). All the chemicals were of analytical grade.

Preparation of apricot kernel milk

For preparing apricot kernel milk, 250 g of apricot kernel was soaked overnight in 1-L ultrapure water at room temperature. The mixture was subjected to agitation with a blender, and filtered using a cheesecloth. The supernatants were stored at -20°C until analyzed. The amount of kernel in the final product was 20 g/100 mL.

Roasting

Apricot kernels were roasted in an oven for 10 min at 170°C, and the roasting process was selected as it was generally applied to nuts.

Chemical composition

The protein contents of apricot kernel and both kinds of milk were determined by Dumas method using LECO-FP 528 analyzer. The protein contents of digested samples were determined using the Bradford (1976) method, and bovine serum albumin (BSA) was used as a standard. The total lipid contents of apricot kernel and apricot kernel milk were detected using the methods proposed by Folch *et al.* (1957) and Bligh and Dyer (1959), respectively.

In vitro gastrointestinal digestion

The samples were subjected to *in vitro* gastrointestinal digestion (Minekus *et al.*, 2014). Accordingly, simulated salivary fluid (SSF), simulated gastric fluid (SGF), and simulated intestinal fluid (SIF) were prepared daily from stock solutions. In this method, the activities of enzymes were determined as per the protocol described by Brodkorb *et al.* (2019). Pepsin and pancreatin were used in gastric digestion and intestinal digestion, respectively. Pefabloc was used to stop enzymatic activity.

Protein profile

The protein profiles of milk from roasted and unroasted apricot kernels and aliquots obtained from *in vitro* gastric and gastrointestinal digestions were determined using SDS-PAGE. Then the samples were diluted to a protein concentration of 1 mg/mL and mixed with sample buffer solution in a 1:1 ratio. The samples were maintained at 95°C for 10 min and then loaded on gels (12% Mini-PROTEAN® TGX™ precast gels) as 40 µL for gastric samples and 20 µL for intestinal samples. Moreover, electrophoretic separations were conducted at 150 V using a running buffer, and gels were stained with Coomassie brilliant blue R-250 solution (50% ethanol and 10% glacial acetic acid).

Analysis of fatty acid

The major fatty acids of apricot kernel were quantified using 7820A GC gas chromatography system (Agilent Technologies, Santa Clara, CA, USA) with a flame ionization detector (FID) and conventional injector. A fused silica capillary column was used (J&W DB-23, 30-m × 0.25-mm inner diameter, 0.25-µm film thickness; Agilent Technologies).

Methyl esters were prepared using the official method Ce 2-66 of American Oil Chemists' Society (AOCS). The procedure described by Wu *et al.* (2011) was applied with slight modifications, and the injection volume was 1 µL. The temperature in both injector and detector was 250°C. The temperature program was started at 45°C, held for 4 min, increased to 175°C at a rate of 15°C/min, held for 15 min, then increased to 215°C at a rate of 4°C/5 min and held for 10 min. Supelco 37 component fatty acid methyl esters (FAME) mixture was used for identifying fatty acids.

Total titratable acid release

The rate of free fatty acid release was monitored using a pH-stat titration unit (Automatic Potentiometric Titrator AT-510; KEM, Kyoto, Japan). NaOH solution, 0.1 M, was used to maintain pH at 7.0 for 2 h at 37°C. Samples obtained from gastric digestion were subjected to pH-stat titration to determine release of free fatty acid. An excessive amount of pancreatic lipase was added to sample at the end of gastric phase to obtain the lipase activity of 2,000 U/mL as recommended by Mat *et al.* (2016).

Measurement of zeta potential

The zeta potentials of apricot kernel milk, roasted apricot kernel milk, and digested samples were measured using Malvern Zeta Sizer Nano ZS. The apricot kernel milk was diluted 100-fold with purified water, gastric digested samples were diluted with citrate buffer (pH = 2.5), and intestinal digested samples were diluted to 100-fold with phosphate buffer (pH = 7.2) according to the procedure proposed by Gallier and Singh (2012).

Optical microscopy

The images of the microstructures of oil bodies of milk and digested samples were taken with motorized light microscope PSARON Floptik (HPTS 150, AIV Labs, Ankara, Turkey) equipped with a controlled vehicular access (CVA) camera using a digital image. A drop of the

sample was placed on a microscope slide, covered with a cover glass, and detected with a 10× objective lens.

Statistical analysis

Parallel proximate analysis was conducted in triplicate. Data were analyzed using ANOVA (SPSS for Windows version 18.0) and comparisons between mean values were performed using a *t*-test. Differences between mean values were considered significant at $p < 0.05$.

Results and Discussion

Chemical composition of apricot kernel and apricot kernel milk

Table 1 lists protein, total lipid, and ash contents of apricot kernel and apricot kernel milk. Protein, total lipid, and ash contents of apricot kernel were higher than that of apricot kernel milk ($p < 0.05$). Different results were reported for protein (15.1%–24.2%) and total lipid contents (27.7–66.7%) (Alpaslan and Hayta, 2006; Gezer *et al.*, 2011). Differences in the chemical compositions of apricot kernels were due to their physical characteristics such as kernel weight and length (Femenia *et al.*, 1995).

Proteins hydrolyze during *in vitro* gastrointestinal digestion

There were 10 protein bands in the SDS-PAGE profile of samples; their molecular weight (MW) was between 97 kDa and 6.5 kDa (Figure 1A). In the unroasted form, three protein bands whose molecular weight was 97, 66, and 66–55 kDa might correspond to storage proteins, specifically nutrient reservoir protein (96 kDa), Prunin 1 (63 kDa), and Prunin 2 (53 kDa) as reported by Ghorab *et al.* (2018). Moreover, the authors indicated that the protein bands with molecular weight of 45, 36, and 29 kDa could be hexosyltransferase (43 kDa), hydroxyisourate hydrolyze activity (37 kDa), and ribosomal protein S18 (31 kDa), respectively. In the roasted form, the disappearance of two protein bands with molecular weight of 97 and 14.2 kDa might be attributed to the breakdown of these proteins during roasting. The SDS-PAGE patterns of *in vitro* gastric digestion of apricot kernel milk (Figure 1B) demonstrated that there were no differences in the protein bands of the samples obtained from gastric chyme at different time intervals. This result indicated that pepsin was not able to hydrolyze proteins with molecular weight of 97 and 66 kDa. Protein band with MW = 20 kDa in the SDS-PAGE profile of gastric digested apricot kernel milk but not in the undigested apricot kernel milk might be a sign of the breakdown of proteins with MW > 20 kDa. A similar SDS-PAGE profile was obtained for *in vitro* gastric digestion of roasted samples (Figure 1C).

Intestinal enzyme pancreatin contains proteases with a molecular weight of 23.8–64 kDa, amylase with a molecular weight of 51–55.4 kDa, lipase with a molecular weight of 45–50 kDa, chymotrypsin with a molecular weight of 25 kDa, trypsin with a molecular weight of 24 kDa, and ribonuclease with a molecular weight of 13.7–14.7 kDa. Protein bands with molecular weight of 45, 24, and ~13 kDa were present in the enzymes of intestinal digestive system (Figures 1D and E). Four protein bands (with MW = 45, 29, 20, and 6.5 kDa) were observed in apricot kernel milk whereas seven protein bands (with MW = 45, 36-37, 29, 24, ~22, 6.5, and <6.5 kDa) were observed in roasted apricot kernel milk during intestinal digestion (Figure 1E). The fact that protein bands with MW > 45 kDa present in the SDS-PAGE profile of the gastric digestion system did not appear in the first 15 min of intestinal digestion indicated that these proteins were hydrolyzed in the first 15 min of intestinal digestion. As reported by Beisson *et al.* (2001), for almond oleosins, the 6.5-kDa protein fraction that was not hydrolyzed during intestinal digestion as a function of time might be the central hydrophobic domain of apricot kernel oleosins. Proteins with MW > 45 kDa were completely hydrolyzed at the end of intestinal digestion.

The disappearance of bands with MW > 45 kDa present in the SDS-PAGE profile of gastric digestion established the hydrolysis of proteins with a higher molecular weight during intestinal digestion. The observation of fractions with molecular weight of 45–6.5 kDa could be attributed to the hydrolysis of proteins with a higher molecular weight.

Table 1. The proximate composition of apricot kernel and apricot kernel milk.

	Apricot kernel	Roasted apricot kernel	Apricot kernel milk	Roasted apricot kernel milk
Protein (%)	21.65 ± 0.08^{a}	22.98 ± 0.98^{a}	3.78 ± 0.72^{b}	3.97 ± 0.81^{b}
Total lipid (%)	26.22 ± 1.40^{c}	25.87 ± 5.67^{c}	7.74 ± 3.79^{d}	6.53 ± 2.45^{d}
Ash (%)	2.55 ± 0.20^{e}	2.36 ± 0.51^{e}	0.15 ± 0.07^{f}	0.11 ± 0.1^{f}

Values are mean ± standard deviation.
Different letters in the same row indicate statistical significance at $p < 0.05$.

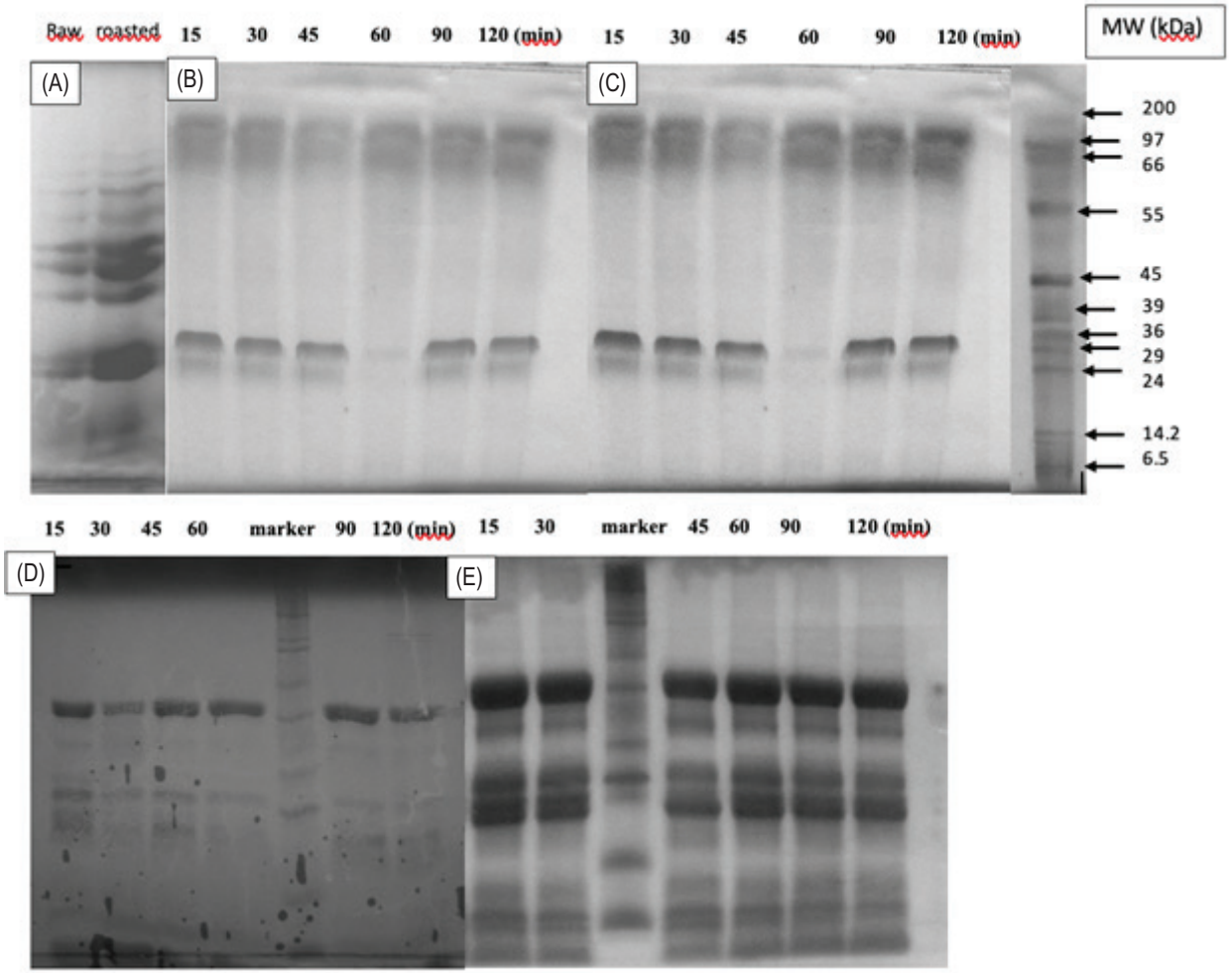

Figure 1. SDS-Page patterns. (A) Apricot kernel milk; (B) *in vitro* gastric digests of apricot kernel milk; (C) *in vitro* gastric digests of roasted apricot kernel milk; (D) *in vitro* intestinal digests of apricot kernel milk; and (E) *in vitro* intestinal digests of roasted apricot kernel milk.

In a study conducted by Gallier and Singh (2012), three primary almond protein bands (20-42 kDa) determined in tricine SDS-PAGE were hydrolyzed in the first 15 min of gastric digestion. The acidic polypeptides were hydrolyzed into smaller peptides in the first 2 min of intestinal digestion and the hydrolysis of all peptides was completed after 5 min of intestinal digestion. Different results obtained in these two studies could be related to pH = 1.5 of gastric chyme used in the study conducted by Gallier and Singh (2012) and difference between the sources of proteins (almond kernel versus apricot kernel) used in both studies.

Composition of fatty acid

The oil and milk extracted from apricot kernels were primarily composed of fatty acids such as palmitic acid, oleic acid, and linoleic acid (Figure 2). Fatty acid profiles of both kernels were identical (Figures 2A and B). Similarly, high amounts of oleic acid and linoleic acid and a low amount of palmitic acid were determined in the apricot kernel oil (Fratianni *et al.*, 2018; Mattheus *et al.*, 2016).

Total titratable acid release

No lag phase was observed during release of total titratable acid from *in vitro* gastric digested apricot kernel milk oil bodies (Figure 3). This indicated that pancreatic lipase easily penetrated the oil-water interface. An early and rapid release of fatty acids from oil bodies was identified in the first 10 min of lipolysis. After 10 min, there was a reduction in the lipolysis rate, although acid release continued slowly to reach a value of 76.5 μM for apricot kernel milk and 85.5 μM for roasted apricot kernel milk at the end of 2-h digestion. During the first 30 min, the rate of free fatty acid release increased rapidly as the oil–water interface was easily accessible by pancreatic lipase. The rate of release of free fatty acid slowed down

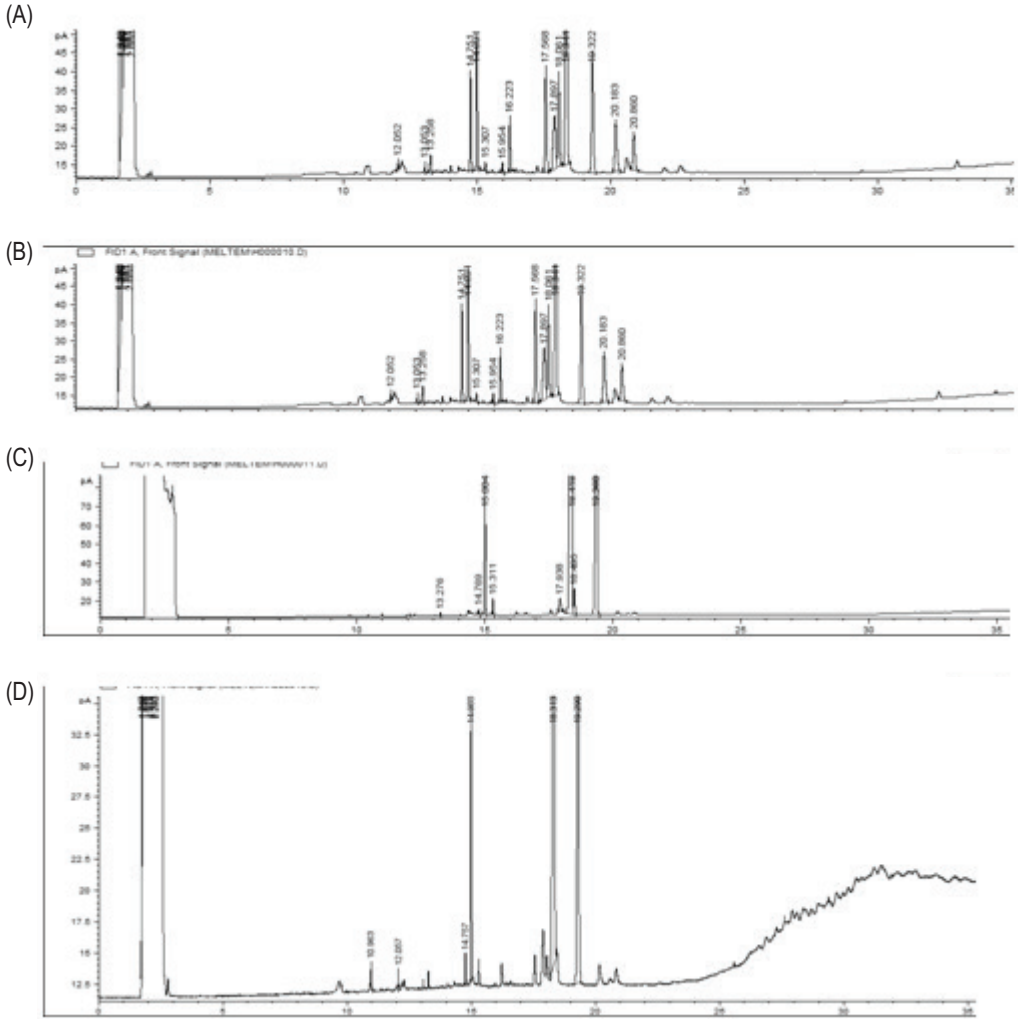

Figure 2. Gas chromatograms of apricot kernels. (A) Raw apricot kernel; (B) roasted apricot kernel; (C) apricot kernel milk; (D) roasted apricot kernel milk.

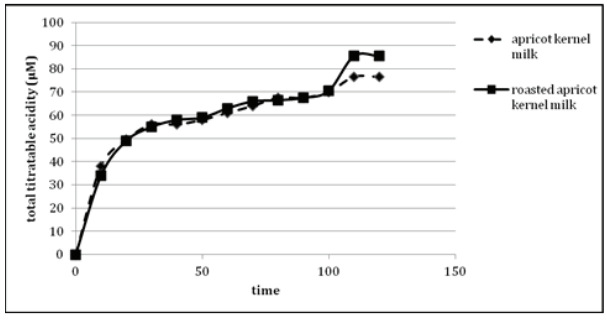

Figure 3. Total titratable acid release from gastric digested apricot kernel milk oil bodies during 120 min of intestinal digestion.

because the interfacial saturation of lipolytic products slowly solubilized into micelles. Unlike our result, Gallier and Singh (2012) observed a lag phase of 2 min, indicating the prevention of lipolysis by the membranes of oil bodies of almond, and the release of 133-μmol/mL free fatty acids of almond oil bodies after *in vitro* intestinal digestion. Moreover, rapid increase in the release rate of fatty acid in the first 25 min of intestinal digestion was also identified.

Measurement of zeta potential

It is important to measure the zeta potential and surface charge of emulsified particles on the stability of emulsions. The power of electrostatic impulsion has a significant contribution to prevent flocculation and coalescence (Çelebi, 2009). Change in the net surface charge on the surface of native apricot kernel bodies was ~0 mV. The zeta potential of oil bodies is governed by the active component oleosins present on the surface.

The zeta potentials of apricot kernel milk and roasted apricot kernel milk were monitored during 2 h of gastric digestion and 2 h of intestinal digestion (Figure 4). The

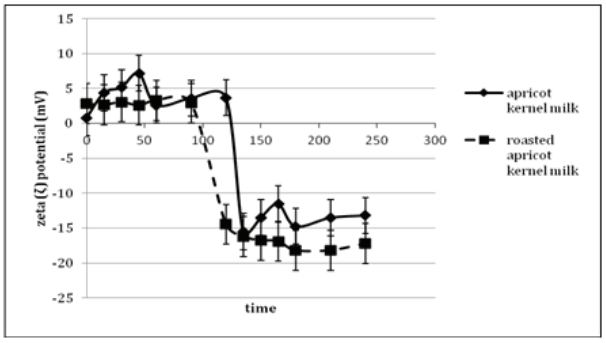

Figure 4. The zeta-potentials of *in vitro* gastric and intestinal digested samples.

zeta potential of apricot kernel milk was ~0 mV at the beginning of *in vitro* gastric digestion; moreover, it was increased to +7.17 mV in the 45th min of gastric digestion. At the end of gastric digestion, the zeta potential of apricot kernel milk was +3.68 mV. The positive value of zeta potential indicated that electrostatic repulsion in protein-stabilized oil droplets decreased and caused flocculation because of the low pH value of gastric environment. During *in vitro* gastric digestion, the zeta potential of roasted apricot kernel milk was different from that of apricot kernel milk. The zeta potential of roasted sample did not change during 0–90 min of *in vitro* gastric digestion and was approximately +3.0 mV (Figure 6). Moreover, zeta potential was –14.47 mV in 120 min of *in vitro* gastric digestion. Low zeta potential (0–±5) indicated that the solution or dispersion might have rapidly coagulated or flocculated. Therefore, the flocculation continued during 90 min of gastric digestion of roasted apricot kernel milk, but solubilization occurred after this point. However, the low positively charged zeta potential of apricot kernel milk did not change during 120 min of gastric digestion. Similarly, Makkhun *et al.* (2015) reported that the emulsion droplets located on the oil bodies of sunflower remained positively charged for 2 h of *in vitro* gastric digestion. The zeta potential of apricot kernel milk became negative at the very beginning (0–15 min) of intestinal digestion. Moreover, the zeta potential of apricot kernel milk was -14.45 mV during the 15 min of intestinal digestion and increased slowly and reached –13.2 mV at the end of intestinal digestion. During intestinal digestion, the zeta potential of roasted apricot kernel milk remained practically the same ranging from –16.23 to –18.2 mV. Although there was an insignificant difference between the zeta potentials of apricot kernel milk and roasted apricot kernel milk, a slightly higher zeta potential of roasted samples could be related to the more extensive association of bile salts with the surface of oil bodies in roasted apricot kernel milk than that in apricot kernel milk, as reported by Makkhun *et al.* (2015) for emulsion droplets located on the oil bodies of sunflower.

Although no research has been conducted on the zeta potential of apricot kernel milk, few studies are determined on the oil bodies of almond, pumpkin seed, soybean, and coconut milk. Gallier and Singh (2012) reported that the charge of native almond oil body was highly negative (-30 mV). At the start of *in vitro* gastric digestion, the zeta potential of almond oil body was highly positive and continued to remain positive during 60 min of gastric digestion. Along with the *in vitro* intestinal digestion of almond milk, the zeta potentials of samples were negatively charged. Dave *et al.* (2019) reported that the zeta potential of oil bodies of coconut milk measured at pH 6.1 was –13 ± 1 mV. At pH 7.5, the zeta potential of oil bodies in washed cream and that of purified oil bodies were –32.6 and -33.8 mV, respectively. The zeta potentials of oil bodies of pumpkin seeds were different at different pH values and salt concentrations. An increase in the concentration of salt up to 10 mM at pH 3 increased the positive charge of zeta potential, which decreased with change in the concentration of salt. However, at pH 7.4, increase in salt concentration from 10 to 100 mM induced negative potentials. Ishii *et al.* (2017) studied the interfacial and emulsifying properties of two types of oil bodies extracted from soybean seeds at different pH values. The zeta potentials of purified oil bodies (OB) and crude oil bodies (OBC), including storage and other minor proteins, were –14.2 and –39.0 mV, respectively. This indicated that there was a strong electrostatic repulsion between crude oil bodies than between purified oil bodies.

Optical microscopy

Spherical and variable size of oil bodies were observed for apricot kernel milk and roasted apricot kernel milk (Figures 5A and B). The size of oil bodies of apricot kernel milk was greater than that of roasted apricot kernel milk. Unlike oil bodies of apricot kernel milk, roasting caused aggregation of oil bodies (Figure 5B, 0 min). Zaaboul *et al.* (2019) reported that roasted peanut oil bodies were larger compared to raw peanut oil bodies. The flocculation started within the 15 min of gastric digestion of both samples (Figures 5A and B). Large aggregates were still present after 90 min of gastric digestion of apricot kernel milk, but disruption in aggregates commenced in roasted apricot kernel milk at 90 min of gastric digestion. This result is supported by the increased zeta potential of roasted apricot kernel milk after 90 min of gastric digestion. The flocculation probably occurred due to the destabilization of oil bodies during hydrolysis of interfacial proteins by pepsin. A similar result indicated that the oil bodies of almond flocculated under low pH conditions (pH 1.5) during gastric digestion (Gallier and Singh, 2012). Moreover, a liquid crystalline phase observed

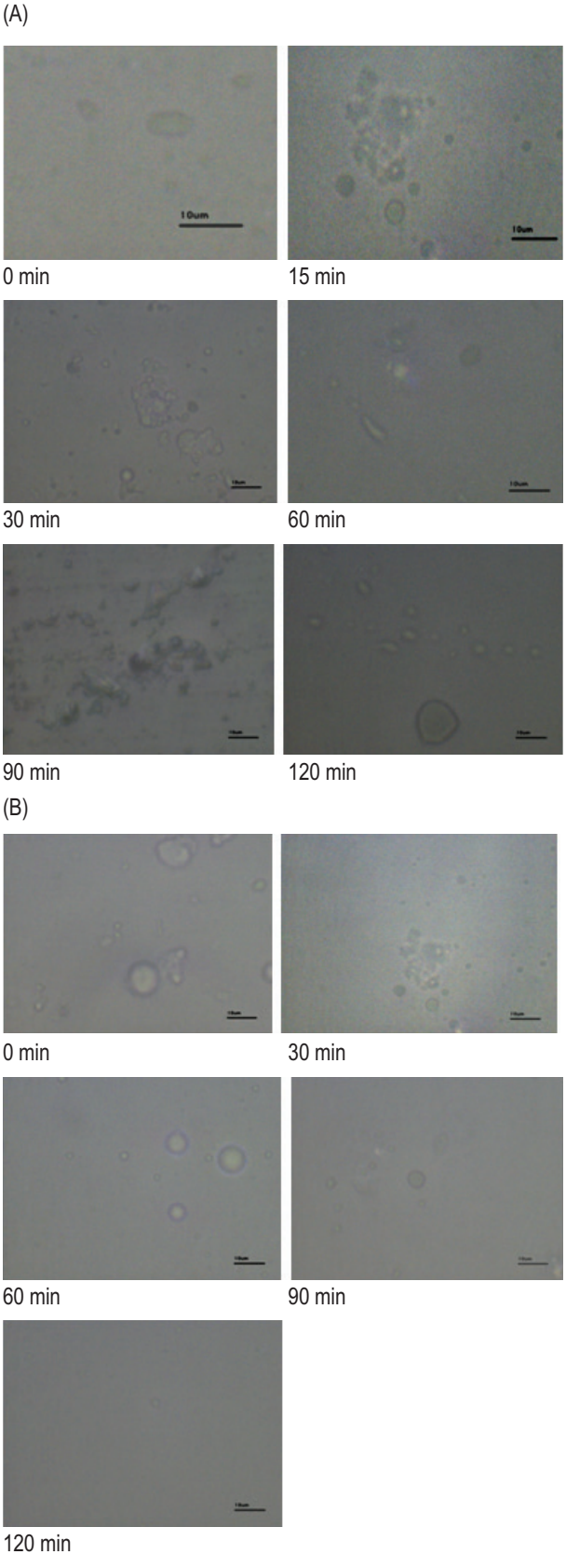

Figure 5. (A) Optical microscopic images of apricot kernel milk and (B) roasted apricot kernel milk digests obtained at different time intervals of *in vitro* gastric digestion.

surrounding lipid droplets at 90 min of *in vitro* gastric digestion (Figure 5B) could be attributed to the presence of insoluble calcium long-chain fatty acid soaps precipitated around oil bodies as reported by Gallier and Singh (2012) in the case of almond oil bodies at 30 min of intestinal digestion.

In the 30th min of intestinal digestion, although large aggregates were still present, marginally disaggregated oil bodies were observed. This disaggregation was probably due to adding bile salts, and pancreatic lipase that they caused to the solubilization of lipolytic products into the mixed micelles formed of bile salts. This solubilization-induced disaggregation of oil bodies after 60 min of intestinal digestion is shown in Figure 6. Gallier and Singh (2012) reported similar behavior of almond oil bodies, revealing the disruption of aggregates after 30 min of intestinal digestion.

Few oil bodies of different sizes were still present at the end of intestinal digestion of apricot kernel milk. However, disaggregation did not occur during 120 min of intestinal digestion of roasted apricot kernel milk (Figure 6B).

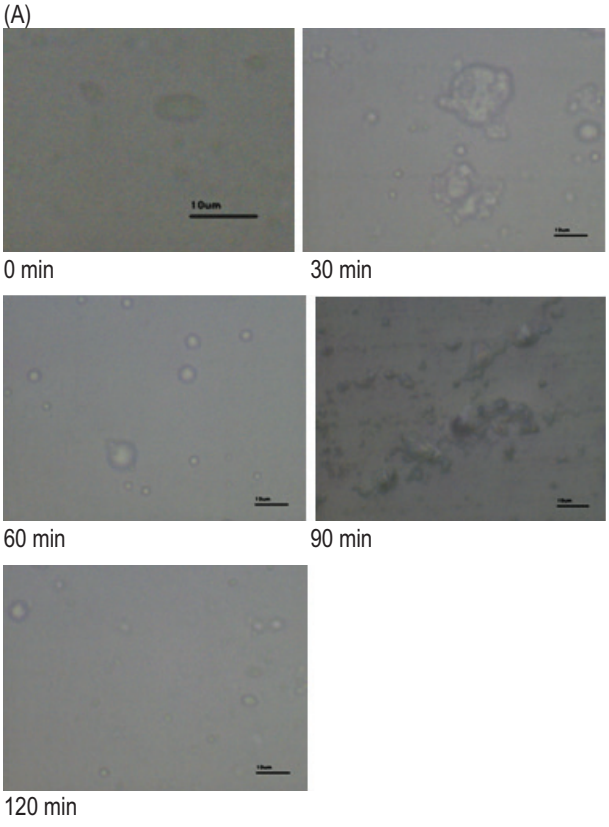

Figure 6. (A) Optical microscopic images of apricot kernel milk and (B) roasted apricot kernel milk digests obtained at different time intervals of *in vitro* intestinal digestion.

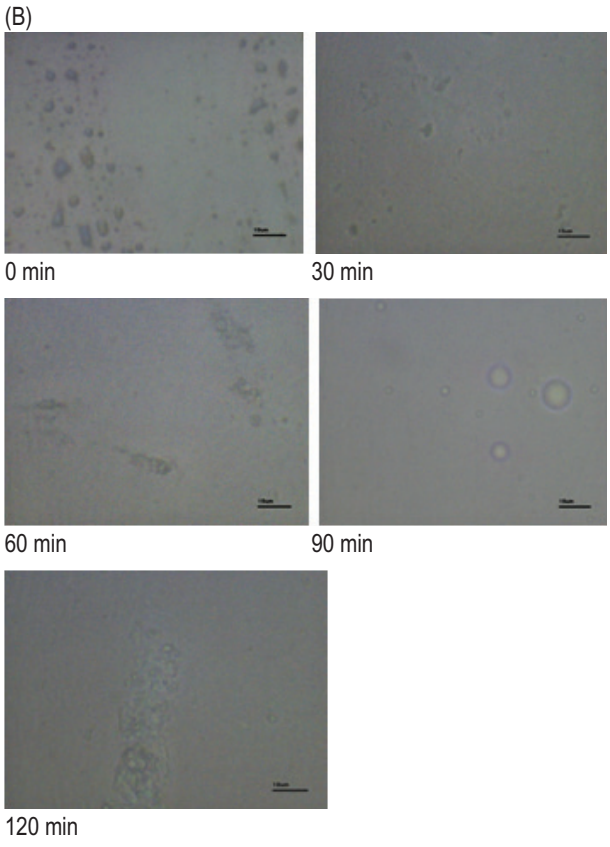

Figure 6. (Continued).

Conclusion

Roasting seems to cause aggregation of oil bodies compared to unroasted apricot kernel milk oil bodies. The proteins of apricot kernel milk and roasted apricot kernel milk were hydrolyzed to a greater or lesser extent during *in vitro* gastrointestinal digestion. However, pepsin-resistant proteins were determined in both samples and the flocculation of oil bodies was observed. No difference was recorded between the pancreatic lipase penetration in the oil-water interface of oil bodies of both milk types. Moreover, a few oil bodies of different sizes were still present at the end of intestinal digestion of apricot kernel milk. However, disaggregation did not occur during 120 min of intestinal digestion of roasted apricot kernel milk. In addition, 250 mL of apricot kernel milk contains 50-g kernel corresponding to 12.5-mg amygdalin, which is considerably lower than the amount (200 mg) that causes poisoning in a child weighing 20 kg, as reported by Karsavuran *et al.* (2015).

In conclusion, the results of the study demonstrated that apricot kernel milk and roasted apricot kernel milk are a good source of alternative vegetable protein. It could be utilized as a value-added product such as a functional food ingredient and/or a novel functional product. The future research must be conducted on the sensory properties of apricot kernel milk.

Acknowledgments

We are grateful to Ege University Corporate Development Planning and Monitoring Coordination Unit and Directorate of Library and Documentation for their support in editing and proofreading of this study.

Disclosure Statement

The authors declare no conflicts of interest.

Funding

This work was supported by the Ege University Scientific Research Project Coordination (Grant Nos. 8295, 13-MUH-015).

References

Abdullah, W. and Zhang H. 2020. Recent advances in the composition, extraction and food applications of plant-derived oleosomes. Trends Food Sci Technol. 106:322–332. https://doi.org/10.1016/j.tifs.2020.10.029

Al Juhaimi F., Özcan M.M., Ghafoor K., and Babiker E.E. 2018. The effect of microwave roasting on bioactive compounds, antioxidant activity and fatty acid composition of apricot kernel and oils. Food Chem. 243:414–419. https://doi.org/10.1016/j.foodchem.2017.09.100

Alpaslan M. and Hayta M. 2006. Apricot kernel: physical and chemical properties. J Am Oil Chem Soc. 83(5):469–471. https://doi.org/10.1007/s11746-006-1228-5

Barre A., Simplicien M., Cassan G., Benoist H., and Rougé P. 2018. Oil bodies (oleosomes): occurrence, structure, allergenicity. Rev Fr Allergol. 58:574–580. https://doi.org/10.1016/j.reval.2018.10.005

Beisson F., Ferté N., Voultoury R., and Arondel V. 2001. Large scale purification of an almond oleosin using an organic solvent procedure. Plant Physiol Biochem. 39(7–8):623–630. https://doi.org/10.1016/S0981-9428(01)01275-X

Bligh E.G. and Dyer W.J. 1959. A rapid method of total lipid extraction and purification. Can J Biochem Physiol. 37(8): 911–917. https://doi.org/10.1139/o59-099

Bradford M.M. 1976. A rapid and sensitive method for the quantitation of microgram quantities of protein utilizing the principle of protein-dye binding. Anal Biochem. 72(1–2):248–254. https://doi.org/10.1016/0003-2697(76)90527-3

Brodkorb A., Egger L., Alminger M., Alvito P., Assunção R., Ballance S., Bohn T., Bourlieu-Lacanal C., Boutrou R., Carrière F., Clemente A., Corredig M., Dupont D., Dufour C., Edwards C.,

Golding M., Karakaya S., Kirkhus B., Le Feunteun S., Lesmes U., Macierzanka A., Mackie A.R., Martins C., Marze S., McClements D.J., Ménard O., Minekus M., Portmann R., Santos C.N., Souchon I., Singh R.P., Vegarud G.E., Wickham M.S.J., Weitschies W., and Recio I. 2019. INFOGEST static *in vitro* simulation of gastrointestinal food digestion. Nat Protoc. 14(4):991–1014. https://doi.org/10.1038/s41596-018-0119-1

Çelebi N. 2009. Emülsiyonlar. In "Modern Farmasötik Teknoloji," F. Acartürk, İ. Ağabeyoğlu, N. Çelebi, T. Değim, Z. Değim, T. Doğanay, S. Takka, and F. Tırnaksız (Eds.), p. 277. Türk Eczacılar Birliği Eczacılık Akademisi Yayını, Ankara, Turkey.

Coman V., Teleky B.E., Mitrea L., Martău G.A., Szabo K., Calinoiu L.F., and Vodnar D.C. 2019. Bioactive potential of fruit and vegetable wastes. Adv Food Nutr Res. 91:157–225. https://doi.org/10.1016/bs.afnr.2019.07.001

Dave A.C., Ye A., and Singh H. 2019. Structural and interfacial characteristics of oil bodies in coconuts (Cocos nucifera L.). Food Chem. 276:129–139. https://doi.org/10.1016/j.foodchem.2018.09.125

Elkot W.F., El-Nawasany L.I., and Sakr H.S. 2017. Composition and quality of stirred yoghurt supplemented with apricot kernels powder. J. Agroaliment Process Technol. 23(3):125–130.

Eyidemir E. and Hayta M. 2009. The effect of apricot kernel flour incorporation on the physicochemical andsensory properties of noodle. Afr J Biotechnol. 8:85–90.

Fasolin L.H., Pereira R.N., Pinheiro A.C., Martins J.J., Andrade C.C.P., Ramos O.L., and Vicente A.A. 2019. Emergent food proteins—towards sustainability, health, and innovation. Food Res Int. 125:108586. https://doi.org/10.1016/j.foodres.2019.108586

Femenia A., Rosselló C., Mulet A., and Cañellas J. 1995. Chemical composition of bitter and sweet apricot kernels. J Agric Food Chem. 43:356–361. https://doi.org/10.1021/jf00050a018

Folch J., Lees M., and Sloane Stanley G.H. 1957. A simple method for the isolation and purification of total lipids from animal tissues. J Biol Chem. 226(1):497–509. https://doi.org/10.1016/S0021-9258(18)64849-5

Food and Agriculture Organization of the United Nations (FAO). 2011. Feeding the future. World Livestock, Livestock in Food Security. Available at: http://www.fao.org/3/i2373e/i2373e03.pdf

Fratianni F., Ombra M.N., d'Acierno A., Cipriano L., and Nazzaro F. 2018. Apricots: biochemistry and functional properties. Curr Opin Food Sci. 19:23–29. https://doi.org/10.1016/j.cofs.2017.12.006

Gallier S., Acton D., Garg M., and Singh H. 2017. Natural and processed milk and oil body emulsions: bioavailability, bioaccessibility and functionality. Food Struct. 13:13–23. https://doi.org/10.1016/j.foostr.2016.07.005

Gallier S., Gordon K.C., and Singh H. 2012. Chemical and structural characterisation of almond oil bodies and bovine milk fat globules. Food Chem. 132:1996–2006. https://doi.org/10.1016/j.foodchem.2011.12.038

Gallier S. and Singh H. 2012. Behavior of almond oil bodies during *in vitro* gastric and intestinal digestion. Food Funct. 3:547–555. https://doi.org/10.1039/c2fo10259e

Gallier S., Zhu X.Q., Rutherfurd S.M., Ye A., Moughan P.J., and Singh H. 2013. *In vivo* digestion of bovine milk fat globules: effect of processing and interfacial structural changes. II. Upper digestive tract digestion. Food Chem. 141:3215–3223. https://doi.org/10.1016/j.foodchem.2013.06.019

Gezer I., Haciseferogullari H., Özcan M.M., Arslan D., Asma B.M., and Ünver A. 2011. Physico-chemical properties of apricot (*Prunus armeniaca L.*) kernels. South West J Hortic Biol Environ. 2(1):1–13.

Ghorab H., Lammi C., Arnoldi A., Kabouche Z., and Aiello G. 2018. Proteomic analysis of sweet algerian apricot kernels (*Prunus armeniaca L.*) by combinatorial peptide ligand libraries and LC–MS/MS. Food Chem. 239:935–945. https://doi.org/10.1016/j.foodchem.2017.07.054

Ishii T., Matsumiya K., Nambu Y., Samoto M., Yanagisawa M., and Matsumura Y. 2017. Interfacial and emulsifying properties of crude and purified soybean oil bodies. Food Struct. 12:64–72. https://doi.org/10.1016/j.foostr.2016.12.005

Karsavuran N., Charehsaz M., Celik H., Asma B.M., Yakıncı C., and Aydın A. 2015. Amygdalin in bitter sweet seeds of apricots. Toxicol Environ Chem. 96(10):1564–1570. https://doi.org/10.1080/02772248.2015.1030667

Makkhun S., Khosla A., Foster T., McClements D.J., Grundy M.M.L., and Gray D.A. 2015. Impact of extraneous proteins on the gastrointestinal fate of sunflower seed (*Helianthus annuus*) oil bodies: a simulated gastrointestinal tract study. Food Funct. 6:125–134. https://doi.org/10.1039/C4FO00422A

Mandalari G., Faulks R.M., Rich G.T., Lo Turco V., Picout D.R., Lo Curto R.B., Bisignano G., Dugo P., Dugo G., Waldron K.W., Ellis P.R., and Wickham M.S.J. 2008. Release of protein, lipid, and vitamin E from almond seeds during digestion. J Agric Food Chem. 56:3409–3416. https://doi.org/10.1021/jf073393v

Mantzouridou F.T., Naziri E., Kyriakidou A., Paraskevopoulou A., Tsimidou M.Z., and Kiosseoglou V. 2019. Oil bodies from dry maize germ as an effective replacer of cow milk fat globules in yogurt-like product formulation. LWT–Food Sci Technol. 105:48–56. https://doi.org/10.1016/j.lwt.2019.01.068

Mat D.J.L., Le Feunteun S., Michon C., and Souchon I. 2016. *In vitro* digestion of foods using pH-stat and the INFOGEST protocol: impact of matrix structure on digestion kinetics of macronutrients, proteins and lipids. Food Res Int. 88:226–233. https://doi.org/10.1016/j.foodres.2015.12.002

Mattheus B., Özcan M.M., and Al Juhaimi F. 2016. Fatty acid composition and tocopherol content of kernel oil from apricot varieties (Hasanbey, Hacıhaliloglu, Kabaasi, and Soganci) collected at different harvest times. Eur Food Res Technol. 242:221–226. https://doi.org/10.1007/s00217-015-2533-8

Minekus M., Alminger M., Alvito P., Ballance S., Bohn T., Bourlieu C., Carrière F., Boutrou R., Corredig M., Dupont D., Dufour C., Egger L., Golding M., Karakaya S., Kirkhus B., Le Feunteun S., Lesmes U., MacIerzanka A., MacKie A., Marze S., McClements D.J., Ménard O., Recio I., Santos C.N., Singh R.P., Vegarud G.E., Wickham M.S.J., Weitschies W., and Brodkorb A. 2014. A standardised static in vitro digestion method suitable for food—an international consensus. Food Funct. 5:1113–1124. https://doi.org/10.1039/C3FO60702J

Mirzaei H. and Rezaei K. 2019. Amygdalin contents of oil and meal from wild almond: effect of different heat pretreatment and extraction methods. J Am Oil Chem Soc. 96:1163–1171. https://doi.org/10.1002/aocs.12257

Morais D.R., Rotta E.M., Sargi S.C., Schmidt E.M., Guntendorfer Bonafe E., Eberlin M.N., Sawaya A.C.H.F., and Visentainer J.V. 2015. Antioxidant activity, phenolics and UPLC–ESI[–]–MS of extracts from different tropical fruits parts and processed peels. Food Res Int. 77(3):392–399. https://doi.org/10.1016/j.foodres.2015.08.036

Sığırcı M., Hasdemir M., Akçay M., and Yurtkulu V. 2015. National Apricot Workshop, p. 80. Turkey Ministry of Agricultural and Forestry, Ankara, Turkey.

Tarım U., Piyasaları-Kayısı. 2020. Turkey Ministry of Agricultural and Forestry, Agricultural Economic and Policy Development Institute. https://arastirma.tarimorman.gov.tr/ tepge/Belgeler/PDF%20Tar%C4%B1m%20%C3%9Cr%C3%BCnleri%20Piyasalar%C4%B1/2020-Ocak%20Tar%C4%B1m%20%C3%9Cr%C3%BCnleri%20Raporu/Kay%C4%B1s%C4%B1%20Tar%C4%B1m%20%C3%9Cr%C3%BCnleri%20Piyasa%20Raporu%202020%20ocak.pdf. Accessed 1 March 2020.

Wang X., Ye A., and Singh H. 2020. Structural and physicochemical changes in almond milk during *in vitro* gastric digestion: impact on the delivery of protein and lipids. Food Funct. 11:4314–4326. https://doi.org/10.1039/C9FO02465D

White D.A., Fisk I.D., Mitchell J.R., Wolf B., Hill S.E., and Gray D.A. 2008. Sunflower seed oil body emulsions: rheology and stability assessment of a natural emulsion. Food Hydrocoll. 22(7):1224–1232. https://doi.org/10.1016/j.foodhyd.2007.07.004

Wu H., Shi J., Xue S., Kakuda Y., Wang D., Jiang Y., Ye X., Li Y., and Subramanian J. 2011. Essential oil extracted from peach (*Prunus persica*) kernel and its physicochemical and antioxidant properties. LWT–Food Sci Technol. 44:2032–2039. https://doi.org/10.1016/j.lwt.2011.05.012

Yan Z., Zhao L., Kong X., Hua Y., and Chen Y. 2016. Behaviors of particle size and bound proteins of oil bodies in soymilk processing. Food Chem. 194:881–890. https://doi.org/10.1016/j.foodchem.2015.08.100

Zaaboul F., Raza H., Cao C., and Yuanfa L. 2019. The impact of roasting, high pressure homogenization and sterilization on peanut milk and its oil bodies. Food Chem. 280:270–277. https://doi.org/10.1016/j.foodchem.2018.12.047

Zderic A., Almeida-Rivera C., Bongers P., and Zondervan E. 2016. Product-driven process synthesis for the extraction of oil bodies from soybeans. J Food Eng. 185:26–34. https://doi.org/10.1016/j.jfoodeng.2016.03.030

Italian Journal of Food Science, 2022; 34 (1): 44–58

Effects of inorganic and organic selenium intervention on resistance of radish to arsenic stress

Liang Hu[1], Xianglian Wang[1]*, Yuntao Zou[1], Daishe Wu[2]*, Guiqing Gao[1], Zhiyao Zhong[1], Yu Liu[3], Shengming Hu[1], Houbao Fan[1], and Baojun Zhang[2,4]

[1]Jiangxi Provincial Key Laboratory for Restoration of Degraded Ecosystems & Watershed Ecohydrology, Nanchang Institute of Technology, Nanchang, China; [2]Key Laboratory of Poyang Lake Environment and Resource Utilization of the Ministry of Education, School of Resource, Environment and Chemical Engineering, Nanchang University, Nanchang, China; [3]Jiagnxi Biotech Vocational College, Nanchang, China; [4]Jiangxi Provincial Key Laboratory of Preventive Medicine, School of Public Health, Nanchang University, Nanchang 330006, China

***Corresponding Authors**: Xianglian Wang, Jiangxi Provincial Key Laboratory for Restoration of Degraded Ecosystems & Watershed Ecohydrology, Nanchang Institute of Technology, Nanchang 330099, China. Email: wangxianglian@nit.edu.cn; Daishe Wu, Key Laboratory of Poyang Lake Environment and Resource Utilization of the Ministry of Education, School of Resource, Environment and Chemical Engineering, Nanchang University, Nanchang 330031, China. Email: daishewuprof@163.com

Received: 26 July 2021; Accepted: 30 December 2021; Published: 27 January 2022

PAPER

Abstract

Arsenic (As) pollution, a potential threat for human health, in vegetables is one of the primary sources of As intake by the human body. In the Pot Experiment, the As content, physiological index and antioxidant enzyme activity of radish were determined. The results demonstrated that the order of As concentration in radish tissues was roots > stems > leaves. Organic selenium (Se) can inhibit the absorption of arsenic in radish more effectively than inorganic Se. The application of organic Se and low concentration of selenite (Se(IV)) significantly enhanced the stress resistance of radish for increasing superoxide dismutase and peroxidase activity, increasing soluble protein, chlorophyll and proline content, and reducing malondialdehyde content. In contrast, the high concentration of Se(IV) and selenate (Se(VI)) treatment group demonstrated stress and toxicological effects on radish. This study provides an idea for further research on the remediation mechanism of Se to As toxicity and provides a reference for the adoption of Se fertilizer in agriculture.

Keywords: arsenic toxicity, selenium intervention, radish, antioxidant enzymes

Introduction

Arsenic (As) is typically a toxic element. Vegetables are the most common food items of people's daily consumption, so their quality and safety directly affect the human health (Fendorf *et al.,* 2010). Related reports of As pollution in vegetables have attracted much public attention (Dahal *et al.,* 2008; Mcbride, 2013; Praveen *et al.*, 2018). Zeng *et al.* (2008) reported that accumulation of As occurred in 44.2% of the soil samples taken from vegetable fields in China, and 9.2% of the samples exceeded the safety limits. Su *et al.* (2005) reported that the excess rate of As pollution in vegetables in Lhasa (China) was as high as 63.64%, and the highest As pollution index was 7.04.

Studies have established that As entering the plant interferes with various metabolic processes of the plant (Tripathi *et al.*, 2012), causing retarded plant growth, chlorosis, membrane damage and even death. Chlorophyll content determines the photosynthetic efficiency of plants and is one of the essential indicators reflecting the growth status of plants. Under As stress, chlorophyll content was reduced in corn (Silva *et al.*, 2015), tobacco (Wu *et al.*, 2015) and eucalyptus (Meng

ISSN 1120-1770 online, DOI 10.15586/ijfs.v34i1.2105

et al., 2017). The research established that As treatment could significantly reduce the germination rate, bud, root elongation and biomass of rice seedlings (Shri *et al.*, 2009). Under As stress, plants produce a large number of reactive oxygen species (ROS), such as superoxide anions ($O_2^{-\bullet}$), hydroxyl radicals ($OH^{-\bullet}$) and hydrogen peroxide (H_2O_2). ROS can damage macromolecules such as nucleic acids, proteins and polysaccharides in cells, resulting in peroxidative damage to membrane lipids. The antioxidant enzyme system plays a vital role in removing ROS. The antioxidant enzyme system primarily includes superoxide dismutase (SOD), catalase (CAT) and peroxidase (POD) (Meng *et al.*, 2017). Changes in antioxidant enzyme activity can reflect the growth and metabolism of plants and resistance to environmental stress. Under high concentrations of As (20 and 30 mg L^{-1}) stress, the activities of SOD, CAT and POD decreased in eucalyptus but the malondialdehyde (MDA) content increased significantly, and eucalyptus suffered severe oxidative damage (Meng *et al.,* 2017).

Nowadays, exploring the prevention and control methods to combat As pollution is a hot topic in the interdisciplinary research of agricultural environment and biology (Dong *et al.*, 2021; Zheng *et al.*, 2022). Selenium (Se) is one of the essential nutrients and plays an essential physiological function in the human body. Se is an essential component of many proteins and enzymes, such as glutathione peroxidase (GSH-Px) and thioredoxin reductase (TR) (Diao *et al.,* 2014). Certain organic forms of Se have antioxidant and anti-cancer functions (Rayman, 2005). Research proposes that Se has a significant alleviating effect on As toxicity and inhibits the anti-cancer properties of As (La porte, 2011). Other scholars have also reported the effects of Se on As toxicity in plants (Camara *et al*., 2018; Pandey and Gupta, 2018), tobacco (Han *et al.,* 2015) and algae (Kramárová *et al.*, 2012). However, these studies primarily focused on the effects of Se application on plants in a single form. However, comparative studies on the effects of Se in various forms (such as inorganic Se and organic Se) on As in plants are relatively lacking, and there are few reports on the effects of Se on As-contaminated vegetables.

Radish, which belongs to the cruciferous family of plant kingdom, has a short duration but high yield. It has been reported that radish absorbs and enriches As more than other daily used vegetables (Huang *et al.,* 2006), and cruciferous vegetables, such as radish, have a higher Se enrichment capacity than other plants (Pedrero *et al.*, 2006). Therefore, this study aimed to investigate the effects of organic and inorganic Se on the antioxidant activity and absorption of As as well as indicators of growth in As-stressed radish, and provided information to alleviate the health risks of As.

Materials and Method

Pot experiment

In this study, red soil and cherry radish were selected as experimental objects (Support Material, Figure S1). The pot experiment and management was carried out in accordance with our previous research (Hu *et al.*, 2020, 2021). The experimental design included the following 21 treatments: (1) 30-mg As kg^{-1} (control group [CK]); (2) 30-mg As kg^{-1} + 1-mg Se kg^{-1} (1Se(IV)); (3) 30-mg As kg^{-1} + 3-mg Se kg^{-1} (3 Se(IV)); (4) 30-mg As kg^{-1} + 6-mg Se kg^{-1} (6Se(IV)); (5) 30-mg As kg^{-1} + 12-mg Se kg^{-1} (12Se(IV)); (6) 30-mg As kg^{-1} + 24-mg Se kg^{-1} (24Se(IV)); (7) 30-mg As kg^{-1} + 1-mg Se kg^{-1} (1Se(VI)); (8) 30-mg As kg^{-1} + 3-mg Se kg^{-1} (3Se(VI)); (9) 30-mg As kg^{-1} + 6-mg Se kg^{-1} (6Se(VI)); (10) 30-mg As kg^{-1} + 12-mg Se kg^{-1} (12Se(VI)); (11) 30-mg As kg^{-1} + 24-mg Se kg^{-1} (24Se(VI)); (12) 30-mg As kg^{-1} + 1-mg Se kg^{-1} (1Se-Y); (13) 30-mg As kg^{-1} + 3-mg Se kg^{-1} (3Se-Y); (14) 30-mg As kg^{-1} + 6-mg Se kg^{-1} (6Se-Y); (15) 30-mg As kg^{-1} + 12-mg Se kg^{-1} (12Se-Y); (16) 30-mg As kg^{-1} + 24-mg Se kg^{-1} (24Se-Y); (17) 30-mg As kg^{-1} + 1-mg Se kg^{-1} (1Se-M); (18) 30-mg As kg^{-1} + 3-mg Se kg^{-1} (3Se-M); (19) 30-mg As kg^{-1} + 6-mg Se kg^{-1} (6Se-M); (20) 30-mg As kg^{-1} + 12-mg Se kg^{-1} (12Se-M) and (21) 30-mg As kg^{-1} + 24-mg Se kg^{-1} (24Se-M). As and Se were added in the form of a solution comprising sodium arsenite (As(III)), sodium selenite (Se(IV)), sodium selenate (Se(VI)), selenium yeast (Se-Y) or Se malt (Se-M), which was then mixed into the soil. The soil moisture content was maintained at 60–80% of the maximum value. After 50 days of equilibration, the seeds were sown. Each treatment was replicated for three times, and the treatments were arranged in random blocks. Plump cherry radish seeds were selected and moistened with ultrapure water, and 10 seeds were distributed evenly in each pot, which were subsequently sprayed with ultrapure water. When the seeds had germinated and developed two true leaves, the seedlings were thinned, leaving three plants in each pot. The photoperiod was 15 h day^{-1}, and the light intensity was 270~360 μE m^{-2} s^{-1}. Furthermore, the indoor temperature was 23°C during the day and 18°C at night. After growing for 35 days, the cherry radish plants were harvested. Their roots, stems and leaves were collected separately, after which they were washed and blotted dry with filter paper. After weighing, the samples were put in a Ziploc bag and stored at –80°C. Radish seeds, Se-Y (containing 2,000-mg kg^{-1} Se) and Se-M (containing 1,600-mg Se kg^{-1}) were purchased from a local market in Nanchang, Jiangxi, China.

Determination of chlorophyll and malondialdehyde content

The chlorophyll content (expressed as mg kg^{-1} fresh weight [FW]) of radish leaves was determined by the 95%

ethanol extraction method (Saelee *et al.*, 2012). Fresh radish leaves (0.2 g) were cut into small pieces. Then the sample was extracted with 20-mL 95% ethanol in darkness for about 24 h. Finally, the absorbance of samples was measured at 665, 649 and 652 nm, and the blank experiment was set up using 95% ethanol.

The MDA content (expressed as mmol g^{-1} FW) was measured by thiobarbituric acid colorimetry according to the study conducted by Hashemi *et al.* (2010). Briefly, the radish root was cut and homogenized, then extracted with 0.1% (w/v) trichloroacetic acid (TCA) in a pre-chilled pestle and mortar. The mixture was centrifuged at 15,000 g for 15 min at 4°C. The obtained supernatant (250 µL) was mixed with 2-mL thiobarbituric acid reagent, then boiled for 30 min in a water bath and centrifuged at 6,000 g for 10 min. Finally, the absorbance of the subsample was tested at 532 nm.

Determination of SOD, POD and soluble protein

Extract for enzymatic assays was prepared according to the study conducted by Bai *et al.* (2013). Fresh radish root samples (0.05 g) were homogenized using phosphate buffer (100 mmol L^{-1}, pH 6.8, 10 mL) and centrifuged under 17,000 g for 15 min at 4°C. The supernatant was used for assays of SOD, POD and soluble protein.

The SOD activity was assayed by using the photochemical nitrogen blue tetrazolium (NBT) method (Beauchamp and Fridovich, 1971). The 3-mL reaction mixture consisted of 50-mM phosphate buffer, pH 7.8; 9.9-mM L-methionine; 57-µM NBT; 0.025% (w/v) Triton X-100 and 0.0044% (w/v) riboflavin. The reaction was allowed to run for 15 min. Blanks and controls were run in the same manner but without irradiation and enzyme, respectively. The absorbance was measured at 560 nm. The unit of SOD activity (expressed as U g^{-1} h^{-1} FW) was defined as being present in the volume of extract that inhibited the NBT photoreduction by 50%.

The POD activity was measured by the method of guaiacol oxidation with guaiacol (Pan *et al.*, 2006) as the substrate in a total volume of 3 mL. The reaction mixture consisted of 50-mM potassium phosphate buffer (pH 6.1); 1% guaiacol; 0.4% H_2O_2 and enzyme extract. The reaction was initiated by the addition of H_2O_2, and changes in the absorbance at 470 nm were recorded for 2 min. Enzyme activity was calculated and expressed as µg g^{-1} min^{-1} FW.

The soluble protein content (expressed as mg g^{-1} FW) was quantified following the study conducted by Bradford (1976). For protein quantification, 1.0-mL extract was mixed with 5-mL Coomassie Brilliant Blue reagent, and vortexed for 30 s. The absorbance of the sample was recorded at 595 nm.

Determination of proline

The proline concentration (expressed as µg g^{-1} FW) was measured by acid ninhydrin colorimetry (Leyva *et al.*, 2011; Yin and Zhang, 2016). The radish root (0.2 g) sample was extracted with 3% sulfosalicylic acid (5 mL) in boiling water for 20 min. After centrifugation, the supernatant (2 mL) was mixed with acetic acid (3 mL) and acid ninhydrin (3 mL). The mixture was then taken into boiling water for 40 min. The cooled mixture was extracted with toluene (5 mL). The absorbance of the organic phase was determined at 520 nm using toluene as a blank.

Determination of As in radish

The total As content in radish roots, shoots and leaves was quantified by inductively coupled plasma mass spectrometry (ICP-MS; Agilent 7700x, USA). The sample pretreatment and detailed steps were performed according to the previously published method (Hu *et al.*, 2019). In brief, the pre-ground raw radish samples were mineralized with nitric acid to analyze total As content. Each sample was filtered through a 0.45-µm microfiltration membrane and stored at 4°C before ICP-MS analysis (Table 1).

Statistical Analysis

The data of biochemical index for radish samples were expressed as fresh weight. All assays were performed at least in triplicate. Data were summarized using mean values and standard deviations (SD) and analyzed statistically using analysis of variance (ANOVA) at a 95% confidence level (95% CL) using SPSS 19.0.

Table 1. Instrument parameter of inductively coupled plasma mass spectrometry (ICP-MS).

ICP-MS	
RF power	1,590 W
Ar plasma gas flow	15.0 L min^{-1}
Ar auxiliary gas flow	0.86 L min^{-1}
Ar nebulizer gas flow	1.0–1.1 L min^{-1}
He gas flow rate	4.2 mL min^{-1}
Spray chamber temperature	2°C
Isotopes monitored	^{75}As
Integration time per isotope for elemental analysis	100 ms
Acquisition mode for elemental analysis	Spectrum

Note: The full name of RF is radio-frequency power.

Results and Discussion

The growth characteristics of radish

Figure 1 shows the growth of radish in the control group, low Se treatment level (1Se) and high Se treatment level (24Se). It was observed that the growth of radish with organic Se source was better than that of inorganic Se source. In the Se(VI) treatment group, the growth of radish was significantly inhibited and root development was limited. It suggested that the organic Se (including Se-Y and Se-M) could significantly promote the growth of radish whereas the expected growth of radish was severely inhibited with the gradual increase of Se application in Se(VI) treatments. The present study suggests that the application of organic Se fertilizer was more beneficial for growth of plants than the application of inorganic Se fertilizer, which was consistent with previous reports (Surai and Dvorska, 2001; Wang and Lovell, 1997). Organic Se could effectively increase the content of organic matter and bioaccessible Se in the soil and improve the content of phosphorus and potassium to increase soil fertility and enhance the absorption and utilization of crop nutrients (Li *et al.,* 2017). Studies have demonstrated that using organic Se fertilizer could significantly improve the growth and nutritional quality of grapes, increase the Se content and reduce the accumulation of heavy metals (Zhu *et al.,* 2017).

In the current study, different exogenous Se had different effects on the growth of radish. The possible reason was that Se(IV) was slightly less mobile because of its ease of

Figure 1. Radish growth in the CK, 1Se and 24Se treatment groups with application of different Se sources: sodium selenite (Se(IV)), sodium selenate (Se(VI)), selenium yeast (Se-Y) and selenium malt (Se-M).

adsorption on the surface of soil particles whereas Se(VI) was more mobile and easily absorbed by plant roots within a short period; this caused the vegetable growth of radish to be limited. The two organic Se fertilizers applied to the soil were absorbed easily by the soil colloid and provided more organic nutrients. During plant growth, the fertilizer effect is gradually released through the action of microorganisms. Hence, the biomass of radish increased to varying degrees.

Characteristics of chlorophyll content in radish

Chlorophyll content determines plant's photosynthetic efficiency and is one of the crucial indicators reflecting the growth status of plants. As shown in Figure 2A, the chlorophyll content at 1Se and 3Se levels in the Se(IV) and Se(VI) treatment groups was significantly higher than the control group ($p < 0.05$), while it was opposite in the 24Se level.

Except for the 24Se level in the Se-M treatment group, the chlorophyll content in all organic Se treatments was higher than that in the control group ($p < 0.05$). With increase in the application of Se, the chlorophyll content of radish in the inorganic Se treatments decreased gradually, while that in the organic Se treatments increased in the beginning but decreased later. It was seen that the application of an appropriate amount of low Se concentration increased chlorophyll to improve the growth of radish, while the application of high Se concentration had an inhibitory effect on the growth of radish. Organic Se had a more pronounced effect on promoting radish growth than inorganic Se, and the tolerance concentration of radish to organic Se was higher than that of inorganic Se. Decrease of chlorophyll content in Se(VI) treatments depicted noticeable toxicological effects on radish growth. This could be related to different types of Se sources in the entire growth cycle of radish. Compared with organic Se, inorganic Se was characterized by immediate effect, short duration and vegetative growth stage. Higher concentrations of inorganic Se, especially Se(VI), inhibited the growth and development of radish, while Se nutrient deficiencies may exist during the reproductive growth stage. Hence, this could affect the chlorophyll content of radish to a certain extent.

Studies have established that the application of Se increased the chlorophyll content of wheat leaves, and the increase of chlorophyll content in the heading and flowering stages was higher than that in other stages (Chu *et al.,* 2013). Magnesium and nitrogen are the primary components of chlorophyll, while copper, zinc, manganese and iron are involved in the biosynthesis of chlorophyll. Under As stress, the chlorophyll content of plants was decreased. This happened after As had entered the plant body, and the decreased concentration of chlorophyll was associated with hindered biosynthesis, and was not due to degradation (Mishra *et al.*, 2016). Li *et al.* (2008) reported that As can replace Mg ions in chlorophyll molecules and interfere with the activity of chlorophyll synthetase, which hinders the synthesis of chlorophyll. The activity of chlorophyll enzymes is degraded and the chlorophyll is decomposed rapidly with the toxicity of As (Li *et al.,* 2008). In general, soil Se application could increase the level of chlorophyll synthesis by promoting the absorption of mineral elements related to chlorophyll synthesis by plant leaves (Yao *et al.,* 2009). Therefore, difference in the effects of different types of exogenous Se treatments on chlorophyll content in this study could be explained by different synergistic effects of various exogenous Se on mineral elements related to chlorophyll synthesis. Since the above results were only a reflection of the results of mature stage, the analysis of carotenoids in

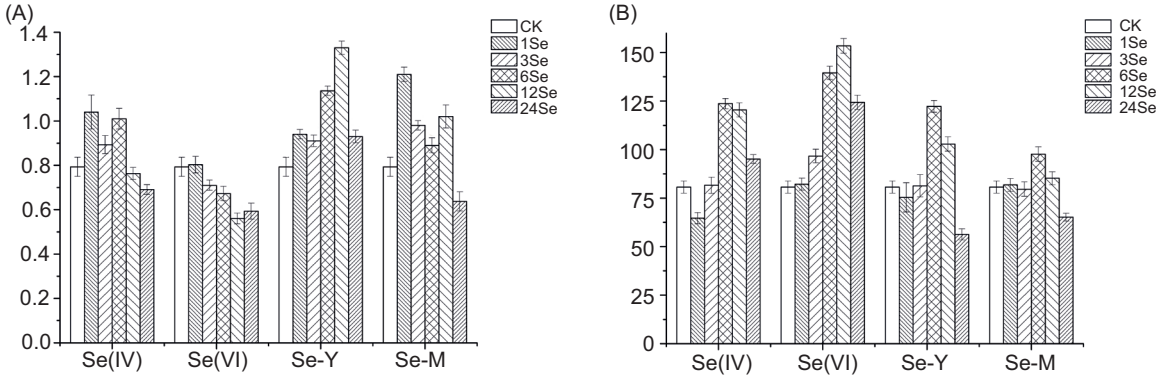

Figure 2. (A) Concentration of chlorophyll content in radish with application of different Se sources: sodium selenite (Se(IV)), sodium selenate (Se(VI)), selenium yeast (Se-Y) and selenium malt (Se-M) (mg kg^{-1} FW). (B) The MDA content in radish with application of different Se sources: sodium selenite (Se(IV)), sodium selenate (Se(VI)), selenium yeast (Se-Y) and selenium malt (Se-M) (mmol g^{-1} FW).

leaves and the dynamic monitoring of chlorophyll at different stages of growth of radish must be strengthened in the future studies.

Characteristics of MDA, SOD, POD, proline and soluble protein content in radish

The MDA content indicates the degree of lipid peroxidation caused by ROS, and the MDA content of each Se treatment group presented a trend of initial increase and subsequent decrease (Figure 2B). In organic Se treatment groups, the MDA content reached the highest value at 6Se level with 122.24 for Se-Y treatment and 97.67 for Se-M treatment. The MDA content decreased to the lowest at the 24Se level, which was significantly lower than in the control group ($p < 0.05$). MDA is the end product of lipid oxidation which aggravates membrane damage. MDA content can be used as an essential indicator of cell lipid peroxidation, biofilm damage and plant stress resistance (Zhu *et al.,* 2017).

The SOD activity at each level in the organic Se group was all higher than that in the control group ($p < 0.05$) (Figure 3A). In comparison with the control group, the highest value of SOD activity was in treatments of 6Se(IV), 1Se(VI), 12Se-Y and 6Se-M, which increased by 49.27%, 22.37%, 59.63% and 84.23%, respectively. The POD activity of Se(IV), Se-Y and Se-M treatment groups was higher than that of the control group ($p < 0.05$), while the Se(VI) group depicted the opposite trend (Figure 3B). In comparison to the control group, the highest value of POD activity was in 12Se(IV), 24Se-Y and 12Se-M treatments, which increased by 78.29%, 104.41% and 123.69%, respectively, while the lowest value of POD activity in Se(VI) was at 565.25 at 1Se level. Compared with the other three kinds of exogenous Se, Se(VI) evidently inhibited SOD, POD, proline and soluble protein in radish, depicting the toxicological effect of Se(VI) on radish. Both SOD and POD are antioxidant enzymes that scavenge excessive ROS in plants and protect cells from ROS poisoning, thus maintaining normal body metabolism.

The proline content initially increased in the Se(IV), Se-Y and Se-M treatment groups but decreased later, while in the Se(VI) treatment group, the proline content gradually increased with the increase of Se application levels (Figure 4A). In the Se(IV) treatment group, the proline content at the 3Se, 6Se and 12Se levels was significantly higher than that in the control group ($p < 0.05$). In the Se(VI) treatment group, the content of proline gradually decreased with the increase of Se content, but was lower than that in the control group ($p < 0.05$). The highest value of proline content was at 6Se level in Se-Y treatment group and at 12Se level in Se-M treatment group, which was 1.31 and 1.39 times, respectively, in comparison to the control group. It was reported that supplement Se could increase proline content in wheat (Khan *et al.,* 2015) and enhance its resistance because of regulatory interaction between ethylene, proline and g*lutathione* (gamma-glutamyl-cysteinyl-glycine [GSH]) metabolism.

The soluble protein content of Se(IV), Se-Y and Se-M treatment groups was significantly higher than that of the control group ($p < 0.05$) (Figuire 4b). There was no significant difference in the soluble protein content of each Se application level in the Se(IV) treatment group, while the Se-Y and Se-M treatments demonstrated a gradual increasing trend. The soluble protein content of the Se(VI) treatment group was significantly lower than that in the control group at high Se levels (12Se and 24Se levels; $p < 0.05$).

The above results indicate that resistance to As-contaminated radish varies with the application of

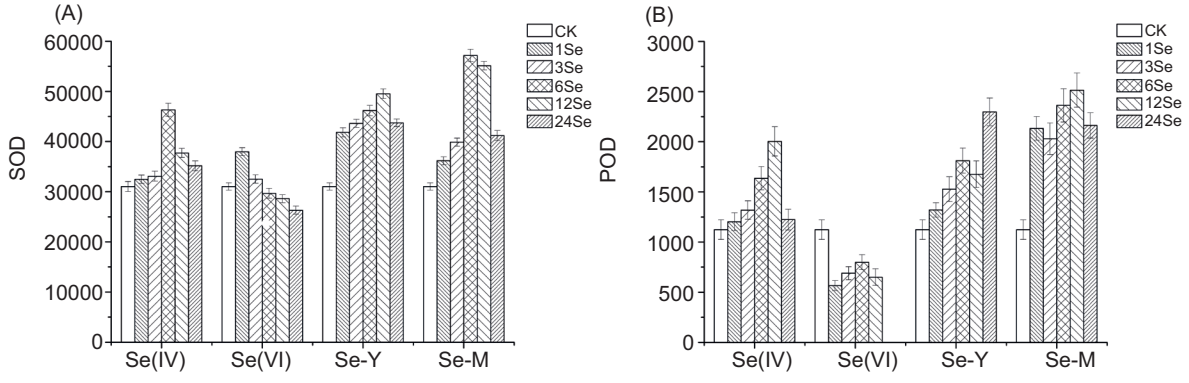

Figure 3. (A) The superoxide dismutase (SOD) activity in radish with application of different Se sources: sodium selenite (Se(IV)), sodium selenate (Se(VI)), selenium yeast (Se-Y) and selenium malt (Se-M) (U g^{-1} h^{-1} FW). (B) The peroxidase activity in radish with application of different Se sources: sodium selenite (Se(IV)), sodium selenate (Se(VI)), selenium yeast (Se-Y) and selenium malt (Se-M) (μg g^{-1} min^{-1} FW).

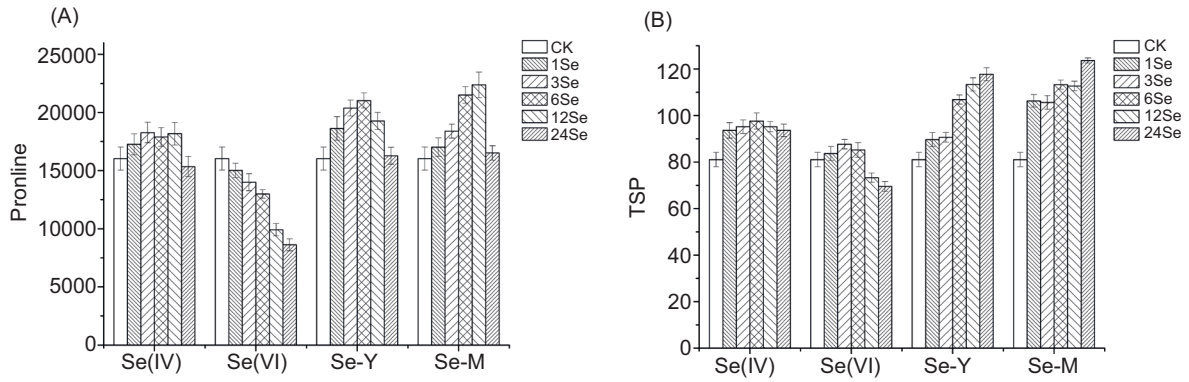

Figure 4. (A) The proline content in radish with application of different Se sources: sodium selenite (Se(IV)), sodium selenate (Se(VI)), selenium yeast (Se-Y) and selenium malt (Se-M) (μg g^{-1} FW). (B) The soluble protein content in radish with application of different Se sources: sodium selenite (Se(IV)), sodium selenate (Se(VI)), selenium yeast (Se-Y) and selenium malt (Se-M) (mg g^{-1} FW).

organic Se and Se(IV). It was observed that after Se was absorbed by radish, it participated in its metabolism and effectively enhanced the resistance of radish contaminated with As. However, its stress resistance varied with different forms of exogenous Se and its application level. Generally, Se is primarily involved in the antioxidant effect of plants in GSH-Px, and regulates the activities of various enzymes in plants and the synthesis of macromolecular substances such as proteins. It was reported that the CAT and POD activities, and proline and chlorophyll content, were significantly increased, while MDA content of wheat seedlings decreased with 1.0-, 2.0- and 3.0-mg Se kg^{-1} treatment (Yao *et al.,* 2009). Application of low Se concentrations (5 and 10 μM) enhanced proline accumulation and antioxidative activity in cucumber seedlings (Hawrylak-Nowak, 2009).

The previous study indicated that application of Se significantly improved the proline, chlorophyll and protein content but reduced the MDA content in rice seedlings subjected to As stress (Pandey and Gupta, 2015). The observations indicated that seedlings supplemented only with As depicted inhibition in growth parameters. However, the application of Se improved the growth of rice seedlings, level of stress indicators (chlorophyll, protein and MDA content) and modulators (cysteine and proline) as compared to the individual treatment of As. The above reports indicated that Se treatment could enhance the resistance of plants to a certain extent.

In the present study, the MDA content in radish was higher than that in the control group with some treatments, indicating an increase in the activity and content of GSH-Px in radish by Se application, but was not enough to offset the As damage to plant cells. It was reported that adding the appropriate amount of Se (0.1 mg L^{-1}) could reduce the toxicity of high-dose As (5 mg L^{-1}) (Han *et al*., 2015). Low Se levels (0.1 mg L^{-1}) reduce the toxicity of high As levels (5 mg L^{-1}) by regulating the antioxidant system of flue-cured tobacco by reducing the transfer of As(III) from the root to the aerial part of the flue-cured tobacco (FCT), thereby promoting FCT growth.

Pandey and Gupta (2018) reported that Se supplementation could significantly reduce the content of H_2O_2, NO and ROS in rice. Se supplementation alleviated the toxicity of As and restored the nutritional deficiency of rice induced by As. Besides, Se treatment increased the activity of thiol metabolism-related enzymes. Yeh *et al.* (2003) reported that the mechanism of Se alleviating the toxicity of As was because Se could regulate glutathione peroxidase (GPX) activity. Malik *et al.* (2012) reported that Se could effectively inhibit the As absorption of mung bean plants, enhance their antioxidant and anti-stress properties, and alleviate the toxic effects of As on the stated plants. Plants treated with Se were also less affected by As-induced cell membrane, chlorophyll and cell viability.

In terms of the mechanism of Se alleviating the toxicity of As, following could be the different reasons: First, Se is involved in regulating antioxidant enzyme activity in plants. Se, as a component of seleno-enzyme activity centers such as GPX, can catalyze GSH to reduce peroxides in plants and participate in the scavenging of free radicals in plants, improve antioxidant enzymes such as SOD, POD, CAT, GPX, ascorbate peroxidase (APX) and dehydroascorbate reductase (DHAR) in plants, thus improving the antioxidant capacity and resistance to adversity in plants. Second, to a certain extent, Se may participate in energy and protein metabolism and interaction with other elements, or Se increases metallothionein (MTs), thiol and glutathione-s-transferase (GST) activity in the plant. Third, Se and As may produce a stable As–Se

complex with low toxicity in plants, thus inhibiting the antioxidant damage caused by As in plants.

Quantify the As content in roots, shoots and leaves of radish

As shown in Figure 5, the content of As in roots, stems and leaves of radish was 3.93, 2.70, 1.61 mg kg^{-1}, respectively, in the control group. The distribution characteristics of As content in radish was: roots > stems > leaves. From bottom to top, the As content depicted a decreasing trend. This pattern was entirely consistent with the results reported by Carbonell-Barrachina *et al.* (1999) and Smith *et al.* (2009). The content of As in the roots of plants was more significant than that in the upper part of the ground, which was due to the binding of As by phytochelatins, which restrict the upward migration of As (Smith *et al.*, 2009). The content of As in radish in the Se(IV), Se(VI), Se-Y, Se-M treatment groups was lower than that in the control group, which indicated that Se could significantly mimic the absorption of As in radish. In the Se(IV) treatment group, the content of As in the root of each treatment's radish depicted the initial decreasing and then increasing trend. However, the content of As in radish stems depicted a decreasing trend with the increase of Se application, while As in radish leaves depicted an initial increasing and then decreasing trend (Figure 5A). The Se(VI) treatment group indicated apparent toxicological effects of Se and inhibited the growth of radish roots, so the data were missed. The As content in radish leaves and stems at each treatment level demonstrated a gradually decreasing trend in Se(VI) treatment, while the As content in leaves, stems and roots at each treatment level gradually decreased in Se-Y treatments (Figures 5B and C). In Se-M treatments, the distribution characteristics of the As content in roots, stems and leaves of radish tissues indicated a gradually decreasing trend with increased Se application (Figure 5D). The present study demonstrated that the application of Se(IV) and organic Se could alleviate the toxicological effects of As better than Se(VI). This result was consistent with the literature report (Camara *et al.*, 2018). This could be because Se and As stimulated the response of plant antioxidant enzyme activities, thereby changing the translocation of heavy metal elements (Feng *et al.*, 2013).

The relationship between different amounts of exogenous Se application and As in radish leaves, stems and roots is shown in Figures S2–S4 (Support Material). The content

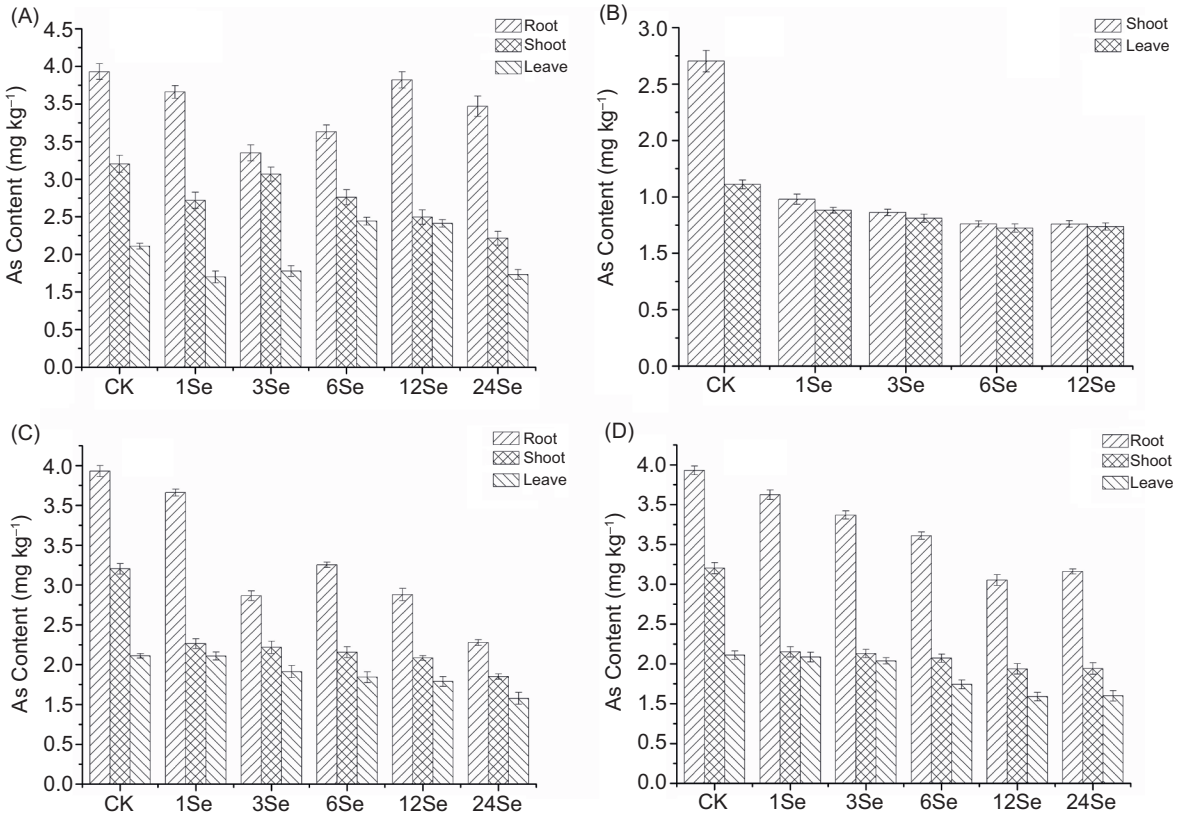

Figure 5. Arsenic concentration in radish roots, shoots and leaves with application of different Se sources: (A) sodium selenite (Se(IV)), (B) sodium selenate (Se(VI)), (C) selenium yeast (Se-Y) and (D) selenium malt (Se-M).

of As in the roots of Se-Y treatment and the amount of Se added depicted a good correlation. The correlation coefficient R^2 was 0.9393, which was better than the linear fitting degree of Se-M and Se(IV) treatments. The curve trend represents the changing trend of As content with increase in Se application. The As content in shoots with each Se treatment depicted a decreasing trend with increasing amount of Se application. The fitting curve coefficients of Se(IV), Se(VI), Se-Y and Se-M treatments were good. The values were 0.88396, 0.98976, 0.96823 and 0.9055, respectively. In Se(IV) treatment, the changing trend of As in leaves depicted an initial increase and then decrease with the increased application of Se, while the other three Se treatments depicted a decreasing trend.

Correlation analysis

In Se(IV) treatments, the As content in roots was significantly negatively correlated with the As content in stems (–0.544, $p < 0.05$) (Support Material, Table S1). This indicates that As content has a competitive effect on roots and stems, possibly because of As and Se interaction, which limits the migration of As from roots to stems. The content of As in roots was significantly positively correlated with SOD activity and soluble protein content but was significantly negatively correlated with chlorophyll content. In Se(VI) treatments, the As content in stems and leaves was significantly positively correlated (0.853, $p < 0.01$) (Support Material, Table S2). In Se-Y treatments, the As content in roots was significantly negatively correlated with POD activity and soluble protein content (Support Material, Table S3). In Se-M treatments, the As content in roots was significantly positively correlated with the As content in stems and leaves. The content of As in roots was significantly negatively correlated with SOD (–0.596, $p < 0.05$) but significantly positively correlated with chlorophyll content (0.612, $p < 0.05$) (Support Material, Table S4). The above results demonstrate that after adding different concentrations of exogenous Se, the correlation between radish As content and plant enzymes is not entirely consistent. This is due to differences in the properties of different Se sources, leading to different chemical and biological effects of As and microorganisms on soil and plants. The results of ANOVA (Table 2) established that different Se sources, Se levels and their interaction factors have incredibly significant effects on As content and enzyme activities in various tissues of radish.

Conclusion

In this study, the influence of inorganic Se and organic Se was studied on the growth, physiological indexes and characteristic of As content on radish plant under As stress. The study demonstrated that supplementing Se at lower concentrations helped to improve the defense ability of radish against As toxicity. The results established that, except for Se(VI), the other three exogenous Se (including Se(IV), Se-Y and Se-M) improved stress resistance in radish. Compared with inorganic Se treatment, organic Se treatment efficiently hindered the absorption of As in radish. Applying organic Se was more beneficial to radish growth than inorganic Se, while the application of Se(VI) demonstrated a significant toxic effect. It was observed that the agronomic effects of different exogenous Se applications were different, which provided a corresponding research basis for applying agricultural soil and crop Se fertilizer. At the same time, it provided related supporting material for the further development of As–Se interaction mechanism. Subsequent research on the mechanism of interaction between As and Se is required to provide theoretical basis for applying Se fertilizer and As pollution control in agriculture.

Acknowledgments

This work was financially supported by the National Key Research and Development Program of China (2017YFD0800900); National Natural Science Foundation of China (42162023); the Natural Science Foundation Project of Jiangxi Provincial Department of Science and Technology (20212BAB204042); College

Table 2. Analysis of two-factor variance of arsenic content and plant enzymes on radish tissues.

Factors	Significance							proline	Chlorophyll
	As content in roots	As content in shoots	As content in leaves	MDA	SOD	POD	Soluble protein		
Se source	**	**	**	**	**	**	**	**	**
Se content	**	**	**	**	**	**	**	**	**
Se source × Se content	**	**	**	**	**	**	**	**	**

$n = 15$, $^{**}p < 0.01$.
Abbreviation: selenium (Se), arsenic (As), malondialdehyde (MDA), superoxide dismutase (SOD), peroxidase (POD).

Students Innovation and Entrepreneurship Training Program of Jiangxi Province in 2020 (S202011319002); Teaching Reform Research Project of Nanchang Institute of Technology in 2020 (2020JG017); the Jiangxi Provincial Key Scientific Research Plan (20203BBGL73220); Research Foundation of Education Bureau of Jiangxi Province, China (GJJ201904); and Water Science and Technology Fund of Jiangxi Province in China (202124ZDKT15).

Conflict of Interest

There was no conflict of interest to disclose among authors.

References

Bai J.H., Liu J.H., Zhang N., Yang J.H., Sa R.L., and Wu L. 2013. Effect of alkali stress on soluble sugar, antioxidant enzymes and yield of oat. J Integr Agric. 12(8):1441–1449. https://doi.org/10.1016/S2095-3119(13)60556-0

Beauchamp C. and Fridovich I. 1971. Superoxide dismutase: improved assays and an assay applicable to acrylamide gels. Anal Biochem. 44(1):276–287. https://doi.org/10.1016/0003-2697(71)90370-8.

Bradford M.M. 1976. A rapid and sensitive method for the quantitation of microgram quantities of protein utilizing the principle of protein-dye binding. Anal Biochem. 72(1–2):248–254. https://doi.org/10.1016/0003-2697(76)90527-3

Camara A.Y., Wan Y., Yu Y., Wang Q., and Li H. 2018. Effect of selenium on uptake and translocation of arsenic in rice seedlings (*Oryza sativa L.*). Ecotoxicol Environ Saf. 148:869–875. https://doi.org/10.1016/j.ecoenv.2017.11.064

Carbonell-Barrachina A., Burlo F., and Valero D.1999. Arsenic toxicity and accumulation in turnip as affected by arsenic chemical speciation. J Agric Food Chem. 47(6):2288–2294. https://doi.org/10.1080/03601239909373220

Chu J., Yao X., Yue Z., Li J., and Zhao J. 2013. The effects of selenium on physiological traits, grain selenium content and yield of winter wheat at different development stages. Biol Trace Elem Res. 151(3):434–440. https://doi.org/10.1007/s12011-012-9575-6

Dahal B.M., Fuerhacker M., Mentler A., Shrestha R.R., and Blum W.E. 2008. Screening of arsenic in irrigation water used for vegetable production in Nepal. Arch Agron Soil Sci. 54(1):41–51. https://doi.org/10.1080/03650340701628197

Diao M., Ma L., Wang J., Cui J., Fu A., and Liu H.Y. 2014. Selenium promotes the growth and photosynthesis of tomato seedlings under salt stress by enhancing chloroplast antioxidant defense system. J Plant Growth Regul. 33(3):671–682. https://doi.org/10.1007/s00344-014-9416-2

Dong Y., Gao M., and Qiu W., 2021. Uptake of microplastics by carrots in presence of As (III): combined toxic effects. J Hazard Mater. 411(1):125055. https://doi.org/10.1016/j.jhazmat.2021.125055

Fendorf S., Michael H.A., and Van Geen A. 2010. Spatial and temporal variations of groundwater arsenic in south and southeast asia. Science. 328(5982):1123–1127. https://doi.org/10.1126/science.1172974

Feng R., Wei C., and Tu S. 2013. The roles of selenium in protecting plants against abiotic stresses. Environ Exp Bot. 87(87):58–68. https://doi.org/10.1016/j.envexpbot.2012.09.002

Han D., Xiong S., Tu S., Liu J., and Chen C. 2015. Interactive effects of selenium and arsenic on growth, antioxidant system, arsenic and selenium species of *Nicotiana tabacum L.* Environ Exp Bot. 117:12–19. https://doi.org/10.1016/j.envexpbot.2015.04.008

Hashemi A., Abdolzadeh A., Sadeghipour H.R. 2010. Beneficial effects of silicon nutrition in alleviating salinity stress in hydroponically grown canola, *Brassica napus L.*, plants. Soil Sci Plant Nutr. 56(2):44–253. https://doi.org/10.1111/j.1747-0765.2009.00443.x

Hawrylak-Nowak B. 2009. Beneficial effects of exogenous selenium in cucumber seedlings subjected to salt stress. Biol Trace Elem Res. 132(1–3):259–269. https://doi.org/10.1007/s12011-009-8402-1

Hu L., Fan H.B., Wu D.S., Liao Y.C., Shen F.F., Liu W.F., Huang R.Z., Zhang B.J., and Wang X.L. 2020. Effects of selenium on antioxidant enzyme activity and bioaccessibility of arsenic in arsenic-stressed radish. Ecotoxicol Environ Saf. 200:110768. https://doi.org/10.1016/j.ecoenv.2020.110768

Hu L., Wang X.L., Wu D.S., Zhang B.J., Fan H.B., Shen F.F., Liao Y.C., Huang X.P., and Gao G.Q. 2021. Effects of organic selenium on absorption and bioaccessibility of arsenic in radish under arsenic stress. Food Chem. 344:128614. https://doi.org/10.1016/j.foodchem.2020.128614

Hu L., Zhang B.J., Wu D.S., Fan H.B., Tu J., Liu W.F., Huang R.Z., and Huang X.P. 2019. Estimation of arsenic bioaccessibility in raw and cooked radish using simulated in vitro digestion. Food Funct. 10:1426–1432. https://doi.org/10.1039/C8FO02003E

Huang R.Q., Gao S.F., Wang W.L., Staunton S., and Wang G. 2006. Soil arsenic availability and the transfer of soil arsenic to crops in suburban areas in Fujian Province, southeast China. Sci Total Environ. 368(2–3):531–541. https://doi.org/10.1016/j.scitotenv.2006.03.013

Khan M.I.R., Nazir F., Asgher M., Per T.S., and Khan N.A. 2015. Selenium and sulfur influence ethylene formation and alleviate cadmium-induced oxidative stress by improving proline and glutathione production in wheat. J Plant Physiol. 173:9–18. https://doi.org/10.1016/j.jplph.2014.09.011

Kramárová Z., Fargašová A., Molnárová M., and Bujdoš M. 2012. Arsenic and selenium interactive effect on alga *Desmodesmus quadricauda*. Ecotoxicol Environ Saf, 86:1–6. https://doi.org/10.1016/j.ecoenv.2012.08.028

La Porte P.F. 2011. Selenium in the detoxification of arsenic: mechanisms and clinical efficacy. PhD Dissertation, The University of Chicago, Chicago, IL.

Leyva R., Sánchez-Rodríguez E., Ríos J.J., Rubio-Wilhelmi M.M., Romero L., Ruiz J.M., and Blasco B. 2011. Beneficial effects of exogenous iodine in lettuce plants subjected to salinity stress. Plant Sci. 181(2):195–202. https://doi.org/10.1016/j.plantsci.2011.05.007

Li Z., Liang D., Peng Q., Cui Z., Huang J., and Lin Z. 2017. Interaction between selenium and soil organic matter and its impact on soil selenium bioavailability: a review. Geoderma. 295:69–79. https://doi.org/10.1016/j.geoderma.2017.02.019

Li S.F., Pu H.P., and Wang H.B. 2008. Advances in the study of effects of arsenic on plant. Photosynthesis Soils 3:6–12. https://doi.org/10.1002/path.1700340417

Malik J.A., Goel S., Kaur N., Sharma S., Singh I., and Nayyar H. 2012. Selenium antagonises the toxic effects of arsenic on mungbean (*Phaseolus aureus Roxb.*) plants by restricting its uptake and enhancing the antioxidative and detoxification mechanisms. Environ Exp Bot. 77:242–248. https://doi.org/10.1016/j.envexpbot.2011.12.001

Mcbride M.B. 2013. Arsenic and lead uptake by vegetable crops grown on historically contaminated orchard soils. Appl Environ Soil Sci. 10:1–8. https://doi.org/10.1155/2013/283472

Meng M., Huang X.F., Li L., Luo Y.C., and Wang W.S. 2017. Effects of arsenic stress on activities of antioxidant enzymes of eucalyptus. Genomics Appl Biol. 12:79–85.

Mishra S., Alfeld M., Sobotka R., Andresen E., Falkenberg G., and Küpper H. 2016. Analysis of sublethal arsenic toxicity to ceratophyllum demersum: subcellular distribution of arsenic and inhibition of chlorophyll biosynthesis. J Exp Bot. 67(15):4639–4646. https://doi.org/10.1093/jxb/erw238

Pan Y., Wu L.J., and Yu Z.L. 2006. Effect of salt and drought stress on antioxidant enzymes activities and SOD isoenzymes of liquorice (*Glycyrrhiza uralensis Fisch*). Plant Growth Regul. 49(2–3):157–165. https://doi.org/10.1007/s10725-006-9101-y

Pandey C. and Gupta M. 2015. Selenium and auxin mitigates arsenic stress in rice (*Oryza sativa L.*) by combining the role of stress indicators, modulators and genotoxicity assay. J Hazard Mater. 287:384–391. https://doi.org/10.1016/j.jhazmat.2015.01.044

Pandey C. and Gupta M. 2018 Selenium amelioration of arsenic toxicity in rice shows genotypic variation: a transcriptomic and biochemical analysis. J Plant Physiol, 231:168–181. https://doi.org/10.1016/j.jplph.2018.09.013

Pedrero Z., Madrid Y., and Cámara C. 2006. Selenium species bioaccessibility in enriched radish (*Raphanus sativus*): a potential dietary source of selenium. J Agric Food Chem. 54(6):2412–2417. https://doi.org/10.1021/jf052500n

Praveen A., Khan E., Ngiimei D.S., Perwez, M., Sardar M., and Gupta M. 2018. Iron oxide nanoparticles as nano-adsorbents: a possible way to reduce arsenic phytotoxicity in Indian mustard plant (*Brassica juncea L.*). J Plant Growth Regul. 37:612–624. https://doi.org/10.1007/s00344-017-9760-0

Rayman M.P. 2005. Selenium in cancer prevention: a review of the evidence and mechanism of action. Proc Nutr Soc. 64(4):527–542. https://doi.org/10.1007/s00203-002-0478-3

Sae-Lee N., Kerdchoechuen O., and Laohakunjit N. 2012. Chemical qualities and phenolic compounds of Assam tea after soil drench application of selenium and aluminium. Plant Soil. 356(1–2):381–393. https://doi.org/10.1007/s11104-012-1139-1

Shri M., Kumar S., Chakrabarty D., Trivedi P.K., Mallick S., Misra P., and Tuli R. 2009. Effect of arsenic on growth, oxidative stress, and antioxidant system in rice seedlings. Ecotoxicol Environ Saf. 72(4):1102–1110. https://doi.org/10.1016/j.ecoenv.2008.09.022

Silva A.J., Nascimento C.W., Neto G., da Silva A., and Silva Junior E.A. 2015. Effects of silicon on alleviating arsenic toxicity in maize plants. Revista Brasileira de Ciência do Solo. 39(1):289–296. https://doi.org/10.13140/RG.2.1.1934.7364

Smith E., Juhasz A.L., and Weber J. 2009. Arsenic uptake and speciation in vegetables grown under greenhouse conditions. Environ Geochem Health. 31(1):125–132. https://doi.org/10.1007/s10653-008-9242-1

Su D., Li Y., and Gladyshev V.N. 2005. Selenocysteine insertion directed by the 3′-UTR SECIS element in *Escherichia coli*. Nucleic Acids Res. 33(8):2486–2492. https://doi.org/10.1093/nar/gki547

Surai P. and Dvorska J. 2001. Is organic selenium better for animals than inorganic sources? Feed Mix. 9(5):8–10.

Tripathi P., Mishra A., Dwivedi S., Chakrabarty D., Trivedi P.K., Singh R.P., and Tripathi R.D. 2012. Differential response of oxidative stress and thiol metabolism in contrasting rice genotypes for arsenic tolerance. Ecotoxicol Environ Saf. 79:189–198. https://doi.org/10.1016/j.ecoenv.2011.12.019

Wang C. and Lovell R.T. 1997. Organic selenium sources, selenomethionine and selenoyeast, have higher bioavailability than an inorganic selenium source, sodium selenite, in diets for channel catfish (*Ictalurus punctatus*). Aquaculture. 152(1–4):223–234. https://doi.org/10.1016/S0044-8486(96)01523-2

Wu M.L., Li H.H., Jia Y.Y., Yang L.T., and Wang G. 2015. Influence of arsenic stress on the photosynthetic pigments and chlorophyll fluorescence characteristics of different tobacco cultivars. Asian J Ecotoxicolo. 10(3):216–223.

Yao X., Chu J., and Wang G. 2009. Effects of selenium on wheat seedlings under drought stress. Biol Trace Elem Res. 130(3):283–290. https://doi.org/10.1007/s12011-009-8328-7

Yeh J.Y., Cheng L.C., Liang Y.C., and Ou B.R. 2003. Modulation of the arsenic effects on cytotoxicity, viability, and cell cycle in porcine endothelial cells by selenium. Endothelium. 10(3):127–139. https://doi.org/10.1080/713715229

Yin B.F. and Zhang Y.M. 2016. Physiological regulation of *Syntrichia caninervis Mitt.* in different microhabitats during periods of snow in the gurbantünggüt desert, northwestern China. J Plant Physiol. 194:13–22. https://doi.org/10.1016/j.jplph.2016.01.015.

Zeng X.B., Li L.F., and Mei X.R. 2008. Heavy metal content in Chinese vegetable plantation land soils and related source analysis. Agric Sci China. 7(9):1115–1126. https://doi.org/10.1016/S1671-2927(08)60154-6

Zheng X.M, Zhang Z.Y, Chen J.C., Liang H.T., Chen X., Qin Y. 2022. Comparative evaluation of *in vivo* relative bioavailability and *in vitro* bioaccessibility of arsenic in leafy vegetables and its implication in human exposure assessment. J Hazard Mater. 423:126909. https://doi.org/10.1016/j.jhazmat.2021.126909

Zhu S., Liang Y., Gao D., An X., and Kong F. 2017. Spraying foliar selenium fertilizer on quality of table grape (*Vitis vinifera L.*) from different source varieties. Sci Hortic. 218:87–94. https://doi.org/10.1016/j.scienta.2017.02.025

Supplementary

Figure S1. Pot experiment of radish with different Se sources application of sodium selenite (Se(IV)), sodium selenate (Se(VI)), selenium yeast (Se-Y) and selenium malt (Se-M).

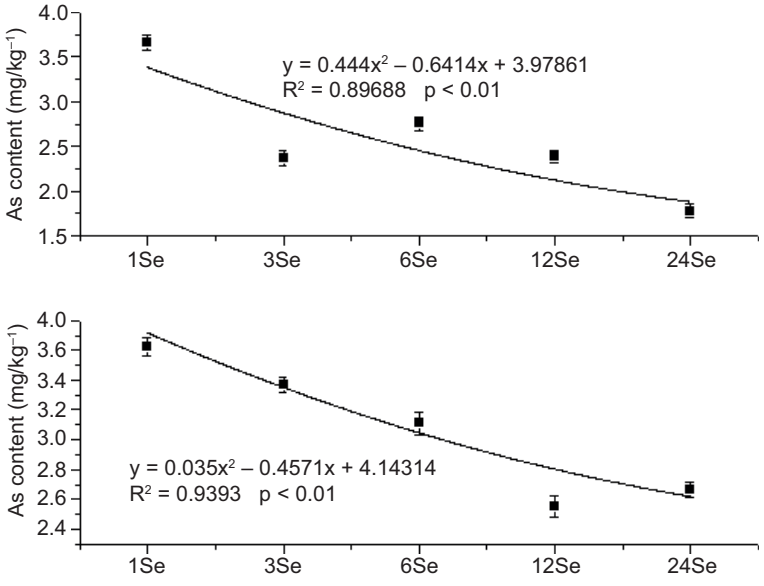

Figure S2. Relationship between arsenic content in radish roots and the adding amount of exogenous selenium of sodium selenite (Se(IV)), sodium selenate (Se(VI)), selenium yeast (Se-Y) and selenium malt (Se-M).

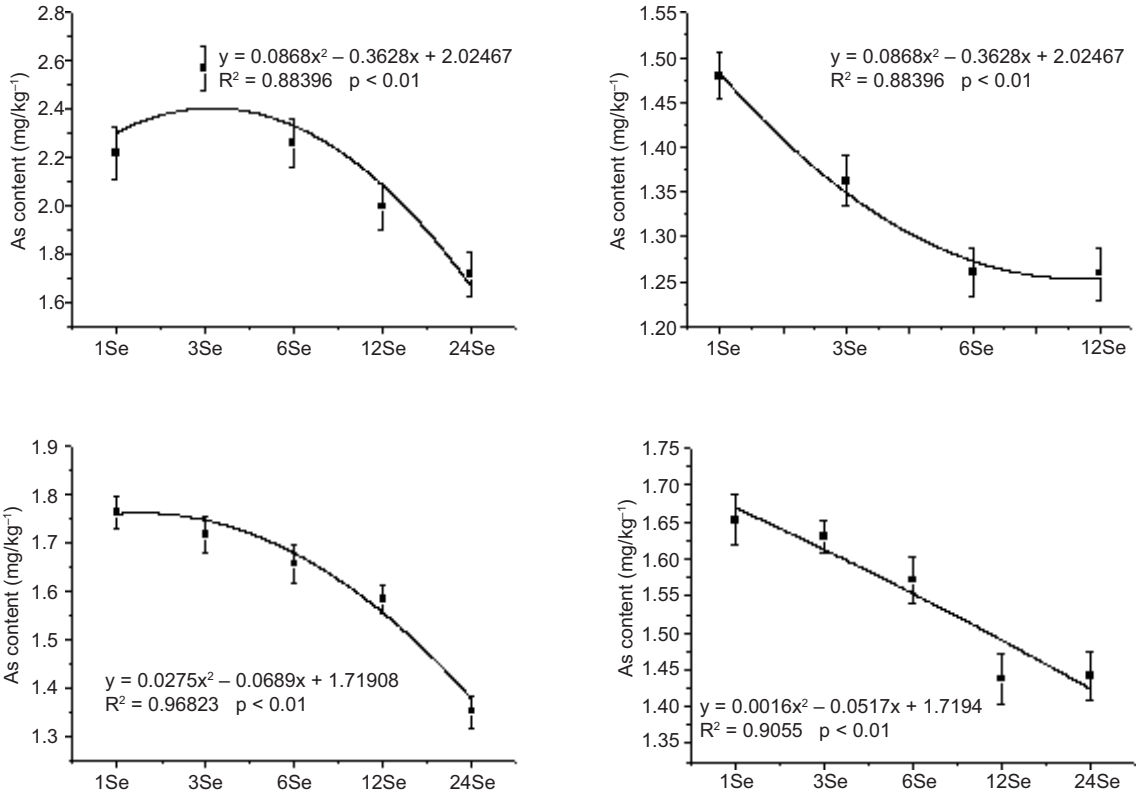

Figure S3. Relationship between arsenic content in radish shoot and the adding amount of exogenous selenium of sodium selenite (Se(IV)), sodium selenate (Se(VI)), selenium yeast (Se-Y) and selenium malt (Se-M).

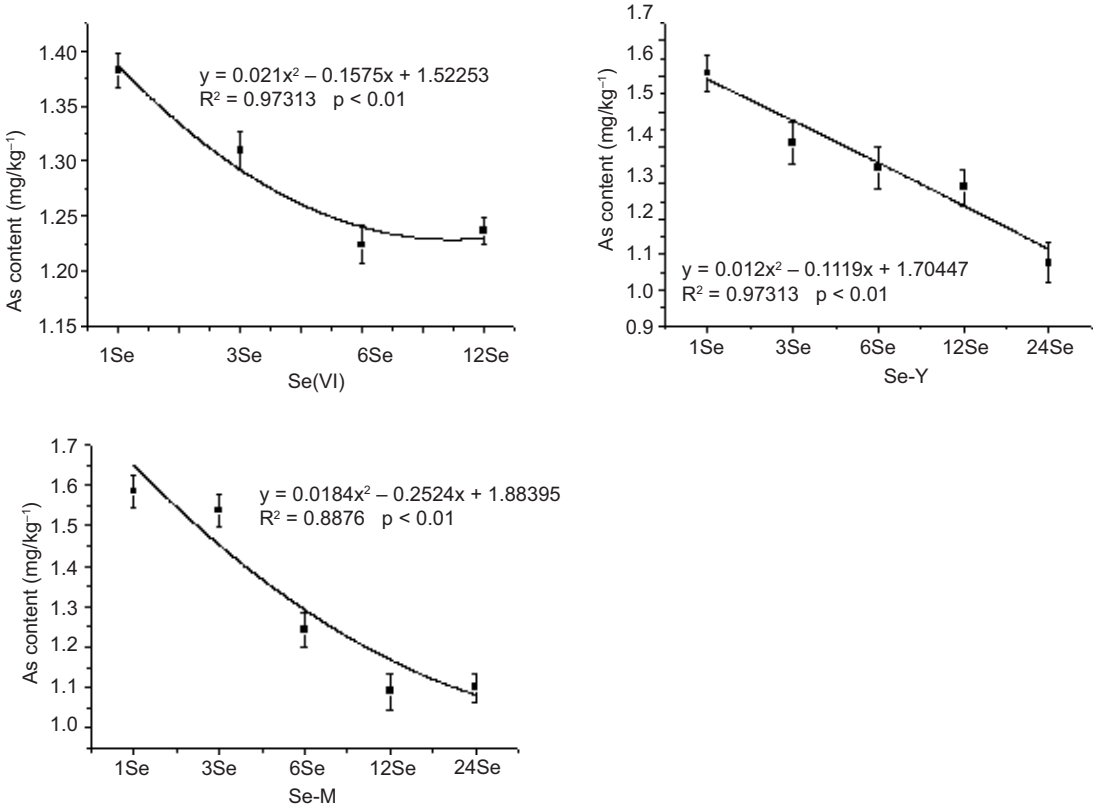

Figure S4. Relationship between arsenic content in radish leaves and the adding amount of exogenous selenium of sodium selenite (Se(IV)), sodium selenate (Se(VI)), selenium yeast (Se-Y) and selenium malt (Se-M).

Table S1. Correlation between arsenic and plant enzymes in radish after addition of selenite (Se(IV)) (*n* = 15).

	As content in roots	As content in shoots	As content in leaves	MDA	SOD	POD	Soluble protein	Proline	Chlorophyll
As content in roots	1								
As content in shoots	–0.544*	1							
As content in leaves	0.131	–0.002	1						
MDA	0.180	–0.198	0.959**	1					
SOD	–0.158	–0.002	0.830**	0.865**	1				
POD	0.351	–0.024	0.901**	0.848**	0.540*	1			
Soluble protein	–0.173	0.365	0.522*	0.430	0.539*	0.425	1		
Proline	–0.093	0.736**	0.478*	0.293	0.236	0.542*	0.582*	1	
Chlorophyll	–0.318	0.871**	–0.222	–0.427	–0.194	–0.255	0.223	0.581*	1

**It represents a significant correlation at the 0.01 level (one-sided). *It represents a significant correlation at the 0.05 level (one-sided).
Abbreviation: selenium (Se), arsenic (As), malondialdehyde (MDA), superoxide dismutase (SOD), peroxidase (POD).

Table S2. Correlation between arsenic and plant enzymes in radish after addition of selenate (Se(VI)) (*n* = 15).

	As content in shoots	As content in leaves	MDA	SOD	POD	Soluble protein	Proline	Chlorophyll
As content in shoots	1							
As content in leaves	0.853**	1						
MDA	–0.888**	–0.856**	1					
SOD	0.973**	0.918**	–0.950**	1				
POD	–0.580*	–0.593*	0.491	–0.537*	1			
Soluble protein	0.396	0.386	–0.609*	0.522*	0.324	1		
Proline	0.777**	0.720**	–0.884**	0.858**	–0.117	0.846**	1	
Chlorophyll	0.916**	0.808**	–0.865**	0.937**	–0.338	0.644*	0.923**	1

**It represents a significant correlation at the 0.01 level (one-sided). *It represents a significant correlation at the 0.05 level (one-sided).
Abbreviation: selenium (Se), arsenic (As), malondialdehyde (MDA), superoxide dismutase (SOD), peroxidase (POD).

Table S3. Correlation between arsenic and plant enzymes in radish after addition of selenium yeast (Se-Y) (*n* = 15).

	As content in roots	As content in shoots	As content in leaves	MDA	SOD	POD	Soluble protein	Proline	Chlorophyll
As content in roots	1								
As content in shoots	0.772**	1							
As content in leaves	0.885**	0.861**	1						
MDA	0.229	0.401	0.198	1					
SOD	–0.313	–0.157	–0.277	0.647**	1				
POD	–0.777**	–0.847**	–0.846**	–0.209	0.211	1			
Soluble protein	–0.687**	–0.806**	–0.827**	0.072	0.596**	0.844**	1		
Proline	0.332	0.691**	0.477*	0.810**	0.345	–0.414	–0.354	1	
Chlorophyll	–0.142	–0.029	–0.161	0.723**	0.952**	0.031	0.503*	0.357	1

**It represents a significant correlation at the 0.01 level (one-sided). *It represents a significant correlation at the 0.05 level (one-sided).
Abbreviation: selenium (Se), arsenic (As), malondialdehyde (MDA), superoxide dismutase (SOD), peroxidase (POD).

Table S4. Correlation between arsenic and plant enzymes in radish after addition of malt selenium (Se-M) (*n* = 15).

	As content in roots	As content in shoots	As content in leaves	MDA	SOD	POD	Soluble protein	Proline	Chlorophyll
As content in roots	1								
As content in shoots	0.872**	1							
As content in leaves	0.949**	0.893**	1						
MDA	0.237	0.372	0.132	1					
SOD	–0.543*	–0.383	–0.619**	0.663**	1				
POD	–0.530*	–0.297	–0.513*	0.525*	0.786**	1			
Soluble protein	–0.730**	–0.596**	–0.746**	–0.395	0.219	0.301	1		
Proline	–0.368	–0.142	–0.355	0.764**	0.903**	0.837**	–0.044	1	
Chlorophyll	0.617**	0.710**	0.620**	0.578*	0.042	–0.077	–0.638**	0.257	1

**It represents a significant correlation at the 0.01 level (one-sided). *It represents a significant correlation at the 0.05 level (one-sided).
Abbreviation: selenium (Se), arsenic (As), malondialdehyde (MDA), superoxide dismutase (SOD), peroxidase (POD).

Italian Journal of Food Science, 2022; 34 (1): 59–66

Quality of frozen stored flavoured olive oils

Giacomo Squeo[1]*, Graziana Difonzo[1], Antonietta Baiano[2], Roccangelo Silletti[1], Antonella Pasqualone[1], Carmine Summo[1], and Francesco Caponio[1]

[1]Department of Soil Plant and Food Sciences, University of Bari "Aldo Moro", Via Amendola, Bari, Italy; [2]Dipartimento di Scienze Agrarie, Alimenti, Risorse Naturali e Ingegneria (DAFNE), University of Foggia, Via Napoli, Foggia, Italy

***Corresponding Author:** Giacomo Squeo, Department of Soil Plant and Food Sciences, University of Bari "Aldo Moro", Via Amendola, Bari, Italy. Email: giacomo.squeo@uniba.it

Received: 2 December 2021; Accepted: 11 January 2022; Published: 27 January 2022

PAPER

Abstract

The purpose of the current research was to study the effects of 6-month frozen storage on the quality parameters and the phenolic profiles of flavoured olive oils (FOO) produced by co-malaxation or infusion using basil, chilli, or chilli–garlic as flavouring ingredients. The results demonstrated that during frozen storage, FOOs underwent degradative processes that caused a progressive depletion of phenolic compounds and the rising of oxidative and hydrolytic markers. A clear interaction appeared between storage time, flavouring ingredient and flavouring technique. Infusion caused a greater quality loss than co-malaxation, and in basil flavoured oils the drawbacks of infusion were greater than in other flavoured oils. The impact of flavouring method on the phenolic profiles of oil became more evident at the end of the storage period. It was confirmed that oleocanthal is less affected by storage in freezing conditions than other secoiridoids.

Keywords: freezing; infusion; malaxation; phenolic compounds; spices; virgin olive oil

Introduction

Aromatic plants have been used since ancient times as food flavouring ingredients as well as in pharmaceutical, cosmetic and perfumery because of the presence of essential oils. Several biological activities, including antimicrobial and antioxidant properties, are assigned to these plants and derived oils or to some of their other constituents (Ayadi *et al.*, 2009; Ijaz Hussain *et al.*, 2008). Along the Mediterranean basin, spices and herbs have been historically used in association with olive oil, as it represented the main source of fats in the area, to improve its nutritional and organoleptic properties (Baiano *et al.*, 2010). Over the time, the importance gained by high-quality virgin olive oils (VOO) has been the driving force for a renewed interest towards flavoured olive oils (FOO), which have been rediscovered as interesting products with unique characteristics as well as these being increasingly appreciated by consumers. Flavouring represents a strategy to increase the use of olive oil among non-traditional consumers for adding value to its organoleptic and good health properties (Perestrelo *et al.*, 2017). In this perspective, FOOs represent an important source of income for producers and sellers.

Oil flavouring is performed by different techniques such as: (i) infusion (Akçar and Gümüşkesen 2011; Ayadi *et al.*, 2009; Baiano *et al.*, 2016; Caporaso *et al.*, 2013; Damechki *et al.*, 2001; Issaoui *et al.*, 2011; Sousa *et al.*, 2015); (ii) ultrasound-assisted maceration (Veillet *et al.*, 2010) and (iii) direct malaxation of olive paste with spices (Baiano *et al.*, 2009; Caponio *et al.*, 2016). The last mentioned technique does not require the implementation of additional equipment in the olive oil mills, and is time-saving without the disadvantages of the other cited methods. In fact, it is reported that ultrasound-assisted technology could determine the off-flavour onset because of the oxidative oil degradation (Chemat *et al.*, 2004), while infusion is time-consuming and could

compromise the quality of olive oil. Previous research conducted by the present authors (Caponio *et al.*, 2016) highlighted that malaxation was more effective in extracting phenolic compounds, with a significantly lower level of hydrolysis of secoiridoids than that occurring with infusion. Moreover, FOOs produced by infusion showed lower antioxidant activity and higher extent of oxidative degradation. Volatile compounds, in generally, were not significantly influenced by the adopted flavouring method. Clodoveo *et al.* (2016) reported that an ultrasound treatment of olive paste mixed with herbs before malaxation determined a higher level of total phenols as well as tyrosol, hydroxytyrosol and oleuropein derivatives in flavoured oils. Yilmazer *et al.* (2016) reported that only the amount of spices influenced the partition of target compounds in FOOs whereas temperature and time of malaxation did not exercise significant effects.

Quality of FOOs is also affected by storage (Ayadi *et al.*, 2009; Baiano *et al.*, 2009; Gambacorta *et al.*, 2007; Issaoui *et al.*, 2011). During storage, FOOs undergo the same degradative processes that commonly affect the quality of VOOs, which are, in turn, dependent on light, oxygen, temperature, water, metals and antioxidants (Choe and Min, 2006). Effects of light, oxygen, metals and water could be controlled by using proper packaging materials and process settings during the extraction process (e.g. settings of the vertical centrifuge, filtration etc.). On the other hand, temperature could be easily managed during storage. Although low-temperature storage could slow down the rate of degradative phenomena, studies on the quality of VOOs stored at low or freezing temperature reported contradictory results, especially considering the fate of phenolic compounds (Cerretani *et al.*, 2005; Li *et al.*, 2014; Mousavi *et al.*, 2021; Mulinacci *et al.*, 2013). However, a study conducted on the subject has highlighted that FOOs stored under freezing conditions and the interactions between storage time and flavouring method and ingredients have been poorly investigated.

In the light of these considerations, our work was aimed at studying changes in the quality features of three different FOOs (basil, chilli, and chilli and garlic) obtained by applying two flavouring methods (co-malaxation and infusion) during 6 months of frozen storage in comparison to unflavoured stored VOOs.

Material and Methods

Sampling

A blend of olives (*Olea europaea* L.) from Peranzana, Coratina and Ogliarola cvs (50%, 30% and 20% w/w, respectively) was used for the experimental trials carried out at a local olive mill (Olearia Clemente, Manfredonia, Italy). Olives were processed by a continuous extraction process. After crushing, the olive paste was malaxed for 30 min at 26°C without any flavouring ingredient to produce the control oil (CTR). Co-malaxed (M) FOOs were produced by direct addition of dried basil (B), dried chili (C), and a combination of dried chili and garlic (CG) during malaxation (30 min at 26°C). The amount of spices used were 5%, 20% and 20% + 10% w/w with respect to the amount of olive processed by addition of dried basil, dried chili, and dried chili and garlic, respectively. To produce FOOs by infusion, the same extraction process as for the control oil was followed. Then the spices were left in infusion (with daily stirring) at 15–18°C for 15 days in the case of oils processed by dried basil and for 7 days in the case of chili and dried chili and garlic. The optimal amount of each flavouring ingredient was identified in preliminary trials based on the best sensory result.

Both CTR and FOOs were stored under freezing conditions (–18°C) and sampled after 3 (T3) and 6 (T6) months. Three independent trials were carried out for each flavouring method, starting from the same olive oil batch.

Routine analyses

Free fatty acid (FFA), peroxide value (PV), and spectrophotometric indices (K_{232}, K_{270} and ΔK) were determined following the analytical methods described by the European Community Regulation (EEC) Regulation 2568/91 and subsequent integrations and amendments (European Commission, 1991).

Extraction of phenolic fraction and determination of phenolic profile

The extraction of phenolic compounds and the quantification of total phenolic content (TPC) were carried out according to the procedure described in Zago *et al.* (2019). TPC was expressed as milligrams of gallic acid equivalents per kilogram of oil. The high-performance liquid chromatography (HPLC) analysis of phenolic extracts was carried out according to Baiano *et al.* (2009). The stationary phase was a Nova-Pack C18 analytical column (150 × 3.9 mm i.d.) with a particle size of 4 μm (Waters, Milford, MA). The mobile phases were (a) water:acetic acid (98:2, v/v) and (b) methanol:acetonitrile (1:1, v/v) at a constant flow rate of 1 mL/min, according to the following gradient programs: 0–30 min 100% mobile phase (a); 30–45 min, 70% mobile phase (); 45–55 min, 50% mobile phase (a); 55–65 min, 40% mobile phase (a); and 65–75 min, 0% mobile phase (a). Phenolic compounds were quantified according to the method of the internal standard considering the response factors, and

identification was carried out comparing peak retention period and spectra with those of pure standards.

Determination of polar compounds

Polar compounds (PCs) were first separated by silica gel column chromatography, according to the Association of Official Analytical Chemists (AOAC) method No. 982.27. The efficacy of the separation was checked by thin layer chromatography (TLC) as recommended by the AOAC. The polar compounds, recovered in tetrahydrofuran (THF), were then analysed by high-performance size-exclusion chromatography (HPSEC) following the conditions reported by Makhlouf *et al.* (2021).

Data elaboration

The paired *t*-test was used to compare the characteristics of oils after 3- and 6-month storage with respect to the time of production. The statistical analysis was carried out with Minitab 17 (Minitab Inc., State College, PA) at a significance level of 0.05. Principal component analysis (PCA) was carried out on the autoscaled data matrix and used as a multivariate tool for data exploration. PCA was carried out in Matlab environment (The MathWorks Inc. MA) by using the PLS_toolbox (Eigenvector Research Inc., USA).

Results and Discussion

The effect of storage on FOOs has been studied by several authors (Ayadi *et al.*, 2009; Baiano *et al.*, 2009; Gambacorta *et al.*, 2007; Issaoui *et al.*, 2011) but without considering the frozen storage. Taking into consideration the frozen storage, the first aim of the present research was to highlight the effect of freezing on quality parameters, the polar compounds and the TPC of FOOs sampled for 3 and 6 months after production. Table 1 shows the significance of the differences in the quality characteristics of T3 and T6 samples with respect to T0. After 3 months, the effect of storage on the characteristics of FOOs was different according to the flavouring method. In fact, in the case of infusion (I-oils), a significant increase in the value of several quality parameters (FFA, PV, spectrophotometric constants and polar compounds) was observed with respect to T0 although with some differences linked to the spice. Notably, the TPC always decreased significantly. On the other hand, after 3-month frozen storage, the characteristics of FOOs from co-malaxation (M-oils) were less affected. Only in the case of co-malaxation with chilli–garlic as flavouring

Table 1. Statistical significance, expressed as *p*-value, of the differences in the characteristics of the samples between T3 or T6 and T0.

	FFA	PV	K232	K270	ΔK	TAGP	ox-TAG	DAG	PC	TPC
					T3 vs. T0					
CTR	0.99	**0.01**↑	0.54	0.86	0.18	**0.05**↑	**0.01**↑	**0.01**↑	**0.00**↑	**0.01**↓
I-B	0.31	**0.00**↑	0.41	**0.00**↑	0.19	0.48	**0.00**↑	**0.05**↑	**0.01**↑	**0.00**↓
I-C	**0.01**↑	**0.01**↑	0.29	0.13	0.10	**0.01**↑	**0.03**↑	0.26	**0.05**↑	**0.01**↓
I-CG	0.11	**0.00**↑	0.07	**0.03**↑	**0.01**↑	0.35	0.07	**0.04**↑	**0.03**↑	**0.04**↓
M-B	0.21	0.20	0.30	0.16	0.06	0.90	0.07	0.16	0.13	**0.02**↓
M-C	0.95	0.65	0.19	0.21	0.30	0.16	0.05	0.29	1.00	**0.03**↓
M-CG	0.87	0.13	0.51	0.09	0.45	0.63	**0.03**↑	0.11	0.09	**0.00**↓
					T6 vs. T0					
CTR	0.16	0.24	0.63	**0.01**↓	0.42	0.06	**0.00**↑	0.11	**0.02**↑	**0.00**↓
I-B	0.67	**0.00**↑	0.20	0.08	0.39	0.60	**0.00**↑	**0.01**↑	**0.02**↑	**0.00**↓
I-C	0.36	0.06	**0.01**↑	**0.02**↑	0.68	0.25	**0.01**↑	0.25	**0.02**↑	**0.00**↓
I-CG	0.07	0.27	**0.05**↑	**0.02**↑	0.07	0.48	**0.02**↑	0.10	0.05	**0.00**↓
M-B	0.73	**0.01**↓	0.07	0.26	**0.00**↑	0.68	**0.01**↑	**0.00**↑	**0.02**↑	0.06
M-C	**0.02**↑	0.13	**0.02**↑	0.07	**0.02**↑	0.11	**0.01**↑	0.26	0.60	**0.00**↓
M-CG	**0.02**↑	**0.04**↓	0.19	0.07	0.42	0.70	**0.02**↑	**0.05**↓	**0.05**↑	**0.00**↓

CTR: unflavoured oils (control); I: infusion; M: co-malaxation; B: basil; C: chilli; CG: chilli and garlic; FFA: free fatty acids; PV: peroxide value; TAGP: triacylglycerol oligopolymers; ox-TAG: oxidated triacylglycerols; DAG: diacylglycerols; PC: total polar compounds; TPC: total phenolic content.
Significant differences ($p \leq 0.05$) are highlighted in bold. Up arrows and down arrows indicate respective significant increase and decrease with respect to T0.

ingredient (M-CG), a significant increase was observed in oxidated triacylglycerols (ox-TAG). However, even in this case, the TPC was always negatively affected by storage. At T6, main differences with the oils at production were the significant increase in polar compounds (in particular, ox-TAG) and depletion of TPC. Other differences were highlighted in the FFA, PV, and spectrophotometric constants. The paired *t*-test afforded to point out differences in characteristics of oils because of storage. However, it did not show the magnitude of these effects and also did not allow considering the complexity of the evolution of features of oils during freeze storage. For this, the data were explored by PCA, and the results are reported in Figure 1.

The score plot in Figure 1A allows discovering the relative effects of flavouring methods, storage and different flavouring agents. First, it clearly appears that the basil

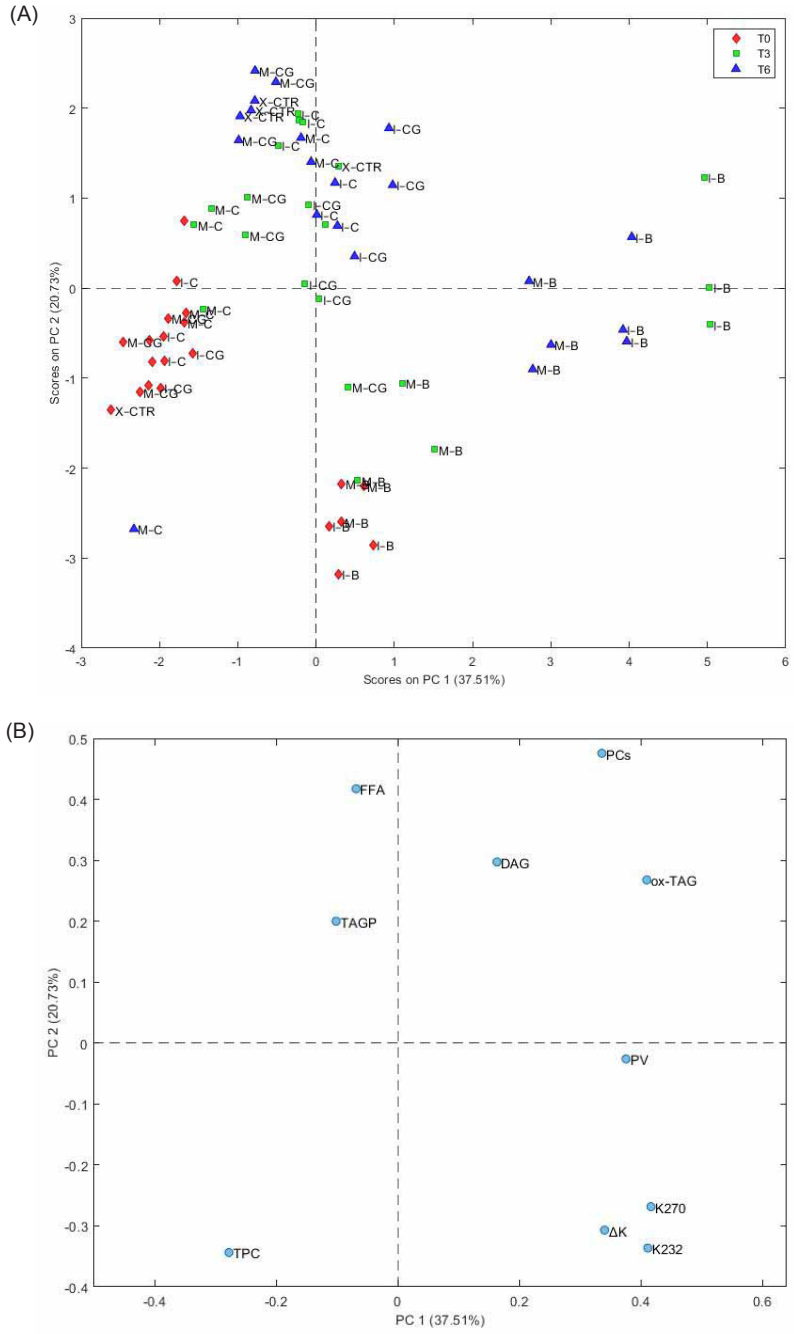

Figure 1. (A) Score plot and (B) loading plot of PCA carried out on quality indices, polar compounds, and total phenolic content of stored flavoured (B, C and CG) and unflavoured (CTR) oils. I: infusion; M: co-malaxation; X: no aromatization; B: basil; C: chilli; CG: chilli and garlic.

FOOs had different characteristics from others. In fact, already at T0, B-oils clustered apart from other samples. It was also observed that technology had a stronger effect than frozen storage on characteristics of B-oils. In fact, B-oils from infusion at T3 and T6 clustered together and showed higher positive scores on PC1 linked to oxidative markers (i.e. PV, K_{232}, K_{270}, ox-TAG and polar compounds) as observed in the corresponding loading plot (Figure 1B). On the other hand, C- and CG-oil followed an evolution similar to that of control samples during storage, indicating a less influence of aromatisation on their chemical characteristics. With time, these samples moved progressively from the negative quadrant of the plot to the positive quadrant because of TPC depletion and increase in hydrolytic and oxidative markers (Figure 1B). Changes in quality parameters because of flavouring practices are well known and observed by several authors (Baiano *et al.*, 2009, 2016; Caponio *et al.*, 2016; Clodoveo *et al.*, 2016; Gambacorta *et al.*, 2007; Sacchi *et al.*, 2017; Sousa *et al.*, 2015).

Overall, the results demonstrated that during frozen storage FOOs underwent degradation that caused progressive depletion of phenolic compounds and increase in oxidative and hydrolytic markers. However, a clear interaction emerged between the storage and the kind of flavouring ingredient and flavouring technique.

Aromatisation effect was also observed on the phenolic profile of VOO (Baiano *et al.*, 2016; Caponio *et al.*, 2016; Sacchi *et al.*, 2017). Table 2 shows the significance of differences in the phenolic profile of oils at T3 and T6 with respect to T0, while Figure 2 reports the results of PCA. In all, 13 phenolic compounds were detected belonging to the common classes found in VOOs (Bendini *et al.*, 2007). It is observed in Table 2 that the most important differences in the phenolic profiles of oils at T3 with respect to production was the increase in hydroxytyrosol acetate (3,4-DHPEA-AC, in all samples) and decrease of almost all the other compounds. This trend could be easily noted by looking at PCA results (Figure 2). In spite of some differences linked to spice and flavouring technique, the samples at T3 depicted similar characteristics.

After 6-month storage, all the oils had significant higher values of 3,4-DHPEA-AC. Phenolic alcohols (3,4-DHPEA and *p*-HPEA) were significantly higher in some cases (I-C, I-CG and M-C) as also secoiridoids such as decarboxymethyl oleuropein aglycon (3,4-DHPEA-EDA), oleocanthal (*p*-HPEA-EDA) and oleuropein aglycon (3,4-DHPEA-EA) (I-B, I-CG, M-B and M-C). On average, C- and CG-oil had the higher amount of complex secoiridoids at T6. PCA results helped in understanding the interaction of storage, flavouring technique and spice on the phenolic profiles. In B-oils, an important effect of flavouring technique was observed with infusion that brought higher amounts of phenolic alcohols at each time point. On the other hand, in C- and CG-oil, effect of flavouring technique appeared more clearly after 6 months when co-malaxation and infusion affected an increase in 3,4-DHPEA-EDA, *p*-HPEA-EDA and 3,4-DHPEA-EA.

An increment in simple phenols (such as tyrosol and hydroxytyrosol) was due to progressive hydrolysis from complex secoiridoids (Bendini *et al.*, 2007) and was observed by Mulinacci and co-workers (2013) in extra virgin olive oils (EVOO) stored for 9 months at room temperature. Our findings suggest that this could happen even during frozen storage, although a critical role was played by other factors (kind of spice and flavouring method). The same could be stated for more complex phenols, such as 3,4-DHPEA-EDA and *p*-HPEA-EDA, that in several cases increased after 6-month storage.

On the other hand, the observed decrements could be explained in different manners. On the one hand, it could be due to the unavoidable oxidation occurring even at low temperatures. On the other hand, as supposed by Cerretani *et al.* (2005), decrement in phenols after freezing was linked to change in the physical state of oil and the consequent solubilisation of phenols into residual water phase. Mousavi *et al.* (2021) reported that secoiridoids (mostly 3,4-DHPEA-EDA, 3,4-DHPEA-EA and *p*-HPEA-EA) decreased during frozen storage, while (*p*-HPEA-EDA) was the most stable phenol. The findings of the present research are in partial agreement with these. In fact, *p*-HPEA-EDA was significantly reduced only in the case of M-CG oils, while 3,4-DHPEA-EDA, 3,4-DHPEA-EA and *p*-HPEA-EA were much more affected by storage in freezing conditions, particularly during the first 3 months (Table 2).

Conclusion

To the best of authors' knowledge, this is the first research centring the effect of storage under frozen conditions on the quality features of FOOs, together with the possible interaction with flavouring methods and flavouring agents. Low temperatures during storage could slow down degradation, thus safeguarding the quality of FOOs.

During storage, the samples had a significant decrease in total phenolic compounds and an increase in some hydrolytic and oxidative markers. The aromatization by infusion was the worse due to significant increase in the values of FFA, PV, spectrophotometric constants and polar compounds. Also, an interaction with the kind of spice was pointed out. In fact, flavouring with basil by infusion had maximum effect on the quality of the product not only at the time of production but also

Table 2. Statistical significance, expressed as *p*-value, of differences in the phenolic profiles of the samples between T3 or T6 and T0.

	3,4-DHPEA	*p*-HPEA	Vanillic ac.	Vanillin	Cumaric ac.	3,4-DHPEA-AC	Ferulic ac.	3,4-DHPEA-EDA	*p*-HPEA-AC	*p*-HPEA-EDA	Pinoresinol	3,4-DHPEA-EA	*p*-HPEA-EA
T3 vs. T0													
CTR	**0.01**↓	**0.00**↓	**0.00**↑	0.83	0.17	**0.01**↑	0.26	**0.00**↑	0.10	**0.03**↑	**0.03**↓	0.36	0.13
I-B	**0.00**↓	**0.00**↓	0.23	0.06	0.11	**0.00**↑	0.10	**0.00**↑	**0.05**↓	**0.00**↑	**0.05**↓	0.18	**0.02**↓
I-C	0.53	0.79	0.51	0.54	**0.02**↓	**0.00**↑	**0.05**↓	**0.02**↓	**0.00**↓	0.08	**0.03**↓	**0.00**↓	**0.03**↓
I-CG	0.06	**0.05**↓	0.33	0.05	**0.00**↓	**0.03**↑	**0.01**↓	**0.00**↓	**0.00**↓	0.94	**0.01**↓	**0.04**↓	**0.00**↓
M-B	0.47	0.23	0.25	0.92	0.07	**0.01**↑	**0.01**↓	**0.00**↓	**0.03**↓	0.44	0.24	**0.05**↓	**0.00**↓
M-C	**0.02**↓	0.77	0.85	0.71	**0.01**↓	**0.02**↑	0.07	0.11	**0.02**↓	0.58	**0.01**↓	**0.01**↓	**0.00**↓
M-CG	0.09	**0.01**↓	0.18	0.25	**0.01**↓	**0.01**↑	0.55	**0.00**↓	**0.00**↓	**0.01**↓	**0.01**↓	**0.01**↓	**0.01**↓
T6 vs. T0													
CTR	**0.00**↓	**0.00**↓	0.09	**0.01**↑	0.73	**0.01**↑	0.48	**0.01**↑	0.13	**0.00**↑	0.07	0.18	0.08
I-B	**0.00**↓	**0.00**↓	0.83	0.09	0.13	**0.00**↑	0.96	**0.00**↑	**0.00**↑	**0.00**↑	**0.01**↓	0.18	**0.01**↓
I-C	**0.02**↓	**0.04**↑	0.08	0.07	**0.01**↓	**0.02**↑	**0.04**↓	0.52	0.33	0.08	0.05	0.08	**0.01**↓
I-CG	**0.01**↑	**0.01**↑	**0.01**↑	**0.03**↑	**0.01**↓	**0.01**↑	0.12	**0.00**↑	**0.05**↓	**0.00**↑	**0.01**↑	**0.04**↑	**0.02**↓
M-B	**0.03**↓	0.77	0.14	0.81	0.14	**0.01**↑	0.24	0.30	**0.00**↑	**0.03**↑	0.29	**0.03**↑	**0.01**↓
M-C	**0.03**↑	**0.03**↑	**0.01**↑	0.52	0.07	**0.00**↑	0.11	**0.00**↑	0.26	**0.01**↑	**0.03**↑	**0.01**↑	0.82
M-CG	**0.03**↓	**0.00**↓	0.80	**0.02**↑	0.07	**0.04**↑	0.68	**0.00**↓	**0.01**↓	**0.01**↓	0.52	0.36	**0.05**↓

CTR: unflavoured oils (control); I: infusion; M: co-malaxation; B: basil; C: chilli; CG: chilli and garlic; 3,4-DHPEA: hydroxytyrosol; *p*-HPEA: tyrosol; 3,4-DHPEA-AC: hydroxytyrosol acetate; 3,4-DHPEA-EDA: decarboxymethyl oleuropein aglycon; *p*-HPEA-AC: tyrosol acetate; *p*-HPEA-EDA: decarboxymethyl ligstroside aglycon; 3,4-DHPEA-EA: oleuropein aglycon; *p*-HPEA-EA: ligstroside aglycon.
Significant differences ($p \leq 0.05$) are highlighted in bold. Up arrows and down arrows indicate respective significant increase and decrease with respect to T0.

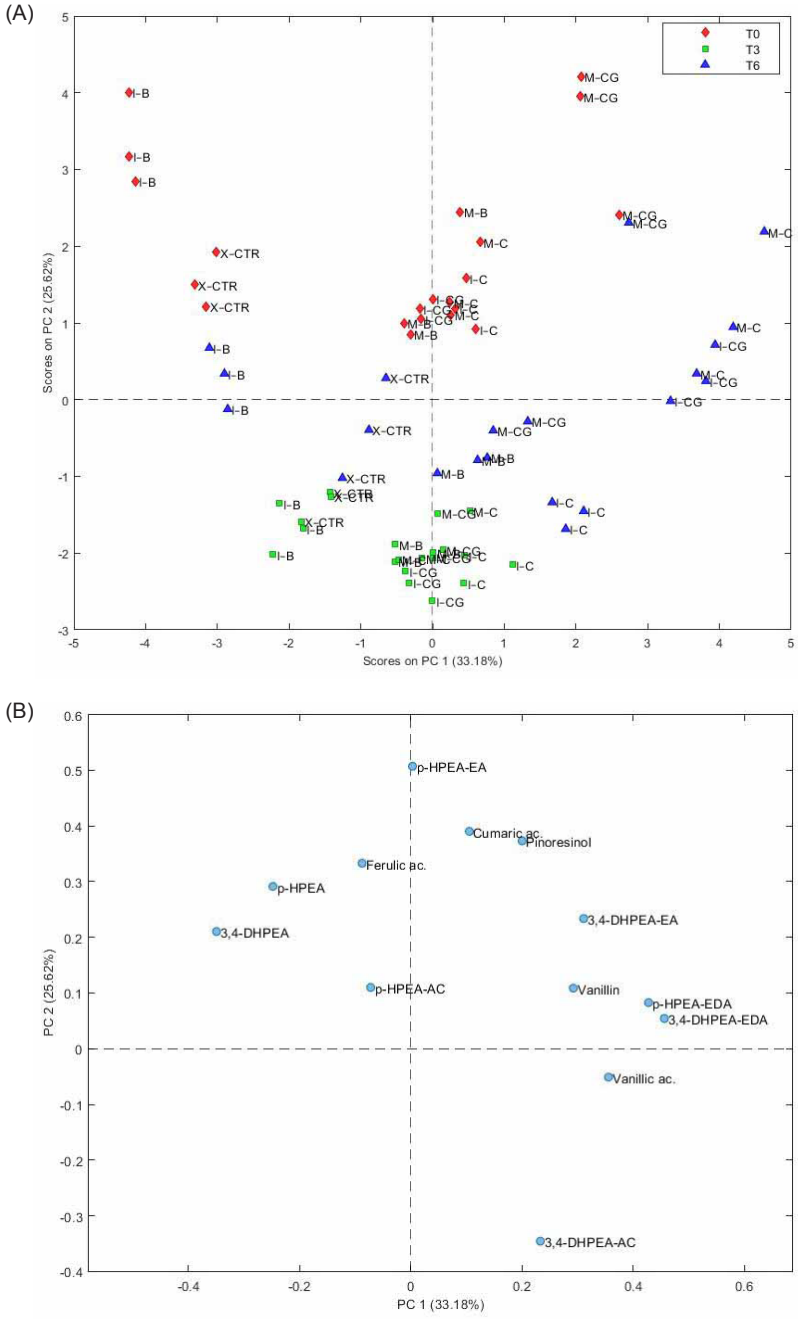

Figure 2. (A) Score plot and (B) loading plot of PCA carried out on the phenolic profile of stored flavoured (B, C and CG) and unflavoured (CTR) oils. I: infusion; M: co-malaxation; X: no aromatization; B: basil; C: chilli; CG: chilli and garlic.

during storage. On the other hand, chilli and chilli–garlic oils followed an evolution similar to that found in unflavoured samples during storage, indicating a lower influence of aromatisation on oil's chemical parameters.

Significant changes were also observed in phenolic profiles. Oleuropein- and ligstroside-related compounds decreased during storage whereas oleocanthal was found to be one of the more stable compounds, as also observed in unflavoured EVOOs.

References

Akçar H.H. and Gümüşkesen A.S. 2011. Sensory evaluation of flavored extra virgin olive oil. J Food (GIDA). 36(5): 249–253.

Ayadi M.A., Grati-Kamoun, N., and Attia H. 2009. Physico-chemical change and heat stability of extra virgin olive oils flavoured by selected Tunisian aromatic plants. Food Chem Toxicol. 47: 2613. https://doi.org/10.1016/j.fct.2009.07.024

Baiano A., Gambacorta G., and La Notte E. 2010. "Aromatization of Olive Oil." Transworld Research Network, Kerala, India. ISBN 978-81-7895-462-2.

Baiano A., Previtali M.A., Viggiani I., Varva G., Squeo G., Paradiso V.M., Summo, C., Gomes, T., and Caponio, F. 2016. As oil blending affects physical, chemical, and sensory characteristics of flavoured olive oils. Eur Food Res Technol. 242: 1693. https://doi.org/10.1007/s00217-016-2669-1

Baiano A., Terracone C., Gambacorta G., and La Notte E. 2009. Changes in quality indices, phenolic content and antioxidant activity of flavored olive oils during storage. J Am Oil Chem Soc. 86: 1083. https://doi.org/10.1007/s11746-009-1446-8

Bendini A., Cerretani L., Carrasco-Pancorbo A., Gómez-Caravaca A.M., Segura-Carretero A., Fernández-Gutiérrez A., and Lercker G. 2007. Phenolic molecules in virgin olive oils: a survey of their sensory properties, health effects, antioxidant activity and analytical methods. An overview of the last decade. Molecules. 12: 1679. https://doi.org/10.3390/12081679

Caponio F., Durante V., Varva G., Silletti R., Previtali M.A., Viggiani I., Squeo G., Summo C., Pasqualone A., Gomes T., and Baiano A. 2016. Effect of infusion of spices into the oil vs. combined malaxation of olive paste and spices on quality of naturally flavoured virgin olive oils. Food Chem. 202: 221. https://doi.org/10.1016/j.foodchem.2016.02.005

Caporaso N., Padano A., Nicoletti G., and Sacchi R. 2013. Capsaicinoids, antioxidant activity, and volatile compounds in olive oil flavoured with dried chilli pepper (*Capsicum annuum*). Eur J Lipid Sci Technol. 115:1434. https://doi.org/10.1002/ejlt.201300158

Cerretani L., Bendini A., Gallina Toschi T., Lercker G., and Biguzzi B. 2005. Freezing storage can affect the oxidative stability of not filtered extra-virgin olive oils. J Commodity Sci. 44: 1000.

Chemat F., Grondin I., Shum Cheong Sing A., and Smadja J. 2004. Deterioration of edible oils during food processing by ultrasound. Ultrason Sonochem. 11: 13. https://doi.org/10.1016/S1350-4177(03)00127-5

Choe E. and Min D.B. 2006. Mechanisms and factors for edible oil oxidation. Compr Rev Food Sci Food Saf. 5: 169. https://doi.org/10.1111/j.1541-4337.2006.00009.x

Clodoveo M.L., Dipalmo T., Crupi P., Durante V., Pesce V., Maiellaro I., Lovece A., Mercurio A., Laghezza A., Corbo F., and Franchini C. 2016. Comparison between different flavored olive oil production techniques: healthy value and process efficiency. Plant Food Hum Nutr. 71: 81. https://doi.org/10.1007/s11130-016-0528-7

Damechki M., Sotiropoulou S., and Tsimidou M. 2001. Antioxidant and pro-oxidant factors in oregano and rosemary gourmet olive oils. Grasas Aceites. 52: 207. https://doi.org/10.3989/gya.2001.v52.i3-4.359

European Commission. 1991. European Community Regulation (EEC) No. 2568/1991. Off J Eur Comm. N. L. 248, Sep. 5, 1991.

Gambacorta G., Faccia M., Pati S., Lamacchia C., Baiano A., and La Notte E. 2007. Changes in the chemical and sensorial profile of extra virgin olive oils flavored with herbs and spices during storage. J Food Lipids. 14: 202. https://doi.org/10.1111/j.1745-4522.2007.00080.x

Hussain A. I., Anwar F., Sherazi S. T. H., and Przybylski R. 2008. Chemical composition, antioxidant and antimicrobial activities of basil (Ocimum basilicum) essential oils depends on seasonal variations. Food Chem. 108: 98. https://doi.org/10.1016/j.foodchem.2007.12.010

Issaoui M., Flamini G., Hajaij M.E., Cioni P.L., and Hammami M. 2011. Oxidative evolution of virgin and flavored olive oils under thermo-oxidation processes. J Am Oil Chem Soc. 88: 1339. https://doi.org/10.1007/s11746-011-1800-5

Li X., Zhu H., Shoemaker C.F., and Wang S.C. 2014. The effect of different cold storage conditions on the compositions of extra virgin olive oil. J Am Oil Chem Soc. 91: 1559. https://doi.org/10.1007/s11746-014-2496-0

Makhlouf F.Z., Squeo G., Difonzo G., Faccia M., Pasqualone A., Summo C., Barkat M., and Caponio F. 2021. Effects of storage on the oxidative stability of acorn oils extracted from three different *Quercus* species. J Sci Food Agric. 101: 131. https://doi.org/10.1002/jsfa.10623

Mousavi S., Mariotti R., Stanzione V., Pandolfi S., Mastio V., Baldoni L., and Cultrera N.G. 2021. Evolution of extra virgin olive oil quality under different storage conditions. Foods. 10: 1945. https://doi.org/10.3390/foods10081945

Mulinacci N., Ieri F., Ignesti G., Romani A., Michelozzi M., Creti D., Innocenti M., and Calamai L. 2013. The freezing process helps to preserve the quality of extra virgin olive oil over time: a case study up to 18 months. Food Res Int. 54: 2008. https://doi.org/10.1016/j.foodres.2013.03.052

Perestrelo R., Silva C., Silva, P., and Câmara J.S. 2017. Global volatile profile of virgin olive oils flavoured by aromatic/medicinal plants. Food Chem. 227: 111. https://doi.org/10.1016/j.foodchem.2017.01.090

Sacchi R., Della Medaglia D., Paduano A., Caporaso N., and Genovese A. 2017. Characterisation of lemon-flavoured olive oils. Food Sci Technol. (LWT) 79: 326. https://doi.org/10.1016/j.lwt.2017.01.025

Sousa A., Casal S., Malheiro R., Lamas H., Bento A., and Pereira J.A. 2015. Aromatized olive oils: influence of flavouring in quality, composition, stability, antioxidants, and antiradical potential. Food Sci Technol. (LWT) 60: 22. https://doi.org/10.1016/j.lwt.2014.08.026

Veillet S., Tomao V., and Chemat F. 2010. Ultrasound-assisted maceration: an original procedure for direct aromatisation of olive oil with basil. Food Chem. 123: 905. https://doi.org/10.1016/j.foodchem.2010.05.005

Yılmazer M., Karagöz S.G., Ozkan G., and Karacabey E. 2016. Aroma transition from rosemary leaves during aromatization of olive oil. J Food Drug Anal. 24: 299. https://doi.org/10.1016/j.jfda.2015.11.002

Zago L., Squeo G., Bertoncini E.I., Difonzo G., and Caponio F. 2019. Chemical and sensory characterization of Brazilian virgin olive oils. Food Res Int. 126: 108588. https://doi.org/10.1016/j.foodres.2019.108588

Italian Journal of Food Science, 2022; 34 (1): 67–85

The virgin coconut oil (VCO) emulsion powder characteristics: effect of pickering emulsion with microcrystalline cellulose (MCC) and different drying techniques

Bambang Nurhadi[1,*], Selly Selly[2], Siti Nurhasanah[1], Rudy Adi Saputra[1], Heni Radiani Arifin[1]

[1]*Faculty of Agricultural Industrial Technology, Universitas Padjadjaran, Indonesia*
[2]*Department of Food Industrial Technology, Universitas Padjadjaran, Indonesia*

***Corresponding Author**: Bambang Nurhadi, Faculty of Agricultural Industrial Technology, Universitas Padjadjaran, Indonesia. Email: bambang.nurhadi@unpad.ac.id

Received: 11 August 2021; Accepted: 21 December 2021; Published: 8 February 2022

PAPER

Abstract

Virgin coconut oil (VCO) has many health benefits; however, drinking of VCO directly is still uncommon. In order to overcome this problem, microencapsulation can be one of the solutions. Unfortunately, emulsion is an unstable system and rapidly separates into two layers. Therefore, in this study, we carried out the explanatory research of microencapsulation process with descriptive analysis. It comprised two emulsion treatments, using homogenization method, and three drying techniques, to determine the effect of Pickering emulsion with microcrystalline cellulose (MCC) and different drying techniques on the characteristics of VCO powder (before drying: creaming index and emulsion droplet size; and after drying: drying yield, color intensity, moisture content, particle morphology, microencapsulation efficiency, peroxide value, rehydration particle size, and dissolving time). The results demonstrated that all emulsion treatments did not depict any emulsion instability up to 21 days of storage, and the obtained VCO powders had different characteristics. The highest microencapsulation efficiency was 33.49 ± 1.59%, obtained from the emulsion using Tween 80 and MCC by spray drying, and the lowest peroxide value was 0.464 ± 0.084 mEq O_2/kg, obtained from the emulsion using Tween 80 and MCC by vacuum drying. The future application of this study is expected to produce VCO powder that can improve the ease handling of VCO and also commercialize for being used as a non-dairy creamer.

Keywords: drying techniques, microcrystalline cellulose, microencapsulation, pickering emulsion, virgin coconut oil

Introduction

Virgin coconut oil (VCO) is well known for being rich in ingredients that are suitable as functional foods. VCO contains about 90% saturated fatty acids and about 10% unsaturated fatty acids (Nurhasanah *et al*., 2019). There are lots of medium chain triglycerides (MCTs) in these saturated fatty acids consisting of caprylic acid (C8:0), capric acid (C10:0) and lauric acid (C12:0). These MCTs are 'unique' due to their physicochemical properties that have shorter chains (6–12 hydrocarbons) and smaller molecular weight compared to long-chain triglycerides (LCT) (13–21 hydrocarbons), making them absorbed and hydrolyzed faster in the body, resulting in rapidly oxidized and producing higher energy (Nurhasanah *et al*., 2019; Parrish, 2017). VCO, compared to copra oil, increases high-density lipoprotein (HDL) and lowers low-density lipoprotein (LDL) significantly, and does not cause coronary heart disease because of the absence of trans fatty acids. Besides the above-mentioned major components, there are also tocopherols, β-carotenes and other phenolic compounds, which are the minor components found in almost all types of vegetable oils, including VCO that has better antioxidant capacity than bleached, refined and deodorized coconut oil. Thus, VCO lowers cholesterol level in the human body, increases

endurance, accelerates recovery rate, activates anti-aging hormones, and prevents cancer, obesity, dementia, heart attack and other diseases associated with premature aging (Hee *et al*., 2017). These are the reasons for using VCO for emulsion.

Unfortunately, the limited use of VCO in food products is due to its liquid form, which complicates the transportation and storage process. It solidifies at room temperature with ease under its melting point (Patil *et al*., 2016). In addition, only a few people consume VCO directly because of people's perception that it is difficult to accept oil consumption (Hee *et al*., 2015). Therefore, it is necessary to process VCO into a more convenient form for general consumption and its wide application in food products while protecting its bioactive components.

Microencapsulation is a method used to solve problems by giving a new perception to the public. Microencapsulation masks the oily taste in the mouth so that it does not leave the unpleasant taste in throat, extends the shelf life to reduce loss during distribution and storage, leads to easy handling, and increases the solubility and bioavailability of bioactive components (Nedovic *et al*., 2011). The process of microencapsulation consists of two stages, which are mixing the core material with the coating material to form an emulsion, followed by drying the formed emulsion (Amaral *et al*., 2019). In this study, mechanism of Pickering emulsion was used for emulsion formation. Pickering emulsion has many advantages, especially it being surfactant-free, having high stability against coalescence, and ostwald ripening (Díaz *et al*., 2020). High stability against coalescence is a major benefit of stabilization using solid particles, with solid particles partially wetted by each of the liquid phases, that is oil and water phases (partial dual wettability) so that the particles are absorbed at the oil and water interface to form a mechanical barrier, which reduces the tendency of flocculation (Xie *et al*., 2019). Pickering emulsion also has advantages in terms of its use in smaller quantities, efficiency, easy of using, good oil retention in dry powder, difficult to extract the surface oil, and not susceptible to environmental changes (Bai *et al*., 2018). That is why, in recent times Pickering emulsion has been widely developed and applied to products, especially to dry products.

Microcrystalline cellulose (MCC) is the solid particle used for Pickering emulsion in this study. MCC has the advantages of having natural ingredients, biocompatibility and biodegradability (Alavi, 2019), and has important functions in preventing emulsion instability (Costa *et al*., 2019). Also, MCC in the emulsion system has the advantage of being able to withstand to high temperatures so that the emulsion system is more stable when exposed to heat during the drying process. In addition, MCC has been used often in food processing compared to cellulose nanocrystals (CNC) because CNC is more expensive and both of them could stabilize the emulsion system. The emulsion formation was carried out in two treatments using homogenization method. MCC was added directly to the coarse emulsion because it stabilizes the emulsion system without the help of surfactants (Costa *et al*., 2019). Besides MCC, Tween 80 with the hydrophile–lipophile balance (HLB) value of 15 was also used as an additional surfactant to MCC because the combination of these emulsifiers could increase the stability of emulsion for a longer period compared to using the surfactant alone (Hu *et al*., 2015). Maltodextrin was used as a glass maker in this study. Maltodextrin has rapid dispersion, high water solubility and low viscosity, strong flavor-binding ability, and is able to form an amorphous glass matrix network to protect the core material so as to facilitate drying process and maintain VCO stability against oxygen (Klinjapo and Krasaekoopt, 2018; Muhamad *et al*., 2018). However, since maltodextrin exhibits poor emulsifying capacity, it is usually combined with other ingredients to maintain emulsion stability (Klinjapo and Krasaekoopt, 2018).

Drying process of emulsion commenced after the emulsion system was formed. Spray drying is one of the drying techniques that is widely used in the food industry (Rajabi *et al*., 2015). This technique uses continuous high temperature and pressure to produce the final product in the form of a dry powder with a very short contact time between the hot air and the product; therefore, it is safe to dry the VCO that contains bioactive components (Anandharamakrishnan and Ishwarya, 2015; Rajabi *et al*., 2015). Apart from spray drying, freeze drying and vacuum drying were also used in this study. Freeze drying uses the principle of freezing at low temperature and ice crystal sublimation so that bioactive components of VCO are not damaged (Liu *et al*., 2008). Vacuum drying uses a low-pressure drying technique (usually lower than the atmosphere pressure), in which the heat required for the drying process is lower and the drying process is faster than a typical dryer so that the bioactive components present in VCO can be maintained (Bazyma and Kutovoy, 2005; Parikh, 2015). These three drying techniques have different drying principles and have their own advantages and do not cause any damage to the bioactive components of VCO. Hence, these three drying techniques were selected for the drying process used to encapsulate VCO.

Thus, in this study Pickering emulsion mechanism was studied to determine the effect of Pickering emulsion with MCC and different drying techniques on the characteristics of VCO powder (measurement before drying: creaming index and emulsion droplet size, and measurement after drying: drying yield, color intensity, particle morphology, moisture content, microencapsulation efficiency, peroxide value, rehydration particle size,

and dissolving time). For oxidation measurement, we chose peroxide value because oxidation reaction occurs in stages, where hydroperoxide is formed as a result of primary oxidation, while other techniques (anisidin and thiobarbituric acid [TBA] values) are used to measure the rancidity of the secondary or further oxidation. If the primary oxidation is bad, then it is possible that the results of the follow-up test would be bad as well. In addition, there is only a small amount of unsaturated fatty acid in VCO and because of limited time (30 days of storage), we only used peroxide value for oxidation measurement in this study.

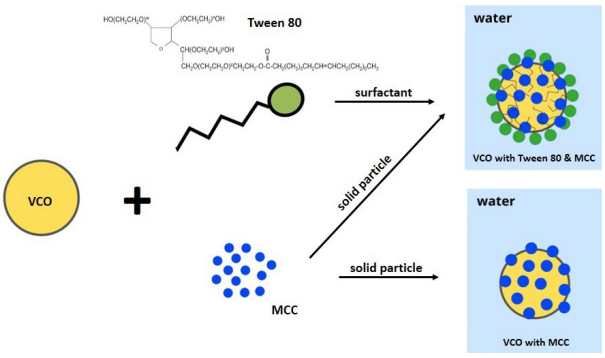

Figure 1. Schematic of VCO Pickering emulsion using the combination of Tween 80 and MCC, or MCC alone.

Materials and Methods

Materials

Virgin Coconut Oil was obtained from Bali Coconut, a local market in Badung, North Kuta, Bali, Indonesia. Tween 80 was obtained from Croda, United Kingdom. Vivapur® MCG 811 F MCC was obtained from JRS Pharma, Germany. Maltodextrin with a dextrose equivalent (DE) of 18 to 20 was obtained from Qin Huang Dao Lihua Starch Co. Ltd., Qin Huang Dao, China. n-Hexane, hydrochloric acid, ammonium thiocyanate, barium chloride dihydrate, iron (III) sulfate heptahydrate, iron (III) chloride, methanol, chloroform, isooctane and 2-propanol were pro-analyst chemicals and obtained from Supelco, Merck KgaA, Darmstadt, Germany.

Preparation of emulsions

The total solid was set at 30% (w/w). The dispersion of maltodextrin and MCC in water was conducted according to the procedure described by Iijima and Takeo (2000) and Lim and Roos (2017) with some modifications. Maltodextrin with DE 18–20 was dissolved in distilled water at 55°C under heating and mechanical stirring by using a magnetic stirrer up to complete dissolution. The heating process was continued up to 70°C. Then, MCC at 5% of VCO (w/w) was added gradually to the maltodextrin dispersion at 70°C with stirring using a magnetic stirrer up to complete dissolution. The MCC and maltodextrin dispersion was then cooled at room temperature to 45 ± 3°C before the core material was added into it.

Emulsion was formed using a homogenization method according to the procedure described by Alcântara *et al.* (2019) and Xu *et al.* (2016) with some modifications. For the first emulsion treatment, Tween 80 at 1% of VCO (w/w) was mixed into distilled water at 25 ± 3°C under mechanical stirring by using a magnetic stirrer until it was thoroughly mixed. Tween 80 at 1% of VCO (w/w) was used in this study because good emulsion stability was obtained with this concentration based on the studies conducted by (Gomes *et al.* (2018) and Vicente *et al.* (2018). VCO at 40% of total solid (w/w) was added gradually to the mixture while stirring. According to conducted studies, the best microencapsulation efficiency is obtained when the concentration of oil is 30% of total solid (w/w). The higher the concentration of oil, the lower the microencapsulation efficiency obtained (Alcântara *et al.*, 2019). In this study, VCO at 40% of the total solid (w/w) was used with the help of Pickering emulsion as the novelty of the study (high oil concentration) because Pickering emulsion can increase emulsion stability for a longer period. The emulsion formed was then homogenized using a rotor-stator homogenizer (DLAB D500, China) (14,000 rpm, 5 min). After this, the emulsion was poured gradually into the MCC and maltodextrin dispersion with mechanical stirring using a magnetic stirrer for 5 min followed by homogenization using the same homogenizer as used before. For the second emulsion treatment, VCO at 40% of the total solid (w/w) was added gradually to the MCC and maltodextrin dispersion with mechanical stirring by using a magnetic stirrer for 5 min followed by homogenization using the same homogenizer. The schematic of VCO Pickering emulsion using the combination of Tween 80 and MCC or using MCC alone is shown in Figure 1. It is observed in Figure 1, how the Tween 80 and MCC solid particles arrange themselves around the VCO droplet to enhance the stabilization of emulsion. The emulsion formed was kept in a glass beaker and stored overnight at room temperature (25 ± 3°C) before drying using the three techniques, spray drying, freeze drying and vacuum drying.

Characterization of emulsions

Stability of emulsions

The emulsion formed was immediately transferred to a test tube, closed and stored at 25 ± 3°C. Monitoring the stability of emulsion was carried out every week for 21

days of storage right after its preparation. The height of the cream formed during storage was calculated using the creaming index (CI) as described by Equation (1) (Akhtar *et al*., 2014):

$$\text{Creaming Index} = \frac{h_c}{h_t} \times 100\%, \quad (1)$$

where h_c is the height of the cream (cm) and h_t is the height of the initial emulsion (cm)

Droplet size of emulsions

The droplet size of emulsion was determined by using the Laser Diffraction Particle Size Analyzer (LS 13 320, Beckman Coulter, United States). The measurement was carried out immediately after the emulsion was formed. The droplet size of the emulsion was expressed as the average size, and the calculation of polydispersity index (PDI) was exercised using Equation (2) (Hirschle *et al*., 2016):

$$\text{PDI} = \left(\frac{\sigma}{d}\right)^2, \quad (2)$$

where σ is the standard deviation of the particle size distribution (μm), and d is the mean diameter of the particle (μm).

Spray drying process

The emulsion was kept in a glass beaker and stored overnight at room temperature (25 ± 3°C); it was diluted with distilled water for as much as 50% of the total emulsion under stirring. The spray drying process was carried out in duplicate according to the procedure described by Sansone *et al*. (2011) with some modifications. A mini spray dryer (Buchi B-290, Flawil-Switzerland) was used for the spray drying process with inlet temperature adjusted at 150 ± 3°C, outlet temperature maintained at 70 ± 3°C, aspirator was set at 85%, pump was set at 25%, and the actual flow rate was maintained at 5 mL/min; the mixture was stirred gently while the feed was pumped to spray dryer to maintain homogeneity. The dried products were collected at collection chamber after the drying process was completed and sieved with a 40-mesh Tyler sieve to obtain a fine powder. All the spray-dried VCO powders were then kept at 4°C while waiting for 'day zero analysis', followed by storage tests at room temperature (25 ± 3°C).

Freeze-drying process

The freeze-drying process also was carried out in duplicate according to the procedure described by Anwar and Kunz (2011) with some modifications. The emulsion was kept in a glass beaker and stored overnight at room temperature (25 ± 3°C) and transferred to a plastic container for the initial freezing process at –50°C for 24 h using a freezer (Thermo Scientific Hera Freeze Basic, United States). After the freezing process, a freeze dryer (Christ Alpha 1-4 LD Plus, Germany) was used for the freeze-drying process with temperature kept at –50°C and pressure at 0.001 mbar for 48 h. The freeze-dried products were then milled in a mortar and pestle, and sieved with a 40-mesh Tyler sieve to obtain a fine powder. All freeze-dried VCO powders were kept at 4°C while waiting for 'day zero analysis', followed by storage tests at room temperature (25 ± 3°C).

Vacuum drying process

The vacuum drying process also was carried out in duplicate according to the procedure described by Nurhadi and Roos (2017) with some modifications. The emulsion was kept in a glass beaker and stored overnight at room temperature (25 ± 3°C), and transferred to a silicone pan for drying using a vacuum oven (VWR Scientific, United States) with temperature and vacuum pressure set at 60°C and 25 inHg, respectively, for 6 h. The vacuum-dried products were then milled in a mortar and pestle, and sieved with a 40-mesh Tyler sieve to obtain fine powder. All vacuum-dried VCO powders were then kept at 4°C while waiting for 'day zero analysis', followed by storage tests at room temperature (25 ± 3°C).

Powder analysis

Drying yield

The drying yield (%) is the ratio between the weight of the microcapsules obtained from the drying process (g) and the total solid of emulsion which consists of VCO, Tween 80, MCC, and maltodextrin (g). The drying yield was calculated using Equation (3) (Zhong *et al*., 2009):

$$\text{Drying Yield}\,(\%) = \frac{M_c}{M_t} \times 100\%, \quad (3)$$

where M_C is the weight of microcapsules obtained from the drying process (g), and M_t is the total solid of the emulsion (g).

Color analysis

Color intensity was determined as described by Yam and Papadakis (2004) using a spectrophotometer (Konica Minolta CM-5 Spectrophotometer, Japan). This measurement was performed on day zero and every 15 days during

the 30-day storage at room temperature (25 ± 3°C). Before analysis, the instrument was calibrated using CM-A210 white calibration plate (Japan). Then the samples were captured and the results obtained were in the form of L* indicating the degree of lightness to darkness, a* indicating the degree of redness to greenness and b* indicating the degree of yellowness to blueness. Hue angle (H*), which indicates the color of VCO powder, was calculated using Equation (4), and chroma (C*) value, which indicates the saturation of VCO powder, was calculated using Equation (5) as described by Kuck and Noreña (2016):

$$H^* = \tan^{-1}\left(\frac{b^*}{a^*}\right), \quad (4)$$

$$C^* = [(a^*)^2 + (b^*)^2]^{1/2}. \quad (5)$$

Morphology of VCO powder

The morphology of VCO powder was observed by using a scanning electron microscope (SEM), Tabletop Microscope Hitachi TM 3000 (Hitachi High-Technologies Corporation, Tokyo, Japan). The sample was placed on a double-sided tape attached to the specimen stub. The specimen stub was then measured at appropriate height and put at a specimen stage. The observation mode was set, and the morphological structure of the particle was observed on computer screen.

Moisture content

The moisture content was measured using the gravimetric method according to official method of Association of Official Analytical Chemistry (AOAC, 2005b), with removal of water vapor by convective heat transfer using an oven at 105°C for 3 h. The moisture content was measured in duplicate and the calculation of moisture content was performed on a wet basis using Equation (6):

$$\text{Moisture Content}\,(\%\text{wb}) = \frac{w_1 - (w_2 - w)}{w_1} \times 100\% \quad (6)$$

where w is the constant weight of empty dish (g), w_1 is the weight of sample (g) and w_2 is the constant weight of dried sample + dish (g).

Microencapsulation efficiency

Total oil (O_T) is the overall oil in a microcapsule and comprises encapsulated oil (O_E) and surface oil (O_S). Total oil was determined by using the soxhlet extraction method according to the official method described by AOAC (2005a). Spray- and vacuum-dried powders were weighed as 2 g and hydrolyzed. Filter paper containing the oil was dried and put into hull to be extracted with soxhlet. Meanwhile, 2-g freeze-dried powder was weighed and put into hull and immediately extracted with soxhlet. The extraction process was carried out with a multi-heater extraction rack (Buchi B-810, Switzerland) for 3 h using n-hexane solvent. Then the oil extract was dried in an oven at 105°C for 30 min to obtain a constant weight. The total oil was calculated using Equation (7):

$$O_T(\%) = \frac{w_2 - w_1}{w} \times 100\%, \quad (7)$$

where w is the weight of the sample (g), w_1 is the constant weight of empty flask (g) and w_2 is the constant weight of extract + flask (g).

Surface oil (O_s) or non-encapsulated oil is determined by the washing method using n-hexane as described by Lim and Roos (2017). This measurement was conducted on day zero and every 15 days during the 30-day storage at room temperature (25 ± 3°C). The sample was weighed as 2 g on a funnel having a filter paper. The sample was washed for four times by using 10-mL n-hexane for each wash. The beaker containing n-hexane and extracted surface oil was then left for two days for evaporation of n-hexane. Then the beaker containing surface oil and remaining hexane was dried using an oven at 105°C for 30 min to obtain a constant weight. The calculation of surface oil was carried out by using Equation (8):

$$O_S(\%) = \frac{w_2 - w_1}{w} \times 100\%, \quad (8)$$

where w is the weight of the sample (g), w_1 is the constant weight of beaker (g) and w_2 is the constant weight of surface oil + beaker (g).

The microencapsulation efficiency was calculated by comparing the encapsulated oil (total oil - surface oil) and the total oil from the sample as described by Anwar and Kunz (2011). The microencapsulation efficiency was calculated by using Equation (9):

$$\text{Microencapsulation Efficiency}\,(\%) = \frac{(O_T - O_S)}{O_T} \times 100\%, \quad (9)$$

where O_T is the amount of total oil (%) and O_S is the amount of surface oil (%).

Peroxide value

Peroxide indicates oil damage because of oxidation, which is characterized by the appearance of rancid odor in the products. The peroxide value of the sample was measured according to the official methods of International Organization for Standardization (ISO) and International

Dairy Federation (IDF) (2006), and the oil extraction process from VCO powder was carried out as described by Partanen *et al*,(2008) with several modifications. This measurement was carried out on day zero and every 15 days during the 30-day storage at room temperature (25 ± 3°C). The sample was weighed as 0.5 g in a test tube and 0.5-mL distilled water was added to it, and homogenized with a vortex mixer for 30 sec. Pipette 400-µL sample solution into a microcentrifuge tube and 1.5-mL isooctane:isopropanol (2:1 ratio) solution was added to it. The solution was centrifuged using a microcentrifuge (Thermo Scientific Sorvall Legend Micro 17R Centrifuge, United Kingdom) (5,000 rpm, 5 min, 25°C). The upper phase (supernatant) was separated for analysis. The extraction process was continued for up to three times of extraction using the same solvent and centrifuge. A 100-µL aliquot of the extraction was moved to a test tube and 9.8 mL of chloroform:methanol (7:3 ratio) solution was added to it. For color formation, 50 µL of Fe^{2+} solution (filtrate from the mixture of barium chloride solution [0.2 g $BaCl_2 \cdot 2H_2O$ was dissolved in 25-mL distilled water] and iron (III) sulfate solution [0.25 g $FeSO_4 \cdot 7H_2O$ was dissolved in 25-mL distilled water]) and 50 µL of 30% ammonium thiocyanate solution (7.5 g dissolved in 25-mL distilled water) were added to samples. The samples were homogenized using a vortex mixer and incubated in dark for 10 min. The absorbance was measured by using a spectrophotometer (VIS-7220G/UV-9200 Ray Leigh Spectrophotometer, Beijing, China) at 500 nm, and the peroxide value was calculated by using a standard curve of Fe^{3+} (0–5 ppm).

Particle size of rehydrated VCO powder

The particle size of rehydrated VCO powder was determined using the laser diffraction particle size analyzer (LS 13 320, Beckman Coulter, United States). For rehydrated microcapsules, 50 mL of distilled water was added to 1 g of sample and stirred by using a magnetic stirrer at a speed of 892 rpm with a 3-mm × 7-mm magnetic bar at 25 ± 3°C until dissolved completely. The measurement was carried out immediately after the rehydration process. The particle size of VCO powder was expressed as the average size, and the PDI was calculated using Equation (10) (Hirschle *et al*., 2016):

$$PDI = \left(\frac{\sigma}{d}\right)^2 \quad (10)$$

where σ is the standard deviation of particle size distribution (µm), and d is the mean diameter of particle (µm).

Dissolving time

Dissolving time was measured as described by Tinay and Ismail (1985). Distilled water, 50 mL, was added to 1 g of sample and stirred using a magnetic stirrer at a speed of 892 rpm with a 3-mm × 7-mm magnetic bar at 25 ± 3°C. The time taken for all solid particles to dissolve completely in the solvent was recorded as the dissolving time.

Results and Discussion

Characterization of emulsions

Creaming index

Emulsion instability usually occurs if the emulsion is stored for a long period. The major cause of emulsion instability is creaming due to gravitational separation, resulting in the separation of emulsion system into two layers. However, the Pickering emulsion system is more stable because it requires more energy to remove solid particles from the emulsion system (Ahsan *et al*., 2020). As observed in Table 1, all VCO emulsions did not depict creaming or other types of instability (creaming index = 0%) up to 21 days of storage. This means that Pickering emulsion with MCC, with or without Tween 80 can maintain the stability of emulsion system for up to 21 days. In the mechanism of Pickering emulsion, MCC is absorbed onto the VCO droplet surface, thus covering the droplet surface by forming a thick layer which acts as a barrier to prevent flocculation between VCO droplets (Xu *et al*., 2016). Apart from this, addition of MCC in high concentrations also result in the presence of MCC in continuous phase, which increases the viscosity to make a gel-like continuous phase (Wei *et al*., 2019; Zhang *et al*., 2017a, 2017b). This happened in this study because the MCC used was

Table 1. The characteristics of VCO Pickering emulsion with MCC.

Sample	Creaming index (%)				Droplet size (µm)	PDI
	Day 0	Day 7	Day 14	Day 21		
VCO emulsion with Tween 80 and MCC	0	0	0	0	1.3620 ± 0.0193	0.2024 ± 0.0103
VCO emulsion with MCC	0	0	0	0	1.4678 ± 0.0163	0.1691 ± 0.0119

Values are mean ± SD of duplicate determination.
PDI: polydispersity index.

a colloidal type Vivapur® MCG 811 F MCC containing 11.30–18.80% carboxymethyl cellulose (CMC). Presence of CMC made droplets in the continuous phase unable to move freely because of the formation of a three-dimensional (3D) network between MCC and water that bound VCO droplets tightly to prevent phase separation (Ahsan *et al*., 2020; Xu *et al*., 2016). This mechanism was in accordance with the terminal velocity equation of Stokes' Law because emulsion stability is directly proportional to viscosity (McClements, 2005). Similar results were observed by Xu *et al*. (2016), where the stability of emulsion system made with low molecular surfactants was increased by MCC adsorption on oil droplet surface. Kargar *et al*. (2012) and Xu *et al*. (2016) also had a similar result, where the addition of MCC to an o/w emulsion without surfactant produced a good emulsion stability.

The VCO emulsion prepared with MCC alone had a higher viscosity than the VCO emulsion prepared with Tween 80 and MCC. The use of surfactant (Tween 80) resulted in the –OH group from Tween 80 binding to the –OH group from water so that it can reduce interaction between MCC particles and water to form a 3D network, resulting in decreased emulsion viscosity (Raman and Aichele, 2020; Vashisth *et al*., 2010). Although the viscosity was different, both emulsions had a good stability of up to 21 days. Therefore, Pickering emulsion with MCC, with or without Tween 80, could maintain the stability of VCO emulsion system for a longer period.

Droplet size of emulsions

The stability of an emulsion system also depends on the size of droplet, where the size of droplet is influenced by the homogenization process (time and speed), and the type and concentration of emulsifier (Hadnadev *et al*., 2013). As observed in Table 1, the VCO emulsion with Tween 80 and MCC had a smaller droplet size. This phenomenon occurred due to the process by which surfactant and solid particles reached the oil–water interface during the emulsification process. At the beginning of the process, the droplet size would be reduced drastically so that the interface area in the emulsion system increased rapidly. The low molecular surfactant (Tween 80) would gather quickly at the oil–water interface and reduced its surface tension, thereby allowing a more efficient breakdown of oil droplets during the emulsification process, resulting in smaller droplet size of emulsion. Besides, the presence of this surfactant could temporarily stabilize the emulsion system (Pichot *et al*., 2010; Raman and Aichele, 2020). Furthermore, the added solid particles (MCC) would coat all the available oil–water interfaces and significantly reduce the coalescence. This mechanism of stabilization of mixed emulsifier system produced smaller emulsion droplets than those produced by using surfactants or solid particles only. This has also been proved by Pichot *et al*. (2010) and Raman and Aichele (2020).

The PDI value demonstrates an overview of the distribution data of particles of different sizes in an emulsion system. PDI is a scale and has no dimensions, with the PDI value are ranging from <0.05 (rarely found) to a maximum of 1.0 (Vicente *et al*., 2018). According to Das and Chaudhury (2011), a PDI value of >0.30 indicates that the particles are no longer homogeneous. According to McClements (2005), a PDI value of >0.50 indicates a very heterogeneous and wide distribution of particle size or very polydispersity, and a PDI value of 1.0 indicates that the sample has the possibility of containing large particles or aggregates which would eventually form a sediment (Vicente *et al*., 2018). As observed in Table 1, both emulsion systems had a PDI < 0.30, which means they had a homogeneous particle size distribution.

Powder analysis

Drying yield

The VCO powder has different drying yield values depending on the microencapsulation process and coating materials. Low drying yield can occur during the drying process because of stickiness in drying chamber, milling and sieving tools, or spill during the drying, milling and sieving processes (Nurhadi *et al*., 2012). As observed in Table 2, spray drying resulted in the lowest drying yield followed by vacuum drying, and the highest drying yield was obtained by freeze drying with the same ratio of oil and coating materials.

Spray drying had the lowest drying yield because of high probability of microencapsules sticking to the drying chamber (Yanuwar *et al*., 2007). Furthermore, the relatively low inlet temperature of spray drying used in this study (150°C) with the aim of maintaining its bioactive components might have contributed to low drying yield (Tonon *et al*., 2008). Vacuum drying had a slightly higher drying yield than spray drying. This was because the vacuum process absorbed water of the sample so that the sample would be sprayed in the oven, resulting in a low drying yield. Meanwhile, freeze drying had the highest drying yield because almost all solids of the freeze-dried emulsion could be used. Freeze-drying process is through water freezing and ice sublimation so that it never causes any product loss. Similar results were observed by Román *et al*. (2020), as the drying yield of rice bran oil powder produced from freeze-drying technique was higher than spray drying technique (96.9% vs. 50.8%). From the viewpoint of different emulsion treatments, the drying yield obtained from VCO emulsion with Tween 80 and MCC

Table 2. Characteristics of VCO powder from Pickering emulsion with MCC and different drying techniques.

Sample	Drying yield (%)	Moisture content (% wb)	Rehydrated particle size (μm)	PDI	Dissolving time (sec)
A	44.98 ± 6.78%	3.83 ± 0.01%	1.5017 ± 0.0099	0.1358 ± 0.0029	108.50 ± 16.26
B	94.03 ± 2.83%	3.51 ± 0.47%	1.4820 ± 0.0139	0.1423 ± 0.0040	78.75 ± 2.47
C	48.98 ± 4.11%	2.19 ± 0.56%	1.5203 ± 0.0155	0.1339 ± 0.0088	156.50 ± 3.54
D	53.86 ± 4.98%	3.49 ± 0.24%	1.5460 ± 0.0104	0.1153 ± 0.0017	188.25 ± 3.18
E	96.43 ± 1.71%	4.74 ± 1.38%	1.5197 ± 0.0025	0.1304 ± 0.0019	101.50 ± 5.66
F	55.66 ± 6.25%	3.42 ± 1.52%	1.5493 ± 0.0064	0.1106 ± 0.0013	258.20 ± 12.73

Values are mean ± SD of duplicate determination.
PDI: polydispersity index; wb = wet basis.
A = VCO + Tween 80 + MCC by spray drying; B = VCO + Tween 80 + MCC by freeze drying; C = VCO + Tween 80 + MCC by vacuum drying; D = VCO + MCC by spray drying; E = VCO + MCC by freeze drying; F = VCO + MCC by vacuum drying.

Table 3. The L*, a*, b*, Hue and Chroma values of VCO powder from Pickering emulsion with MCC and different drying techniques during storage.

Sample		L*	a*	b*	Hue	Chroma
A	Day 0	92.46 ± 1.17	−0.30 ± 0.10	3.29 ± 1.13	95.28 ± 0.15	3.30 ± 1.13
	Day 15	91.78 ± 1.39	−0.26 ± 0.02	2.91 ± 1.07	95.40 ± 1.56	2.92 ± 1.07
	Day 30	91.85 ± 1.75	−0.24 ± 0.04	3.01 ± 0.56	94.56 ± 0.04	3.02 ± 0.56
B	Day 0	93.32 ± 0.17	−0.14 ± 0.09	1.83 ± 0.47	94.96 ± 4.02	1.84 ± 0.46
	Day 15	93.83 ± 0.34	−0.17 ± 0.09	2.01 ± 0.17	94.82 ± 3.00	2.02 ± 0.16
	Day 30	93.72 ± 0.42	−0.16 ± 0.10	2.03 ± 0.02	94.37 ± 2.81	2.04 ± 0.01
C	Day 0	79.64 ± 0.22	−1.45 ± 0.44	10.21 ± 3.26	98.12 ± 0.13	10.31 ± 3.29
	Day 15	80.22 ± 0.22	−1.21 ± 0.39	8.31 ± 2.36	98.23 ± 0.30	8.39 ± 2.39
	Day 30	79.14 ± 0.70	−1.24 ± 0.36	2.33 ± 0.40	117.78 ± 2.91	2.64 ± 0.53
D	Day 0	95.17 ± 0.46	−0.12 ± 0.07	2.48 ± 0.56	92.91 ± 2.28	2.48 ± 0.55
	Day 15	94.60 ± 0.15	−0.09 ± 0.09	2.74 ± 0.49	92.09 ± 2.30	2.74 ± 0.49
	Day 30	94.22 ± 0.11	−0.09 ± 0.08	2.62 ± 0.45	92.16 ± 2.22	2.62 ± 0.44
E	Day 0	93.54 ± 0.26	−0.18 ± 0.03	1.82 ± 0.15	95.63 ± 1.45	1.83 ± 0.14
	Day 15	93.19 ± 0.29	−0.18 ± 0.04	1.78 ± 0.15	95.70 ± 1.84	1.79 ± 0.15
	Day 30	92.84 ± 0.17	−0.18 ± 0.04	1.66 ± 0.01	96.12 ± 1.31	1.66 ± 0.01
F	Day 0	86.77 ± 1.76	−0.84 ± 0.47	7.49 ± 1.26	96.18 ± 2.50	7.54 ± 1.30
	Day 15	85.99 ± 1.70	−0.74 ± 0.39	7.63 ± 0.73	95.39 ± 2.38	7.66 ± 0.76
	Day 30	85.05 ± 2.05	−0.69 ± 0.43	7.23 ± 0.24	95.41 ± 3.23	7.27 ± 0.28

*Values are mean ± SD of duplicate determination.
A = VCO + Tween 80 + MCC by spray drying; B = VCO + Tween 80 + MCC by freeze drying; C = VCO + Tween 80 + MCC by vacuum drying; D = VCO + MCC by spray drying; E = VCO + MCC by freeze drying; F = VCO + MCC by vacuum drying.

was lower than that obtained from VCO emulsion only with MCC. Low viscosity from the emulsion system caused low drying yield, and *vice versa* (Sarungallo *et al.*, 2019). This result was in accordance with the literature, where the emulsion system with Tween 80 and MCC had a lower viscosity, resulting in a lower drying yield.

Color analysis

According to Table 3, the high *degrees of lightness to darkness* (L* value) in VCO powder resulted from spray and freeze drying. However, lower L* value was obtained from vacuum-dried powder. Similar results were observed by Horszwald *et al.* (2013) and Michalska and Lech (2018). The long-term use of heat in the vacuum drying process allowed the product to be oxidized and could even be burnt due to caramelization reaction (nonenzymatic browning). Meanwhile, the spray drying process used high temperatures in a very short time, so it did not significantly affect the characteristics of VCO powder. Similarly, the freeze-drying process also did not use heat so that the original color of the product could be maintained. However, all VCO powders obtained from all

drying techniques had white to light cream color, which met the commercial standards of consumer acceptance based on SNI 4444:2009 (Badan Standarisasi Nasional, 2009).

All samples of VCO powder produced by different drying techniques had a slightly greenish color with different *degrees of redness to greenness* (a* value) but still close to zero, which is neutral, except for vacuum-dried VCO powder with a more greenish color. The lengthy process of vacuum drying resulted in the formation of green pigments from colorless precursors present in VCO. The pigments were not from the chlorophyll group, and as described by Joslyn and Sano (1956), the specific compound responsible for the green pigment formed in garlic maceration tissue was not yet known.

All VCO powders also had a positive *degrees of yellowness to blueness* (b* value), which means that powders tended to have a yellowish color. Vacuum-dried VCO powder had the highest b* value, because of Tween 80 and MCC or MCC alone. These results were in accordance with the results obtained by Nurhadi *et al*. (2012), where the vacuum-dried honey powder had the highest b* value because of the long-term heating effect of drying process. After 30 days of storage, there was a decrease in the b* value of vacuum-dried VCO powder, especially in sample C, caused by a greenish pigment formed due to lengthy vacuum drying process. During storage, the greenish pigment turned brown due to exposure to oxygen and would gradually turn yellowish and finally to a light cream color, as described by Joslyn and Sano (1956).

The VCO powder obtained from Pickering emulsion with MCC and different drying techniques demonstrated no significant difference in lightness after 30 days of storage. In addition, VCO powder obtained from an emulsion using Tween 80 and MCC also had lower L* and a* values but a higher b* value because of the yellowish color of Tween 80 that affected the lightness and the color of VCO powder.

The color or shade (hue angle value) of VCO powders ranged from 92.09 to 98.23, confirming that the sample was tended yellow in hue, with the highest hue angle value found in sample C (vacuum-dried VCO powder from the emulsion using Tween 80 and MCC). All VCO powders had stable hue angle values, except sample C, and increased up to 117.78 ± 2.91 on the 30th day of storage because of decrease in b* value.

The spray- and freeze-dried VCO powders had a low saturation (chroma value) compared to vacuum-dried VCO powder, especially sample C, and were stable for up to 30 days of storage. Meanwhile, the chroma value of sample C decreased steadily until the 30th day of storage, resulting in a more faded color.

Overall, VCO powders obtained from all drying techniques had a white to slightly yellowish hue. However, VCO powder obtained from spray drying (samples A and D) and freeze drying (samples B and E) had a slightly yellowish and a little bit of greenish in white hue but still having a bright coloration. Meanwhile, the VCO powder obtained from vacuum drying tended to be more yellowish and greenish than the powders obtained from other two drying techniques because of the long vacuum drying process.

Morphology of VCO powder

As observed in Figure 2, the spray-dried VCO powders (samples A and D) had a specific particle morphology, which was spherical in shape with a smooth surface

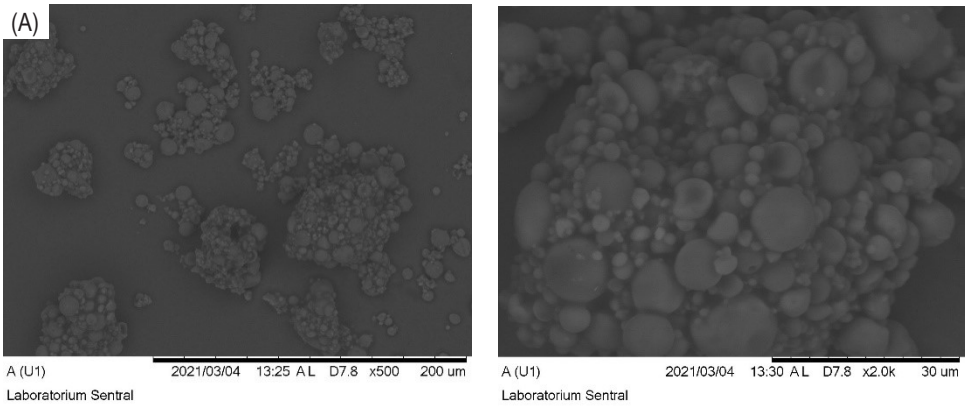

Figure 2. Morphology of VCO powder from Pickering emulsion with MCC and different drying techniques. A = VCO + Tween 80 + MCC by spray drying; B = VCO + Tween 80 + MCC by freeze drying; C = VCO + Tween 80 + MCC by vacuum drying; D = VCO + MCC by spray drying; E = VCO + MCC by freeze drying; F = VCO + MCC by vacuum drying.

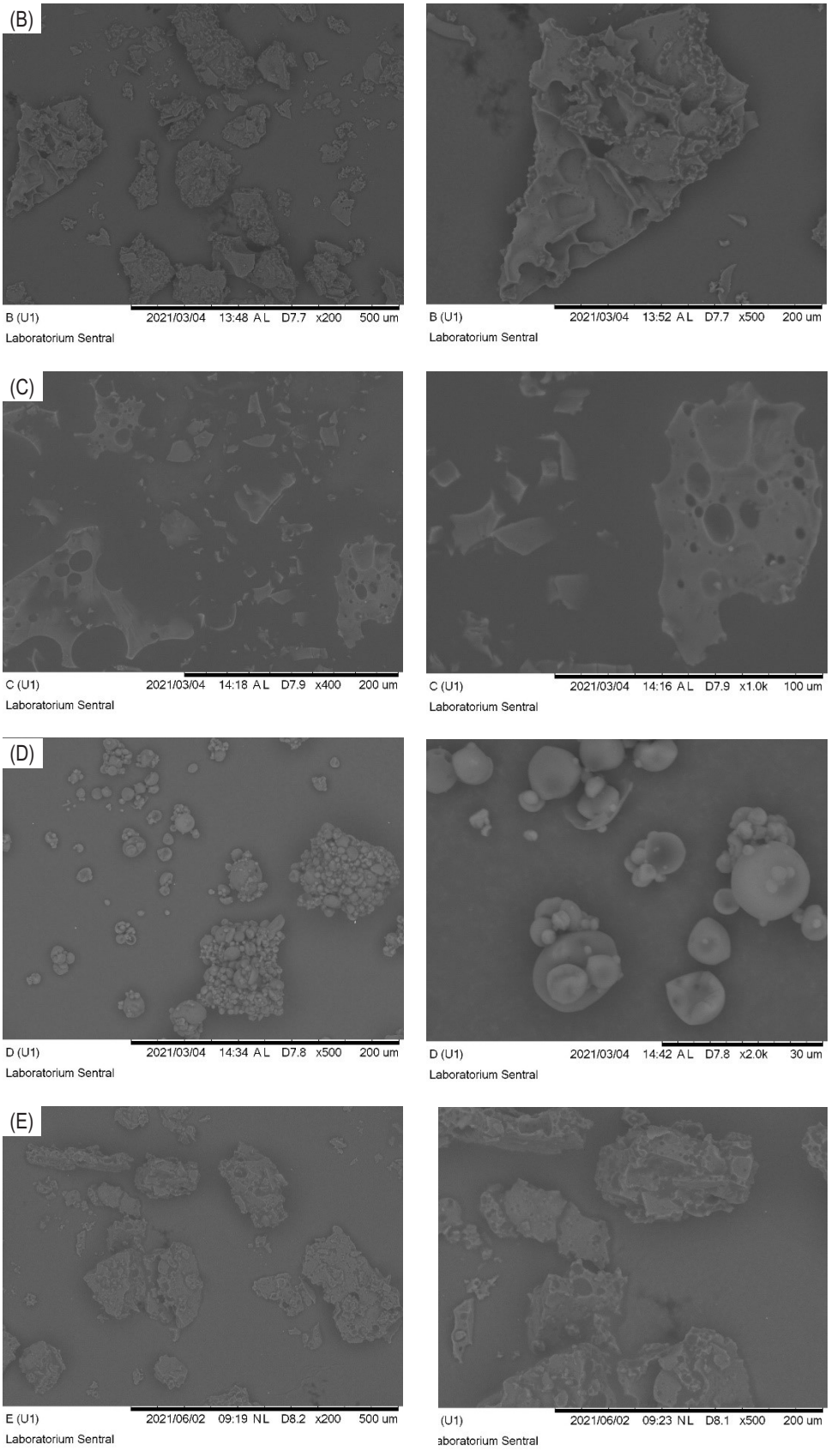

Figure 2. (Continued)

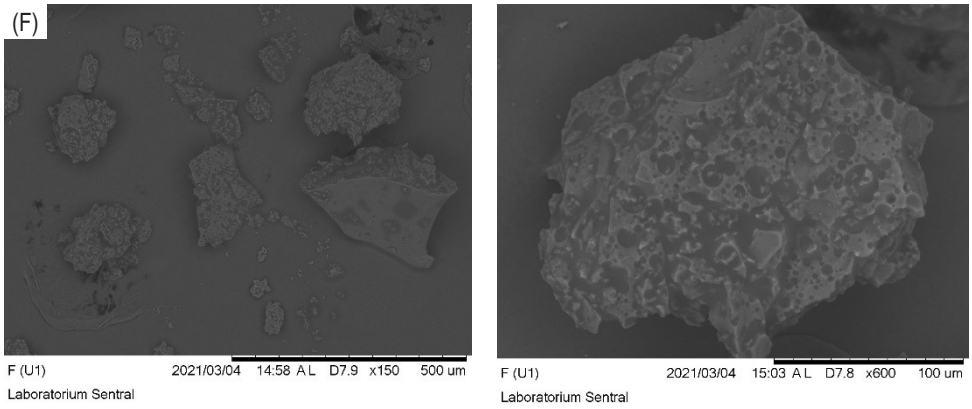

Figure 2. (Continued)

and no pores but some dents caused by rapid water loss during the initial drying process (Ré, 1998; Román *et al*., 2020; Wilkowska *et al*., 2017). The smooth surface of spray-dried particles was caused by the atomization process of spray drying (Pasrija *et al*., 2015). Similar results have been reported by several studies using different coating materials, such as modified starch (Melgosa *et al*., 2019), pea protein (Moreno *et al*., 2016), various biopolymers (Gallardo *et al*., 2013), a combination of maltodextrin and pea protein isolate (Román *et al*., 2020) or a combination of maltodextrin and soy protein isolate (Carneiro *et al*., 2013). In addition, there were also small particles adhered to the surface of spray-dried particles that could be the oil non-capsulized by the matrix, thus inducing other particles to stick to the surface and form a cluster (Román *et al*., 2020). These spherical-shaped particles were perfect for microencapsulation with bioactive components perfectly protected inside the coating agent. Likewise, spray-dried VCO powder had a more regular and uniform shape and size so that the solubility would be more uniform.

Samples B and E, which were freeze-dried VCO powders, had a wrinkled sponge-like morphology with an irregular surface and nonuniform shape, and very light and high porosity. Therefore, these particles had a large surface area. The presence of pores and wrinkles in the particles because of the usage of MCC fastened water removal from the material (Dhar *et al*., 2012) as well as the fast sublimation process of ice crystals on the matrix during freeze drying, resulting in the formation of pores which previously were ice crystals (Smrdel *et al*., 2008). Similar particle morphology has been reported by other studies using different coating materials, such as sodium alginate in anthocyanin extract microcapsules (Zhang *et al*., 2020), a combination of various polymers in fish oil microcapsules (Anwar and Kunz, 2011), and a combination of maltodextrin and pectin in the microcapsules of Moringa stenopetala leaf extract (Dadi *et al*., 2020). High porosity of this freeze-dried VCO powder made it suitable for instant powder drink because it caused rapid dissolution in solvent, but the dissolution was just not uniform because of the nonuniform shape compared to spherical-shaped particles' dissolution.

Samples C and F, which were vacuum-dried VCO powders, had an angular and nonuniform morphology with large cavities on their surfaces. Similar result was observed by Mutlu *et al*. (2020). The presence of cavities in the particles was caused by the suction/vacuum process of water vapor from the heated material to produce dry products with large hollows (Reis, 2014). This particle morphology was almost the same as that of freeze-dried particles but not porous and also had a high surface oil, so it was very oily resulting in low wettability and solubility, making it unsuitable for instant powder drinks.

Moisture content

The VCO powders had different moisture contents depending on the drying techniques and ranged from 2.19% to 4.74% (Table 2). The moisture content obtained was under 5%, which means all of the VCO powders were still accepted in the food industry (Díaz *et al*., 2020). The freeze-dried VCO powder from emulsion with only MCC had the highest moisture content because of its porous structure, so it was more hygroscopic with a higher adsorption capacity than other dried samples (Gong *et al*., 2007). The freeze-drying process that used temperatures lower than –40°C also resulted in the obstruction of mass transfer and sublimation process because of rapid freezing of outer layer pores, thereby increasing the retention of moisture in microcapsules. Similar results were observed by Kuck and Noreña (2016), where the grape skin phenolic extract powder produced by freeze drying had a higher water content than spray drying.

The vacuum-dried VCO powder from emulsion using Tween 80 and MCC had the lowest moisture content caused by vacuum conditions of drying that reduced the heat required to evaporate water so that water evaporation occurred quickly at low pressure (Piwińska *et al*., 2015). Similar results of the moisture content were also obtained by Nurhadi *et al*. (2012), where the vacuum-dried honey powder had a lower moisture content than spray-dried honey powder.

VCO powders obtained from emulsions with MCC only (samples D and F) had a higher moisture content. This was due to the higher viscosity of emulsion, resulting in decreased water diffusion during the drying process because the total solid concentration was more than 20% (Frascareli *et al*., 2012). In addition, use of Tween 80 also produced VCO powder with a low moisture content because of foam formation in the emulsion system (Mayasari *et al*., 2019). The foam layer dried faster than the liquid under the same drying conditions. As a result, the drying process was completed quickly and produced microcapsules with a lower moisture content (Kamsiati, 2006).

Microencapsulation efficiency

Microencapsulation efficiency is defined as the ratio between encapsulated oil and total oil contained in particles (Tonon *et al*., 2012). The microencapsulation efficiency depends on several factors, such as the ratio of core material to coating material, chemical properties, effect of material interactions, and the microencapsulation techniques (Dadi *et al*., 2020).

In Figure 3, all VCO powders had a low microencapsulation efficiency, which is <50%. The low microencapsulation efficiency is caused by the high concentration of oil (40%), so there would be a lack of coating material to encapsulate oil, thus resulting in high surface oil and low encapsulated oil (Frascareli *et al*., 2012). Similar results were also demonstrated in the study conducted by McNamee *et al.* (1998) on encapsulation of soybean oil with gum arabic, where the encapsulation efficiency was reduced from 100% to 48% with oil and gum arabic ratio increasing from 0.25 to 5.00. Several other studies have also demonstrated similar results (Ahn *et al*., 2008; Alcântara *et al*., 2019).

The freeze-dried VCO powder from both emulsion treatments had the lowest microencapsulation efficiency because of high surface oil on particles. The freezing process induced demulsification in the emulsion system because some droplets froze first and the volume of frozen droplets increased, resulting in collisions between droplets, thus damaging water and emulsifier layers that covered the droplets. Many droplets froze together to form larger ice domains due to coalescence, and also some droplets froze because of partial contact with other ice, which is commonly referred to as 'partial coalescence'. The coalescence of particles produced an even larger particle, which at a certain particle size triggered phase separation resulting in high non-encapsulated oil

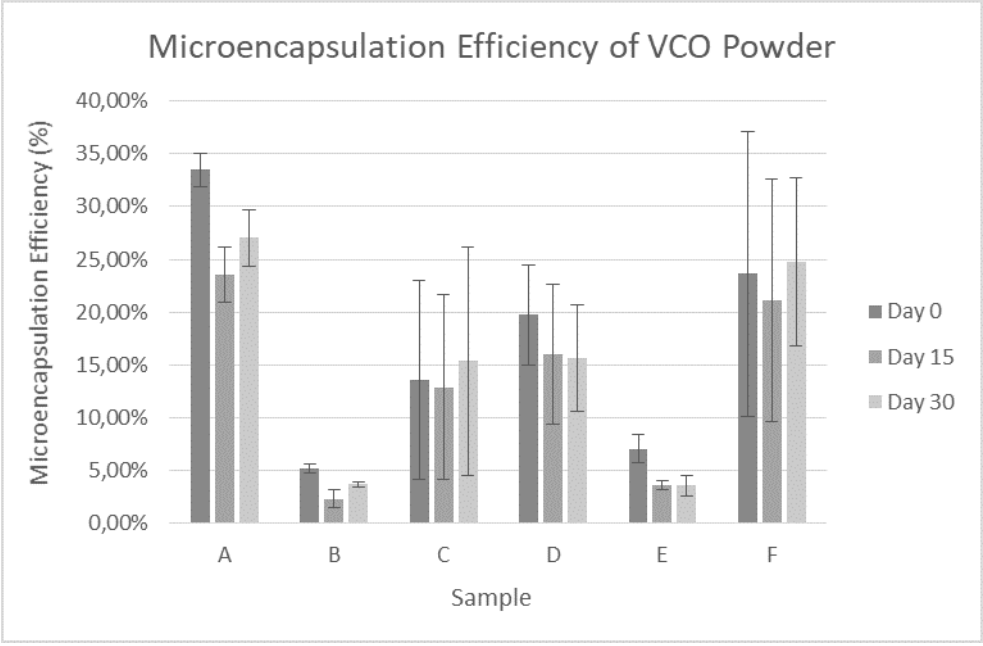

Figure 3. Microencapsulation efficiency of VCO powder from Pickering emulsion with MCC and different drying techniques during storage. A = VCO + Tween 80 + MCC by spray drying; B = VCO + Tween 80 + MCC by freeze drying; C = VCO + Tween 80 + MCC by vacuum drying; D = VCO + MCC by spray drying; E = VCO + MCC by freeze drying; F = VCO + MCC by vacuum drying

in freeze-dried samples (Lin *et al*., 2007). Similar results were obtained by Anwar and Kunz (2011) in microencapsulationof fish oil using freeze drying.

The highest microencapsulation efficiency was obtained by spray drying in the emulsion using Tween 80 and MCC (sample A), with a microencapsulation efficiency of 33.49 ± 1.59%. As observed in Figure 2, particles produced by the spray-drying technique had no cracks and pores in their microstructure, so they would have a good microencapsulation efficiency (Pereira *et al*., 2019). Besides this, using Tween 80 in the emulsion system resulted in a smaller emulsion droplet size, which would result in a higher microencapsulation efficiency. Similar results were observed by Soottitantawat *et al*. (2005), and also supported by Shamaei *et al*. (2017), where there was no correlation between microencapsulation efficiency and microparticle size (or emulsion droplet size).

In addition to spray drying, freeze- and vacuum-dried VCO powders obtained from the emulsion with MCC only had a higher microencapsulation efficiency. This may be affected by the viscosity of emulsion, where using Tween 80 resulted in a lower emulsion viscosity, but the emulsion with MCC only had a higher viscosity. Thus, a stronger matrix was formed in the emulsion using MCC only that helped to prevent the diffusion/migration of oil from matrix to produce microcapsules with higher encapsulated oil (Sarungallo *et al*., 2019).

The microencapsulation efficiency of VCO powder demonstrated decrease on the 15th and 30th day of storage, which means that more oil was diffused from matrix, resulting in high surface oil. Similar results were observed by Esparza *et al*. (2020), where the microencapsulation efficiency of hempseed oil powder stabilized with nanocrystalline cellulose Pickering emulsion decreased after 30 days of storage.

Peroxide value

Peroxide is an indicator to determine the level of oxidation of fats and oil products. The peroxide value of all VCO powders depicted a higher value compared to the characterization result of VCO, which was only 0.052 mEq O_2/kg. This indicated that exposure to light, oxygen and heat during the microencapsulation process could facilitate oxidation (Mubarak, 2017). However, increase in the peroxide value was still below the maximum limit of the quality requirements of VCO peroxide value, which is 2.0 mEq O_2/kg based on SNI 01-7381-2008 (Badan Standardisasi Nasional, 2008), which established that VCO powder was still safe for consumption. A slight increase in the peroxide value of VCO powder was due to a small amount of unsaturated fatty acids (about 10%) that we discovered in VCO, which could be oxidized easily.

In Figure 4, the spray-dried VCO powder (samples A and D) demonstrated the highest peroxide value, and the

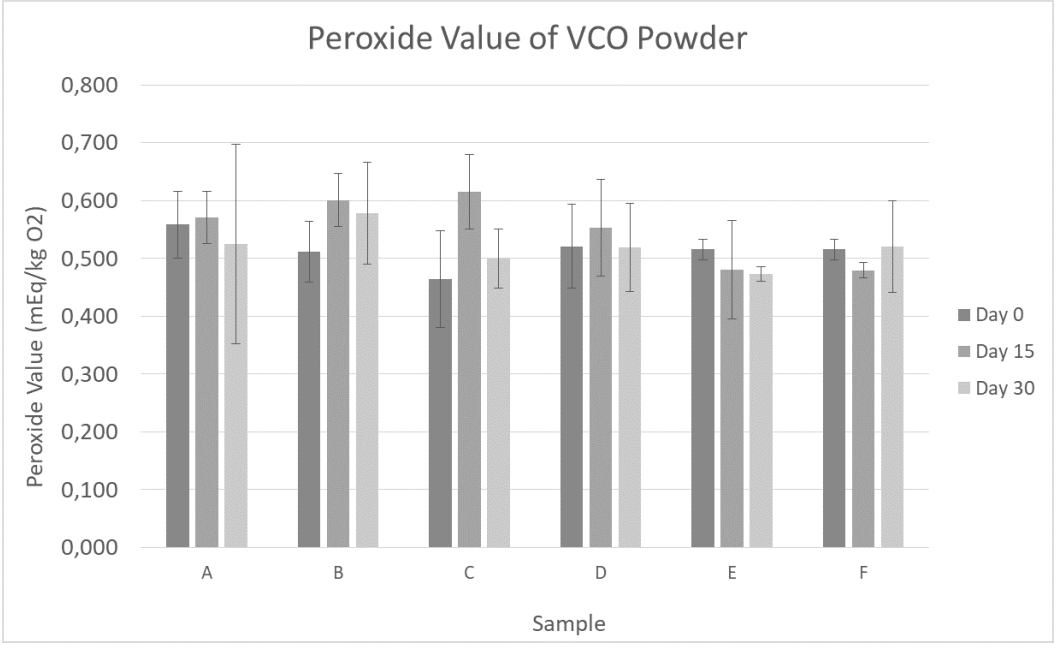

Figure 4. Peroxide value of VCO powder from Pickering emulsion with MCC and different drying techniques during storage. A = VCO + Tween 80 + MCC by spray drying; B = VCO + Tween 80 + MCC by freeze drying; C = VCO + Tween 80 + MCC by vacuum drying; D = VCO + MCC by spray drying; E = VCO + MCC by freeze drying; F = VCO + MCC by vacuum drying.

vacuum-dried VCO powder depicted the lowest peroxide value on day zero. Exposure to high temperatures of heat during the spray drying process could be the reason for accelerated oxidation, resulting in high peroxide formation in the sample (Anwar and Kunz, 2011). The vacuum process helped to minimize the oxygen that was contacted with the sample, so it prevented peroxide formation. However, peroxide values from all drying techniques did not differ significantly because basically VCO only contained a small amount of unsaturated fatty acids (about 10%), which could be easily oxidized (Nurhasanah *et al*., 2019).

During storage, the peroxide value of VCO powder first depicted an increase on the 15th day then a decrease on the 30th day. Similar trends were obtained in different VCO powder samples. These results indicated that the oxidation would gradually increase to reach a peak, then it would decrease. However, the increase in peroxide value on the 15th day tended to be higher in vacuum-dried VCO powder, and the lowest increase was observed in spray-dried VCO powder. Previous study conducted by Anwar and Kunz (2011) established that spray-dried powder tended to be unstable due to the presence of pro-oxidants at high temperatures, which could result in rapid peroxide decomposition after its formation. Therefore, only a slight increase in peroxide value during the 15 days of storage was observed compared to other dried samples.

The stability of VCO powder during storage was also influenced by several other factors, such as particle morphology and surface oil (Tolun *et al*., 2016). VCO powders obtained from freeze drying (samples B and E) and vacuum drying (samples C and F) had an irregular morphology. As a result, the surface area was larger, so that it was more likely to be exposed to oxidation than fine particles (Pereira *et al*., 2019; Tolun *et al*., 2016). In addition, the freeze- and vacuum-dried VCO powders had high porosity and large cavities. These conditions facilitated the diffusion of oxygen on particles' surface and even the particles in surface, so that oxygen easily decomposed the non-encapsulated oil (Anwar and Kunz, 2011). Moreover, the freeze- and vacuum-dried VCO powders had a higher surface oil than the spray-dried VCO powder. Therefore, this could be one of the reasons for high increase in peroxide value on the 15th day of storage because surface oil tended to be oxidized more easily (Condori *et al*., 2011).

A different trend was observed in sample E of VCO powder, where its peroxide value depicted a downward trend up to the 30th day of storage. Sample F of VCO powder also depicted a decrease in peroxide value on the 15th day, and then an increase occurred on the 30th day of storage. Decrease in peroxide value during storage was because only a few new peroxides were formed compared to high degradation rate, resulting in secondary oxidation products in the form of aldehyde and ketone compounds (Ketaren, 1986). Some of the main aldehyde compounds produced from secondary oxidation were n-alkanal, trans-2-alkenes, 4-hydroxy-trans-2-alkenes and malondialdehyde (Chaijan and Panpipat, 2017). These aldehyde compounds would undergo an oxidation process to form carboxylic acids, which belong to the free fatty acid group. Hydrogen present in this carboxylic acid would form fatty acid radicals that react with oxygen to again produce peroxides during storage (Widodo *et al*., 2020). This increased the peroxide value of sample F on the 30th day of storage.

VCO powder obtained from emulsion with Tween 80 and MCC (samples A–C) also demonstrated a higher increase in peroxide value on the 15th day of storage. This could be due to the use of Tween 80, which belonged to the triglyceride group, allowing the fatty acid components of Tween 80 to be oxidized during storage, resulting in a higher peroxide value compared to the non-Tween 80 samples.

Particle size of rehydrated VCO powder

As observed in Table 2, all rehydrated VCO powders had a slight increase in the particle size compared with their emulsions' droplet size but not different significantly (Table 1). These results indicated that the emulsion systems had the possibility of slight coalescence because of heating and freezing during the microencapsulation process.

All rehydrated VCO powders had the same PDI value, which was still below 0.30, indicating that there hydrated dried particles were homogeneous. However, the rehydrated freeze-dried VCO powder from both emulsions depicted higher PDI values than other dried samples with the same emulsion treatment. These phenomena occurred due to the greater coalescence process during freezing than heating so that a higher PDI was obtained (Lin *et al*., 2007).

Dissolving time

Dissolving time is the time required for all particles to dissolve homogeneously in solvent through stirring (Pereira *et al*., 2019). The dissolving time is one of the parameters of microcapsule rehydration properties and is important for producing instant powder drinks. The lower the dissolving time, the better it would be for instant powder drink. As presented in Table 2, the dissolving time of VCO powders was in the range of 78.75–258.50 sec, while the dissolving time of microencapsulated pink

pepper essential oil observed by Pereira *et al*. (2019) was in the range of 329–351 sec. Relatively fast dissolving time of VCO powders in water is one of the important requirements of the food industry, because it can expand the possible use of VCO in food products that are insoluble in water in their original form (Pereira *et al*., 2019).

The dissolving time is influenced by different structural characteristics of VCO powders related to matrix and drying conditions (Farias and Ratti, 2009; Rahman and Perera, 2007). Freeze-dried VCO powder (samples B and E) had the minimum dissolving time compared to other drying principles whereas vacuum-dried VCO powder had the longest dissolving time. This was due to the high porosity of freeze-dried VCO powder, as depicted in Figure 2, so that it had the shortest dissolving time because particle porosity also played an important role in powder rehydration (Farias and Ratti, 2009; Fernandes *et al*., 2013; Stapley, 2008). Similar results were observed by Karthik and Anandharamakrishnan (2013). The spray-dried VCO powder had a longer dissolving time than freeze-dried VCO powder but faster than vacuum-dried VCO powder. This was in line with particle morphology, because the spray-dried VCO powder had nonporous particles compared to freeze-dried VCO powder, but it also had a larger surface area than vacuum-dried VCO powder, so that its dissolving time was in between freeze- and vacuum-dried VCO powders. Meanwhile, the vacuum-dried VCO powder, with a sticky characteristic, had the smallest surface area among all VCO powders obtained from different drying techniques. It tended to stick together due to wetness of surface oil, affecting the wettability of particles, resulting in the longest dissolving time in samples C and F.

VCO powders from emulsion with Tween 80 and MCC (samples A–C) had a faster dissolving time because of Tween 80, which formed foam in the emulsion system, resulting in a porous microcapsule (Ngamwonglumlert and Devahastin, 2017). The high porous structure resulted in high solvent penetration of particles, hence shorter time required to dissolve all particles homogeneously in the solvent (Farias and Ratti, 2009).

Conclusion

The Pickering emulsion method (with or without Tween 80) could be used to produce VCO powders of good characteristics, which, of course, were also affected by drying techniques. Usage of MCC resulted in thicker emulsion system. However, addition of Tween 80 decreased emulsion viscosity (but both emulsion treatments had a good stability of up to 21 days of storage) and resulted in a emulsion of smaller droplet size than without addition of Tween 80. So did the drying techniques. Spray drying produced VCO powder with the lowest drying yield (44.98–53.86%), had bright and white spherical shape particles, smooth surface and no pores, but with some dents on the particle surface. It has the highest microencapsulation efficiency (33.49 ± 1.59%) and peroxide value on day zero (0.558 ± 0.058 mEq O_2/kg) with not too slow dissolving time. Freeze drying produced VCO powder with the highest drying yield (94.03–96.43%), had bright and white wrinkled sponge-like particles with an irregular and very porous surfaces. It had the smallest rehydrated particle size (1.4820 ± 0.0139 μm) and the fastest dissolving time in solvent (78.75 ± 2.47 sec), with the highest peroxide value on the 30th day of storage (0.578 ± 0.088 mEq O_2/kg). Vacuum drying produced VCO powder with a more yellowish color with angular shape particles with large cavities on the surface. It had the lowest moisture content (2.19 ± 0.56%), the highest peroxide value on the 15th day of storage (0.615 ± 0.065mEq O_2/kg), and the longest dissolving time (258.20 ± 12.73 sec).

Based on the results, spray drying was the best technique to produce VCO powder with good characteristics compared to other techniques; hence, Sample A (VCO emulsion using Tween 80 and MCC with spray drying) had no creaming index up to 21 days of storage, had small size of emulsion droplet, and bright and white color VCO powder. It had spherical shape particles, high microencapsulation efficiency and not too slow dissolving time. Therefore, spray drying technique is worth applying in various applications of microencapsulation than other two drying techniques. Overall, the characteristics of VCO powders obtained in this study were quite good, but had low microencapsulation efficiency. Further research is required to study and increase the concentration of solid emulsifier and to replace MCC with CNC with a lower concentration but providing better stability and higher microencapsulation efficiency to VCO powder so that it could be used as a non-dairy creamer in accordance with quality requirements and consumer requirements.

References

Ahn, J.-H., Kim, Y.-P., Lee, Y.-M., Seo, E.-M., Lee, K.-W., & Kim, H.-S. (2008). Optimization of microencapsulation of seed oil by response surface methodology. *Food Chemistry*, *107*(1), 98–105. https://doi.org/10.1016/j.foodchem.2007.07.067

Ahsan, H. M., Zhang, X., Liu, Y., Wang, Y., Li, Y., Li, B., Wang, J., & Liu, S. (2020). Stable cellular foams and oil powders derived from methylated microcrystalline cellulose stabilized pickering emulsions. In Professor Pete Williams DSc PhD (Ed.), *Food Hydrocolloids* (Vol. 104). Elsevier Ltd. https://doi.org/10.1016/j.foodhyd.2020.105742

Akhtar, M., Murray, B. S., Afeisume, E. I., & Khew, S. H. (2014). Encapsulation of flavonoid in multiple emulsion using spinning

disc reactor technology. *Food Hydrocolloids*, *34*, 62–67. https://doi.org/10.1016/j.foodhyd.2012.12.025

Alavi, M. (2019). Modifications of microcrystalline cellulose (MCC), nanofibrillated cellulose (NFC), and nanocrystalline cellulose (NCC) for antimicrobial and wound healing applications. *E-Polymers*, *19*(1), 103–119. https://doi.org/10.1515/epoly-2019-0013

Alcântara, M. A., Lima, A. E. A. de, Braga, A. L. M., Tonon, R. V., Galdeano, M. C., Mattos, M. da C., Brígida, A. I. S., Rosenhaim, R., Santos, N. A. dos, & Cordeiro, A. M. T. de M. (2019). Influence of the emulsion homogenization method on the stability of chia oil microencapsulated by spray drying. *Powder Technology*, *354*, 877–885. https://doi.org/10.1016/j.powtec.2019.06.026

Amaral, P. H. R. do, Andrade, P. L., & Conto, L. C. de. (2019). Microencapsulation and Its Uses in Food Science and Technology: A Review. In F. Salaun (Ed.), *Microencapsulation - Processes, Technologies and Industrial Applications* (pp. 1–18). IntechOpen. https://doi.org/10.5772/intechopen.81997

Anandharamakrishnan, C., & Ishwarya, S. P. (2015). Introduction to spray drying. In C. Anandharamakrishnan & S. P. Ishwarya (Eds.), *Spray Drying Techniques for Food Ingredient Encapsulation* (pp. 1–36). John Wiley & Sons Inc. https://doi.org/10.1002/9781118863985.ch1

Anwar, S. H., & Kunz, B. (2011). The influence of drying methods on the stabilization of fish oil microcapsules: Comparison of spray granulation, spray drying, and freeze drying. *Journal of Food Engineering*, *105*(2), 367–378. https://doi.org/10.1016/j.jfoodeng.2011.02.047

AOAC. (2005a). *Association of Official Analytical Chemistry (AOAC) Official Method 963.15, Lipid Content.*

AOAC. (2005b). Solids (Total) and Moisture in Flour, Method 925.10. *Official Methods of Analysis, 18th Edition*.

Badan Standardisasi Nasional. (2008). *SNI 01-7381-2008 Minyak Kelapa Virgin (VCO)* (pp. 1–28). Badan Standarisasi Nasional.

Badan Standarisasi Nasional. (2009). *SNI 4444:2009 Krimer Nabati Bubuk* (pp. 1–37). Badan Standarisasi Nasional.

Bai, L., Huan, S., Xiang, W., & Rojas, O. J. (2018). Pickering emulsions by combining cellulose nanofibrils and nanocrystals: Phase behavior and depletion stabilization. *Green Chemistry*, *20*(7), 1571–1582. https://doi.org/10.1039/c8gc00134k

Bazyma, L. A., & Kutovoy, V. A. (2005). Vacuum drying and hybrid technologies. *Stewart Postharvest Review*, *1*(4), 1–4. https://doi.org/10.2212/spr.2005.4.7

Carneiro, H. C. F., Tonon, R. V., Grosso, C. R. F., & Hubinger, M. D. (2013). Encapsulation efficiency and oxidative stability of flaxseed oil microencapsulated by spray drying using different combinations of wall materials. *Journal of Food Engineering*, *115*(4), 443–451. https://doi.org/10.1016/j.jfoodeng.2012.03.033

Chaijan, M., & Panpipat, W. (2017). Mechanism of Oxidation in Foods of Animal Origin. In R. Banerjee, K. A. Verma, & M. W. Siddiqui (Eds.), *Natural Antioxidants* (1st ed., pp. 1–37). Taylor & Francis Group. https://doi.org/10.1201/9781315365916-2

Condori, S. Q., Saldaña, M. D. A., & Temelli, F. (2011). Microencapsulation of flax oil with zein using spray and freeze drying. *LWT - Food Science and Technology*, *44*(9), 1880–1887. https://doi.org/10.1016/j.lwt.2011.01.005

Costa, Medronho, Filipe, Mira, Lindman, Edlund, & Norgren. (2019). Emulsion Formation and Stabilization by Biomolecules: The Leading Role of Cellulose. *Polymers*, *11*(10), 1570. https://doi.org/10.3390/polym11101570

Dadi, D. W., Emire, S. A., Hagos, A. D., & Eun, J. B. (2020). Physical and Functional Properties, Digestibility, and Storage Stability of Spray- and Freeze-Dried Microencapsulated Bioactive Products from Moringa stenopetala Leaves Extract. *Industrial Crops and Products*, *156*(2020), 1–10. https://doi.org/10.1016/j.indcrop.2020.112891

Das S., & Chaudhury A. (2011). Recent Advances in Lipid Nanoparticle Formulations with Solid Matrix for Oral Drug Delivery. AAPS PharmSciTech. 12(1): 62–76. https://doi.org/10.1208/s12249-010-9563-0

Dhar, N., Akhlaghi, S. P., & Tam, K. C. (2012). Biodegradable and biocompatible polyampholyte microgels derived from chitosan, carboxymethyl cellulose and modified methyl cellulose. *Carbohydrate Polymers*, *87*(1), 101–109. https://doi.org/10.1016/j.carbpol.2011.07.022

Díaz, C. B.-, Navarrete, M. O.-, Añual, M. S.-, Calderón, F. L.-, & Bustamante, M. (2020). Food-grade Pickering emulsion as a novel astaxanthin encapsulation system for making powder-based products: Evaluation of astaxanthin stability during processing, storage, and its bioaccessibility. *Food Research International*, *134*, 109244. https://doi.org/10.1016/j.foodres.2020.109244

Esparza, Y., Ngo, T. D., & Boluk, Y. (2020). Preparation of powdered oil particles by spray drying of cellulose nanocrystals stabilized Pickering hempseed oil emulsions. *Colloids and Surfaces A: Physicochemical and Engineering Aspects*, *598*(March), 124823. https://doi.org/10.1016/j.colsurfa.2020.124823

Farias, M. A., & Ratti, C. (2009). Dehydration of Foods : General Concepts. In C. Ratti (Ed.), *Advances in Food Dehydration* (pp. 1–36). Taylor & Francis Ltd.

Fernandes, R. V. de B., Borges, S. V., & Botrel, D. A. (2013). Influence of spray drying operating conditions on microencapsulated rosemary essential oil properties. *Ciência e Tecnologia de Alimentos*, *33*, 171–178. https://doi.org/10.1590/S0101-20612013000500025

Frascareli, E. C., Silva, V. M., Tonon, R. V., & Hubinger, M. D. (2012). Effect of process conditions on the microencapsulation of coffee oil by spray drying. *Food and Bioproducts Processing*, *90*(3), 413–424. https://doi.org/10.1016/j.fbp.2011.12.002

Gallardo, G., Guida, L., Martinez, V., López, M. C., Bernhardt, D., Blasco, R., Pedroza-Islas, R., & Hermida, L. G. (2013). Microencapsulation of linseed oil by spray drying for functional food application. *Food Research International*, *52*(2), 473–482. https://doi.org/10.1016/j.foodres.2013.01.020

Gomes, A., Costa, A. L. R., & Cunha, R. L. (2018). Impact of oil type and WPI/Tween 80 ratio at the oil-water interface: Adsorption, interfacial rheology and emulsion features. *Colloids and Surfaces B: Biointerfaces*, *164*, 272–280. https://doi.org/10.1016/j.colsurfb.2018.01.032

Gong, Z., Zhang, M., & Sun, J. (2007). Physico-chemical properties of cabbage powder as affected by drying methods. *Drying Technology*, *25*(5), 913–916. https://doi.org/10.1080/07373930701372239

Hadnadev, T. D., Dokić, P., Krstonošić, V., & Hadnadev, M. (2013). Influence of oil phase concentration on droplet size distribution and stability of oil-in-water emulsions. *European Journal of Lipid Science and Technology*, *115*(3), 313–321. https://doi.org/10.1002/ejlt.201100321

Hee, Y. Y., Tan, C. P., Rahman, R. A., Adzahan, N. M., Lai, W. T., & Chong, G. H. (2015). Influence of Different Wall Materials on the Microencapsulation of Virgin Coconut Oil by Spray Drying. *International Journal of Food Engineering*, *11*(1), 61–69. https://doi.org/10.1515/ijfe-2014-0215

Hee, Y. Y., Tan, C. P., Rahman, R. A., Noranizan, M., Smith Jr, R. L., & Chong, G. H. (2017). Production of virgin coconut oil microcapsules from oil-in-water emulsion with supercritical carbon dioxide spray drying. *The Journal of Supercritical Fluids*, *130*, 118–124. https://doi.org/10.1016/j.supflu.2017.07.037

Hirschle, P., Preiß, T., Auras, F., Pick, A., Völkner, J., Valdepérez, D., Witte, G., Parak, W. J., Rädler, J. O., & Wuttke, S. (2016). Exploration of MOF nanoparticle sizes using various physical characterization methods-is what you measure what you get? *CrystEngComm*, *18*(23), 4359–4368. https://doi.org/10.1039/c6ce00198j

Horszwald, A., Julien, H., & Andlauer, W. (2013). Characterisation of Aronia powders obtained by different drying processes. *Food Chemistry*, *141*(3), 2858–2863. https://doi.org/10.1016/j.foodchem.2013.05.103

Hu, Z., Ballinger, S., Pelton, R., & Cranston, E. D. (2015). Surfactant-enhanced cellulose nanocrystal Pickering emulsions. *Journal of Colloid and Interface Science*, *439*, 139–148. https://doi.org/10.1016/j.jcis.2014.10.034

Iijima, H., & Takeo, K. (2000). Microcrystalline Cellulose : An Overview. In G. O. Phillips & P. A. Williams (Eds.), *Handbook of Hydrocolloids* (pp. 331–346). Woodhead Publishing Ltd.

ISO, & IDF. (2006). *Milk Fat - Determination of Peroxide Value (ISO 3976 - IDF 74)* (2nd ed., pp. 1–13). ISO and IDF.

Joslyn, M. A., & Sano, T. (1956). The Formation and Decomposition of Green Pigment in Crushed Garlic Tissue. *Journal of Food Science*, *21*(2), 170–183. https://doi.org/10.1111/j.1365-2621.1956.tb16908.x

Kamsiati, E. (2006). Pembuatan Bubuk Sari Buah Tomat (Licopersicon esculentum) dengan Metode "Foam-Mat Drying." *Teknologi Pertanian*, *7*(2), 113–119.

Kargar, M., Fayazmanesh, K., Alavi, M., Spyropoulos, F., & Norton, I. T. (2012). Investigation into the potential ability of Pickering emulsions (food-grade particles) to enhance the oxidative stability of oil-in-water emulsions. *Journal of Colloid and Interface Science*, *366*(1), 209–215. https://doi.org/10.1016/j.jcis.2011.09.073

Karthik, P., & Anandharamakrishnan, C. (2013). Microencapsulation of Docosahexaenoic Acid by Spray-Freeze-Drying Method and Comparison of its Stability with Spray-Drying and Freeze-Drying Methods. *Food and Bioprocess Technology*, *6*(10), 2780–2790. https://doi.org/10.1007/s11947-012-1024-1

Ketaren, S. (1986). *Pengantar Teknologi Minyak dan Lemak Pangan*. UI Press.

Klinjapo, R., & Krasaekoopt, W. (2018). Microencapsulation of Color and Flavor in Confectionery Products. In A. M. Grumezescu & H. A. Maria (Eds.), *Natural and Artificial Flavoring Agents and Food Dyes* (pp. 457–494). Elsevier Inc. https://doi.org/10.1016/B978-0-12-811518-3.00014-4

Kuck, L. S., & Noreña, C. P. Z. (2016). Microencapsulation of grape (Vitis labrusca var. Bordo) skin phenolic extract using gum Arabic, polydextrose, and partially hydrolyzed guar gum as encapsulating agents. *Food Chemistry*, *194*, 569–576. https://doi.org/10.1016/j.foodchem.2015.08.066

Lim, A. S. L., & Roos, Y. H. (2017). Carotenoids stability in spray dried high solids emulsions using layer-by-layer (LBL) interfacial structure and trehalose-high DE maltodextrin as glass former. *Journal of Functional Foods*, *33*, 32–39. https://doi.org/10.1016/j.jff.2017.03.006

Lin, C., He, G., Li, X., Peng, L., Dong, C., Gu, S., & Xiao, G. (2007). Freeze/thaw induced demulsification of water-in-oil emulsions with loosely packed droplets. *Separation and Purification Technology*, *56*(2), 175–183. https://doi.org/10.1016/j.seppur.2007.01.035

Liu, Y., Zhao, Y., & Feng, X. (2008). Exergy analysis for a freeze-drying process. *Applied Thermal Engineering*, *28*(7), 675–690. https://doi.org/10.1016/j.applthermaleng.2007.06.004

Mayasari, E., Rahayuni, T., & Manalu, J. (2019). Pengaruh Formulasi Maltodekstrin Dan Tween 80 Pada Karakteristik Fisikokimia Bumbu Herbal Instan. *Pro Food*, *5*(2), 479. https://doi.org/10.29303/profood.v5i2.102

McClements, D. J. (2005). Food Emulsions: Principles, Practices, and Techniques. In D. J. McClements (Ed.), *Food Emulsions: Principles, Practices, and Techniques, Sec* (2nd ed.). Taylor & Francis Inc.

McNamee, B. F., O'Riorda, E. D., & O'Sullivan, M. (1998). Emulsification and Microencapsulation Properties of Gum Arabic. *Journal of Agricultural and Food Chemistry*, *46*(11), 4551–4555. https://doi.org/10.1021/jf9803740

Melgosa, R., Román, Ó. B., Sanz, M. T., Paz, E. de, & Beltrán, S. (2019). Omega–3 encapsulation by PGSS-drying and conventional drying methods. Particle characterization and oxidative stability. *Food Chemistry*, *270*, 138–148. https://doi.org/10.1016/j.foodchem.2018.07.082

Michalska, A., & Lech, K. (2018). The Effect of Carrier Quantity and Drying Method on the Physical Properties of Apple Juice Powders. *Beverages*, *4*(1), 2. https://doi.org/10.3390/beverages4010002

Moreno, T., de Paz, E., Navarro, I., Rojo, S. R., Matías, A., Duarte, C., Buenhombre, M. S., & Cocero, M. J. (2016). Spray Drying Formulation of Polyphenols-Rich Grape Marc Extract: Evaluation of Operating Conditions and Different Natural Carriers. *Food and Bioprocess Technology*, *9*, 2046–2058. https://doi.org/10.1007/s11947-016-1792-0

Mubarak, S. (2017). Pengaruh Penyimpanan Minyak Jelantah Terhadap Bilangan Peroksida. *Jurnal Ilmiah Kesehatan Iqra*, *5*(1), 42–47.

Muhamad, I. I., Jusoh, Y. M. M., Nawi, N. M., Aziz, A. A., Padzil, A. M., & Lian, H. L. (2018). Advanced Natural Food Colorant Encapsulation Methods: Anthocyanin Plant Pigment. In M. A. Grumezescu & H. A. Maria (Eds.), *Natural and Artificial Flavoring Agents and Food Dyes* (pp. 495–526). Elsevier. https://doi.org/10.1016/B978-0-12-811518-3.00015-6

Mutlu, C., Koç, A., & Erbaş, M. (2020). Some physical properties and adsorption isotherms of vacuum-dried honey powder with different carrier materials. *LWT*, *134*, 110166. https://doi.org/10.1016/j.lwt.2020.110166

Nedovic, V., Kalusevic, A., Manojlovic, V., Levic, S., & Bugarski, B. (2011). An overview of encapsulation technologies for food applications. *Procedia Food Science*, *1*, 1806–1815. https://doi.org/10.1016/j.profoo.2011.09.265

Ngamwonglumlert, L., & Devahastin, S. (2017). Microstructure and its relationship with quality and storage stability of dried foods. In S. Devahastin (Ed.), *Food Microstructure and Its Relationship with Quality and Stability*. Elsevier Ltd. https://doi.org/10.1016/B978-0-08-100764-8.00008-3

Nurhadi, B., Andoyo, R., Mahani, & Indiarto, R. (2012). Study the properties of honey powder produced from spray drying and vacuum drying method. *International Food Research Journal*, *19*(3), 849–854.

Nurhadi, B., & Roos, Y. H. (2017). Influence of anti-caking agent on the water sorption isotherm and flow-ability properties of vacuum dried honey powder. *Journal of Food Engineering*, *210*, 76–82. https://doi.org/10.1016/j.jfoodeng.2017.04.020

Nurhasanah, S., Wulandari, N., Munarso, S. J., & Hariyadi, P. (2019). Production of structured lipids rich in triacylglycerols containing medium-chain fatty acids and unsaturated fatty acids at the Sn-2 position through enzymatic interesterification. *International Journal on Advanced Science, Engineering and Information Technology*, *9*(5), 1624–1630. https://doi.org/10.18517/ijaseit.9.5.10076

Parikh, D. M. (2015). Vacuum Drying: Basics and application. *Chemical Engineering (United States)*, *122*(4), 48–54.

Parrish, C. R. (2017). The Use of Medium-Chain Triglycerides in Gastrointestinal Disorders. *Nutrition Issues in Gastroenterology, Series #160*, *160*(February), 20–28.

Partanen, R., Raula, J., Seppaünen, R., Buchert, J., Kauppinen, E., & Forssell, P. (2008). Effect of Relative Humidity on Oxidation of Flaxseed Oil in Spray Dried Whey Protein Emulsions. *Journal of Agricultural and Food Chemistry*, *56*(14), 5717–5722. https://doi.org/10.1021/jf8005849

Pasrija, D., Ezhilarasi, P. N., Indrani, D., & Anandharamakrishnan, C. (2015). Microencapsulation of green tea polyphenols and its effect on incorporated bread quality. *LWT - Food Science and Technology*, *64*(1), 289–296. https://doi.org/10.1016/j.lwt.2015.05.054

Patil, U., Benjakul, S., Prodpran, T., Senphan, T., & Cheetangdee, N. (2016). Characteristics and quality of virgin coconut oil as influenced by maturity stages. *Carpathian Journal of Food Science and Technology*, *8*(4), 103–115.

Pereira, A. R. L., Cattelan, M. G., & Nicoletti, V. R. (2019). Microencapsulation of pink pepper essential oil: Properties of spray-dried pectin/SPI double-layer versus SPI single-layer stabilized emulsions. *Colloids and Surfaces A: Physicochemical and Engineering Aspects*, *581*(August), 123806. https://doi.org/10.1016/j.colsurfa.2019.123806

Pichot, R., Spyropoulos, F., & Norton, I. T. (2010). O/W emulsions stabilised by both low molecular weight surfactants and colloidal particles: The effect of surfactant type and concentration. *Journal of Colloid and Interface Science*, *352*(1), 128–135. https://doi.org/10.1016/j.jcis.2010.08.021

Piwińska, M., Wyrwisz, J., Kurek, M., & Wierzbicka, A. (2015). Hydration and physical properties of vacuum-dried durum wheat semolina pasta with high-fiber oat powder. *LWT - Food Science and Technology*, *63*(1), 647–653. https://doi.org/10.1016/j.lwt.2015.03.022

Rahman, M. S., & Perera, C. O. (2007). Drying and Food Preservation. In M. S. Rahman (Ed.), *Handbook of Food Preservation* (2nd ed., pp. 403–432). Taylor & Francis Inc.

Rajabi, H., Ghorbani, M., Jafari, S. M., Sadeghi, A., & Rajabzadeh, G. (2015). Retention of saffron bioactive components by spray drying encapsulation using maltodextrin, gum Arabic and gelatin as wall materials. *Food Hydrocolloids*, *51*, 327–337. https://doi.org/10.1016/j.foodhyd.2015.05.033

Raman, A. K. Y., & Aichele, C. P. (2020). Influence of non-ionic surfactant addition on the stability and rheology of particle-stabilized emulsions. *Colloids and Surfaces A: Physicochemical and Engineering Aspects*, *585*, 124084. https://doi.org/10.1016/j.colsurfa.2019.124084

Ré, M. I. (1998). Microencapsulation by Spray Drying. *Drying Technology*, *16*(6), 1195–1236. https://doi.org/10.1080/07373939808917460

Reis, F. R. (2014). *Studies on Conventional Vacuum Drying of Foods* (pp. 7–18). https://doi.org/10.1007/978-3-319-08207-3_2

Román, Ó. B., Sanz, T., & Beltrán, S. (2020). Microencapsulation of rice bran oil using pea protein and maltodextrin mixtures as wall material. *Heliyon*, *6*(4), e03615. https://doi.org/10.1016/j.heliyon.2020.e03615

Sansone, F., Mencherini, T., Picerno, P., D'Amore, M., Aquino, R. P., & Lauro, M. R. (2011). Maltodextrin/pectin microparticles by spray drying as carrier for nutraceutical extracts. *Journal of Food Engineering*, *105*(3), 468–476. https://doi.org/10.1016/j.jfoodeng.2011.03.004

Sarungallo, Z. L., Santoso, B., Roreng, M. K., & Murni, V. (2019). *Karakteristik Mutu Mikroenkapsulat Minyak Buah Merah (Pandanus conoideus) Dengan Perbandingan Konsentrasi Bahan Pengemulsi dan Bahan Pelapis*. *5*(2).

Shamaei, S., Seiiedlou, S. S., Aghbashlo, M., Tsotsas, E., & Kharaghani, A. (2017). Microencapsulation of walnut oil by spray drying: Effects of wall material and drying conditions on physicochemical properties of microcapsules. *Innovative Food Science & Emerging Technologies*, *39*, 101–112. https://doi.org/10.1016/j.ifset.2016.11.011

Smrdel, P., Bogataj, M., Zega, A., Planinšek, O., & Mrhar, A. (2008). Shape optimization and characterization of polysaccharide beads prepared by ionotropic gelation. *Journal of Microencapsulation*, *25*(2), 90–105. https://doi.org/10.1080/02652040701776109

Soottitantawat, A., Bigeard, F., Yoshii, H., Furuta, T., Ohkawara, M., & Linko, P. (2005). Influence of emulsion and powder size on the stability of encapsulated d-limonene by spray drying. *Innovative Food Science & Emerging Technologies*, *6*(1), 107–114. https://doi.org/10.1016/j.ifset.2004.09.003

Stapley, A. G. F. (2008). Freeze drying, in: Evans J. A. (Ed.). *Frozen Food Science and Technology, Blackwell, Oxford, UK*, 248–275.

Tinay, I. A. El, & Ismail, A. H. (1985). Effect of some additives and processes on the characteristics of agglomerated and granulated spray-dried Roselle powder, Acta Aliment. In *Hungaricae 14* (pp. 238–295).

Tolun, A., Altintas, Z., & Artik, N. (2016). Microencapsulation of grape polyphenols using maltodextrin and gum arabic as two alternative coating materials: Development and characterization. *Journal of Biotechnology*, *239*, 23–33. https://doi.org/10.1016/j.jbiotec.2016.10.001

Tonon, R. V., Brabet, C., & Hubinger, M. D. (2008). Influence of process conditions on the physicochemical properties of açai (Euterpe oleraceae Mart.) powder produced by spray drying. *Journal of Food Engineering*, *88*(3), 411–418. https://doi.org/10.1016/j.jfoodeng.2008.02.029

Tonon, R. V., Pedro, R. B., Grosso, C. R. F., & Hubinger, M. D. (2012). Microencapsulation of Flaxseed Oil by Spray Drying: Effect of Oil Load and Type of Wall Material. *Drying Technology*, *30*(13), 1491–1501. https://doi.org/10.1080/07373937.2012.696227

Vashisth, C., Whitby, C. P., Fornasiero, D., & Ralston, J. (2010). Interfacial displacement of nanoparticles by surfactant molecules in emulsions. *Journal of Colloid and Interface Science*, *349*(2), 537–543. https://doi.org/10.1016/j.jcis.2010.05.089

Vicente, J., Pereira, L. J. B., Bastos, L. P. H., Carvalho, M. G. de, & Rojas, E. E. G. (2018). Effect of xanthan gum or pectin addition on Sacha Inchi oil-in-water emulsions stabilized by ovalbumin or tween 80: Droplet size distribution, rheological behavior and stability. *International Journal of Biological Macromolecules*, *120*, 339–345. https://doi.org/10.1016/j.ijbiomac.2018.08.041

Wei, Z., Cheng, J., & Huang, Q. (2019). Food-grade Pickering emulsions stabilized by ovotransferrin fibrils. *Food Hydrocolloids*, *94*, 592–602. https://doi.org/10.1016/j.foodhyd.2019.04.005

Widodo, H., Adhani, L., Solihatun, Prastya, M., & Annisa, A. (2020). Pemanfaatan Minyak Cengkeh Sebagai Antioksidan Alami untuk Menurunkan Bilangan Peroksida Pada Produk Minyak Goreng. *Jurnal Penelitian Dan Karya Ilmiah Lembaga Penelitian Universitas Trisakti*, *5*(1), 77–90.

Wilkowska, A., Czyżowska, A., Ambroziak, W., & Adamiec, J. (2017). Structural, physicochemical and biological properties of spray-dried wine powders. *Food Chemistry*, *228*, 77–84. https://doi.org/10.1016/j.foodchem.2017.01.115

Xie, J., Luo, Y., Chen, Y., Liu, Y., Ma, Y., Zheng, Q., Yue, P., & Yang, M. (2019). Redispersible Pickering emulsion powder stabilized by nanocrystalline cellulose combining with cellulosic derivatives. *Carbohydrate Polymers*, *213*, 128–137. https://doi.org/10.1016/j.carbpol.2019.02.064

Xu, D., Zhang, J., Cao, Y., Wang, J., & Xiao, J. (2016). Influence of microcrystalline cellulose on the microrheological property and freeze-thaw stability of soybean protein hydrolysate stabilized curcumin emulsion. *LWT - Food Science and Technology*, *66*, 590–597. https://doi.org/10.1016/j.lwt.2015.11.002

Yam, K. L., & Papadakis, S. E. (2004). A simple digital imaging method for measuring and analyzing color of food surfaces. *Journal of Food Engineering*, *61*(1), 137–142. https://doi.org/10.1016/S0260-8774(03)00195-X

Yanuwar, W., Widjanarko, S. B., & Wahono, T. (2007). Characteristics and antioxidant stability of red fruit (Pandanus conoideus Lam) protein based microcapsule. *Jurnal Teknologi Pertanian*, *8*(2), 127–135.

Zhang, M., Yang, B., Liu, W., & Li, S. (2017). Influence of hydroxypropyl methylcellulose, methylcellulose, gelatin, poloxamer 407 and poloxamer 188 on the formation and stability of soybean oil-in-water emulsions. *Asian Journal of Pharmaceutical Sciences*, *12*(6), 521–531. https://doi.org/10.1016/j.ajps.2017.05.009

Zhang, R., Zhou, L., Li, J., Oliveira, H., Yang, N., Jin, W., Zhu, Z., Li, S., & He, J. (2020). Microencapsulation of anthocyanins extracted from grape skin by emulsification/internal gelation followed by spray/freeze-drying techniques: Characterization, stability and bioaccessibility. *LWT*, *123*, 109097. https://doi.org/10.1016/j.lwt.2020.109097

Zhang, S., Chen, J., Yin, X., Wang, X., Qiu, B., Zhu, L., & Lin, Q. (2017). Microencapsulation of tea tree oil by spray-drying with methyl cellulose as the emulsifier and wall material together with chitosan/alginate. *Journal of Applied Polymer Science*, *134*(13), 1–10. https://doi.org/10.1002/app.44662

Zhong, Q., Jin, M., Davidson, P. M., & Zivanovic, S. (2009). Sustained release of lysozyme from zein microcapsules produced by a supercritical anti-solvent process. *Food Chemistry*, *115*(2), 697–700. https://doi.org/10.1016/j.foodchem.2008.12.063

Italian Journal of Food Science, 2022; 34 (1): 86–113

Environmental impact of the main household cooking systems—A survey

Alessio Cimini and Mauro Moresi*

Department of Innovation in Biological, Agrofood and Forestry Systems, University of Tuscia, Viterbo, Italy

***Corresponding Author:** Mauro Moresi, Department of Innovation in Biological, Agrofood and Forestry Systems, University of Tuscia, Viterbo, Italy. Email: mmoresi@unitus.it

Received: 9 January 2022; Accepted: 4 February 2022; Published: 23 February 2022

REVIEW ARTICLE

Abstract

The food cooking energy may represent the primary hotspot in the cradle-to-grave life cycle of several foods and drinks. It is mainly affected by the type of food and its cookery method, cooking appliance and the fuel selected as well as the number of portions to be cooked. The primary aim of this survey was to demonstrate the basic characteristics of the main cooking methods, appliances, and fuels as well as energy required for some key foods. The secondary aim was to assess the environmental impacts of a generic cooking system as a function of few household cookers fueled by different fuels (i.e., firewood, charcoal, coal, natural gas, liquefied petroleum gas, kerosene and biogas) and electricity in the Italian scenario by using the ReCiPe 2016 and product environmental footprint (PEF) standard methods and Ecoinvent v. 3.7 database. A functional unit equal to per capita useful energy delivered to the pot for cooking (1.41 gigajoule [GJ]) in 27 European Union countries in 2019 was used as the basis of comparison. The use of natural gas resulted in minimum impact in nine of the 18 mid-point impact categories of ReCiPe 2016 method and two damage categories (human health and ecosystem quality) with a minimum overall weighted damage score ($OWDS_R$) of ~5 Pt. Thus, such a cookstove appeared to be more apt to minimize both indoor and outdoor air pollution. Even if the electric cookstove yielded a greater $OWDS_R$ (8.6 Pt) because the Italian electricity grid mix was mainly based on fossil sources, it was possible to forecast that new-generation, smart cooktops driven by hydro- and wind-power electricity would minimize $OWDS_R$ to as low as 0.9 and 1.4 Pt, respectively, thus not only avoiding the consumption of any fossil energy source but also improving people's health.

Keywords: clean cooking, cooking appliances, cooking fuels, cooking systems, environmental impacts, life cycle assessment, PEF standard method, ReCiPe 2016 standard method

Introduction

Nowadays, cooking of food has become mandatory for humans (Wrangham and Conklin-Brittain, 2003). Its associated energy requirements represent the preponderant share of energy used in the cradle-to-grave life cycle of several foods and drinks, as in the case of vegetal products with low to medium degree of processing (Carlsson-Kanyama and Boström-Carlsson, 2001), dry pasta (Bevilacqua *et al*., 2007; Cimini *et al*., 2019, 2021a, 2021b) and coffee brewing (Cibelli *et al*., 2021). Energy use for cooking is largely affected by the food type and its cookery method, and the cooking appliance selected. Energy utilization reduces as the number of portions cooked increases (Carlsson-Kanyama and Boström-Carlsson, 2001).

About one-third of the human population (that is 2.5-billion people), generally living in low- and middle-income countries, still relies on solid biomass fuels (i.e., firewood, crop residue, charcoal and dung) for cooking, while the remaining 5-billion people rely on fossil energy, such as coal, natural gas (NG), kerosene, liquefied petroleum gas (LPG) and electricity (Wright *et al*., 2020).

ISSN 1120-1770 online, DOI 10.15586/ijfs.v34i1.2170

The combustion products emitted by solid fuels give rise to by far higher levels of indoor air pollution than those recommended by the World Health Organization (WHO, 2018), especially in poorly ventilated dwellings. These harmful emissions have been associated with respiratory diseases and other health problems (i.e., lung cancer, chronic obstructive pulmonary disease [COPD], pneumonia, tuberculosis, cardiovascular events, low birth weight and cataracts; Fullerton *et al*., 2008), and are responsible for as many as 4 million premature deaths per year globally (WHO, 2021). WHO is thus committed to attaining the so-called 'Sustainable Development Goals' (SDG) on health (SDG 3) and energy (SDG 7) as scheduled by the United Nations Development Program (UNDP, 2021) in order to improve the health and well-being of the people still using polluting technologies and fuels not only for cooking but also for heating and lighting. So far, numerous programs have been implemented globally to introduce cleaner and more efficient cooking technologies. All the attempts to improve the performance of biomass-burning stoves have until now caused limited health benefits, while the use of other cleaner fuels (i.e., LPG, ethanol and biogas) has offered not only greater health benefits but also smaller greenhouse gas (GHG) emissions (Rosenthal *et al*., 2018). In particular, the replacement of solid biofuels with LPG was quite successful in several countries, such as Brazil (Wright *et al*., 2020), Ecuador (Martínez-Gómez *et al*., 2016), Ghana (Afrane and Ntiamoah, 2011, 2012), Indonesia (Thoday *et al*., 2018), India (Gould and Urpelainen, 2018; Jungbluth *et al*., 1997; Singh *et al*., 2014), and a few countries of the Indo-Chinese Peninsula (Aberilla *et al*., 2020) for at least two reasons: (i) lower GHG emissions compared to burning solid fuels, and (ii) lower infrastructure requirement compared to NG and electricity (Wright *et al*., 2020). Unfortunately, although use of such a clean cooking technology improves people's health conditions, it still relies on fossil energy sources. A long-term sustainable cooking should alternatively rely on renewable energy sources only (i.e., solar or wind energy, biogas and bioethanol; Aro, 2016).

Several life cycle assessment (LCA) studies have so far dealt with cooking appliances, such as cookstoves fired by different fuels (Aberilla *et al*., 2020; Afrane and Ntiamoah, 2011, 2012; Jungbluth *et al*., 1997; Singh *et al*., 2014), induction and gas hobs (Favi *et al*., 2018) and electric and gas ovens (Landi *et al*., 2019) in the Italian context as well as induction hobs with different electronic boards (Elduque *et al*., 2014), using diverse life cycle impact assessment (LCIA) methods, some of which, unfortunately, use old databases.

The primary aim of this survey was to review the basic characteristics of main cooking methods, appliances and fuels as well as energy requirements for some key foods. The secondary aim was to account for a generic cooking system capable of delivering the useful per capita energy transferred to the cooking pot in 27 European Union (EU) countries in 2019 (Eurostat, 2021a). The final goal of this study was to assess its life cycle environmental impacts by using the well-known ReCiPe 2016 (Huijbregts *et al*., 2016) and product environmental footprint (PEF) (European Commission [EC], 2018b) LCIA methods and Ecoinvent v. 3.7 database (Ecoinvent, 2020). By using different fuels (i.e., firewood, charcoal, coal, NG, LPG, kerosene, and biogas) and electricity used in the Italian scenario, it was possible to identify the cooking system with overall minimum environmental impact and, thus, prospect promising new eco-smart household cooktops.

Basic Characteristics of Main Cooking Methods

Cooking makes food as more edible, easily digestible and relishing. In this way, cooked foods exhibit quite significant variations in their physical aspect, structure, composition and nutritional value. Any food-cooking operation is characterized by a heating element (i.e., open flame etc.) and a heat transfer medium that allows cooking by:

1. *expansion* if the hot medium is made of water or oil, and
2. *concentration* if the heating element transmits heat to food through a pan, plate or grill.

Mixed cooking methods include both modes. Generally, the first part of cooking is carried out by concentration, while the second one by expansion, thanks to the addition of a liquid. Alternatively, the dry heat cookery methods (i.e., baking, steaming, grilling and roasting) can be discriminated from the moist heat cookery ones (i.e., boiling, stewing, shallow frying, deep frying and basting). In the former, the heating element conveys heat directly to the food (which in turn is cooked in its own juice and the steam generated by the evaporation of water added to the food during its preparation) mainly by means of convection and/or irradiation. On the contrary, in the moist heat methods a liquid medium (i.e., water, milk, coconut cream, molted butter, oil etc.) is heated before or after the food to be cooked is placed in the cooking pan.

Table 1 briefly describes both basic cooking methods and some combined and microwave cooking methods by pointing out heat propagation media, range of cooking temperature and main heat transfer modes.

Table 1. Main food cooking methods (Hager and Morawicki, 2013; McGee, 2004).

Main cooking methods	Cooking system	Description	Heat propagation medium	Cooking temperature (°C)	Heat transfer mode	Uses
Dry heat cooking	Baking	Food is put in an oven.	Air	140–250	Air convection + wall radiation + pan conduction	Cereal-based foods
	Grilling	Food is placed on a grill tray, which is heated by burning charcoal and gas, or by electricity.	Air	220–250	Air convection + grill conduction + grill or flame radiation	Meat, vegetables, cheeses, and marshmallow
	Steaming	Food is cooked by the hot steam rising from an underlying pot filled with water.	Steam at ambient or steam pressure	100–120	Vapor convection and condensation	Meat and filled pastas
	Roasting in an oven	Food is flavored, tied with strings and placed in a saucepan containing a very hot fatty substance to wet the external surface of the food and avoid its drying.	Air and fats	200–220	Air convection + wall radiation + pan conduction	Meat and nuts
	Roasting on a spit	Pieces of food are skewered, salted and flavored to be heated by wood, charcoal, coal, electricity and gas.	Air	250	Air convection + burner radiation + spit conduction	Poultry and meat
	Cooking au gratin	Food is placed in a shallow oven-proof container and baked or cooked under an overhead grill with a topping of seasoned breadcrumbs, grated cheese, egg, or butter.	Air	250–300	Air convection + grill radiation + pan conduction	Vegetables and pastas
	Barbequing	Food is variously cooked over live fire from glowing firewood, charcoal or coal and smoke using direct or indirect heating with several national and regional differences.	Smoke	200–250	Smoke convention + flame radiation	Meat, vegetables and breads
Moist heat cooking	Boiling	A water-filled pot is used to cook food over the fire. Except for rice and meat, the cooking water is thrown away at the end of cooking.	Water	≤100	Water convection	Pastas, rice, meat and vegetables
	Stewing	Food is chopped, diced and cubed, and added to a pot partially filled with a liquid. Stewed food is served with the thickened liquid.	Water and oil	≤100	Vapor condensation + liquid convection + pan conduction	Meat, vegetables and grains
	Deep frying	Food is submerged in hot boiling oil contained in a deep pan till it turns brown on the outside. A piece of brown paper helps soaking up any oil from the food before it is served.	Oils and fats	150–200	Convention + pan conduction	Meat, vegetables and dough
	Pan or shallow frying	Food pieces are stirred around a few times in a frying pan coated with a small amount of oil and fat, and must be properly heated to prevent cooked foods from becoming too oily, greasy or burnt outside and uncooked inside.	Oils and fats	150–200	Oil and pan conduction	Meat, vegetables and dough

	Basting	Meat is cooked in its own juices, or a sauce or marinade in an oven using a lidded oven-pan. Any juice is often spooned over the outer part of the meat to avoid its drying during cooking. Use of a closed oven-bag traps evaporating moisture, the condensation of which forming the real cooking juice of food.	Air, steam oils, and fats	100–120	Pan conduction + liquid convection + wall radiation	Meat
Mixed cooking	Braising	Food is first browned at a high temperature, and then simmered in a lidded pot in a cooking liquid (i.e., wine, broth, coconut milk and beer). It differs from stewing for about 3/4 of the product being submerged by the cooking liquid.	Air, steam, oils and fats	~150	Pan conduction + liquid convention	Meat, vegetables and grains
	Cooking in a casserole	Small and tender pieces of meat are salted, placed over finely chopped vegetables sprinkled with melted butter in a lidded oven-pot, and cooked in the oven on a very low flame.	Air, oils and fats	150–220	Pan conduction + liquid convection + wall radiation	Meat and vegetables
	Microwave cooking	Electromagnetic radiation at a frequency of 915 or 2,450 MHz is used to heat directly and rapidly the only polar molecules of foods, while the oven air and nonpolar container materials (i.e., glass, stoneware and plastic) are heated by the food itself as it heats up. While infrared energy is almost entirely absorbed at the food surface, microwaves can penetrate food to a depth of about 2.5 cm.	Polar molecules	Variable	Microwave radiation	Meat and vegetables

Main cooking appliances

Open wood fires were used for cooking by humans for approximately two million years (Wrangham, 2009). The energy performance and resulting emissions from biomass cookstoves depend on various factors, such as the stove design, fuel feeding practice, lighting, and combustion temperature (Okino *et al*., 2021; Rasoulkhani *et al*., 2018). Generally, traditional biomass stoves, largely used indoor in developing nations, are improperly ventilated, which leads to a significant increase in indoor levels of particulate matters ($PM_{2.5}$) and carbon monoxide that cause lung inflammation and lead to chronic obstructive pulmonary disease. Excessive consumption of biomass fuels has led to natural forest degradation and deforestation, as already observed in South Italy during period of Roman Empire, as well as shortage of firewood for cooking in some areas of Africa even today (Okino *et al*., 2021). In order to improve the efficiency of cooking energy and thus reduce the biomass consumption of the so-called *three-stone fire stove*, quite numerous improved stoves have been developed (Okoko *et al*., 2018; Wikipedia, 2021a). For instance, Darlami *et al*. (2019) reported that the thermal efficiency (η_{CS}) of a traditional Nepalese cookstove increased from 18.0% to 25.6% when it was modified with mud, while Okino *et al*. (2021) improved the thermal efficiency (η_{CS}) of a cooking stove insulated with sawdust from 13–21% to 19–35% with the use of a few indigenous wood fuels available in Uganda. Nevertheless, a recent review has found that the use of such improved cookstoves has so far had a small mitigating effect on the health results of household air pollution and called for more initiatives and policies to favor the adoption of cleaner fuels and improved cookstoves in households (Pratiti *et al*., 2020). In fact, more than 2.5-billion people in developing countries are still relying on quite polluting cooking fuels, such as wood, crop residues, animal dung, charcoal, coal and kerosene.

For instance, wood and coal burning cookstoves are still manufactured by the Amish in Lancaster County (PA, USA) to satisfy not only cooking and baking requirements but also heating and hot water requirements. In India (Jungbluth *et al*., 1997) and Nigeria (Anozie *et al*., 2007), kerosene stoves replaced most of the traditional biomass cookstoves, thanks to governmental fuel subsidies to prevent deforestation for cooking fuels. Cheaper and more efficient gas stoves fueled by NG and LPG started to disseminate once a distribution network for gas pipeline and bottled LPG transport was available. This allowed their increasing diffusion either in Europe or the United States since the beginning of the 20th century. Gas ignition was originally done by matchsticks. Then it became possible with a pilot light, a continuously burning gas flame under the cooktop to immediately light the gas leaving the burner if the stove was

turned on. Nowadays, gas stoves have electronic ignition to avoid any gas consumption when the stove is not used, a flame failure device to stop gas flowing without igniting and prevent from accidental explosion, and an extractor hood to evacuate fumes and minimize indoor air pollution (Wikipedia, 2021b).

By the end of the 19th century, several electric stoves were patented in Canada, the United States and Australia, even though their diffusion in household kitchens was conditioned by the extension of urban and rural electrification. Whereas gas cooktops heat food with flame and disperse much of the heat in the air, electric cooktops mainly transfer heat to the cooking surface and thus are more efficient than gas cooktops. Electric cooktops include both open coil and smooth (or radiant) cooktop types. The former is made of resistive wires encased in hollow metal tubes arranged in a spiral to directly support the cookware, and thus is quite affordable and durable. On contrary, smooth and radiant types consist of a hotplate surface or a smooth glass-ceramic surface heated locally via electrical heating coils or halogen lamps. The latter guarantees less heat loss with easier cleanability but, unfortunately, higher stretchability and breakability. Nowadays, in such cooktops, the maximum temperature of the heating element is controlled thermostatically while power supply is regulated either discretely or continuously between minimum and maximum heat settings (Wikipedia, 2021c). Different studies have indicated that hotplates are least efficient among electric stoves (Hager and Morawicki, 2013), even if the glass–ceramic cooktops are found to be up to 20% less efficient than hotplate surfaces (Carlsson-Kanyama and Böstrom-Carlsson, 2001). Moreover, reflective trays beneath electric coils in coiled cooktops appeared to increase the energy efficiency and reduce heating period by 20% (Hager and Morawicki, 2013). Induction stoves are *de facto* the latest version of electric stoves. In fact, these use electricity to generate electromagnetic induction in just ferromagnetic cookware, which is thus directly heated instead of being heated by beneath smooth surface of glass–ceramic. Such cooktops are not only highly safe but also the most energy-efficient appliances. Their accurate control of cooking temperature could be improved by using a low-cost, open-source electronic platform pilotable via smartphone, as in the case of the novel home eco-sustainable pasta cooker previously developed by Cimini *et al.* (2020).

Among the diverse renewable fuel stoves, it is worth citing the biogas, ethanol and solar stoves.

Biogas stoves resemble the conventional NG and LPG stoves with just some modifications in burner design to maximize their combustion effectiveness and reduce unburned methane and soot from incomplete combustion (International Renewable Energy Agency [IRENA], 2017).

Alcohol burning stoves are like existing kerosene stoves, their main differences being related to the use of stainless steel to minimize corrosion and fuel type used. Interest for such stoves is mainly due to the use of bioethanol, its combustion practically providing pollutant-free emissions. Unfortunately, such stoves are expensive and suffer from the costs of bioethanol supply chain. In the EU, such stoves are used for marine and mobile leisure applications in conjunction with an aqueous mixture of 85% (v/v) ethanol. Their use was extended to a few developing countries, especially in Brazil, where the above mixture is available as a biofuel (Benka-Coker *et al*., 2018; Stokes and Ebbeson, 2005; Zuzarte, 2007). In order to avoid using such an inflammable mixture, other safer prototypes were developed in India and South Africa to utilize diluted ethanol mixtures at 50% (v/v) (Rajvanshi *et al*., 2004) or enriched with colorants and thickeners (i.e., calcium acetate) and flavoring agents (*Greengel*; Climate Technology Center & Network [CTCN], 2017; Okusanya *et al*., 2019), respectively.

Solar cooking appliances started to be commercialized in the 1980s as 100% emission-free devices capable of concentrating solar thermal energy to cook foods. Each one consists of three components: concentrator, absorber and retainer. The first one, being made of shiny materials, such as silver, chromium or aluminum, allows the sunlight to be concentrated at a fixed point, where it is absorbed by a black-painted cookware to cook food. To minimize heat loss, the cookware is to be properly insulated and lidded. Four types of solar cookers are currently available (Pandey *et al*., 2021), as shown in Table 2. The *box cooker* simply consists of a box inside another one and is the cheapest type of solar cooker. The transparent cover on the top of the outer box allows entrance of the sunlight, where it is absorbed by the black-painted inner box. A mirror in the inner side of the outer box helps in reflecting the heat energy radiated from the inner black box. The *panel solar cooker* has a large flat panel, which mainly reflects and focuses the sunlight falling vertically on the cooker for cooking. Owing to the instability of panel to high wind, such a solar cooker is not used frequently. The *parabolic solar cooker* collects the solar radiation in the central focus point of a collector dish, where a pressure cooker with black-painted bottom is placed. In this way, temperatures as high as those causing the burning of food can be achieved. Finally, the *vacuum-tube solar cooker* entails two tubes, one inside the other. The inner tube contains food to be cooked and is black painted to maximize heat absorption, while the outer one is transparent. Vacuum is created in the space between these tubes to minimize heat loss and trap the heat absorbed for a longer period. Such type of cooker is highly efficient (Pandey *et al*., 2021).

Table 2. Main types of cookstoves and performances together with cooking fuels used, some typical models, fuel availability and cookstove efficiency (η_{cs}).

Category	Fuel type used	Some typical models	Fuel availability	η_{cs} (%)	References
Traditional biomass stove	Firewood		Usually, easily available *in situ*	11 13.5 14 17 20 13–21	Aberilla *et al*., 2020 Singh *et al.*, 2014 Afrane and Ntiamoah, 2011, 2012 Hager and Morawicki, 2013 Benka-Coker *et al*., 2018 Okino *et al*., 2021
	Crop residues		Usually easily available *in situ*	11	Singh *et al*., 2014 Aberilla *et al*., 2020
	Charcoal		Supply chain required	14 17.5 18 23 24–32	Aberilla *et al*., 2020 Singh *et al*., 2014 Afrane and Ntiamoah, 2011, 2012 Benka-Coker *et al*., 2018 Okoko *et al*., 2018
Coal stove	Coal		Supply chain required	15.5	Singh *et al*., 2014
Improved biomass stove	Firewood		Usually, easily available *in situ*	25.0–42.8	Mehetre *et al*., 2017
Modern fossil fuel stove	Kerosene		Supply chain required	35 40 45 46 47 42–64	Afrane and Ntiamoah, 2012 Benka-Coker *et al*., 2018 Hager and Morawicki, 2013 Aberilla *et al*., 2020 Singh *et al*., 2014 Jungbluth *et al*., 1997
	LPG		Supply chain required	24–34 45 46* 49 50 56 57 60–72	Cimini and Moresi, 2017 Afrane and Ntiamoah, 2012 Cimini and Moresi, 2017 Aberilla *et al*., 2020 Hager and Morawicki, 2013 Benka-Coker *et al*., 2018 Singh *et al*., 2014 Afrane and Ntiamoah, 2011 Jungbluth *et al*., 1997
	Natural gas		Supply infrastructure required	50	Hager and Morawicki, 2013
Electric stove	Electricity	Generic electric stove	Supply infrastructure required	55 59 65 70 80	Benka-Coker *et al*., 2018 Aberilla *et al*., 2020 Afrane and Ntiamoah, 2012 Singh *et al.*, 2014 Hager and Morawicki, 2013
		(a) Hotplate hob		42–50 57*	Cimini and Moresi, 2017
		(b) Coil stove		49	Wollele, 2020
		(c) Induction cooktop		27–39 65* 45–59§ 66–68#	Cimini and Moresi, 2017 Cimini *et al.*, 2020
Renewable fuel stove	Biogas		Supply chain required	55 50	Singh *et al.*, 2014 Aberilla *et al*., 2020 Afrane and Ntiamoah, 2011, 2012
	Ethanol	(a) Low-grade ethanol stove (b) Ethanol-gel stove	Supply chain required	43–45 55 43	Rajvanshi *et al*., 2004 Benka-Coker *et al*., 2018 Okusanya *et al.*, 2019
	Solar	(a) Box cooker (b) Panel cooker (c) Parabolic cooker (d) Vacuum tube cooker	Weather-dependent	20 26.6	Hager and Morawicki, 2013 Arenas, 2007 Xu *et al*., 2015

* As referred to dry pasta cooking with a water-to-pasta ratio (WPR) of 10 L/kg when using the environmentally sustainable cooking practice set up by Cimini and Moresi (2017).
# As referred to dry pasta cooking with WPR = 10 L/kg when using the home eco-sustainable pasta cooker (Cimini *et al*., 2020).
§ As referred to dry pasta cooking with the minimum WPR of 2–4 L/kg when using the home eco-sustainable pasta cooker (Cimini *et al*., 2020).

Table 2 provides an overview of main cooking stoves in use together with the cooking fuels used, fuel availability and cookstove efficiency (η_{CS}).

Besides the cooking stoves mentioned above, useable for the so-called *surface* (or stovetop or cooktop) *cooking*, oven cooking, must also be considered, since it is essential for cooking quite numerous food products (i.e., bread, cakes, biscuits and various meat products) requiring diverse cooking methods, such as baking, grilling, roasting etc. (Table 1). An oven is a device liable to expose foods to a hot environment. It consists of a hollow chamber that can be heated in a controlled manner using a burning gas, electricity or microwaves. When an oven is combined with cook-tops (*range*), the fuel used for the oven may be the same as, or different from, that used for the burners on the stovetops. Generally, the food placed in an oven is heated from below, as in the case of baking and roasting. It can be also heated from the top, as in the case of broiling and grilling. In a *conventional oven*, the air is naturally circulated in the oven chamber, while in *a convection oven*, air recirculation is assisted by a small fan, thus resulting in faster and more energy-efficient cooking of food. Such ovens make use of a thermostat for on and off mode in order to maintain about constant the temperature selected, and a timer to turn off the oven automatically after selected period. The so-called *smart ovens* may use computer-based controls to program quite different cooking modes and even the possibility of automatically shutting it off when the minimum core temperature of the food has been attained. Moreover, self-cleaning ovens are earning an increasing popularity among consumers, their manual cleaning being complicated and asking for critical cleaning chemicals. There are two types of self-cleaning ovens (Barratt, 2021; Hager and Morawicki, 2013):

(i) *Pyrolytic ovens*, which feature a self-cleaning mode that heats the oven to about 500°C for as long as 2 h to convert food and fat residues into a white ash that can be wiped away easily.
(ii) *Catalytic ovens*, their porous surfaces being embedded with catalysts, which oxidize residual food by converting it into ash during cooking of food.

Currently, the pyrolytic version of self-cleaning ovens is not only that most widespread since it needs no expensive catalyst (Hager and Morawicki, 2013), but also because it is more thermally efficient due to greater wall insulation density required to withstand the high self-cleaning temperatures used. Generally, the thermal efficiency (η_{CS}) of well-insulated conventional electric ovens ranges from 10% to 15%, while that of gaseous counterparts ranges from 6% to 7% because of the higher air flows and electric glow-bar that run continuously to reignite the gas flame should it blow out (Barratt, 2021; Hager and Morawicki, 2013). The energy requirements of convection ovens are less than those of conventional ovens by 20–30% (Barratt, 2021). Finally, the mean efficiency of a microwave oven was reported to range between 56% and 60% depending on the class of microwave (Hager and Morawicki, 2013), although efficiency of as low as 35% was reported by Probert and Newboroug (1985).

In addition to the above oven types, it is necessary to acknowledge wood-fired ovens, which are used globally in restaurants, rotisserie shops and bakeries. For instance, about 6,400 pizza restaurants are operating in the city of São Paulo in Brazil and using about 48 megagram (Mg)/year of wood as fuel in their pizza ovens. These are responsible for an average emission factor of $PM_{2.5}$ = 0.38 g per kg of wood burned (Lima *et al*., 2020). The average $PM_{2.5}$ concentration at the exit of their chimneys was quite high (6,171 μg/m^3), while indoor, it was about two orders smaller in magnitude (68 μg/m^3) (Lima *et al*., 2020), although it definitively exceeded the indoor 24-h mean level of 15 μg/m^3 of $PM_{2.5}$ recommended by WHO (2018). In order to limit such a high $PM_{2.5}$ emission in Delhi (India), it was proposed to replace coal-fired with electric- and gas-fired appliances in all restaurants with a seating capacity of more than 10 persons (Apurva, 2016). Also, San Vitaliano, a town with a population of 5,000 people located near Naples (Italy), banned the use of wood-fired ovens in restaurants and bakeries during the cold season unless their chimneys were equipped with pollution-reducing filters (Singh and Highway, 2016). However, wood-fired ovens are specifically used to bake the well-known *Pizza Napoletana* (TSG), registered as a traditional specialty guaranteed by the EC (2010) Regulation No. 97/2010. Such ovens consist of a base of tuff bricks covered with a circular cooking floor over which is built a dome made of refractory materials to minimize heat dispersion. Their appropriate geometric dimensions (i.e., mouth of an having a width of 45–50 cm and a height of 22–25 cm, a cooking floor with a diameter of 105–140 cm and a vault height of 40–45 cm) allow the temperature of the dome and cooking floor maintained at about 485 °C and 430 °C, respectively; this ensures the baking quality of the Pizza Napoletana TSG (EC, 2010).

The thermal efficiency (η_{CS}) of such ovens should be like that of conventional gas ovens. According to Igo *et al*. (2020), the thermal efficiency of a metal fired-wood oven to heat 20 liters of water from 35 to 90°C was found to be of ~19%, about 55% of the energy consumed being lost by hot fumes and 26% dispersed through the oven walls. Alternatively, the specific consumption of two types (indirect and semi-direct) of bakery ovens resulted in 0.55 and 0.90 kg of wood used per kg of wheat flour baked, respectively (Manhiça *et al*. 2012). This was equivalent to an estimated oven efficiency of 3–5% when assuming an increment in temperature from 25 to 150°C

for dough having a moisture content of 36.5% (w/w) and the lower heating value of firewood as shown in Table 3.

Cooking fuels

According to Eurostat (2021a), the final energy consumption in households in EU-27 in 2019 amounted to about 10.3×10^{18} J, 63.6% of which was used for space heating, 14.8% for water heating, 14.1% for lighting and appliances, 6.1% for cooking devices and 0.4% for space cooling. The share of energy consumption for cooking ranged from 1% in Finland to as much as 36% in Portugal, while it was 6.5% in Italy. The cooking energy consumption in EU-27 was mainly supplied by electricity (49.8%), gas (31%), oil and petroleum products (13%), renewables and wastes (5.7%) and solid fuels (0.6%). In Italy, it was primarily supplied by gas (69.2%), then by electricity (15.8%), oil and petroleum products (10.2%) and renewables and wastes (4.8%).

The specific energy consumption for cooking was thus estimated by referring the overall cooking energy consumed in 2019 (628.67 petajoule [PJ]) by EU-27 population (~447 million) (Eurostat, 2021b), and it amounted to about 1.41 gigajoule [GJ] (i.e., 391 kWh) per capita/year.

The main characteristics of the cooking fuels used globally are shown in Table 3.

Biomass fuel

The use of biomass as a fuel in thermal and electrical applications is related to the fact that its combustion is CO_2 neutral that is, CO_2 released into the air equals to that absorbed during photosynthesis. The ultimate composition of wood biomass is slightly dependent on species. Roughly, it is made of 50% carbon, 6% hydrogen, 44% oxygen and 0.1–0.5% nitrogen (Vassilev *et al.*, 2010). Such composition may vary in other agricultural residues (i.e., rice husk, straw, cotton stalk and grasses), mainly because of higher hemicellulose and ash contents (Shen *et al.*, 2010). Ash is an inorganic fraction of biomass fuel that remains after its burning, and it includes calcium, potassium, sodium, magnesium and other elements. The heating value of biomass is often expressed as the higher (HHV) and lower (LHV) heating values, provided the heat released by its complete combustion leading to the production of water vapors includes or does not include the latent heat of water condensation. Such values decrease as the initial moisture content of biomass increases. These can be determined experimentally via an adiabatic bomb calorimeter or predicted based on the weight fraction of carbon (x'_C), hydrogen (x'_H), oxygen (x'_O) and moisture content (x_M) of the biomass under

Table 3. Characteristics of the main cooking fuels: density, moisture (x_M), elemental composition (C, H, O, N, S) and ash (x_A) content on a dry matter (DM) basis; raw formula; CO_2 generated per kg of burned fuel (CFR); and higher heating value (HHV) and lower heating value (LHV) (EPA, 1998; Singh *et al.*, 2014).

Fuel type	Density (kg m^{-3})	x_M (g/100 g)	x'_C (g/100 DM)	x'_H (g/100 DM)	x'_O (g/100 DM)	x'_N (g/100 DM)	x'_S (g/100 DM)	x'_A (g/100 DM)	Raw formula	CFR (kg/kg)	HHV (MJ/kg)	LHV (MJ/kg)
Firewood	450–980[1] 300–450[2]	22.4	46.00	5.80	44.87	0.30	0.01	3.02	$CH_{1.513}O_{0.732}N_{0.006}S_{0.002}$	1.74	15.84	13.95
Crop residues	200–400[3]	14.0	42.10	6.30	48.37	0.36	0.17	2.70	$CH_{1.796}O_{0.862}N_{0.007}S_{0.002}$	1.59	14.62	12.84
Charcoal	180–220	1.7	80.00	1.80	10.00	0.74	0.06	7.40	$CH_{1.513}O_{0.270}N_{0.094}S_{0.000}$	3.17	27.86	27.41
Coal	640–930[4]	10.0	39.00	4.00	15.00	1.50	0.50	40.00	$CH_{1.231}O_{0.288}N_{0.033}S_{0.005}$	2.38	16.30	15.14
Natural gas	0.57–0.72	0.0	72.38	23.58	1.37	2.66	0.01	0	$CH_{3.909}O_{0.014}N_{0.032}S_{0.0005}$	2.65	58.25	52.92
LPG	508–573	0.0	82.29	17.70	0.00	0.00	0.01	0.00	$CH_{2.581}$	3.02	53.37	49.37
Kerosene	780–810	0.0	85.90	13.80	0.05	0.05	0.20	0.00	$CH_{1.928}S_{0.001}$	3.15	48.97	45.85
Biogas	0.85–0.93	0	56.50	11.90	27.86	3.47	0.27	0.00	$CH_{2.527}O_{0.37}N_{0.053}S_{0.002}$	2.07	31.28	28.59
Ethanol	785–794	4[5]	52.17	13.04	34.78	0	0	0	$CH_3O_{0.5}$	1.91	26.8–29.7	21.4–26.9

[1] Density at 13% moisture content (Francescato *et al.*, 2008).
[2] Bulk density of wood logs at 15% moisture content (Francescato *et al.*, 2008).
[3] Bulk density of agricultural residues at 7–11% moisture content (Makavana *et al.*, 2018).
[4] Bulk density (https://www.tapcoinc.com/images/uploads/Tapco_Catalog_09_p88-94.pdf).
[5] Water content of the ethanol mixture used by CleanCook ethanol stove (Appropedia, 2008; Benka-Coker *et al.*, 2018).

study on dry basis using one of the mathematical models available in literature (Vargas-Moreno *et al.*, 2012). In this work, HHV and LHV (expressed in MJ/kg) were calculated as follows (Mukunda, 2009):

$$HHV = 33.823\ x'_C + 144.249\ (x'_H - x'_O/8) + 9.418\ x'_S, \quad (1)$$

$$LHV = HHV - 22.604\ x'_H - 2.581\ x_M. \quad (2)$$

Table 3 shows the elemental composition and moisture content of typical firewood and crop residues (Singh *et al*., 2014), together with their estimated raw formula, theoretical amount of CO_2 produced by the overall combustion of a unitary mass of biofuel, and higher and lower heating values calculated using Equations (1) and (2), respectively.

The heating value of anhydrous wood biomass varies between 18.5 MJ/kg and 19 MJ/kg, whatever be the wood species examined. Owing to their higher lignin, resin, wax and oil contents, the heating value of conifers is about 2% higher than that of broad leave trees. The calorific value of anhydrous lignin (26–27 MJ/kg) is higher than that of cellulose (17.2–17.5 MJ/kg) or hemicellulose (16 MJ/kg). Further variability in the heating value is due to slight variation in hydrogen content and especially to diverseness in ash and moisture contents (Francescato *et al*., 2008).

Several crop residues (i.e., rice husk, wheat straw, cotton stalk, corn stover etc.), which are mostly left on fields after harvesting, and forestry residues (i.e., branches, leaves, bark etc.) are usually collected and burned by households. These are characterized by low bulk density and heating values in the range of 12–20 MJ/kg, depending on their ash and moisture contents. Most of the woody biomass free from leaves and needles has an ash content of less than 2%, while in some agricultural residues, it could be as high as 21% as in the case of rice husk (Shen *et al*., 2010).

Table 3 shows the ultimate composition of a typical mixture of crop residues used in India (Singh *et al*., 2014). Emissions in the air resulting from the combustion of typical firewood and crop residues as shown in Table 4 are derived from Singh *et al.* (2014). The resulting ash contents are generally disposed of in landfills. The theoretical CO_2 emissions shown in Table 3 were greater than those obtained under conditions of real combustion, probably because of an inappropriate mass ratio of air to the solid fuel used.

Charcoal

Charcoal (CHC) is a high-carbon solid fuel obtained from the carbonization of wood and wood wastes, which

Table 4. Emissions to air and waste generated by the combustion of typical cooking fuels (EPA, 1998; Singh *et al*., 2014).

Emissions to air/waste	Firewood (g/kg)	Crop residues (g/kg)	Charcoal (g/kg)	Coal (g/kg)	Natural gas (g/STPm^3)	Kerosene (g/kg)	LPG (g/kg)	Biogas (g/kg)
CO_2 (biogenic)	326	1,302	625	0	0	0	0	1,450
CO_2	1,032	0	1,979	1,559	1,918.5	2,943	3,085	0
CO	69	65.6	275	49	1.3	62	14.9	1.88
CH_4	4.2	6.8	7.9	4.69	0.04	0.74	0.074	0.43
NO	0.41	0.54	0.62	0.55	1.60	0.58	0.98	0.38
NO_2	0.35	0.54	0.51	0.45	0.00	0.52	0.78	0.24
N_2O	0.09	0.05	0.08	0.08	0.04	0.09	0.015	0.009
Non-methane volatile organic compounds (NMVOC)	7.35	8.2	10.3	10.5	0.09	13.2	10.59	0.56
$PM_{2.5}$	3.3	7.5	0.4	12.2	0.12	1.9	0.32	0.66
PM_{10}	4.34	7.54	0.43	17.9	0.00	0.52		0.66
Total suspended particulate (TSP)	1.04	0.63	2.19	1.3	0.00	0.7	0.51	0.52
Black carbon	0.6	0.51	0.2	5.42	0.00	0.16	0.01	0.01
Organic carbon	0.95	1.46	1.18	6.75	0.18	0.12	0.02	0.02
SO_2	0.32	0.27	0.34	2.67	0.01	2.56	2.12	0.85
Formaldehyde	0	0	0.03	0	0	0	0	0
Ash	30.2	27	74	400.0	0	0	0	0
Digested slurry	0	0	0	0	0	0	0	1060.0

are heated under limited aeration to remove water and volatile components. Such a process can be carried out in traditional earth mound kilns with a yield of about 14%, or in closed retorts with yields as high as 25–40%, thanks to the heat recovered from the combustion of volatile components baked off (Singh *et al*., 2014; Wikipedia, 2021d). Generally, the carbon content of charcoal ranges from 0.68 to 0.82 kg per kg of charcoal, which upon combustion gives rise to 2.5–3 kg of biogenic CO_2 (Table 3). The main disadvantage of this process is the emission of unburnt methane, combustion gases, and particulates harmful to human health and the environment (Table 4).

Coal

Coal (CO) is a common resource of energy and chemicals. It is a complex heterogeneous solid composed of organic and inorganic matter with quite different chemico-physical properties. It is generally ranked on the basis of its carbon content into four types, namely, (1) *anthracite* with 86–97% carbon content (x'_C) and the highest heating value, (2) *bituminous coal* with x'_C = 45–86%, (3) *sub-bituminous coal* with x'_C = 35–45% and (4) *lignite* with x'_C = 25–35%. Table 3 shows the ultimate composition of a typical sub-bituminous coal generally used for cooking purposes. Its combustion gives rise to the emissions to air as listed in Table 4, and to coal ash usually disposed in landfills like that resulting from biomass fuels.

Kerosene

Kerosene (KER) is a combustible hydrocarbon liquid obtained from the fractional distillation of petroleum between 150 °C and 275 °C. It is mainly used as aviation fuel and indoor cooking fuel. Its typical physico-chemical properties are shown in Table 3, while main emissions after its combustion are shown in Table 4. Even in this case, the theoretical CO_2 emissions (Table 3) were greater than those obtained under the real combustion conditions of this liquid fuel (Table 4).

Natural Gas

Natural gas is a nonrenewable mixture consisting of methane (85–96% mol/mol), other alkanes (1.9–7.4% mol/mol) and inert compounds (i.e., carbon dioxide, nitrogen and hydrogen sulfide) (Florida Power & Light Co., 2003).

Table 3 shows typical properties and composition of NG. It is used as a fuel for generating electric and thermal energy, household heating and cooking, in vehicles as well as a chemical feedstock for manufacturing plastics and organic chemicals. It is primarily transported in its gaseous form using specific gas transmission network in industrialized countries. It can also be compressed and cooled into a liquid form and transported by sea. Emissions to the air resulting from its combustion are listed in Table 4 (US Environmental Protection Agency [EPA], 1998).

Liquified Petroleum Gas

Liquified petroleum gas is a fossil fuel mixture consisting of propane (C_3H_8) and butane (C_4H_{10}) with smaller percentage of isobutene and propylene. Its composition may range from 100% propane to 20% propane and 80% butane depending on the local winter and summer weather conditions, respectively. LPG can be manufactured during the refining of crude oil or extracted from petroleum or NG streams. It can be used as a fuel gas for heating and cooking, and in vehicles. To this end, it can be stored in portable steel cylinders, barbecue gas bottles and larger tanks. It is considered a clean cooking fuel because it gives rise to by far smaller indoor air pollution than biomass fuels. For this reason, LPG supply chains have been developed in several countries (e.g., Brazil, India, Indonesia, Bangladesh, Ethiopia, Haiti, Burundi, Mozambique etc.) to convert people in rural and urban areas to cleaner and healthier cooking solutions because its supply chain requires no investment in infrastructure as in the case of electricity grid and NG network (Rosenthal *et al*., 2018; Wright *et al*., 2020).

Table 3 shows the typical properties and composition of LPG, while Table 4 reports the main emissions to air as resulting from LPG cookstoves. Beyond the fact that LPG is ideal for users living in areas not accessible to NG lines, it has the advantage of a greater calorific value of 93.2 MJ/m^3 against 38.7 MJ/m^3 for NG. Moreover, because of the easier regulation of mass ratio of air to LPG, the CO_2 emitted during real burning is near to the theoretical amount shown in Table 3.

Biogas

Biogas (BG) is obtained from the process of anaerobic digestion of organic wastes, such as agricultural waste, manure, municipal waste, sewage, green waste and food waste, in anaerobic digesters (Bedoić *et al*., 2020). It mainly comprises methane (50–75% v/v), carbon dioxide (25–45% v/v) and nitrogen (0–10% v/v). It also contains small amounts of oxygen, ammonia, hydrogen and hydrogen sulfide, each being less than 1% v/v, and siloxanes. Its moisture varies from 2% v/v at 20 °C to 7% v/v at 40 °C. It is regarded as a renewable energy source, since its combustion practically releases the CO_2 absorbed from

the atmosphere in the growth of primary bio-resource. It can be used for different purposes, such as electricity and heat generation, cooking etc. A greater percentage of household-scale biogas digesters are installed in China and India. Economic governmental subsidies are provided to encourage rural population in Asia, Africa and South America to produce and use biogas at household levels, and thus avoid health problems associated with the use of biomass cookstoves (Wright *et al*., 2020).

Table 3 shows the typical properties and composition of biogas, while Table 4 reports the main emissions to air resulting from biogas cookstoves.

Bioethanol

Bioethanol is a renewable fuel used as a low-carbon alternative to fossil-derived fuels. It is the main fermentation product of yeast (e.g., *Saccharomyces cerevisiae*) or bacteria (e.g., *Zymomonas mobilis*) cultured on the media rich in simple sugars under anaerobic conditions. The so-called *first-generation* bioethanol stems from sugar-based raw materials (i.e., sugarcane, corn, sweet sorghum and cassava), while the *second-generation* bioethanol is derived from lignocellulose raw materials (such as straw, corn stover, wood trimmings, sawdust, bamboo, citrus peels etc.), which are presented for preliminary enzymatic treatment to hydrolyze cellulose (Kang *et al*., 2014). Brazil and the United States currently cover ~85% of global supply of bioethanol by utilizing sugarcane and corn as substrates, respectively (Bertrand *et al*., 2016).

Numerous life cycle assessment studies attempted to estimate the environmental impact of bioethanol from different substrates with contradictory results. According to Jeswani *et al*. (2020), if no land-use change is involved, only bioethanol from sugarcane can meet the EU Renewable Energy Directive (EC, 2018a) of 60% reduction in GHG emissions relative to petrol, while lignocellulosic bioethanol from agricultural and forest residues appears to have a greater mitigation effect. Among the several initiatives aiming at testing the use of ethanol cookstoves, it is worth citing the case of Gaia Association in Addis Ababa (Ethiopia), where the stoves are fed with 96% (v/v) technical ethanol, which cannot be used as power ethanol for vehicles and is denatured with a bitter additive and dyed blue to make it unpalatable for drinking and unmistakable for water (Appropedia, 2008).

Table 3 shows the typical properties and composition of bioethanol. No information was found in the literature about the emissions in the air generated by ethanol cookstoves, although several studies monitored emissions to air resulting from the combustion of different ethanol-gasoline mixtures in spark-ignition engines (Iodice *et al*., 2018; Manzetti and Andersen, 2015). The ethanol blend of 85% (v/v), generally used as a vehicle fuel in Brazil, generated 90%, 15% and 50% less particulates, CO and NO_X, respectively, or benzene and 1,3-butadiene with respect to 100% gasoline, but almost 3.5 times higher carbonylic compound emissions were noted, mainly acetaldehyde (Costagliola *et al*., 2013).

Electricity

The use of electric energy (EL) for cooking results in no indoor emissions and smoke, and thus is a minimum health risk source. Nevertheless, such use affects ambient air pollution and climate change in a smaller or greater manner, especially if the electricity is made from wind turbines and solar photovoltaic panels or coal, respectively. Globally, about 26,603 TWh of electricity was generated in 2018, about 38% of which being made from coal, 23% from NG, 10% from nuclear power plants and 25.5% from renewables (International Energy Agency [IEA], 2019). In industrialized countries, where electrification rates are very high, about 50% and 61% of the cooking energy consumption in the EU-27 (Eurostat, 2021a) and the United States (IEA, 2018) is supplied by electricity whereas 31% and 33% by NG, respectively. Nevertheless, cooking devices consume about 6% of the overall energy consumption in the EU-27 and the US households, while the energy consumption for noncooking purposes (e.g., space and water heating, lighting and air conditioning) is by far dominating (Eurostat, 2021a). In low- and middle-income countries, use of electricity for cooking is limited, being even lower than the electricity access rate, for its high specific cost (Wright *et al*., 2020).

Food Cooking Energy Requirements

Several studies have attempted to measure the energy required to cook some food items in single or multiple portions using different cookstove or oven types, cooking fuels, and methods, and in some cases to assess the resulting GHG emissions (Carlsson-Kanyama and Boström-Carlsson, 2001; Foster *et al*., 2006; Frankowska *et al*., 2020; Martinez-Gómez *et al*., 2016; Nielsen, 2003). Many of these studies pointed out different thermal energy efficiencies of the main cooking systems used.

As an example, Table 5 shows the specific life cycle energy use (LCEU) and cooking time (t_C) of a few food items as a function of different appliances and cooking modes, number of portions, including mass of food and water used, as interpreted by Carlsson-Kanyama and Boström-Carlsson (2001). For instance, these authors demonstrated that boiling water in an electric kettle or

Table 5. Specific life cycle energy use (LCEU) and cooking time (t_c) of a few food items as a function of different appliances and cooking modes used, number of portions, including the overall masses of food and water used (Carlsson-Kanyama and Boström-Carlsson, 2001).

No.	Food Item	Appliance & cooking mode	No. of portions	Food mass (g)	Water mass (g)	t_c (min)	LCEU (MJ/kg)
1	Wheat	Hotplate	4	180	350	17	1.8
2	Wheat	Hotplate	1	45	88	15	11.3
3	Wheat	Microwave oven	4	180	350	15	2.1
4	Wheat	Microwave oven	1	45	85	12	14.9
5	Barley	Hotplate	4	160	700	23	2.3
6	Barley	Hotplate	1	40	175	30	16.5
7	Barley	Microwave oven	4	160	700	26	2.9
8	Barley	Microwave oven	1	40	160	23	23.8
9	Couscous	Electric kettle	4	240	300	1.00	4.0
11	Couscous	Hotplate	4	240	300	2.42	4.2
12	Couscous	Hotplate	1	80	100	2.00	13.8
13	Boiled potatoes	Hotplate	4	800	1,000	32.4	1.1
14	Boiled potatoes	Hotplate	1	190	600	28.3	6.8
15	Boiled potatoes	Hotplate[1]	4	800	1,000	32.4	1.1
16	Boiled potatoes	Hotplate[1] method	1	190	600	28.3	6.3
17	Baked potatoes	Microwave oven	4	1,200	-	28.0	1.2
18	Baked potatoes	Microwave oven	1	300	-	7.0	5.0
19	Baked potatoes	Conventional oven	4	1,200	-	65.0	1.8
20	Baked potatoes	Conventional oven	1	300	-	65.0	20.0
21	Mashed potatoes	Electric kettle	4	140	650	4.25	7.1
22	Mashed potatoes	Electric kettle	1	35	175	2.25	28.6
23	Mashed potatoes	Hotplate	4	140	650	1.83	7.9
24	Mashed potatoes	Hotplate	1	35	175	0.83	34.3
25	Swedish-made pasta	Hotplate	4	280	2,500	18	4.3
26	Italian-made pasta	Hotplate	4	280	2,500	18	4.6
27	Swedish-made pasta	Hotplate	1	70	1,000	14	21.4
28	Italian-made pasta	Microwave oven	1	70	1,000	14	22.9
29	Fresh pasta	Microwave oven	4	520	2,500	12	3.5
30	Fresh pasta	Microwave oven	1	130	1,000	8	16.2
31	Rice	Hotplate	4	240	600	20	4.2
32	Rice	Hotplate	1	60	150	20	21.7
33	Rice	Microwave oven	4	240	600	17	5.0
34	Rice	Microwave oven	1	60	150	17	25.0

[1] Energy-saving method.

baking a single portion of potatoes in a microwave oven was by far more energy-efficient than a hotplate or conventional oven. Moreover, Lakshmi *et al*. (2007) observed that an electric rice cooker was more energy-efficient than a pressure cooker or microwave cooker. Similarly, Martinez-Gómez *et al*. (2016) analyzed several cooking parameters for eight typical Ecuadorian meals when cooked using LPG-, coil- or induction-stoves. For example, the energy requirements to cook four hard-boiled eggs or grill 400-g chicken reduced from about 0.44 to 0.29 or 0.2 kWh. This clearly indicated that induction stove was more efficient thermally than other stoves examined.

According to Frankowska *et al*. (2020), the cooking of vegetables (e.g., cabbage, carrots, cauliflower, onions and potatoes) and meat and fish accounts for around 61% and 8–27% of total GHGs emitted during their overall life cycle, respectively. Similarly, home cooking of 1 kg of conventional dry pasta in 10 L of boiling water laced

with 70 g of table salt consumed as much as 2.8 kWh/kg, which represented about 50% of the cradle-to-grave carbon footprint, while wheat-milling and pasta-making and packaging or durum wheat cultivation covered 24.8% and 21.7% of total GHG emissions respectively (Cimini *et al.*, 2020). By using the innovative Arduino®-based eco-sustainable pasta cooker, operating with a water-to-dry pasta ratio of 3 ± 1 L/kg and consuming just 0.6 ± 0.1 kWh/kg (Cimini *et al.*, 2020), the cradle-to-grave carbon footprint of dry pasta reduced by 27% (Cimini *et al.*, 2020). In the case of brewing of a cup of coffee using different coffee makers, the use phase represented the secondary hotspot (12.5–18.2% of cradle-to-grave carbon footprint), coffee bean cultivation and green coffee production phase embodying 59–70% of total GHG emissions (Cibelli *et al.*, 2021).

The cooking of lamb and beef is highly energy-intensive in consequences of their long cooking period (>1 h) as in the case of roasting in an oven. Nevertheless, the contribution of their cooking to the total GHGs emitted was found to be lower than 10% because their cradle-to-grave carbon footprint was by far higher than that of vegetables. Under these circumstances, it would be much more environment-friendly to reduce the consumption of lamb and beef than to improve the energy efficiency of cooking method of choice (Frankowska *et al.*, 2020).

Table 6 summarizes the specific energy requirements for cooking different food items using either a few ordinary moist (e.g., boiling, and frying), dry (grilling) and combined (microwave) heat cookery methods, as interpreted by Foster *et al.* (2006).

Description of the Cooking Systems Studied

A cooking system does not entail just the cookstove and oven but it accounts for the stove technology, cooking fuels and their supply chains, cookware, food materials as well as all the stages involved in the process of cooking from collection, handling, transportation and use of raw materials, extraction and/or refining, transportation to consumers, cooking, as well as post-consumer waste disposal. Its system boundary is sketched in Figure 1.

Table 6. Specific energy requirements for cooking different food items using a few ordinary cookery methods (Foster *et al.*, 2006).

Cookery methods	Specific energy required (MJ/kg of raw food)
Boiling	3.5
Frying	7.5
Grilling	8.5
Microwave cooking	0.34

If the per capita cooking energy consumption per year is known as (E_C), the mass of cooking fuels consumed (m_{CF}) and the electric energy absorbed from the national grid (E_{EE}) can be estimated as follows:

$$m_{CF} = \frac{E_C}{LHV\,\eta_{CS}}, \quad (3)$$

and

$$E_{EE} = \frac{E_C}{\eta_{CS}(1-\eta_{EG})}, \quad (4)$$

where LHV is the lower heating value of each cooking fuel (see Table 3), η_{CS} is the average thermal efficiency of cookstove, and η_{EG} is the average loss of electric grid. While the range of values for η_{CS} is shown in Table 2, the latter was about 5.8% for the Italian grid in 2020 (Terna, 2020).

Specific emissions into the air, water and solid wastes resulting from the use of different cooking fuels are reported in Table 4. In Italy, electricity is produced mainly from fossil fuels (52% of total, that is, 43% from NG, 4.3% from coal and 1.0% from petroleum products etc.), and from renewable energy sources (37.6% of total, that is, 15.3% from hydroelectric sources, 8.3% from solar, 6.0% from wind and 1.94% from geothermic power, and 6.3% from biofuels) (Terna, 2020).

Methodology

The life-cycle analysis (LCA) was carried out according to specific international standards (International

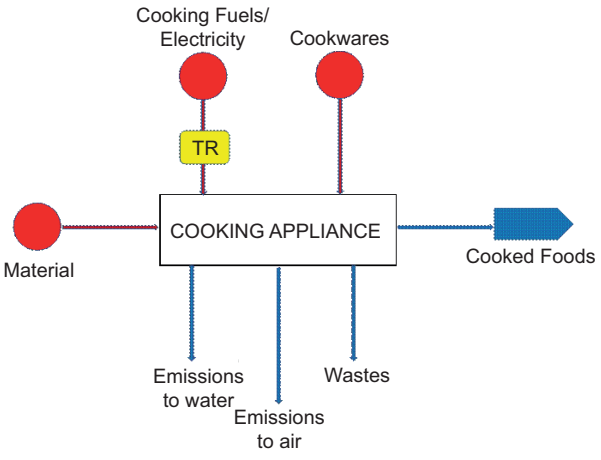

Figure 1. Schematic of a generic cooking system, including the transportation stage (TR) of cooking fuels.

Organization for Standardization [ISO], 2006a, 2006b), and included the following stages: Goal and scope definition, inventory analysis, impact assessment and interpretation of results.

Goal and scope definition

The goal of this study was to determine the potential life cycle environmental impacts of different cooking fuels (i.e., firewood, charcoal, kerosene, NG, LPG, biogas and electricity) in Italy using the LCA software Simapro 9.2.0.2 (Prè Consultants, Amersfoort, NL) with embedded background Ecoinvent v. 3.7 database. The cooking energy requirements depend not only on the thermal efficiency (η_{CS}) of the cookstove used but also on the type and energy (LHV) value of each fuel, as shown in Tables 2 and 3. For a valid comparison between different cooking systems, the production of useful EU-27 per capita cooking energy consumption of 1.41 GJ/yr, as transferred to the cooking pot after the combustion of each fuel in the cookstove, was used as the functional unit. In this way, differences in the fuel energy values and efficiencies of end-use cookstoves were accounted for.

As suggested by the guidelines established by the Publicly Available Specification (PAS) 2050 standard method (British Standards Institution [BSI], 2011), the production of capital goods (cookstoves, cookware etc.) as well as their cleaning and disposal (Section 6.4.4; BSI, 2011), was not included in the system boundary. Such assumption was also corroborated by a few LCA analyses which confirmed that the use phase was responsible for the greatest environmental impact in several impact categories in the case of mud stoves for firewood (Afrane and Ntiamoah, 2012), gas and induction hobs (Favi *et al*., 2018), electric and gas ovens (Landi *et al*., 2019) as well as domestic induction hobs equipped with different electronic boards (Elduque *et al*., 2014). Additionally, the lifespan of each cookstove was, in general, more than 10 years, this being the average life of the appliances installed in Italy (Favi *et al*., 2018). In addition, the production and transportation of food materials, as well as the transportation and disposal of food wastes, were excluded from the system boundaries, as they were assumed to be the same for all the cookstoves examined.

Inventory analysis

The production processes of all cooking fuels, as well as electricity drawn from the Italian grid mix, were extracted from the Ecoinvent v. 3.7 database (Table 7).

Solid (i.e., firewood, charcoal and coal) and liquid (i.e., kerosene and LPG) cooking fuels were distributed by road using Euro5 lorries with a load capacity of 3.5–7.5 Mg for an average distance of 50 km. Kerosene was packed in 20-L high-density polyethylene tanks weighing 0.75 kg each and LPG was filled into 10-kg steel bottles, weighing 11 kg each. Finally, gaseous fuels (i.e., NG and biogas) were distributed by 50-km pipelines, while electricity was drawn from the Italian grid mix.

Pollutants from cookstoves are mainly derived from incomplete combustion processes. They included biogenic and/or fossil CO_2, carbon monoxide, methane, oxides of nitrogen (NO_X), non-methane volatile organic compounds (NMVOC), particulate matter (PM), black carbon, organic carbon compounds and sulfur dioxide. These pollutants are of great concern because of their harmful effects on human health. Electric cookstoves have no direct indoor emissions but a more or less severe indirect environmental impact depending on the electric power supply.

Emissions and solid wastes resulting from the combustion of fuels (Singh *et al*., 2014) are shown in Table 4, as referred to 1 kg of cooking fuel or 1 standard temperature and pressure (STP) m^3 of NG. The effective mass of cooking fuels burnt and electricity drawn from the electric grid were calculated by using Equations (3) and (4), respectively.

Finally, solid wastes (wood and coal ash) from cookstoves were disposed of in landfills.

Impact assessment

The impact assessment was carried out using the ReCiPe 2016 (Huijbregts *et al*., 2016), and PEF (EC, 2018b; Manfredi *et al*., 2012; Sala *et al*., 2017, 2018) standard methods, all these methods being embedded in the software SimaPro 9.2.0.2.

Any generic impact category (IC_j) was estimated by summing up release into the air, water and soil (ψ_i, expressed in mass, energy, and mass-km basis) associated to the system boundaries times its corresponding characterization factor ($F_{i,j}$) as:

$$IC = \sum_i (\Psi_{i,j} F_{i,j}) \quad (5)$$

The updated ReCiPe 2016 method (Huijbregts *et al*., 2016) included the following 18 midpoint impact categories; the reference substance of each is indicated in parentheses: global warming (kg CO_{2e}); stratospheric

Table 7. Production processes for the cooking fuels used in this work (extracted from the Ecoinvent v. 3.7 database).

Cooking fuels	Ecoinvent v. 3.7 database	Description
Firewood	Wood pellet, measured as dry mass (RoW)| wood pellet production| cut-off, S	Wood pellets are produced in a wood pellets factory, which uses wood residue from sawmills and woodchips as raw materials. The raw materials are first pre-treated and dried; then comminuted, mixed, pelletized, cooled and bagged. 20% of the production was packed in 15-kg bags, while the remaining 80% was sold unpacked.
Charcoal	Charcoal (GLO)| production| cut-off, S	Charcoal with an average carbon content of 80% (w/w) is produced from hardwood from forest plantations.
Coal	Hard coal (Europe, without Russia and Turkey)| market for hard coal| cut-off, S	This activity starts at the hard coal preparation plant with coal ready to be loaded on rail, truck, barge or conveyor. The activity ends with the unloading of hard coal at domestic consumers or export hubs. The inventory refers to the average transport distance specific to the domestic market of hard coal in Europe without Russia and Turkey.
Natural gas	Natural gas, high pressure (IT)| import from RU| cut-off, S	This dataset represents the extraction of NG in the Russian Federation and includes the following activities: exploration, production, processing, underground storage of NG, and feeding of produced gas in the pipeline for transport to the country where it is consumed. The leakages of production and processing of the raw gas are included. This dataset describes the transport required for the export of Russian NG to Italy (expressed in Mg km). Gas losses and emissions during seasonal storage are included. An average distance of 6,400 km is estimated for the export.
LPG	Liquefied petroleum gas (Europe without Switzerland)| liquefied petroleum gas production, petroleum refinery operation| cut-off, S	This dataset describes the operation of a representative average petroleum oil refinery in Europe without Switzerland. It includes the following activities: crude oil and product storage on refinery grounds and energy provision, refinery infrastructure, wastewater treatment, freshwater supply (from nature), refined petroleum products leaving the refinery. Its sulfur content was 1.03%.
Kerosene	Kerosene (Europe without Switzerland) | kerosene production, petroleum refinery operation| cut-off, S	This dataset describes the operation of a representative average petroleum oil refinery in Europe without Switzerland. Activity starts with crude oil entering the petroleum refinery. Wastewater treatment, freshwater supply (from nature), refinery infrastructure, crude oil and product storage on refinery grounds and energy provision are included. Electricity requirements are met by the on-site generation mix. Activity ends with refined petroleum products leaving the refinery.
Biogas	Biogas (RoW)| anaerobic digestion of manure| cut-off, S	This activity produces biogas and digestate from manure and includes the following activities: input of livestock manure (cattle slurry, pig slurry and cattle manure) to incoming storage at the biogas plant, storage of the substrates, anaerobic fermentation, and storage of digestate after fermentation. The activity ends with the biogas and digestate being available at the biogas plant. The calorific value of the biogas only accounts for the methane content excluding the presence of H_2S in it.
Electricity	Electricity, low voltage (IT)| market for| cut-off, S	This dataset describes the electricity available on the low-voltage level in Italy in 2017 as well as grid losses. It includes electricity inputs produced in this country and from imports and transformed to low voltage, the transmission network over aerial lines and cables, direct emissions to air (SF_6 from the insulation gas in the high-voltage level switchgear are allocated to the electricity demand on medium voltage), and electricity losses during transmission.
	Electricity, low voltage (FR)| market for| cut-off, S	This dataset describes the electricity available on low-voltage level in France in 2017. It includes electricity inputs produced in France from imports and transformed to low voltage, the transmission network, direct emissions to air (SF_6 from the insulation gas in the high-voltage level switchgear are allocated to the electricity demand on medium voltage), and electricity losses during transmission. This dataset excludes electricity losses during transformation from high to medium voltage or medium to low, as these are included in the dataset for transformation, leakage of insulation oil from cables and electro technical equipment, SF_6 emissions during production and deconstruction of the switchgear, as these are accounted for in the transmission network dataset.
	Electricity, low voltage (PL)| market for| cut-off, S	This dataset describes the electricity available on low-voltage level in Poland in 2017. It includes electricity inputs produced in Poland and from imports and transformed to low voltage, the transmission network, direct emissions to air (SF_6 from the insulation gas in the high-voltage level switchgear are allocated to the electricity demand on medium voltage level), electricity losses during transmission. This dataset excludes electricity losses during transformation from high to medium voltage or medium to low, as these are included in the dataset for transformation, leakage of insulation oil from cables and electro technical equipment (transformers, switchgear and circuit breakers) because this only happens in case of accidental release, SF_6 emissions during production and deconstruction of the switchgear, as these are accounted for in the transmission network dataset.

(*continues*)

Table 7. Continued

Cooking fuels	Ecoinvent v. 3.7 database	Description
	Electricity, high-voltage (IT)| electricity production, hydro, reservoir, alpine region| cut-off, S	This dataset represents the production of high-voltage electricity at grid-connected reservoir hydropower plants in Italy in 2012. Net average electrical efficiency, including pipe losses, is 78%. This dataset starts from the power plant ready to produce electricity, i.e., the reservoir filled with water, and ends with 1 kWh of high-voltage electricity produced at the power plant and arrived at the busbar. This dataset doesn't include land use for access roads to the reservoir, emissions of carbon dioxide, raw materials extraction, decommissioning and waste treatment as these activities are already included in the infrastructure datasets, transformation of the electricity produced.
	Electricity, high-voltage (IT)| electricity production, wind, 1–3-MW turbine, onshore| cut-off, S	This dataset represents the production of high-voltage electricity at on-shore grid-connected wind power plants with a capacity between 1 MW and 3 MW in Italy in 2005–2020. It includes operation and maintenance expenditures as well as infrastructure inputs.
	Electricity, low-voltage (IT)| electricity production, photovoltaic, 570-kWp open ground installation, multi-Si | cut-off, S	This dataset represents the production of grid-connected low-voltage electricity with a 570-kWp open ground photovoltaic plant in Italy in 2008–2020. An inverter is used to convert the low-voltage DC power into AC power. Use of tap water for cleaning the module and its treatment is included.

FR - France; GLO, global; IT - Italy; PL - Poland; RoW - Rest of world; RU - Russia, S - system.

ozone depletion (kg trichlorofluoromethane or freon-11, CFC-11_e); ionizing radiation (kBq $^{60}Co_e$); fine PM formation (kg $PM_{2.5e}$); ozone formation-human health, and ozone formation-terrestrial ecosystems (kg NO_{xe}); terrestrial acidification (kg SO_{2e}); freshwater (kg P_e) and marine (kg N_e) eutrophication; terrestrial, freshwater, and marine ecotoxicity (kg 1,4-Dichlorobenzene [DCB]); human carcinogenic and noncarcinogenic toxicity (kg 1,4-DCB); land use (m^2 annual $crop_e$); mineral (kg Cu_e) and fossil (kg oil_e) resource scarcity; and water consumption (m^3). Finally, the PEF method accounted for the following 16 impact categories, the reference substance of each is indicated in parentheses: climate change (kg CO_{2e}), ozone depletion (kg CFC-11_e), ionizing radiation-human health (kBq $^{235}U_e$), photochemical ozone formation (kg $NMVOC_e$), PM (diseases included), human toxicity, noncancer (Human Comparative Toxic Unit, CTU_h); human toxicity, cancer (CTU_h), acidification (mol H^+_e), freshwater eutrophication (kg P_e), marine eutrophication (kg N_e); terrestrial eutrophication (mol N_e), freshwater ecotoxicity (ecotoxicity Comparative Toxic Unit, CTU_e), land use (point [Pt]), water scarcity (m^3 depriv.), resource use-fossils (MJ), and resource use-mineral and metals (kg Sb_e).

Both standard methods combine the above-mentioned environmental impacts into one point value. More specifically, the ReCiPe 2016 method groups the aforementioned impact categories into the following three endpoint indicators: (i) damage to *human health* (HH), expressed in DALY, that is, the number of years of life lost as a result of premature mortality and/or disability after an exposure to toxic chemicals; (ii) damage to *ecosystem quality* (EQ), expressed in loss of species during a year; and (iii) damage to *resource availability* (RA), expressed in US$ 2013 to quantify the extra costs involved for future mineral and fossil resource extraction. Such damage categories are then normalized with respect to the global population and aggregated using specific weights. Finally, the three damage categories may be grouped into individualistic, hierarchic, or egalitarian perspective, according to the 'Cultural Theory' (Thompson *et al*., 1990). In this study, hierarchic perspective was used to estimate the *overall weighted damage score* ($OWDS_R$), since such a perspective is regarded as the most balanced one between future and present impacts, and risks and benefits (Huijbregts *et al*., 2016). Thus, the midpoint ReCiPe-Hierarchic (H) version-Europe was used to characterize the results of LCIA, while the environmental impacts were calculated according to the ReCiPe endpoint - Hierarchic (H) version-Europe H/A - with the average weighting set (A), both methods being encoded in the LCA software SimaPro 9.2.0.2.

Concerning the PEF method, any impact category was normalized with respect to its corresponding global impact as recommended by Sala *et al*. (2017), weighted as suggested by Sala *et al*. (2018), and finally summed up to yield another *overall weighted score* (OWS_p).

Sensitivity analysis

Uncertainty in the outputs of the above-mentioned LCA models was mainly apportioned to the range of variations in thermal efficiency (η_{CS}) of the cooking fuels used (see Table 2) and to the electric power supply (i.e., the French or Polish grid mix, hydro, solar photovoltaic and

wind power). In particular, the French electricity mix is largely dominated by the nuclear power, while coal governs the power sector of Poland (www.iea.org/countries). Once the default triangular and/or normal distribution uncertainty range for η_{CS} was accounted for, it was possible to resort to the well-known Monte Carlo analysis (Theodoridis, 2015).

Results and Discussion

Mid-point environmental profile of the cooking systems examined

Environmental impacts of the cooking fuels examined in this work at the first stage of cause–effect chain are shown in Table 8, depicted according to the ReCiPe 2016 and PEF standard methods.

According to the ReCiPe 2016 method, the use of coal appeared to have the maximum impact in 12 of the 18 categories (i.e., global warming, fine PM formation, ozone formation affecting human health and terrestrial ecosystems, terrestrial acidification, freshwater and marine eutrophication and ecotoxicity, human carcinogenic and noncarcinogenic toxicity, and fossil resource scarcity). The use of charcoal, electricity and firewood largely affected three impact categories (namely, stratospheric ozone depletion, land use and water consumption), two impact categories (e.g., ionizing radiation and mineral resource scarcity), and one (terrestrial ecotoxicity) impact category, respectively. In contrast, the use of NG gave rise to the minimum impact in 9 of the 18 categories (i.e., ionizing radiation, fine PM formation, terrestrial acidification, freshwater eutrophication, terrestrial, freshwater and marine ecotoxicity, human noncarcinogenic toxicity, and land use). The use of biogas, LPG and kerosene minimized the impact of four impact categories (i.e., global warming, ozone formation affecting human health and terrestrial ecosystems, and fossil resource scarcity), four impact categories (namely, stratospheric ozone depletion, marine eutrophication, human carcinogenic toxicity, and mineral resource scarcity) and one impact category (water consumption), respectively.

In addition, with the PEF method, the use of coal appeared to have the maximum impact in 10 of the 16 categories (i.e., climate change, photochemical ozone formation, PM, acidification, freshwater, marine and terrestrial eutrophication, freshwater ecotoxicity, resource use, that is, fossils and mineral and metals). The use of charcoal, NG and electricity had the maximum impact on four impact categories (namely, human noncancer and cancer toxicity, land use, and water scarcity), one impact category (ozone depletion), and one impact category (ionizing radiation), respectively. In agreement with the other LCIA method, the use of NG led to minimum impact in 10 of the 16 categories (i.e., ionizing radiation, photochemical ozone formation, PM, noncancer and cancer human toxicity, acidification, eutrophication freshwater, ecotoxicity freshwater, land use, and resource use, that is, -mineral and metals). The use of kerosene and biogas exerted minimum impact on the remaining three (i.e., marine, terrestrial eutrophication, and water scarcity) and three (namely, climate change, ozone depletion, and resource use, that is, fossils) impact categories, respectively.

Whereas the PEF method refers to the 100-year time horizon global warming potentials (Myhre *et al*., 2013), in the ReCiPe 2016 method, the characterization factors for global warming differ from the former because climate–carbon feedback for non-CO_2 GHGs is included (Huijbregts *et al*., 2017). Therefore, scores of the global warming category, as estimated using both methods, resulted to be slightly different. These ranged from as high as 1,210 kg CO_{2e} in the case of coal cookstoves to as low as 153 kg CO_{2e} in the case of biogas cookstoves. Except for charcoal cookstoves (which emitted about 607 kg CO_{2e}), all other cookstoves emitted 188–256 kg CO_{2e} per person per year. By contrast, thanks to the model developed by van Zelm *et al.* (2016), it was possible to assess maximum formation of fine PM if using coal, firewood and charcoal cookstoves (i.e., 7.5, 2.3 and 0.46 kg $PM_{2.5e}$ per person per year, respectively), and minimum formation of fine PM if using NG cookstoves (~0.1-kg $PM_{2.5e}$). LPG and kerosene cookstoves emitted about 0.15–0.27 kg $PM_{2.5e}$ per person per year. These results were similar to those obtained with the PEF method, despite this method estimates the impact of such a category in terms of disease incidence using the United Nation Environment Program (UNEP) model (Fantke *et al*., 2016).

End-point environmental profile of the cooking systems examined

The ReCiPe 2016 standard method groups its 18 midpoint impact categories into three damage categories (DC) to highlight the environmental compartments damaged by any cooking system during its life cycle. In particular, the impact categories of global warming and water consumption exerted their damage to both human health and ecosystem quality compartments. By contrast, the categories of stratospheric ozone depletion, ionizing radiation, fine PM and ozone formation affecting human health, and human carcinogenic and noncarcinogenic toxicity affected the human health compartment only, while categories of ozone formation affecting terrestrial ecosystems, terrestrial acidification, freshwater and marine eutrophication, terrestrial, freshwater and marine

Table 8. Environmental profile at the first stages of the cause–effect chain of different cooking systems used, as provided by the mid-point impact categories of the ReCiPe 2016 and product environmental footprint (PEF) standard methods per person per year.

Impact category	Cooking fuels								Unit
	FW	CHC	CO	NG	LPG	KER	BG	EL	
ReCiPE 2016									
Global warming (GW_{100})	2.28E+02	6.07E+02	1.21E+03	2.35E+02	1.88E+02	2.27E+02	1.53E+02	2.56E+02	kg CO_{2e}
Stratospheric ozone depletion	6.57E-04	1.75E-03	5.89E-04	1.27E-04	6.11E-05	1.24E-04	3.34E-04	1.59E-04	kg CFC-11_e
Ionizing radiation	8.22E+00	2.82E+00	9.71E+00	2.71E-01	1.77E+00	2.07E+00	1.87E+00	2.75E+01	kBq $^{60}Co_e$
Fine particulate matter formation	2.30E+00	4.63E-01	7.50E+00	9.73E-02	1.46E-01	2.73E-01	2.53E-01	2.67E-01	kg $PM_{2.5e}$
Ozone formation, human health	1.75E+00	1.58E+00	3.07E+00	3.44E-01	3.31E-01	3.79E-01	1.91E-01	4.37E-01	kg NO_{xe}
Ozone formation, terrestrial ecosystems	2.23E+00	2.12E+00	3.72E+00	3.56E-01	3.97E-01	4.82E-01	2.00E-01	4.45E-01	kg NO_{xe}
Terrestrial acidification	8.49E-01	5.94E-01	2.81E+00	2.79E-01	4.01E-01	4.67E-01	7.48E-01	7.77E-01	kg SO_{2e}
Freshwater eutrophication	4.70E-02	2.80E-02	7.89E-01	1.55E-03	1.83E-03	2.08E-03	2.41E-02	6.25E-02	kg P_e
Marine eutrophication	8.64E-03	1.08E-02	4.90E-02	2.06E-04	1.87E-04	2.26E-04	1.68E-03	4.57E-03	kg N_e
Terrestrial ecotoxicity	4.75E+02	3.02E+02	3.64E+02	7.32E+00	1.41E+02	1.14E+02	9.60E+01	2.88E+02	kg 1,4-DCB
Freshwater ecotoxicity	9.70E+00	8.44E+00	5.75E+01	2.02E-01	3.12E-01	3.44E-01	1.86E+00	2.18E+01	kg 1,4-DCB
Marine ecotoxicity	1.34E+01	1.19E+01	7.90E+01	2.83E-01	5.85E-01	6.24E-01	2.47E+00	2.69E+01	kg 1,4-DCB
Human carcinogenic toxicity	1.04E+01	5.53E+00	7.50E+01	2.41E+00	1.51E+00	1.66E+00	4.06E+00	1.16E+01	kg 1,4-DCB
Human noncarcinogenic toxicity	3.11E+02	3.10E+02	3.89E+03	3.81E+00	1.03E+01	1.13E+01	5.33E+01	1.69E+02	kg 1,4-DCB
Land use	2.65E+02	4.11E+02	1.49E+01	9.66E-02	3.14E-01	3.32E-01	5.68E+00	6.40E+00	m^2 annual $crop_e$
Mineral resource scarcity	2.54E-01	1.18E-01	3.57E-01	5.00E-02	4.28E-02	5.19E-02	9.00E-02	4.51E-01	kg Cu_e

(*continued*)

Table 8. Continued

Impact category	Cooking fuels								Unit
	FW	CHC	CO	NG	LPG	KER	BG	EL	
Fossil resource scarcity	3.67E+01	2.05E+01	3.79E+02	8.54E+01	6.43E+01	7.62E+01	1.38E+01	7.78E+01	kg oil_e
Water consumption	7.64E-01	5.99E+00	8.57E-01	3.82E-02	3.85E-02	2.55E-02	1.67E-01	3.62E+00	m^3
PEF									
Climate change (GW_{100})	2.36E+02	6.17E+02	1.26E+03	2.36E+02	1.89E+02	2.34E+02	1.59E+02	2.56E+02	kg CO_{2e}
Ozone depletion	1.03E-05	8.05E-06	1.87E-05	6.64E-05	4.52E-05	5.36E-05	2.96E-06	3.47E-05	kg CFC-11_e
Ionizing radiation, human health (HH)	1.18E+01	5.01E+00	1.51E+01	3.82E-01	1.25E+01	1.48E+01	2.61E+00	3.01E+01	kBq $^{235}U_e$
Photochemical ozone formation, HH	5.25E+00	5.56E+00	9.14E+00	3.94E-01	8.62E-01	1.35E+00	4.41E-01	5.65E-01	kg $NMVOC_e$
Particulate matter (PM)	6.08E-04	4.14E-05	2.13E-03	3.22E-06	7.12E-06	3.49E-05	2.90E-05	4.50E-06	disease inc.
Human toxicity, noncancer	1.84E-06	6.46E-05	3.56E-05	2.59E-07	1.18E-06	4.81E-06	4.35E-06	1.79E-06	CTU_h
Human toxicity, cancer	6.85E-08	2.25E-07	1.77E-07	1.39E-08	1.45E-08	1.43E-08	4.09E-08	8.66E-08	CTU_h
Acidification	1.38E+00	9.79E-01	4.26E+00	4.52E-01	5.85E-01	6.69E-01	1.12E+00	1.14E+00	mol H^+_e
Eutrophication freshwater	4.70E-02	2.80E-02	7.89E-01	1.55E-03	1.82E-03	2.07E-03	2.41E-02	6.24E-02	kg P_e
Eutrophication marine	4.05E-01	3.16E-01	9.57E-01	1.27E-01	8.71E-02	8.26E-02	9.18E-02	1.81E-01	kg N_e
Eutrophication terrestrial	4.36E+00	3.28E+00	9.39E+00	1.38E+00	9.53E-01	9.03E-01	3.38E+00	2.01E+00	mol N_e
Ecotoxicity freshwater	2.78E+03	2.72E+03	2.92E+04	3.77E+02	1.42E+03	1.71E+03	2.39E+03	3.04E+03	CTU_e
Land use	3.07E+04	4.668E+04	2.54E+03	6.26E+01	3.36E+02	3.91E+02	7.93E+02	1.21E+03	Pt
Water scarcity	2.20E+01	2.530E+02	1.71E+01	1.23E+00	9.78E-01	3.46E-01	4.41E+00	1.32E+02	m^3 depriv.
Resource use, fossils	1.72E+03	9.337E+02	1.69E+04	3.51E+03	2.78E+03	3.29E+03	6.31E+02	3.78E+03	MJ
Resource use, mineral and metals	6.75E-04	2.050E-04	1.26E+03	1.61E-05	3.93E-05	4.08E-05	2.14E-04	2.38E-03	kg Sb_e

FW: firewood; CHC: charcoal; CO: coal; NG: natural gas; LPG: liquified petroleum gas; KER: kerosene; BG: biogas; EL: electricity; CTU_e: comparative toxic unit of ecotoxicity; NMVOC: non-methane volatile organic compounds.

ecotoxicity, and especially land use distressed the ecosystem quality compartment. Finally, the categories of mineral and fossil resource scarcities limited the resource availability compartment.

Table 9 shows single scores of the three damage categories for any cooking system examined, which were first normalized and then aggregated to complete assessment to the end-point approach.

The use of coal appeared to have maximum impact on two of the three damage categories (i.e., human health and resource availability). The use of charcoal affected maximum the other damage category (ecosystem quality). In contrast, the use of NG exerted the least impact on human health and ecosystem quality, while the use of biogas had a minimum impact on resource availability. The resulting single score ($OWDS_R$) was maximum in the case of coal cookstoves (118 Pt) and minimum in the case of LPG cookstoves (~5 Pt). The contribution of damage to human health ranged from 91% to 98% of $OWDS_R$ in the case of charcoal and coal cookstoves, respectively. Moreover, the overall weighted damage score for NG, biogas, kerosene and electricity cookstoves were 5.2, 5.7, 7.0 and 8.6 Pt, respectively; these scores confirmed their suitability for being included in the category of the so-called clean cooking fuels (IEA and the World Bank, 2014).

As suggested by the PEF method, all mid-point impact categories were normalized with respect to their corresponding global impact and weighted to obtain another single score (OWS_p). Even with this method, the overall environmental impact of coal cookstoves was maximum (425 millipoint [mPt]), while that of LPG cookstoves was minimum (12.6 mPt). Higher scores characterized the NG (12.9 mPt), biogas (14.2 mPt), kerosene (19.7 mPt) and electricity (21.8 mPt) cookstoves, while the overall environmental impact of firewood and charcoal cookstoves represented just 27% and 11% of OWS_p of coal cookstoves (Table 9). It also confirmed the predominant contribution of PM on OWS_p for coal (75%) and firewood (79%) cookstoves; it was minimum in the case of electric (3%) and NG (4%) cookstoves. It is worth pointing out that such a contribution grew to 13%, 27% and 31% in the case of charcoal, kerosene and biogas cookstoves (Table 9).

Sensitivity analysis

Figure 2 shows how the environmental single scores, $OWDS_R$ and OWS_p, of cooking systems under study were affected by uncertainty of thermal efficiency (η_{CS}) of the cooktops used (Table 2). Such mean values were derived from the Monte Carlo analysis (using a fixed number of 2,000 runs) and characterized by standard deviations ranging from ~3% (in the case of biogas cookstove) to 19% (in the case of charcoal cookstove). Moreover, at a probability level of 0.05, there was no statistically significant difference between the overall scores for NG and LPG cookstoves. Under these circumstances, both cooking fuels appeared to be less damaging to the compartments of human health and ecosystem quality, and thus more apt to minimize both indoor and outdoor air pollution. As shown in Figure 2, $OWDS_R$ increased from a minimum value of ~5 Pt to 6 Pt, 7 Pt and 9 Pt if biogas, kerosene and electric cookstoves are used, respectively. Quite similar results were obtained by comparing the overall weighted scores OWS_p according to the PEF method (Figure 2).

In the case of electric cookstoves, both single scores were related to different primary energy sources producing electricity in Italy. To point out the effect of different nonrenewable and/or renewable sources used to generate electricity, it was assumed to draw electricity from the French and Polish grid mix, or from hydro, solar photovoltaic and wind power plants. Table 10 shows the mean values and standard deviations for damage categories of human health, ecosystem quality and resource availability, as such or normalized, as well as the overall weighted score $OWDS_R$ and OWS_p for the electric cooking system examined.

If using the Italian grid mix, which uses about 52% fossil sources (mainly NG) and 37.6% renewable ones (mainly hydroelectric and wind power) (Terna, 2020), $OWDS_R$ was equal to about 8.7 Pt and was practically controlled by damage to ecosystem quality. By contrast, large use of electricity from nuclear power in France had positive effects of reducing $OWDS_R$ to about one-third (3.1 Pt); however, this being predominantly affected by damage to human health. Such a damage enhanced up to 28.8 Pt when using the electricity produced by coal power plants as in Poland, while the total environmental score $OWDS_R$ amounted to ~30 Pt (Table 10). By using renewable energy sources only, $OWDS_R$ reduced to as low as ~0.9 Pt if hydropower electricity was used. It slightly increased to 1.4 and 2.8 Pt if electricity was generated through wind and solar photovoltaic plants, respectively (Table 10).

According to the PEF method, the single environmental score OWS_p was maximum in the case of Polish grid mix (59 mPt) but almost indifferent in the case of Italian and French grid mix (21–22 mPt). It reached a minimum value if electricity from wind was used (1.8 mPt) but increased to 6.3 mPt and 8.4 mPt if electricity was used from hydropower and solar energy, respectively.

Table 9. Endpoint characterization of the environmental profile of cooking systems examined according to the ReCiPe 2016 and PEF standard methods: single and weighted damage scores of each damage category (DC), and overall weighted scores (OWDSR, and OWSP).

Parameter	Cooking fuels								Unit
	FW	CHC	CO	NG	LPG	KER	BG	EL	
ReCiPe 2016									
Single DC score									
Human health (HH)	1.77E-03	9.59E-04	6.98E-03	2.88E-04	2.73E-04	3.91E-04	3.27E-04	4.89E-04	DALY
Ecosystem quality (EQ)	3.51E-06	5.85E-06	5.18E-06	7.65E-07	6.67E-07	8.04E-07	6.84E-07	1.07E-06	Loss of Species yr
Resource availability (RA)	1.01E+01	6.11E+00	4.11E+01	3.05E+01	2.89E+01	3.43E+01	2.42E+00	2.32E+01	US$2013
Weighted DC score									
Human health (HH)	2.95E+01	1.60E+01	1.16E+02	4.81E+00	4.56E+00	6.52E+00	5.46E+00	8.15E+00	Pt
Ecosystem quality (EQ)	9.49E-01	1.58E+00	1.40E+00	2.07E-01	1.80E-01	2.17E-01	1.85E-01	2.91E-01	Pt
Resource availability (RA)	7.24E-02	4.36E-02	2.93E-01	2.18E-01	2.07E-01	2.45E-01	1.73E-02	1.66E-01	Pt
$OWDS_R$	30.5	17.6	118.0	5.2	5.0	7.0	5.7	8.6	Pt
PEF									
OWS_P	116.0	46.2	425	12.9	12.6	19.7	14.2	21.8	mPt
Particulate matter score	91.6	6.23	320	0.49	1.07	5.25	4.36	0.68	mPt

FW: firewood; CHC: charcoal; CO: coal; NG: natural gas; LPG: liquified petroleum gas; KER: kerosene; BG: biogas; EL: electricity.
$OWDS_R$: overall weighted damage score; OWS_P: overall weighted score.

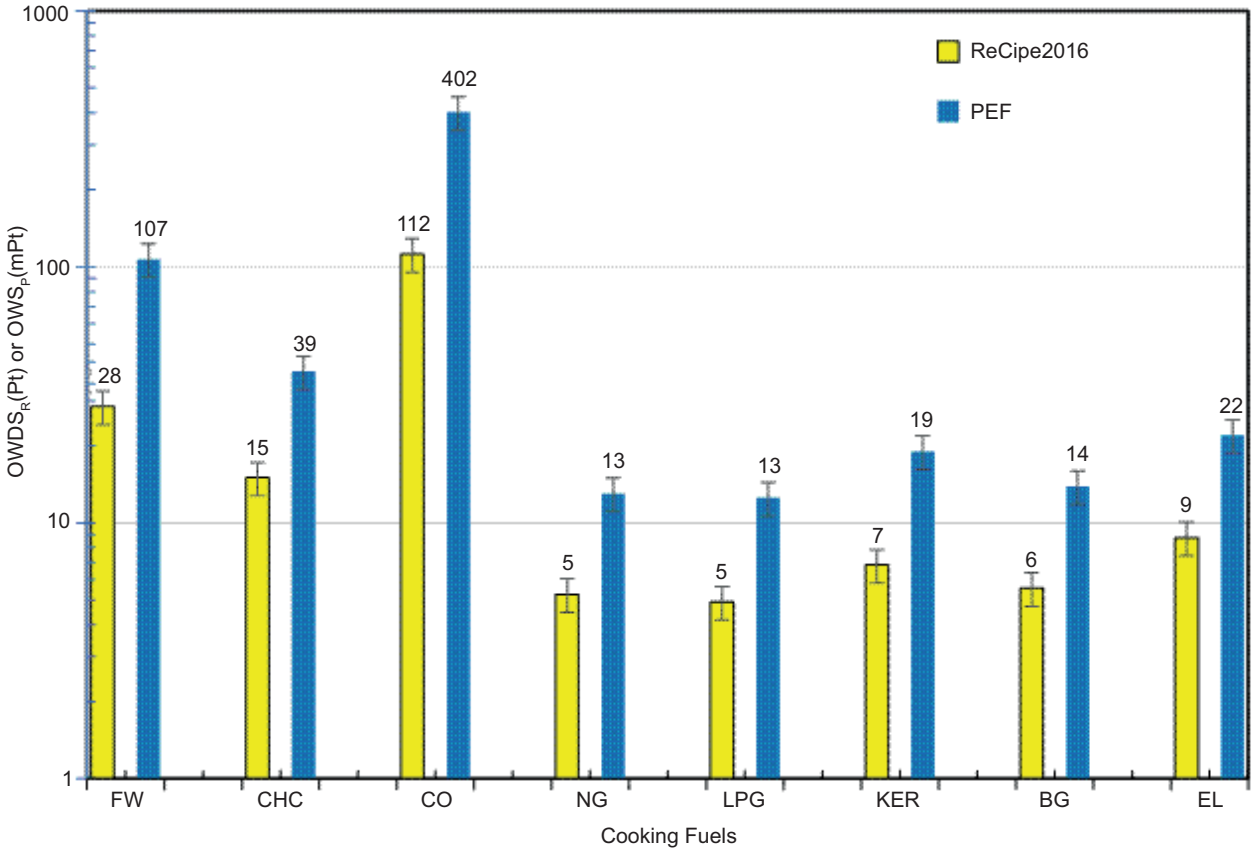

Figure 2. Comparison of environmental impact of different cooking systems examined using the overall weighted scores $OWDS_R$ and OWS_P as estimated according to the ReCiPe 2016 end-point—Hierarchic (H) version—Europe H/A and PEF standard methods, respectively: FW, firewood; CHC, charcoal; CO, coal; NG, natural gas; LPG, liquified petroleum gas; KER, kerosene; BG, biogas, and EL, electricity.

Discussion of results and the future perspectives

The main results of this LCA study pointed out quite similar environmental effects despite the different life cycle impact assessment methods used, and can be summarized as follows:

1. Among the cooking fuels used in the Italian context, the lowest environmental impact was associated with the use of NG and LPG if using the ReCiPe 2016 method, their overall weighted damaged scores being not statistically different at 5% probability level. Such impact was, in turn, significantly smaller than that induced by burning biogas at 95% Confidence Level (CL) despite the fact that use of such a biofuel exerted just 8% of the damage to resource availability induced by other fossil fuels accounted for (Table 10). This was further corroborated by the fact that the database used excluded the infrastructure required to distribute biogas to final users (Table 7). According to the PEF method, LPG cookstoves exerted a lesser impact than that derived from NG and biogas cookstoves, probably because the average distance travelled by LPG bottles was assumed as short as 50 km.
2. When using solid fuels derived from fossils (coal) and renewable (firewood and charcoal) sources, damage to the human health compartment increased by approximately 25 or six and three times, respectively, with respect to that caused by the cooking fuels mentioned above. This was similar to the previous findings from a few LCA studies relative to other countries, such as India (Singh *et al*., 2014), Ghana (Afrane and Ntiamoah, 2011, 2012) and remote communities in the Southeast Asia Pacific region (Aberilla *et al*., 2020) despite different LCIA methods used. Likewise, a recent meta-analysis of 50 studies from Africa, Asia, South and Latin America confirmed that indoor $PM_{2.5}$ concentrations were very low if cooking is done with LPG and electricity (Pope *et al*., 2021). Finally, the LCA study of cooking fuel systems in India, China, Kenya and Ghana pointed out the primary requirement to reduce indoor PM formation, especially in China (its cooking fuel mix includes 31% LPG, 29% coal, 15% firewood and 12% crop residues) and India (its cooking fuel mix being

Table 10. Endpoint characterization of the environmental profile of cooking systems supplied with different electricity grid mixes according to the ReCiPe 2016 and PEF standard methods: single and weighted damage scores of each damage category (DC), and overall weighted scores (OWDSR, and OWSP).

Parameter	EL-IT	EL-FR	EL-PL	EL-HY	EL-SP	EL-WI	Unit
ReCiPe 2016							
Single DC score							
Human health (HH)	$(4.94 \pm 0.49) \times 10^{-4}$	$(1.78 \pm 0.18) \times 10^{-4}$	$(1.72 \pm 0.17) \times 10^{-3}$	$(5.13 \pm 0.51) \times 10^{-5}$	$(1.61 \pm 0.16) \times 10^{-4}$	$(7.98 \pm 0.80) \times 10^{-5}$	DALY
Ecosystem quality (EQ)	$(1.09 \pm 0.11) \times 10^{-6}$	$(3.25 \pm 0.32) \times 10^{-7}$	$(3.40 \pm 0.33) \times 10^{-6}$	$(6.48 \pm 0.64) \times 10^{-8}$	$(3.70 \pm 0.37) \times 10^{-7}$	$(5.73 \pm 0.57) \times 10^{-8}$	Species yr
Resource availability (RA)	23.5 ± 2.3	5.97 ± 0.59	12.7 ± 1.24	$(1.86 \pm 0.18) \times 10^{-1}$	2.82 ± 0.28	$(8.71 \pm 0.87) \times 10^{-1}$	US$2013
Weighted DC score							
Human health (HH)	0.29 ± 0.03	2.97 ± 0.29	28.8 ± 2.8	$(8.56 \pm 0.85) \times 10^{-1}$	2.69 ± 0.27	1.33 ± 0.13	Pt
Ecosystem quality (EQ)	8.24 ± 0.81	$(8.80 \pm 0.86) \times 10^{-2}$	$(9.19 \pm 0.90) \times 10^{-1}$	$(1.75 \pm 0.17) \times 10^{-2}$	$(1.00 \pm 0.10) \times 10^{-1}$	$(1.55 \pm 0.16) \times 10^{-2}$	Pt
Resource availability (RA)	0.17 ± 0.02	$(4.27 \pm 0.42) \times 10^{-2}$	$(9.09 \pm 0.89) \times 10^{-2}$	$(1.33 \pm 0.13) \times 10^{-3}$	$(2.01 \pm 0.20) \times 10^{-2}$	$(6.22 \pm 0.62) \times 10^{-3}$	Pt
$OWDS_R$	*8.71 ± 0.86*	*3.10 ± 0.31*	*29.8 ± 2.90*	*0.88 ± 0.09*	*2.81 ± 0.28*	*1.35 ± 0.14*	Pt
PEF							
OWS_P	*22 ± 2*	*21 ± 2*	*59 ± 6*	*6.3 ± 0.6*	*8.4 ± 0.8*	*1.8 ± 0.2*	mPt

EL-IT: Italian electricity grid mix; EL-FR, French electricity grid mix; EL-PL, Polish electricity grid mix; EL-HY, electricity from hydropower plants; EL-SP, electricity from solar photovoltaic power plants; EL-WI, electricity from wind power plants.
$OWDS_R$: overall weighted damage score; OWS_P: overall weighted score.

formed by 49% firewood, 25% LPG, 11% dung and 9% crop residues), and secondarily to replace traditional stoves with improved ones so as to allow the use of traditional cooking fuels in more appropriate forms and thus enhance their thermal efficiency and limit their environmental burden (Morelli *et al.*, 2017). For instance, in China, substituting conventional honeycomb coal briquettes with coal powder would reduce the impact of climate change and PM formation by about 70% and 97%, respectively (Morelli *et al.*, 2017).

3. Electric cookstove accounted for more than 174% of overall weighted damage score of NG hob. This reflects the environmental impact of two typical cooking appliances, induction hob vs. gas hob and electric oven vs. gas oven, in Italian kitchens, as assessed by Favi *et al.* (2018) and Landi *et al.* (2019), respectively. Obviously, such unfavorable comparison stems from the nature of electricity grid mix in the Italian scenario, which is mainly based on fossil sources (Terna, 2020). Alternatively, use of French electricity grid mix, mainly established from nuclear energy, had the advantage of reducing damage to human health, ecosystem quality and resource availability by about 66%, 49% and 21%, respectively. More favorable environmental impact would arise by using renewable electricity from hydro and wind plants. In this way, electric cooking would not only improve people's health but also avoid the consumption of any fossil energy source.
4. Electricity is currently the only means of cooking suitable for developing new-generation, energy-efficient home smart cookers. In fact, the prospective diffusion of low-cost, open-source platforms would in all probability reduce their selling price and thus promote their market penetration. Such platforms would, for instance, keep the selected cooking temperature practically constant or variable according to specific cooking programs, and shut the cooktop after preset period or as soon as the minimum core temperature is achieved. In this way, it would be possible to minimize both food cooking period and energy requirements. As an example, it is worth citing the eco-sustainable pasta cooking system developed by Cimini *et al.* (2021b). It consisted of a commercial 2-kW induction-plate hob, an induction stainless steel cooking pot, a stainless steel rod mixer piloted by a direct current electric motor welded to pot lid, a digital temperature sensor to monitor temperature of cooking water and a current sensor to register consumption of electric energy. All operations were accomplished via Arduino® platform and an application installed in a smartphone with android system. It allowed short and long dry pastas to be cooked even at lower temperatures than the water boiling point at ambient pressure with as low as 2.7–3.2 L of cooking water per kg of dry pasta. Although the cooked pasta

did not differ from that conventionally cooked at 100 °C with 10-L water per kg of dry pasta in terms of chemico-physical quality parameters and ultrastructure, the pasta cooking energy requirement reduced from the default value of 2.8 kWh/kg to 0.45 kWh/kg, and the overall GHG emissions reduced to about one-sixth of those resulting from the use of average European home appliances.

5. Finally, even if the energy used for cooking represents just 6% of a household's typical energy consumption in the United States and EU-27 countries, such a percentage is quite high in some European, Asian and African countries. Above all, reduction of indoor and outdoor household air pollution and personal exposure to health damaging pollutants, such as PM and carbon monoxide, is a top-priority environmental goal.

Conclusions

After reviewing the basic characteristics of main cooking methods, appliances and fuels, and assessing environmental impact of a few household cookers fired by different fuels and electricity in the Italian scenario in compliance with the ReCiPe 2016 and PEF standard methods, it is pointed out that NG cookstove generates minimum indoor and outdoor air pollution. This finding was comforting, because the Italian cooking energy requirements are predominantly fulfilled by gas (69.2%), although such cookers still rely on fossil energy sources.

To avoid finishing such sources and concurrently improving people's health, household cooking appliances must be replaced by new-generation smart-cooktops driven by hydropower or wind-power electricity, of course, on condition that global electricity generation from renewable energy sources is accelerated faster than done ever before.

Acknowledgements

This research was supported by the Italian Ministry of Instruction, University and Research within the research project entitled 'The Neapolitan pizza: processing, distribution, innovation and environmental aspects'; special grant PRIN 2017-prot. 2017SFTX3Y_001.

References

Aberilla J.M., Gallego-Schmid A., Stamford L., and Azapagic A. 2020. Environmental sustainability of cooking fuels in remote communities: life cycle and local impacts. Sci Total Environ. 713:136445. https://doi.org/10.1016/j.scitotenv.2019.136445

Afrane G. and Ntiamoah A. 2011. Comparative life cycle assessment of charcoal, biogas, and liquefied petroleum gas as cooking fuels in Ghana. J Indus Ecol. 15(4):539–549. https://doi.org/10.1111/j.1530-9290.2011.00350.x

Afrane G. and Ntiamoah A. 2012. Analysis of the life-cycle costs and environmental impacts of cooking fuels used in Ghana. Appl Energy. 98:301–306. https://doi.org/10.1016/j.apenergy.2012.03.04

Anozie A.N., Bakare A.R., Sonibare J.A., and Oyebisi T.O. 2007. Evaluation of cooking energy cost, efficiency, impact on air pollution and policy in Nigeria. Energy. 32:1283–1290. https://doi.org/10.1016/j.energy.2006.07.004

Appropedia. 2008. Ashden Awards. CleanCook ethanol stove. Available at: https://www.appropedia.org/CleanCook_ethanol_stove (accessed: 19 Jan 2022).

Apurva. 2016. Tandoors, burning of solid waste adding to dirty Delhi air: IIT Study. *Indian Express*. Available at: https://indianexpress.com/article/india/india-news-india/tandoors-burning-of-solid-waste-adding-to-dirty-delhi-air-iit-study/ (accessed: 13 Dec 2021).

Arenas J.M. 2007. Design, development and testing of a portable parabolic solar kitchen. Renew Energy. 32:257–266. https://doi.org/10.1016/j.renene.2006.01.013

Aro E.M. 2016. From first generation biofuels to advanced solar biofuels. Ambio. 45(Suppl 1):S24–S31. https://doi.org/10.1007/s13280-015-0730-0

Barratt N. 2021. Different oven types explained! Available at: https://www.canstarblue.co.nz/appliances/ovens/different-types-of-ovens-explained/ (accessed: 2 Dec 2021).

Bedoić R., Ćosić B., Pukšec T., and Duić N. 2020. Anaerobic digestion of agri-food by-products. In Holden N.M., Wolfe M.L., Ogejo J.A., and Cummins E.J. (Eds.) Introduction to Biosystems Engineering. American Society of Agricultural and Biological Engineers (ASABE) in association with Virginia Tech, Blacksburg, VA, pp. 1–23. Available at: https://vtechworks.lib.vt.edu/bitstream/handle/10919/93254/Anaerobic_Digestion.pdf?sequence=27&isAllowed=y (accessed: 11 Dec 2021). https://doi.org/10.21061/IntroBiosystemsEngineering/Anerobic_Digestion

Benka-Coker M.L., Tadele W., Milano A., Getaneh D., and Stokes H. 2018. A case study of the ethanol CleanCook stove intervention and potential scale-up in Ethiopia. Energy Sustain Develop. 46:53–64. https://doi.org/10.1016/j.esd.2018.06.009

Bertrand E., Vandenberghe L.P.S., Soccol C.R., Sigoillot J.C., and Faulds C. 2016. First generation bioethanol. In: Soccol C., Brar S., Faulds C., and Ramos L. (Eds.) Green fuels technology. Green Energy and Technology. Springer, Cham, Denmark. https://doi.org/10.1007/978-3-319-30205-8_8

Bevilacqua M., Braglia M., Carmignani G., and Zammori F.A. 2007. Life cycle assessment of pasta production in Italy. J Food Qual. 30:932–952. https://doi.org/10.1111/j.1745-4557.2007.00170.x

British Standards Institution (BSI). 2011. PAS 2050:2011. Specification for the Assessment of the Life Cycle Greenhouse Gas Emissions of Goods and Services. British Standards Institution, London.

Carlsson-Kanyama A. and Boström-Carlsson K. 2001. Energy Use for Cooking and Other Stages in the Life Cycle of Food. A Study

of Wheat, Spaghetti, Pasta, Barley, Rice, Potatoes, Couscous and Mashed Potatoes. Report No. 160. Stockhoms Universitet, Stockholm, Sweden.

Cibelli M., Cimini A., Cerchiara G., and Moresi M. 2021. Carbon footprint of different methods of coffee preparation. Sustain Prod Consump. 27:1614–1625. https://doi.org/10.1016/j.spc.2021.04.004

Cimini A., Cibelli M., and Moresi M. 2019. Cradle-to-grave carbon footprint of dried organic pasta: Assessment and potential mitigation measures. J Sci Food Agricul. 99:5303–5318 https://doi.org/10.1002/jsfa.9767.

Cimini A., Cibelli M., and Moresi M. 2020. Development and assessment of a home eco-sustainable pasta cooker. Food Bioprod Proc. 122:291–302. https://doi.org/10.1016/j.fbp.2020.05.009

Cimini A., Cibelli M., and Moresi M. 2021a. Environmental impact of pasta. In Galanakis C. (Ed.) Environmental Impact of Agro-Food Industry and Food Consumption. Chp. 5; pp. 101–127. Academic Press, San Diego, CA. https://doi.org/10.1016/B978-0-12-821363-6.00005-9

Cimini A., Cibelli M., Taddei A.R., and Moresi M. 2021b. Effect of cooking temperature on cooked pasta quality and sustainability. J Sci Food Agricul. 101:4946–4958. https://doi.org/10.1002/jsfa.11138

Cimini A. and Moresi M. 2017. Energy efficiency and carbon footprint of home pasta cooking appliances. J Food Eng. 204:8–17. https://doi.org/10.1016/j.jfoodeng.2017.01.012

Climate Technology Center & Network (CTCN). 2017. Ethanol cook stoves. Available at: https://www.ctc-n.org/technologies/ethanol-cook-stoves (accessed: 19 Jan 2022).

Costagliola M.A., De Simio L., Iannaccone S., and Prati M.V. 2013. Combustion efficiency and engine out emissions of a S.I. engine fueled with alcohol/gasoline blends. Appl Energy. 111:1162–1171. https://doi.org/10.1016/j.apenergy.2012.09.042

Darlami H.B., Ale B.B., and Pokharel G.R. 2019. Experimental analysis of thermal efficiency of mud improved cookstove with variation of different parameters and economic analysis. J Inst Eng. 15(3):385–392. https://doi.org/10.3126/jie.v15i3.32228

Ecoinvent. (2020) Ecoinvent v3.7.1. Available at: https://ecoinvent.org/the-ecoinvent-database/data-releases/ecoinvent-3-7-1/ (accessed: 11 Feb 2022).

Elduque D., Javierre C., Pina C., Martínez E., and Jiménez E. 2014. Life cycle assessment of a domestic induction hob: Electronic boards. J Clean Prod. 76:74–84. https://doi.org/10.1016/j.jclepro.2014.04.009

European Commission (EC). 2010. Commission Regulation (EU) No. 97/2010, "Entering a name in the register of traditional specialities guaranteed [Pizza Napoletana (TSG)]." Off J EU. L 34, 05 February. Available at: https://eur-lex.europa.eu/legal-content/EN/TXT/HTML/?uri=OJ:L:2010:034:FULL (accessed: 13 Dec 2021).

European Commission (EC). 2018a. Directive (EU) 2018/2001 of the European Parliament and of the Council of 11 December 2018 on the promotion of the use of energy from renewable sources. Off J EU. L 328/82, 21 December. Available at: https://eur-lex.europa.eu/legal-content/EN/TXT/PDF/?uri=CELEX:32018L2001&from=fr (accessed: 24 Jan 2022).

European Commission (EC). 2018b. Product Environmental Footprint Category Rules Guidance—Version 6.3. European Commission, Brussels, Belgium. Available at: https://eplca.jrc.ec.europa.eu/permalink/PEFCR_guidance_v6.3-2.pdf (accessed: 18 Dec 2021).

Eurostat. 2021a. Energy consumption in households. Available at: https://ec.europa.eu/eurostat/statistics-explained/index.php?title=Energy_consumption_in_households#Energy_products_used_in_the_residential_sector (accessed: 20 Nov 2021).

Eurostat. 2021b. Population projections in the EU. Available at: https://ec.europa.eu/eurostat/statistics-explained/index.php?oldid=497115#Population_projections (accessed: 4 Dec 2021).

Fantke P., Evans J., Hodas N., Apte J., Jantunen M., Jolliet O., and McKone T.E. 2016. Health impacts of fine particulate matter. In Frischknecht R. and Jolliet O. (Eds.) Global Guidance for Life Cycle Impact Assessment Indicators. Vol. 1, pp 76–99. UNEP/SETAC Life Cycle Initiative, Paris, France.

Favi C., Germani M., Landi D., Mengarelli M., and Rossi M. 2018. Comparative life cycle assessment of cooking appliances in Italian kitchens. J Clean Prod. 186:430–449. https://doi.org/10.1016/j.jclepro.2018.03.140

Florida Power & Light Co. 2003. Natural gas specs sheet. Available at: https://www.naesb.org/pdf2/wgq_bps100605w2.pdf (accessed: 19 Jan 2022).

Foster C., Green K., Blea M., Dewick P., Evans B., Flynn A., and Mylan J. 2006. Environmental Impacts of Food Production and Consumption. Report to the Department of the Environment, Food, and Rural Affairs (DEFRA). Manchester Business School London.

Francescato V., Antonini E., and Zuccoli Bergomi L. 2008. Wood Fuels Handbook. Italian Agroforestry Energie Association (AIEL), Legnaro (PD), Italy. Available at: https://www.yumpu.com/pt/document/read/2571080/wood-fuels-handbook-biomasstradecentres (accessed: 6 Dec 2021).

Frankowska A., Schmidt Rivera X., Bridle S.L., Kluczkovski A., da Silva J., Martins C., Rauber F., Levy R.B., Cook J., and Reynolds C. 2020. How home cooking methods and appliances affect the GHG emissions of food. Nature Food. 1:787–791. https://doi.org/10.1038/s43016-020-00200-w

Fullerton D.G., Bruce N., and Gordon S.B. 2008. Indoor air pollution from biomass fuel smoke is a major health concern in the developing world. Trans Royal Soc Trop Med Hygiene. 102:843–851. https://doi.org/10.1016/j.trstmh.2008.05.028

Gould C.F. and Urpelainen J. 2018. LPG as a clean cooking fuel: Adoption, use, and impact in rural India. Energy Policy. 122:395–408. https://doi.org/10.1016/j.enpol.2018.07.042

Hager T.J. and Morawicki R. 2013. Energy consumption during cooking in the residential sector of developed nations: A review. Food Policy. 40:54–63. https://doi.org/10.1016/j.foodpol.2013.02.003

Huijbregts M.A.J., Steinmann Z.J.N., Elshout P.M.F., Stam G., Verones F., Vieira M., Zijp M., Hollander A., and van Zelm R. 2017. ReCiPe 2016: A harmonised life cycle impact assessment method at midpoint and endpoint level. Int J Life Cycle Assess. 22:138–147. https://doi.org/10.1007/s11367-016-1246-y

Huijbregts M.A.J., Steinmann Z.J.N., Elshout P.M.F., Verones F., Vieira M.D.M., Hollander A., Zijp M., van Zelm R., and Stam G. 2016. ReCiPe2016: A Harmonized Life Cycle Impact Assessment Method at Midpoint and Endpoint LevelS. Report I: Characterization. RIVM Report 2016. National Institute for Public Health and the Environment, Bilthoven, the Netherlands. https://doi.org/10.1007/s11367-016-1246-y

Igo S.W., Kokou N., Compaoré A., Kalifa P., Sawadogo G.L., and Namoano D. 2020. Experimental analysis of the thermal performance of a metal fired-wood oven. Iranian (Iranica) J Energy Environ. 11(3):225–230. https://doi.org/10.5829/IJEE.2020.11.03.08

International Energy Agency (IEA). 2018. World energy outlook 2018. Available at: https://iea.blob.core.windows.net/assets/77ecf96c-5f4b-4d0d-9d93-d81b938217cb/World_Energy_Outlook_2018.pdf (accessed: 13 Dec 2021).

International Energy Agency (IEA). 2019. World energy outlook 2019. Available at: https://iea.blob.core.windows.net/assets/98909c1b-aabc-4797-9926-35307b418cdb/WEO2019-free.pdf (accessed: 13 Dec 2021).

International Energy Agency (IEA) and the World Bank. 2014. Sustainable Energy for All 2013–2014: Global Tracking Framework Report. World Bank, Washington, DC. https://doi.org/10.1596/978-1-4648-0200-3.

International Organization for Standardization (ISO). 2006a. 14040-Environmental Management e Life Cycle Assessment—Principles and Framework. International Organization for Standardization, Genève, CH.

International Organization for Standardization (ISO). 2006b. 14044-Environmental Management—Life Cycle Assessment—Requirements and Guidelines. International Organization for Standardization, Genève, CH.

International Renewable Energy Agency (IRENA). 2017. Biogas for Domestic Cooking: Technology Brief. International Renewable Energy Agency, Abu Dhabi. Available at: https://irena.org/-/media/Files/IRENA/Agency/Publication/2017/Dec/IRENA_Biogas_for_domestic_cooking_2017.pdf (accessed: 1 Jan 2022).

Iodice P., Langella G., and Amoresano A. 2018. Ethanol in gasoline fuel blends: Effect on fuel consumption and engine out emissions of SI engines in cold operating conditions. Appl Therm Eng. 130:1081–1089. https://doi.org/10.1016/j.applthermaleng.2017.11.090

Jeswani H.K., Chilvers A., and Azapagic A. 2020. Environmental sustainability of biofuels: A review. Proc Royal Soc A. 476:20200351. https://doi.org/10.1098/rspa.2020.0351

Jungbluth N., Kollar M., and Koß V. 1997. Life cycle inventory for cooking. Some results for the use of liquefied petroleum gas and kerosene as cooking fuels in India. Energy Policy. 25(5):471–480. https://doi.org/10.1016/S0301-4215(97)00022-0

Kang Q., Appels L., Tan T., and Dewil R. 2014. Bioethanol from lignocellulosic biomass: Current findings determine research priorities. Sci World J. 2014:Arte ID 298153, 13 p. http://dx.doi.org/10.1155/2014/298153

Lakshmi S., Chakkaravarthi A., Subramanian R., and Singh V. 2007. Energy consumption in microwave cooking of rice and its comparison with other domestic appliances. J Food Eng. 78(2):715–722. https://doi.org/10.1016/j.jfoodeng.2005.11.011

Landi D., Consolini A., Germani M., and Favi C. 2019. Comparative life cycle assessment of electric and gas ovens in the Italian context: An environmental and technical evaluation. J Clean Prod. 221:189–201. https://doi.org/10.1016/j.jclepro.2019.02.196

Lima F.D.M., Pérez-Martínez P.J., de Fatima Andrade M., Kumar P., and de Miranda R.M. 2020. Characterization of particles emitted by pizzerias burning wood and briquettes: A case study at Sao Paulo, Brazil. Environ Sci Pollution Res. 27:35875–35888. https://doi.org/10.1007/s11356-019-07508-6.

Makavana J.M., Agravat V.V., Balas P.R., Makwana P.J., and Vyas V.G. 2018. Engineering properties of various agricultural residue. Int J Curr Microbiol App. Sci. 7(6):2362–2367. https://doi.org/10.20546/ijcmas.2018.706.282

Manfredi S., Allacker K., Chomkhamsri K., Pelletier N., and Maia de Souza D. 2012. Product Environmental Footprint (PEF) Guide. European Commission, Ispra, Italy.

Manhiça F.A., Lucas C., and Richards T. 2012. Wood consumption and analysis of the bread baking process in wood-fired bakery ovens. Appl Ther Eng. 47:63–72. https://doi.org/10.1016/j.applthermaleng.2012.03.007

Manzetti S. and Andersen O. 2015. A review of emission products from bioethanol and its blends with gasoline. Background for new guidelines for emission control. Fuel. 140:293–301. https://doi.org/10.1016/j.fuel.2014.09.101

Martínez-Gómez J., Ibarra D., Villacis S., Cuji P., and Cruz P.R. 2016. Analysis of LPG, electric and induction cookers during cooking typical Ecuadorian dishes into the national efficient cooking program. Food Policy. 59:88–102. https://doi.org/10.1016/j.foodpol.2015.12.010

McGee H. 2004. On Food and Cooking – The Science and Lore of the Kitchen. Scribner, New York, NY.

Mehetre S.A., Panwar N.L., Sharma D., and Kumar H. 2017. Improved biomass cookstoves for sustainable development: A review. Renew Sustain Energy Rev. 73:672–687. https://doi.org/10.1016/j.rser.2017.01.150

Morelli B., Cashman S., Rodgers M. 2017. Life Cycle Assessment of Cooking Fuel Systems in India, China, Kenya and Ghana. Report No. EPA/600/R-17/225. US Environmental Protection Agency, Washington, DC. Available at: https://cfpub.epa.gov/si/si_public_record_Report.cfm?Lab=NRMRL&dirEntryId=339679 (accessed: 30 Dec 2021).

Mukunda H.S. 2009. Understanding Combustion, 2nd edition. Orient Blackswan, New Delhi, India.

Myhre G., Shindell D., Bréon F.-M., Collins W., Fuglestvedt J., Huang J., Koch D., Lamarque J.-F., Lee D., Mendoza B., Nakajima T., Robock A., Stephens G., Takemura T., and Zhang H. 2013. Anthropogenic and natural radiative forcing. Ch. 8. In Stocker T.F., Qin D., Plattner G.-K., Tignor M., Allen S.K., Boschung J., Nauels A., Xia Y., Bex V., Midgley P.M. (Eds.) Climate Change 2013: The Physical Science Basis. Contribution of Working Group I to the Fifth Assessment Report of the Intergovernmental Panel on Climate Change, pp. 731–738. Cambridge University Press, Cambridge, UK.

Available at: https://www.ipcc.ch/site/assets/uploads/2018/02/WG1AR5_Chapter08_FINAL.pdf (accessed: 18 Dec 2021).

Nielsen H. 2003. Cooking food in ovens and stoves. Available at: http://www.lcafood.dk/ (accessed: 25 Nov 2021).

Okino J., Komakech A.J., Wanyama J., Ssegane H., Olomo E., and Omara T. 2021. Performance characteristics of a cooking stove improved with sawdust as an insulation material. J Renew Energy, vol. 2021, Art ID 9969806: 1–12. https://doi.org/10.1155/2021/9969806

Okoko A., Wymann von Dach S., Reinhard J., Kiteme B., and Owuor S. 2018. Life cycle costing of alternative value chains of biomass energy for cooking in Kenya and Tanzania. J Renew Energy. 2018(Article ID 3939848):1–12. https://doi.org/10.1155/2018/3939848

Okusanya M.A., Ibrahim G.W., and Ogunlade C.B. 2019. The use of ethanol gel cook-stove as a more accessible alternative cooking energy. Int J Eng Sci Invent. 8(10):15–22. www.ijesi.org

Pandey S., Goswami S., Saini P., Powar S., and Dhar A. 2021. Hybrid electrical-solar oven: A new perspective. In Tyagi H., Chakraborty P.R., Powar S., Agarwal A.K. (eds.) New Research Directions in Solar Energy Technologies. Energy, Environment, and Sustainability, pp. 237–255. Springer, Singapore. https://doi.org/10.1007/978-981-16-0594-9_8

Pope D., Johnson M., Fleeman N., Jagoe K., Duarte R., Maden M., Ludolph R., Bruce N., Shupler M., Adair-Rohani H., and Lewis J. 2021. Are cleaner cooking solutions clean enough? A systematic review and meta-analysis of particulate and carbon monoxide concentrations and exposures. Environ Res Lett. 16:083002. https://doi.org/10.1088/1748-9326/ac13ec

Pratiti R., Vadala D., Kalynych Z., and Sud P. 2020. Health effects of household air pollution related to biomass cook stoves in resource limited countries and its mitigation by improved cookstoves. Environ Res. 186:109574. https://doi.org/10.1016/j.envres.2020.109574

Probert D. and Newborough M. 1985. Designs, thermal performances and other factors concerning cooking equipment and associated facilities. Appl Energy. 21:81–222. https://doi.org/10.1016/0306-2619(85)90069-8

Rajvanshi A.K., Patil S.M., and Mendoca B. 2004. Development of Stove Running on Low Ethanol Concentration. Nimbkar Agricultural Research Institute (NARI), Maharashtra, India.

Rasoulkhani M., Ebrahimi-Nik M., Abbaspour-Fard M.H., and Rohani A. 2018. Comparative evaluation of the performance of an improved biomass cookstove and the traditional stoves of Iran. Sustain Environ Res. 28(6):438–443. https://doi.org/10.1016/j.serj.2018.08.001

Rosenthal J., Quinn A., Grieshop A.P., Pillarisetti A., and Glass R.I. 2018. Clean cooking and the SDGs: Integrated analytical approaches to guide energy interventions for health and environment goals. Energy Sustain Develop. 42:152–159. https://doi.org/10.1016/j.esd.2017.11.003

Sala S., Cerutti A.K., and Pant R. 2018. Development of a Weighting Approach for the Environmental Footprint. Publications Office, European Union, Luxembourg. http://dx.doi.org/10.2760/945290. Available at: https://publications.jrc.ec.europa.eu/repository/handle/JRC106545 (accessed: 18 Dec 2021).

Sala S., Crenna E., Secchi M., and Pant R. 2017. Global Normalisation Factors for the Environmental Footprint and Life Cycle Assessment. JRC Scientic Report. Publications Office, European Union, Luxembourg. http://dx.doi.org/10.2760/88930 Available at: https://publications.jrc.ec.europa.eu/repository/handle/JRC109878 (accessed: 18 Dec 2021).

Shen J., Zhu S., Liu X., i Zhang H., and Tan J. 2010. The prediction of elemental composition of biomass based on proximate analysis. Energy Convers Manag. 51:983–987.

Singh P., Gundimeda H., and Stucki M. 2014. Environmental footprint of cooking fuels: A life cycle assessment of ten fuel sources used in Indian households. Int J Life Cycle Assess. 19:1036–1048. https://doi.org/10.1007/s11367-014-0699-0

Singh B. and Highway D. 2016. What is your restaurant's carbon footprint? Available at: https://www.pizzamarketplace.com/articles/what-is-your-restaurants-carbon-footprint/ (accessed: 13 Dec 2021).

Stokes H. and Ebbeson B. 2005. Project Gaia: Commercialising a new stove and new fuel in Africa. Boiling Point. 50:31–33.

Terna. 2020. Dati statistici sull'energia elettrica in Italia. Available at: https://www.terna.it/it/sistema-elettrico/statistiche/pubblicazioni-statistiche (accessed: 24 Jan 2022).

Theodoridis S. 2015. Monte Carlo methods. In Machine Learning. A Bayesian and Optimization Perspective, Chp. 14, pp 707–744. Academic Press, London. https://doi.org/10.1016/B978-0-12-801522-3.00014-8

Thoday K., Benjamin P., Gan M., and Puzzolo E. 2018. The mega conversion program from kerosene to LPG in Indonesia: Lessons learned and recommendations for future clean cooking energy expansion. Energy Sustain Dev J Int Energy Initiative. 46:71–81. https://doi.org/10.1016/j.esd.2018.05.011

Thompson M., Ellis R., and Wildavsky A. 1990. Cultural Theory. Westview Press, Boulder, CO.

United Nations Development Program (UNDP). 2021. What are the sustainable development goals? Available at: https://www.undp.org/sustainable-development-goals (accessed: 29 Dec 2021).

US Environmental Protection Agency (EPA). 1998. Natural gas combustion. Available at: https://www3.epa.gov/ttnchie1/ap42/ch01/final/c01s04.pdf (accessed: 10 Dec 2021).

van Zelm R., Preiss P., Van Goethem T., van Dingenen R., and Huijbregts M.A.J. 2016. Regionalized life cycle impact assessment of air pollution on the global scale: Damage to human health and vegetation. Atmos Environ. 134:129–137. https://doi.org/10.1016/j.atmosenv.2016.03.044

Vargas-Moreno J.M., Callejón-Ferre A.J., Pérez-Alonso J., and Velázquez-Martí B. 2012. A review of the mathematical models for predicting the heating value of biomass materials. Renew Sustain Energy Rev. 16:3065–3083. https://doi.org/10.1016/j.rser.2012.02.054

Vassilev S.V., Baxter D., Andersen L.K., and Vassileva C.G. 2010. An overview of the chemical composition of biomass. Fuel. 89:913–933. https://doi.org/10.1016/j.fuel.2009.10.022

Wikipedia. 2021a. Improved cookstove. Available at: https://en.wikipedia.org/wiki/Improved_cookstove (accessed: 26 Nov 2021).

Wikipedia. 2021b. Gas stove. Available at: https://en.wikipedia.org/wiki/Gas_stove (accessed: 29 Nov 2021).

Wikipedia. 2021c. Electric stove. Available at: https://en.wikipedia.org/wiki/Electric_stove (accessed: 26 Nov 2021).

Wikipedia. 2021d. Charcoal. Available at: https://en.wikipedia.org/wiki/Charcoal (accessed: 9 Dec 2021).

Wollele M.B. 2020. Quantifying energy losses on electric cooking stove. Int J Eng Res Technol. 9(5):753–756. https://doi.org/10.17577/IJERTV9IS050577

World Health Organization (WHO). 2018. Ambient (outdoor) air pollution. Available at: http://www.who.int/mediacentre/factsheets/fs313/en/index.html (accessed: 13 Dec 2021).

World Health Organization (WHO). 2021. Household air pollution and health. Available at: https://www.who.int/news-room/fact-sheets/detail/household-air-pollution-and-health (accessed: 29 Dec 2021).

Wrangham R. 2009. Catching Fire: How Cooking Made Us Human. Basic Books, New York, NY.

Wrangham R. and Conklin-Brittain N. 2003. Cooking as a biological trait. Comp Biochem Physiol Mol Integ Physiol. 136(1):35–46. https://doi.org/10.1016/S1095-6433(03)00020-5

Wright C., Sathre R., and Buluswar S. 2020. The global challenge of clean cooking systems. Food Secur. 12:1219–1240. https://doi.org/10.1007/s12571-020-01061-8

Xu Z., Sun D.-W., Zhang Z., and Zhu Z. 2015. Research developments in methods to reduce carbon footprint of cooking operations: A review. Trends Food Sci Technol. 44:49–57. https://doi.org/10.1016/j.tifs.2015.03.004

Zuzarte F. 2007. Ethanol for cooking—Feasibility of Small-Scale Ethanol Supply and Its Demand as a Cooking Fuel: Tanzania Case Study. KTH School of Energy and Environmental Technology, Heat and Power Technology, Stockholm, Sweden.

Italian Journal of Food Science, 2022; 34 (1): 114–123

Phytochemical component, and antioxidant and vasculo-protective activities of Taiwan cocoa polyphenols by different processing methods

Heuy-Ling Chu[1], Hong-Xuan Fu[2], En-Kuang Chou[2], and Ying-Chun Lin[1]*

[1]Department of Food Science and Technology, and [2]Department of Pharmacy (with Master's program), Chia Nan University of Pharmacy and Science, Tainan City, Rende Dist., Taiwan (ROC)

***Corresponding Author:** Ying-Chun Lin, Department of Food Science and Technology, Chia Nan University of Pharmacy and Science, No. 60, Sec. 1, Erren Rd., Tainan City, Rende Dist. 71710, Taiwan (ROC). Email: ifelin@mail.cnu.edu.tw

Received: 28 September 2021; Accepted: 8 February 2022; Published: 25 February 2022

PAPER

Abstract

Cocoa tree (*Theobroma cacao* L.) is a recently planted crop in Taiwan, a country located in East Asia. Taiwanese cocoa beans are appreciated globally because of their distinctive flavor and aroma. The effects of the water extracts of unfermented Taiwan cocoa beans (WUFCB) and fermented and roasted Taiwan cocoa beans (WFRCB) on the anti-oxidation, vascular protection, and variation in phytochemical components were investigated. Variations in the catechins components of WUFCB and WFRCB were examined by high performance liquid chromatography. The values of catechin compounds in WUFCB (epicatechin [EC]: 52.32 ± 0.56 mg/g, and catechin (C): 15.14 ± 0.26 mg/g) were approximately two times higher than those found in WFRCB (EC: 26.22 ± 0.48 mg/g, and C: 4.56 ± 0.10 mg/g), indicating that the fermentation and roasting steps caused decline in catechins compounds of WFRCB. In the range of 50–300 μg mL^{-1}, both WUFCB and WFRCB depict noncytotoxicity in endothelial cells; they protect cells from H_2O_2-induced cytotoxicity as established by MTT assay. Meanwhile, nitric oxide (NO) levels in endothelial cells were elevated by WUFCB. In addition, WUFCB displayed radical scavenging in the acellular model and inhibited increase in reactive oxygen species (ROS) noted in endothelial cell induced by H_2O_2. Overall, the significant vascular protection of WUFCB is associated with increased NO formation. The decreased ROS generation against oxidative damage was attributed to abundant catechin compounds. This study establishes Taiwan cocoa polyphenol as an effective and complementary tool for preventing endothelial dysfunction and cardiovascular disease.

Keywords: endothelial cells, fermentation and roasting, oxidative damage, Taiwan cocoa polyphenol, vascular protection

Introduction

The impression of humans toward chocolate products has gradually shifted from desserts to healthcare products, emphasizing the amount of bioactive substances found in cocoa beans. Polyphenols in cocoa beans not only bring out unique astringency and bitterness of chocolate flavor but also possess numerous benefits to human health, for instance, eyesight protection (Puell and de Pascual-Teres, 2021); prevention of Parkinson's and Alzheimer's diseases, improved recognition ability, prevention of obesity, increasing the amounts of adiponectin and glucose transporter, decreasing the production of lipid, and insulin resistance (Magrone *et al*., 2017). Moreover, Buijsse *et al*. (2010) discovered that polyphenols relax the smooth muscles, having the potential to reduce blood pressure. Heiss *et al.* (2010) demonstrated that polyphenols prevent the aggregation of platelets and moderate inflammation (Monagas *et al*., 2009). All these mentioned benefits are related to a critical neurotransmitter in the

ISSN 1120-1770 online, DOI 10.15586/ijfs.v34i1.2132

cardiovascular system, that is, nitric oxide (NO). Nitric oxide serves as a second messenger for signaling the cardiovascular smooth muscles. Small molecular weight and lipophilicity of NO allow it to rapidly pass through cell membranes and reach the smooth muscle cells. Sufficient NO bioavailability is associated with normal vasodilation and normal blood pressure. The factors influencing NO levels are as follows: (1) Most NO is synthesized from L-arginine in a reaction catalyzed by the enzyme of endothelial NO synthase (eNOS). The NO level depends on eNOS expression and activity. (2) NO reacts with superoxide anion (O_2-) to form peroxynitrite (ONOO-), which can oxidize cell components, eliminate NO levels and suppress NO bioavailability. (3) The major sources of reactive oxygen species (ROS) (including H_2O_2, OH**.** and O_2-**.**) are related to mitochondrial electron transport chain and nicotinamide adenine dinucleotide phosphate (NADPH) oxidase (NOX) pathway. The elimination of ROS production is associated with decreasing cellular oxidative stress, generation of ONOO- and increased NO levels (Fraga *et al*., 2011 ; Oteiza *et al*., 2021). As indicated, cocoa polyphenol is involved in these phenomena.

According to the statistics provided by the International Cocoa Organization (ICCO), global cocoa bean production in 2018–2019 season exceeded 4.78 million tons, and the production of 2019–2020 season exceeded 4.69 million tons (International Cocoa Organization, 2020; Olga *et al*., 2020). In Taiwan, the planting area of cocoa has increased in recent years, particularly in Neipu and Wanluan counties of Pingtung, Southern Taiwan, where cocoa plantation is done in about 350 hectares. Nowadays, the distribution of cocoa tree planting area has even reached to the middle of Taiwan, indicating cocoa trees have become a recently developed crop in Taiwan. This has led the government and academic institutions to conduct cocoa-relevant research, for instance, the effect of choice of fermentation of starter cocoa cultures, roasting temperature of cocoa beans leading changes in flavanols and procyanidins and sensory properties of cocoa end products. All these investigations aim to enrich the competitiveness and value of Taiwan's cocoa products. However, few studies are conducted involving the cytoprotection of Taiwan cocoa beans and content levels of catechins and methylxanthine compounds in fermented and unfermented cocoa beans, both of which are expected to have higher phytochemical contents.

The present study was designed to prepare two types of cocoa beans under different processing methods (i.e., fermented and unfermented) to explore the effect of their extracts concerning phytochemical level, antioxidant activity, diminishing oxidative stress and vascular protection of endothelial cells. The study also evaluated function of Taiwan cocoa beans to effectively improve endothelial function.

Material and Methods

Materials

3-(4,5-dimethylthiazol-2-yl)-2,5-diphenyltetrazolium bromide (MTT), epicatechin, catechin, theobromine, caffeine, and dimethyl sulfoxide (DMSO) were purchased from Sigma-Aldrich Chemical Co. (St Louis, MO, USA). Mouse vascular endothelial cells, SVEC4-10 (BCRC No. 60220) were purchased from the Bio-resource Collection and Research Center (BCRC, Food Industry Research and Development Institute, Hsinchu, Taiwan). All chemicals of analytical grade were used in the research.

Preparation of cocoa beans

Cocoa pods were purchased from a Pingtung farm in Taiwan. The husk and damaged parts of the cocoa pods were removed. Then 60-kg cocoa beans were fermented for 7 days and sun-dried until the moisture level was 6%. Following fermentation and sun-drying, the cocoa beans were randomly sampled for roasting. The beans were roasted for 25 min at a temperature of 130°C. The final roasted cocoa beans were known as fermented and roasted cocoa beans.

On the other hand, another 20 kg of harvested cocoa beans were in boiling water for 15 min at 90°C and at once cooled in ice water. Then, the boiled cocoa beans were washed and sun-dried until the moisture level dropped to 6%. These bean samples were known as unfermented cocoa beans.

Extraction

A total of 100 g of cocoa beans were peeled manually for each processing method and the nibs were ground into powder in a grinder with liquid nitrogen. The cocoa powder was defatted for 20 min and extracted with boiling water in 1:10 (w/v) ratio. After filtering through Advantec No, 2. filter paper, the residue was reextracted using the same steps. The supernatant was collected and concentrated through a rotary evaporator, freeze-dried, and stored under -20°C. Two different cocoa extracts were obtained, viz. water extracts of fermented and roasted cocoa beans (WFRCB) and water extracts of unfermented cocoa beans (WUFCB).

High-performance liquid chromatography (HPLC) analysis marker components in cocoa extract

The analysis was performed with HPLC according to the method enumerated by Zhang *et al*. (2016). HPLC

chromaster (Hitachi Ltd., Tokyo, Japan) comprised 7725i injector, 5110 pump and 5430 diode array detector (DAD). Sample (1 mg mL^{-1}) was filtered through a hydrophilic PVDF 0.22-µm membrane and injected with a 20-µL sample into an RP-18 column (5µm particle, 4.6 × 250 mm, Mightysil [Kanto Chemical, Tokyo, Japan]). The elution buffer consisted of acetonitrile (Solvent A) and 1% (v/v) phosphoric acid in water (Solvent B) at a flow rate at 0.8 mL/min. The solvent gradient was as follows: 0–8 min, 5–15% B, 8–30 min, 15–25% B, 30–40 min, 25–30% B followed by equilibration of the column prior to new injection. All compounds were detected at 280 nm. Based on the profile of the concentration (x, µg mL^{-1}) versus peak area (y), the linear regression equation and the correlation coefficients (r^2) were as follows: theobromine: y = 7,810.1x -14,896 (r^2 = 0.997); epigallocatechin (EGC): y = 2,700x -21.0 (r^2 = 0.999); caffeine: y = 31,668x +9,043.1 (r^2 = 0.999); catechin (C): y = 8,278.9x –1,790.9 (r^2 = 0.999); epicatechin (EC): y = 9,274.6x +13,850 (r^2 = 0.994); epigallocatechin gallate (EGCG): y = 9,929.2 x -474.1 (r^2 = 0.999); and epicatechin gallate (ECG): y = 10,790x -445.4 (r^2 = 0.999). The HPLC analysis for each sample was performed in triplicate.

Total polyphenolic content (TPC)

Total polyphenol content was analyzed as gallic acid equivalent (GAE). Different concentrations of cocoa extracts were added in a 10-mL volumetric flask, to which 2-mL sodium carbonate (20% w/v) was added. After 5 min, 0.1-mL Folin–Ciocalteu reagent (50% v/v) was added and the volume was made up to 10 mL with H_2O. After 1-h incubation at 30°C, the absorbance was measured at 750 nm and compared to a gallic acid calibration curve.

Proanthocyanidins content (PAC)

The working solution consisted of 0.25-mL cocoa extract, 1.5-mL n-BuOH/HCl (95:5, v/v) and 50-µL 2% solution of $NH_4Fe(SO_4)_2$ $12H_2O$ in 2-M HCl. The reaction mixture was capped, shaken and incubated for 1 h at 95°C. The solution was cooled at room temperature and the absorbance was measured at 550 nm using an enzyme-linked-immunosorbent assay (ELISA) reader (Molecular DevicesVMax, MA, USA). The concentration of proanthocyanidin was measured from a standard curve of cyanidin chloride with the same protocol, and was indicated as mg cyanidin chloride equivalent (CyE/g) of cocoa extract.

DPPH radical scavenging activity

The effect of cocoa extracts on reducing the 2,2-diphenyl-1-picrylhydrazyl (DPPH) radical scavenging activity was determined. The samples were added to a methanolic solution (1 mL) of DPPH radicals (final concentration of DPPH was 0.2 mM). The mixture was shaken vigorously for 30 min at room temperature and then placed in dark. Absorbance of the resulting solution was measured at 517 nm. Trolox equivalent (TE) was used as a reference standard.

Trolox equivalent antioxidant capacity (TEAC) assay

The 2,2'-azino-bis(3-ethylbenzothiazoline-6-sulfonic acid) ($ABTS^+$) cation-free radical inhibitory activity was measured as described previously (Mellinas, *et al*., 2020). The $ABTS^+$ was generated by reacting 1-mM $ABTS^+$ with 0.5-mM hydrogen peroxide and 10 units/mL horseradish peroxidase in dark at 30°C for 2 h. After addition of 1-mL $ABTS^+$ to cocoa extract, absorbance was measured after 10 min at 734 nm. A lower level of absorbance indicated a stronger inhibitory activity of samples. Trolox equivalent was again used to obtain calibration curve.

SVEC4-10 cell line culture

SVEC cells were obtained from BCRC, Taiwan. The cells were cultured in Dulbecco's Modified Eagle Medium (DMEM) containing 10% heat-inactivated fetal bovine serum and 1.5 g L^{-1} L-glutamine at 37°C in a humidified 5% CO_2/95% air-controlled incubator.

Cell viability assay

Cell viability was performed by MTT assay. MTT is a tetrazolium salt and was converted into insoluble formazan by mitochondrial succinate dehydrogenase of living cells. Briefly, cells were seeded in 96-well plates cultured for 24 h. Next, the cells were treated with sample for 1 h, H_2O_2 was added to the medium and incubated for 24 h. Then 5 mg mL^{-1} MTT stock solution was added in each well and incubated for 2 h. Subsequently, the medium was removed and the plates were incubated for 30 min to solubilize colored formazan dye by the addition of DMSO. Then the absorbance of each well was measured with a Thermo Model 355 microplate reader at 550 nm.

Intercellular reactive oxygen species

In order to determine the generation of ROS in cells, 2',7'-dichlorofluorescein-diacetate (DCFH-DA) was used. It penetrates cell membranes and is hydrolyzed by intracellular esterase to form dichlorodihydro-fluorescein (DCFH). DCFH reacts with ROS generated by intracellular stress to produce highly fluorescent DCF, which

emits fluorescence when excited at 485 nm. The SVEC4-10 cells were cotreated with cocoa extract and 0.2-mM H_2O_2. Subsequently, DCFH-DA (50 μM) was added to the medium and incubated for 240 min. The treatment medium was removed, and the cells were washed twice with phosphate buffer solution (PBS). The ROS produced from intracellular stress was detected using a Bio-Tek FLX800 microplate fluorescence reader (Winoosky, VT, USA) with an excitation wavelength of 485 nm and an emission wavelength of 530 nm.

Intercellular nitric oxide

Nitrite levels in cell-cultured media, reflecting the intracellular NO synthase activity, were determined by the Griess reaction. Briefly, the cells were cultured for 18 h with cocoa extracts. Then the growth medium was added with the same volume of Griess reagent (1% sulfanilamide in 5% phosphoric acid and 0.1% N-(1-naphthyl)ethylenediamine dihydrochloride in water) at room temperature. Then the absorbance of mixture at 550 nm was detected.

Statistical analysis

Each experiment was performed at least for three times and the average was calculated. Data are expressed as mean ± SD, and ANOVA was conducted using the SPSS software (version 12.0, SPSS Inc., Chicago, IL, USA). When a significant F-ratio (mean square between treatments / mean square within treatments) was obtained ($p < 0.05$), a *post hoc* analysis was conducted between groups using Duncan's multiple range tests. A significant difference between treatments was considered for $p < 0.05$.

Results and Discussion

Principle phytochemicals present in WUFCB and WFRCB using HPLC

Phytochemicals are plant-derived small molecules possessing multifunctional effects and significantly inhibit oxidative stress. It is worth evaluating the variation in the phytochemical components of Taiwan cocoa beans with different processing procedures. The analysis and separation of the phytochemical components present in WUFCB and WFRCB were performed by HPLC-DAD using an RP-18 analytical column. The qualitative analysis of the phytochemicals utilized linear regression equation of commercial standard compound as described in 'Methods' section. Seven principle compounds were identified and quantified, including theobromine (49.57 ± 1.06 mg/g WUFCB and 71.22 ± 1.24 mg/g WFRCB), epigallocatechin (2.22 ± 0.31 mg/g WUFCB and 1.06 ± 0.11 mg/g WFRCB), caffeine (5.38 ± 0.07 mg/g WUFCB and 8.90 ± 0.16 mg/g WFRCB), catechin (15.14 ± 0.26 mg/g WUFCB and 4.56 ± 0.10 mg/g WFRCB), epicatechin (52.32 ± 0.56 mg/g WUFCB and 26.22 ± 0.48 mg/g WFRCB), epigallocatechin gallate (EGCG, 10.78 ± 0.12 mg/g WUFCB and 5.00 ± 0.50 mg/g WFRCB) and epicatechin gallate (ECG, 0.40 ± 0.15 mg/g WUFCB and 0.48 ± 0.05 mg/g WFRCB), by comparison between retention time (RT), UV-Vis spectrum, the characteristic maximum wavelength (λ_{max}), and literature data from commercial standard and samples. Variation in methylxanthine and catechin levels between WUFCB and WFRCB was investigated as shown in Table 1. The data indicated that WUFCB was rich in catechin compounds, including catechin, epicatechin, EGCG, and EGC. The values of catechin compounds present in WUFCB were approximately two times higher than those found in WFRCB, except for ECG. Alternatively, there was a lower content of methylxanthines (theobromine and caffeine) in WUFCB involved in the pretreatment; it was boiled in hot water at 90°C for 15 min for inactivating polyphenoloxidase and peroxidase. In the latter situation, a lot of methylxanthines (theobromine and caffeine) were found soluble in hot water (Febrianto and Zhu, 2020) that retained a lower concentration of methylxanthines present in WUFCB. Theobromine, caffeine, catechin, epicatechin and procyanidins are related to the astringency and bitter taste of cocoa products. The bitter taste of cocoa is largely influenced by the content of theobromine and caffeine, and to a lesser degree by polyphenolic compounds. Additionally, theobromine and caffeine have a physiological stimulatory activity on the central nervous system (CNS) with beneficial health effects on cognition, satiety function, and mood (Letricia *et al*., 2021).

As described in Table 1, the main polyphenol present in both WUFCB and WFRCB was epicatechin. Current research has found that epicatechin can serve as a free radical scavenger, metal chelator, eNOS activator and arginase inhibitor (Fraga *et al*., 2011), modulating oxidative stress and contributing to the prevention of cardiovascular diseases. Therefore, epicathchin was used as a reference control in the following assay.

Effect of cocoa extracts on antioxidant activity

Polyphenol and proanthocyanidins naturally occur in cocoa beans, playing important roles in different biofunctional activities and have positive health effects in humans. The TPC values in WUFCB and WFRCB are shown in Figure 1A, displaying significant difference ($p < 0.05$). At 400 μg mL^{-1} of WUFCB and WFRCB, TPC was quantified in 16.93 ± 1.71 mg GAE and 13.84 ± 1.48 mg GAE, respectively. It was suggested that fermentation and

Table 1. HPLC analysis of principle polyphenols present in WUFCB and WFRCB.

Compound	Retention time (min)	λ_{max} (nm)	Content (mg/g extract)	
			WUFCB	WFRCB
Theobromine	10.1	272	49.57 ± 1.06	71.22 ± 1.24
EGC	13.6	271	2.22 ± 0.31	1.06 ± 0.11
Caffeine	14.9	272	5.38 ± 0.07	8.90 ± 0.16
Catechin	15.3	278	15.14 ± 0.26	4.56 ± 0.10
Epicatechin	18.1	278	52.32 ± 0.56	26.22 ± 0.48
EGCG	18.9	275	10.78 ± 0.12	5.00 ± 0.50
ECG	26.7	276	0.40 ± 0.15	0.48 ± 0.05

The data were indicated with mean ± SD.
EGC: epigallocatechin; EGCG: epigallocatechin gallate; ECG: epicatechin gallate; WUFCB: water extracts of unfermented cocoa beans; WFRCB: water extracts of fermented and roasted cocoa beans.

roasting of the processing stage significantly decreased TPC, that is, WFRCB is 18.3% lower in TPC after these processing steps.

Proanthocyanidins have depicted potential beneficial effects on human health, in addition to a pleasant sensory ingredient found in cocoa products (Pedan *et al.*, 2018). The effect of WUFCB and WFRCB on PAC display significant differences, as shown in Figure 1B ($p < 0.05$). PAC was influenced by fermentation and roasting steps; it decreased from 3.43 ± 0.02 mg CyE/g WUFCB to 2.97 ± 0.09 mg CyE/g WFRCB.

Proanthocyanidins play a potential role in the prevention of cardiovascular disease and this includes the monomer, catechin and epicatechin, and oligomer units. The obtained data from Figures 1A and B confirm the observation that operational process decreased the levels of PAC and TPC. The results were consistent with previous studies, and the following reasons explain the higher levels of PAC and TPC in WUFCB than in WFRCB: (1) WUFCB (unfermented cocoa beans) were raw cocoa beans and had not undergone the process of fermentation and roasting. Polyphenolic compounds diffused from cellular compartments and oxidized to produce insoluble high molecular weight tannins during the fermentation period. These oxidation reactions were catalyzed by polyphenol oxidase (PPO), which could be the remaining 5–10% of enzymatic activity between the first and the second day of fermentation (Febrianto and Zhu, 2020); and (2) the pretreated WUFCB were heated at 90°C for 15 min, which almost completely inhibited PPO activity. Lower PPO activity retained more TPC and PAC. Further, lower PAC and TPC contents in WFRCB could be because these compounds were susceptible to oxidative degradation during fermentation and roasting (Quiroz-Reyes and Fogliano, 2018).

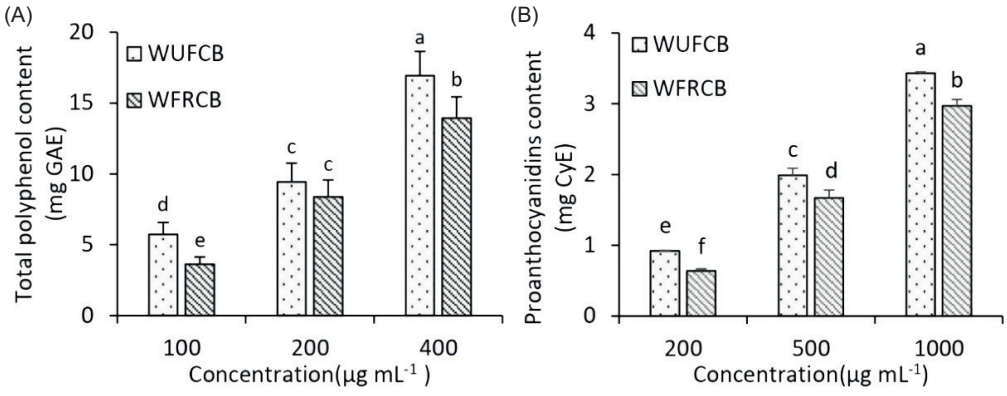

Figure 1. Determination of (A) total polyphenol content (TPC) and (B) proanthocyanidins content (PAC) in water extracts of unfermented cocoa beans (WUFCB) and water extracts of fermented and roasted cocoa beans (WFRCB). Different superscript letters indicate significant differences ($p < 0.05$).

DPPH and ABTS methods, associated with free radical scavenging activities, were selected to assay antioxidant activity. The effect of WUFCB and WFRCB on DPPH and ABTS radical scavenging activities are shown in Table 2. Both WUFCB and WFRCB exhibit a concentration-dependent effect for these two methods in terms of free radical scavenging assay and display a significant difference ($p < 0.05$). The values of antiradical activity by DPPH were similar to that of ABTS. Although similar results were obtained in both DPPH and ABTS assays, properties of each of the extracted compounds differed. In DPPH assay, it easily interacted with hydrophobic compounds; however, it interacted with both hydrophilic and hydrophobic molecules in ABTS assay (Carmen L.D.T.S. *et al.*, 2021). The DPPH radical scavenging activities for WUFCB and WFRCB at concentrations of 150 μg mL^{-1} were equal to 9.70 ± 0.82 mg TE and 8.86 ± 0.62 mg TE, respectively. The ABTS radical scavenging activities were 11.81 ± 0.26 mg TE and 9.26 ± 0.39 mg TE, respectively. WUFCB exhibited more antiradical activity than WFRCB. The obtained results demonstrated that more of processing steps decreased both free radical scavenging activities.

The data obtained in Figure 1 and Table 2 show that less processing steps implies higher retention of TPC and PAC, and DPPH and ABTS radical scavenging activities. The results also established that the antioxidant capacity is directly related to TPC and PAC, which, of course, are affected by the process of fermentation, drying and roasting. The main polyphenolic compounds present in cocoa beans are epicatechin and PAC, which are composed of aromatic rings and functional groups such as hydroxyl group. These structures allow TPC and PAC to chelate metal ions, resulting in the formation of inactive complexes, or the activity to stabilize and reduce hydroxyl, peroxyl or superoxide radicals (Noelia *et al.*, 2021). Free radicals play a crucial role in causing oxidative damage and pathological events, including inflammation, aging and cardiovascular diseases. These observations demonstrated that antiradical activities were potentially affected by TPC and PAC found in cocoa and the low-processing cocoa extract (i.e., WUFCB), rich in TPC and PAC and higher antiradical activity, was a promising candidate for becoming a potential health-promoting food.

In order to examine whether the antiradical activity is related to TPC and PAC, a correlation coefficient test (r^2) was performed. Previous studies have reported a strong correlation between polyphenolic compounds with the antiradical activity of extracts (Carmen L.D.T.S. *et al.*, 2021). Based on the concentration of TPC (x, mg GAE) or PAC (x, mg CyE) versus DPPH (y, mg TE) and ABTS scavenging activities (y, mg TE), the linear regression equation and the correlation coefficient (r^2) are as follows: TPC-DPPH /WUFCB: y = 1.1383x + 5.007 (r^2 = 0.992); TPC-ABTS/WUFCB: y = 2.5858x - 5.6934 (r^2 = 0.999); PAC-DPPH/WUFCB: y = 12.108x + 3.889 (r^2 = 0.990); PAC-ABTS/WUFCB: y = 31.462x - 10.461 (r^2 = 0.998); TPC-DPPH/WFRCB: y = 1.6322x + 4.1053 (r^2 = 0.987); TPC-ABTS/WFRCB: y = 1.9505x - 0.0044 (r^2 = 0.965); PAC-DPPH/WFRCB: y = 16.93x + 3.4375 (r^2 = 0.996); PAC-ABTS/WFRCB: y = 15.483x + 0.6961 (r^2 = 0.972).

The high correlation values observed for antiradical activity are related to both TPC and PAC. The r^2 varied from 0.965 to 0.999.

Effect of cocoa extracts on cell viability in endothelial cells

Endothelial cells are susceptible to oxidative damage, resulting in disturbed cardiovascular homeostasis.

Table 2. The effect of WUFCB (water extracts of unfermented cocoa beans), and WFRCB (water extracts of fermented and roasted cocoa beans) on DPPH and ABTS scavenging activity.

Sample	Concentration (μg mL^{-1})	DPPH scavenging activity (mg TE)	ABTS scavenging activity (mg TE)
Epicatechin	50	4.37 ± 0.39^{e}	3.59 ± 0.57^{e}
	100	5.43 ± 0.49^{de}	6.82 ± 0.34^{d}
	150	6.87 ± 0.90^{bcd}	10.60 ± 0.31^{ab}
WUFCB	50	7.50 ± 0.85^{bc}	4.48 ± 0.71^{e}
	100	8.74 ± 0.94^{ab}	8.25 ± 0.43^{c}
	150	9.70 ± 0.82^{a}	11.81 ± 0.26^{a}
WFRCB	50	6.68 ± 0.52^{cd}	3.48 ± 0.65^{e}
	100	8.09 ± 0.66^{abc}	6.52 ± 0.53^{d}
	150	8.86 ± 0.62^{ab}	9.26 ± 0.39^{bc}

The data were indicated with mean ± SD.
The different letters indicated significant differences ($p < 0.05$).

For this reason, the endothelial cell line SVEC4-10 was used in this study. MTT assay is widely used to measure cell growth. The cytotoxicity of cocoa extract and epicatechin was determined by an MTT assay. Figure 2A shows the response of endothelial cells incubated with samples for 24 h. The cell viabilities of two cocoa extracts of 50–300 μg mL^{-1} and epicatechin at 5–20 μg mL^{-1} were from 91.46% to 127.31% compared to untreated control cells. In other words, WUFCB, WFRCB and epicatechin demonstrated non-cytotoxicity in endothelial cells at all studied concentrations.

Effect of cocoa extracts on cytoprotection by H_2O_2-induced oxidative stress in endothelial cells

Free radicals, including O_2^{-}.,OH., and H_2O_2, are toxic to vascular endothelial cells. H_2O_2 has no charge and can diffuse through the cell membrane. Therefore, in this research H_2O_2 was selected as an oxidant reagent to induce oxidative stress in endothelial cells. In order to evaluate whether Taiwan cocoa polyphenol was involved in protecting endothelial cells from H_2O_2-induced oxidative stress, direct cytotoxicity effect of H_2O_2 on endothelial cells was examined by MTT assay. This included 50, 100 and 300 μg mL^{-1} of cocoa extracts and 5, 10 and 20 μg mL^{-1} of epicatechin. Endothelial cells were damaged by H_2O_2 for 1 h, and the samples were added and incubated for 24 h. The viability of untreated or treated cells by 0.2-mM H_2O_2 in the absence of samples was 223.85% and 100%, indicating that H_2O_2 demonstrated significant cytotoxicity on endothelial cells (Figure 2B). Treatment of 300 μg mL^{-1} of WUFCB and WFRCB and 20 μg mL^{-1} of epicatechin with 0.2-mM H_2O_2 resulted in increased survival rates of endothelial cells, viz. 121.52%, 115.75% and 143.97%, respectively, compared with untreated cells (100%). The results in Figure 2B indicated the cytoprotective effects of WUFCB, WFRCB, and epicatechin from H_2O_2-induced cytotoxicity and depicted a dose-dependent increase in cell growth. In this study, epicatechin, a major component of Taiwan cocoa beans, acted as an effective free radical scavenger in acellular and cellular models, and modulated oxidative stress.

Effect of cocoa extracts on ROS generation in endothelial cells

Many studies have revealed that the development of endothelial dysfunction and cardiovascular disease displayed altered redox status compared with normal cells, including increased ROS generation. Additionally, accumulating studies reported that natural phytochemicals, such as EGCG, EGC, ECG, and proanthocyanin, demonstrate a preventive effect, and are involved in ameliorating intracellular accumulation of ROS. To verify whether the cytoprotection of Taiwan cocoa polyphenol was ascribed to the amelioration of oxidative stress, the effects of the WUFCB and WFRCB were examined on the intracellular ROS formation of SVEC4-10 damaged by H_2O_2. Figure 3 displays the effect of WUFCB, WFRCB and epicatechin on ROS formation in endothelial cells. The intensity of florescence DCF was determined in endothelial cells pretreated with samples for 1 h and then exposed to 0.2-mM H_2O_2. If the endothelial cells were damaged by H_2O_2 for 30 min, intracellular ROS increased to 207.8% compared with the corresponding control value (100%). In addition, pretreatment of endothelial cells with 300 μg mL^{-1} of WUFCB and WFRCB, and 5 μg mL^{-1} of epicatechin, together with H_2O_2, decreased intracellular ROS to 82.31%, 86.41% and 106.58%, respectively (Figure 3). There was a statistically significant decrease in ROS formation, indicating that WUFCB, WFRCB and epicatechin significantly ameliorated intracellular accumulation of ROS. Moreover, the identification of catechins compounds by HPLC-DAD, such as epicatechin, against oxidative damage induced by H_2O_2 may help researchers to better understand protective association of WUFCB with oxidative stress induced by H_2O_2. This demonstrated that Taiwan cocoa polyphenol could be expected to protect endothelial cells against ROS formation by H_2O_2-induced oxidative damage.

Effect of cocoa extracts on NO production in endothelial cell

Endothelial nitric oxide synthase produces NO, a freely diffusible gas, acting as a second messenger for signaling vascular smooth muscle relaxation, causing vasodilation and lowering of blood pressure. However, a fall in NO steady-state level results in endothelial dysfunction, failure of smooth muscle relaxation, and consequent hypertension (Engler and Engler, 2004; Fraga, *et al*., 2011). In this regard, we determined whether WUFCB, WFRCB and epicathchin modulated NO generation in endothelial cells. NO is a short-lived free radical that rapidly reacts with molecular oxygen to yield nitrogen dioxide, dinitrogen trioxide and nitrite. Nitrite is the only stable product. Nitrite levels in the culture medium were determined as an index of NO synthesis by using the Griess reagent (Chu *et al*., 2017). Incubation with samples for 18 h demonstrated that epicatechin had no significant effect on NO generation (Figure 4). Alternatively, treatment of endothelial cells with 300-μg mL^{-1} WUFCB resulted in 116.38% NO generation compared with the untreated cells (100%). In other words, WUFCB has the potency to increase NO generation in endothelial cells. This result is in agreement with previous reports (Engler and Engler, 2004) that demonstrated that polyphenol-rich cocoa could activate eNOS for synthesis NO, inhibit arginase and NADPH oxidase, leading to lower levels of O_2^{-}.; it

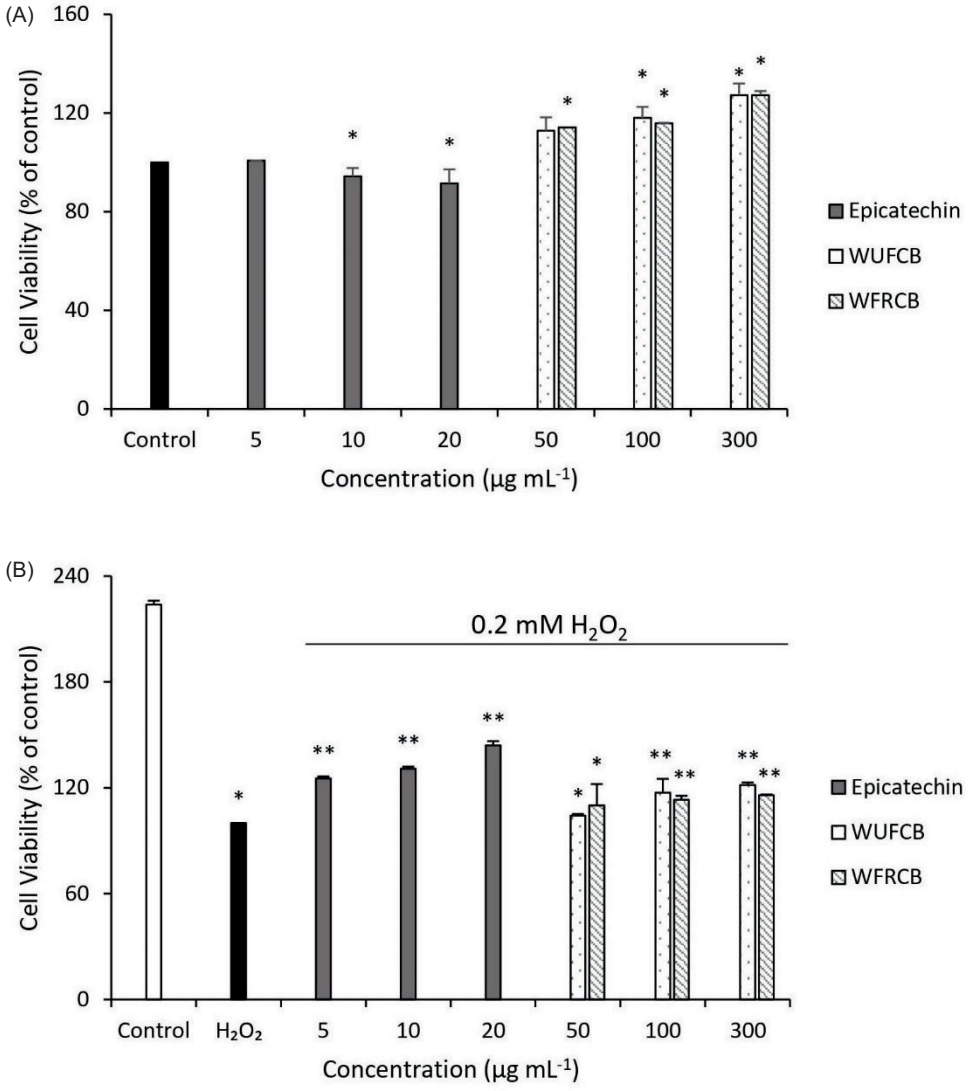

Figure 2. Cell viability relative to (A) untreated control and (B) damage of endothelial cells by 0.2-mM H_2O_2 following different concentrations of water extracts of unfermented cocoa beans (WUFCB), water extracts of fermented and roasted cocoa beans (WFRCB) and epicatechin, estimated with MTT assay. The data were indicated as mean ± SD. Different markers indicate significant differences ($p < 0.05$).

could also raise the level of NO (Giovanni *et al*., 2014). Moreover, tetramers and higher polymers of procyanidin were related to the activation of eNOS. According to the analysis of WUFCB using HPLC-DAD (data not shown), the content of tetramer and higher degree of polymerization (DP) procyanidins were abundant in WUFCB.

Conclusion

This study demonstrated the basis for the exploitation of polyphenolic compounds extracted from Taiwan cocoa beans. The results provided profiles of polyphenol compounds of WFRCB compared to WUFCB. WUFCB is rich in catechins compounds; additionally, WUFCB exerts a marked vascular protective activity in endothelial cells induced by H_2O_2 that could be attributed to the higher levels of polyphenols, such as epicatechin, catechin, EGC, EGCG and other compounds, present in WUFCB. These exert their protective action against oxidative stress through scavenging ROS, and modulate NO generation. Therefore, WUFCB has a great potential for preventing endothelial dysfunction and related complications.

Declaration of Interest

The authors declared no conflicts of interest.

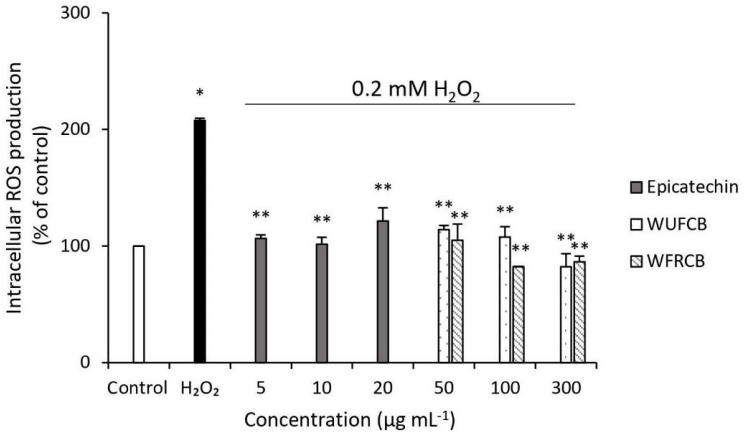

Figure 3. Effect of water extracts of unfermented cocoa beans (WUFCB), water extracts of fermented and roasted cocoa beans (WFRCB) and epicatechin on intercellular ROS formation in endothelial cells induced by 0.2-mM H_2O_2. ROS formation is relative to untreated control of endothelial cells and those treated with different concentrations. The data were indicated as mean ± SD. Different markers indicate significant differences ($p < 0.05$).

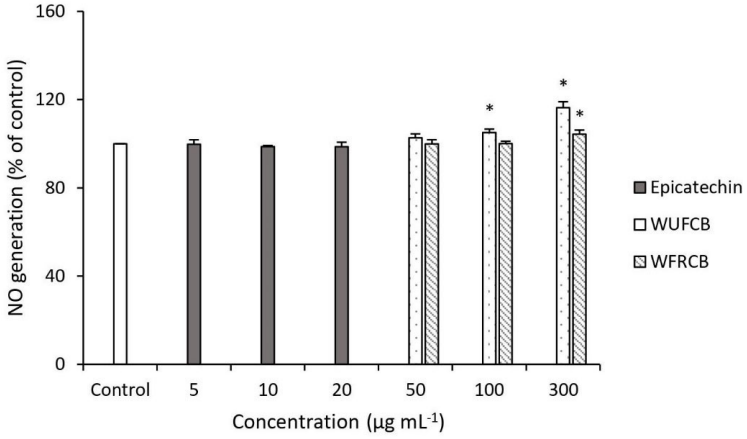

Figure 4. Effect of water extracts of unfermented cocoa beans (WUFCB), water extracts of fermented and roasted cocoa beans (WFRCB) and epicatechin on intercellular NO production in endothelial cell. NO production is relative to untreated control of endothelial cells and those treated with different concentrations. The data were indicated as mean ± SD. Different markers indicate significant differences ($p < 0.05$).

Acknowledgments

This work was funded by the Ministry of Science and Technology of the Republic of China [MOST 108-2221-E-041-001].

Contribution of Authors

Ying-Chun Lin designed the study and Heuy-Ling Chu supervised data collection. Hong-Xuan Fu and En-Kuang Chou analyzed the data. Heuy-Ling Chu and Ying-Chun Lin interpreted the data and reviewed the manuscript for publication. All authors approved the final manuscript.

References

Buijsse B., Weikert C., Drogan D., and Bergmann M. 2010. Chocolate consumption in relation to blood pressure and risk of cardiovascular disease in German adults. Eur Heart J. 31(13):1616–1623. https://doi.org/10.1093/eurheartj/ehq068

Carmen L.D.T.S., Francisco R.F., Francisco J.C.M., Josue' J., Sau'l R.C., Francisco J.W.C., Jesu's B.F., Daniela D.C., Carlos G.B.U., Jose' A.T.H. 2021. Recovery of phytochemical from three safflower (*Carthamus tinctorius* L.) by-products: antioxidant properties, protective effect of human erythrocytes and profile by UPLC-DAD-MS. J Food Process Preserv. *45*(9):e15765. http://doi.org/10.1111/jfpp.15765

Chu C.C., Wu W.S., Shieh J.P., Chu H.L., Lee C.P., and Duh P.D. 2017. The anti-inflammatory and vasodilating effects of three

selected dietary organic sulfur compounds from allium species. J Funct Biomat. 8(1):5. https://doi.org/10.3390/jfb8010005

Engler M.B. and Engler M.M. 2004. The vasculoprotective effects of flavonoid-rich cocoa and chocolate. Nutr Res. 24(9):695–706. https://doi.org/10.1016/j.nutres.2004.05.001

Febrianto N.A. and Zhu F. 2020. Changes in the composition of methylxanthines, polyphenols, and volatiles and sensory profiles of cocoa beans from the Sul 1 genotype affected by fermentation. J Agric Food Chem. *68*(32):8658–8675. https://doi.org/10.1021/acs.jafc.0c02909

Fraga C.G., Litterio M.C., Prince P.D., Calabró V., Piotrkowski B., and Galleano M. 2011. Cocoa flavanols: effects on vascular nitric oxide and blood pressure. J Clin Biochem Nutr. 48(1):63–67. https://doi.org/10.3164/jcbn.11–010FR

Giovanni S., Sergio D., Laura D.R., Antonino De L., Hector H.O., Giuseppe M., Arrigo F.C., and Salvador G. 2014. Cocoa bioactive compounds: significance and potential for the maintenance of skin health. Nutrients. 6(8):3202–3213. https://doi.org/4145303/pdf/nutrients-06-03202

Guillermo S., Mosca S., Cienfuegos-Jovellanos E., Pasamar M.A., Muguerza B., Ramón D. and Ríos J.L. 2010. Antioxidant properties of polyphenol-rich cocoa products industrially processed. Food Res Int. 43:20101614. https://doi.org/10.1016/j.foodres.2010.04.032

Heiss C., Keen C.L., and Keml M. 2010. Flavanols and cardiovascular disease prevention. Eur Heart J. 31(21):2583–2592. https://doi.org/10.1093/eurheartj/ehq332

International Cocoa Organization (ICCO). 2020, Dec 02. The Quarterly Bulletin of Cocoa Statistics, Vol. XLVI, No. 4, Cocoa year 2019/2020. The International Cocoa Organization, Abidjan, Ivory Coast. Available at: https://www.icco.org/november-2020-quarterly-bulletin-of-cocoa-statistics/

Letricia B.P., Simona B., Ilario F., Olga R.P., and Giuseppe Z. 2021. Characterization and classification of cocoa bean shells from different regions of Venezuela using HPLC-PDA-MS/MS and spectrophotometric techniques coupled to chemometric analysis. Foods. 10:1791. https://doi.org/10.3390/foods10081791

Magrone T., Russo M.A., and Jirillo E. 2017. Cocoa and dark chocolate polyphenols: from biology to clinical applications. Front Immunol. 9(8):677. https://doi.org/10.3389/fimmu.2017.00677

Mellinas, A.C., Jimenez, A. and Garrigós, M.C. 2020. Optimization of microwave-assisted extraction of cocoa bean shell waste and evaluation of its antioxidant, physicochemical and functional properties. LWT-Food Science and Technology. 127:1–13. https://doi.org/10.1016/j.lwt.2020.109361

Monagas M., Khan N., Andres-Lacueva C., Casas R., Urpí-Sardà M., and Llorach, R. 2009. Effect of coca powder on the modulation of inflammatory biomarkers in patients at high risk of cardiovascular disease. Am J Clin Nutr. 90:1144–1150. https://doi.org/10.3945/ajcn.2009.27716

Noelia D.M., Mónica C. S., Gonzalo S.M., Dolores R.P., and Pilar M. 2021. Cytotoxicity study of bakery product melanoidins on intestinal and endothelial cell lines. Food Chem. 343:128405. https://doi.org/10.1016/j.foodchem.2020.128405

Olga R.P., Letricia B.P., Giuseppe Z. and Caroline, S. 2020. Cocoa bean shell—a by-product with nutritional properties and biofunctional potential. Nutrients. 12(4):1123. https://.doi.org/10.3390%2Fnu12041123

Oteiza P.I., Fraga C.G., and Galleano M. 2021. Linking biomarkers of oxidative stress and disease with flavonoid consumption: from experimental models to humans. Redox Biol. 42:101914. https://doi.org/10.1016/j.redox.2021.101914

Pedan V., Weber C., Do T., Fischer N., Reich E., and Rohn S. 2018. HPTLC fingerprint profile analysis of cocoa proanthocyanidins depending on origin and genotype. Food Chem. 267:277–287. https://doi.org/10.1016/j.foodchem.2017.08.109

Puell M.C. and de Pascual-Teres S. 2021. The acute effect of cocoa and red-berries on visual acuity and cone-mediated dark adaptation in healthy eyes. J Funct Foods. 81:104435. https://doi.org/10.1016/j.jff.2021.104435

Quiroz-Reyes C.N. and Fogliano V. 2018. Design cocoa processing towards healthy cocoa products: the role of phenolics and melanoidins. J Funct Foods. 45:480–490. https://doi.org/10.1016/j.jff.2018.04.031

Zhang Y. N., Yin J.F., Chen J.X., Wang F., Du Q.Z., Jiang Y.W., and Xu Y.Q. 2016. Improving the sweet after-taste of green tea infusion with tannase. Food Chem. 192:470–476. https://doi.org/10.1016/j.foodchem.2015.07.046

Italian Journal of Food Science, 2022; 34 (1): 124–131

Effects of different concentrations of pineapple core extract and maceration process on free-range chicken meat quality

Norhayati Hussain[1,2*], Choy Hew Weng[1], Nursabrina Munawar[1,3]

[1]*Department of Food Technology, Faculty of Food Science and Technology, Universiti Putra Malaysia, 43000, Serdang, Selangor, Malaysia;* [2]*Halal Products Research Institute, Putra Infoport, 43400 UPM Serdang, Selangor, Malaysia;* [3]*Alliance of Research and Innovation for Food (ARIF), Universiti Teknologi MARA, Cawangan Negeri Sembilan, Kampus Kuala Pilah, 72000 Kuala Pilah, Negeri Sembilan, Malaysia*

***Corresponding Author:** Hussain N, Department of Food Technology, Faculty of Food Science and Technology, Universiti Putra Malaysia, 43000, Serdang, Selangor, Malaysia. Email: aryatihussain@upm.edu.my

Received: 10 June 2021; Accepted: 18 October 2021; Published: 26 February 2022

PAPER

Abstract

The tenderisation effects of pineapple (Josephine variety) core extracts on the quality of free-range chicken meat using different maceration concentrations (30%, 50%, and 100%) and duration (15, 25, and 35 min) were analysed. Texture profile analysis, colour, pH, bromelain content, and microbiological analyses of the macerated meat samples were assessed. Broiler breast meat macerated with core extract (100%, 35 min) showed 86% reduction in hardness and the pH decreased from 5.87 to 4.99. The pineapple core extract has great potential as a meat tenderiser thus reduces the agriculture by-product and converts it into natural food ingredients.

Keywords: bromelain content; broiler breast; maceration; meat quality; pineapple core extract; tenderisation process

Introduction

Increased export capacity and processing of pineapple are estimated to reach RM320 billion. In Malaysia, the pineapple plantation covering 13,433 hectares of farmland with a yield of about 32.37 tonnes of pineapple per hectare produce a total volume of 434,811 metric tonnes (Nor Mazila, 2020). This mass production generates a substantial by-product consisting of residual pulp, leaf, stem, peels, cores, crowns high in sugar, pectin (insoluble fibre), crude fibre, and proteins. The increasing volume of waste is detrimental to health because pineapple waste takes quite a long time to degrade and attract pests, leading to an increased risk of various dangerous diseases. Thus, there is a need to convert this core into a value-added commodity. It consists of a sizeable amount of antioxidant property, sugar, fibre, vitamin C, protein, phenolic compound, carotenoids, and flavonoids (Hanafi and Abdullah, 2008). Pineapple core waste contains a high amount of bromelain enzyme, widely used in the food industry for tenderising meat (Janhvi *et al*., 2016), chill proofing beer (Ketnawa and Rawdkuen, 2011), leather tanning process, in latex manufacturing (Christner *et al*.,1992), skincare products (Frank and Schulze, 2010), and pharmaceuticals (Bhattacharyya, 2008).

Bromelain acts on meat by breaking down the collagen fibres and shows hydrolytic activity on the connective tissue, leading to the tenderisation of meat. The bromelain action on meat is affected by various factors such as pH, water-holding capacity, moisture content, and concentration (Janhvi *et al*., 2016). A method to tenderise the tough meat is essential to increase its acceptability. According to Gok and Bor (2016), the typical way to tenderise meat is by the maceration technique. The maceration time may vary according to the type of marinade used to over-tenderise the meat surface, leading to undesirable "mushy" meat (Han *et al*., 2009).

ISSN 1120-1770 online, DOI 10.15586/ijfs.v34i1.2086

Therefore, this study aims to determine the effect of using different concentration core extracts and maceration durations on free-range chicken meat quality. According to the United States Department of Agriculture (USDA), free-range-chicken means that the chicken has full access and freedom to roam outdoors, outside of their pens, at any given time. The pineapple core by product of Josephine in this study could be considered as a potential meat tenderiser for a broiler chicken quality, commonly associated with tough and rigid texture among local people.

Materials and Methods

Preparation of pineapple core extract

Josephine pineapple was purchased from the New Seng Kee (NSK) hypermarket located at Jalan Peel, Kuala Lumpur, Malaysia. The basis of selection was the size (1.2–1.5 kg), firmness (C3 maturation stage), and skin colour (yellow/orange on two thirds), with no secretion from the skin. These parameters were measured visually using the naked eye (Yuris and Lee, 2014). The pineapples were washed thoroughly using tap water, cored, and then weighed (Mettler Toledo, US). The pineapples' cores were extracted out and subjected to the juicing process using a juicer (Panasonic, Malaysia), filtered using muslin cloth with a mesh size of 2 mm, and stored in a sterile bottle. The yield after the extraction of 20 cores was about 1000 mL of extract. The extracted juice was kept at 4°C before the maceration treatment.

Proximate analysis, pH, and total soluble solid analysis of pineapple juice core extract

Following proximate analysis, ash, moisture content, and crude fibre were determined by using the standard AOAC Method 2006. The pH value was recorded using a digital pH meter (PT-15, Sartorius, Germany). Total soluble solids (TSS) in the core extract were determined using a handheld analog refractometer (0-32°) (Atago, Japan), and the results were expressed as per cent soluble solids (° Brix)

Bromelain content analysis

The enzyme activity of fresh pineapple core and macerated broiler breast meat was determined according to the casein digestion method and tyrosine standard (Edmund and Isaac, 2018). The assay mixture contained 5 mL of freshly prepared 1% casein, which was pre-warmed at 37°C, to be used as substrate and 1 mL of the freshly prepared solubilised bromelain was added in the mixture. The mixture was vortexed immediately and incubated at 37°C for 10 min. The reaction was stopped by the addition of 5 mL of 1% Trichloroacetic acid. The reaction mixture was filtered and the absorbance of the filtrate was measured at 280 nm using a spectrophotometer. Using tyrosine as a standard, concentrations of 50 µg/mL, 100 µg/mL, 150 µg/mL, 200 µg/mL, and 250 µg/mL were prepared, and their absorbance read at 280 nm. A standard curve of tyrosine absorbance (Y axis) against tyrosine concentration (X axis) was plotted, refer to equation (1):

$$\text{Activity(CDU / mL)} = \frac{\text{Et} - \text{Eb}}{\text{Es}} \text{Concentration of Standard L} - \text{tyrosine} \times \frac{\text{Vr}}{\text{tr}} \times \text{Df}, \quad (1)$$

where

CDU = casein digestion unit
Et = absorbance of enzyme sample
Df = dilution factor
Eb = absorbance of enzyme blank
Vr = reaction volume
Es = absorbance of standard l-tyrosine
tr = reaction time

Browning inhibition in pineapple core extract juice

A low browning inhibition value indicates a high level of browning in the core, as described by Kim *et al.* (2005) The absorbance was read at 420 nm for every 45 min using a UV-VIS Spectrophotometer (UV-1900, Shimadzu, Japan). The browning inhibition percentages were calculated using equation (2):

$$\text{Inhibition (\%)} = [(\text{AF}_{\text{blank}} - \text{AI}_{\text{blank}}) - (\text{AF}_{\text{sample}} - \text{AI}_{\text{sample}}) \times 100] / \text{A}_{\text{blank}}, \quad (2)$$

where

$\text{AF}_{\text{sample}}$ is the final absorption of the sample

AF_{blank} is the final absorption of the control

AI_{blank} is the initial absorption of the control

Maceration process for tenderisation effect in broiler breast meat

The broiler cuts from the breast part were selected and purchased from the local market in Pudu, Selangor, Malaysia. The breast meat was chosen, as it displays a firmer, more rigid, and thicker texture than the other

broiler chicken meat parts (Debora *et al*., 2017). The visible fats and connective tissue were removed before maceration. The maceration procedure of the meat was performed, as described by Bhaskar *et al*. (2007). Meats were manually cut into uniform size, approximately 2 × 2 × 2 cm before further analysis. The meat and pineapple core extract ratio was maintained as 1:1 (meat: marinade) (Gok and Bor, 2016). The broiler meat chunks were macerated in the core extract for 15, 25, and 35 min at three different concentrations: 100% (1:0), which contains 250 mL of the whole core extract/without dilution; 50% (1:1), which contains 125 mL of the core extract and 125 mL of distilled water; and 30% (1:2), which contains 75 mL of the core extract diluted with 175 mL of distilled water, respectively, to obtain the maximum effect of up to 250 mL of the total volume. Meat samples were macerated at room temperature (27 ± 3°C) and placed in a zip lock bag during the maceration process. Fresh meat samples macerated using distilled water was used as a control.

Texture profile analysis of macerated broiler breast meat

Texture profile analysis was carried out using the texture analyser (Stable Micro System, UK) with a flat-ended cylindrical probe. The test samples were compressed to 50% of their original height with the setting of 1.0 mm/s, 4.2 mm/s, and 5.0 mm/s for pre-set speed, test speed, and post-test speed, respectively. The textural parameters of the meat were hardness and chewiness (Nadzirah *et al*., 2016). All the analyses were performed in triplicate at room temperature of 27°C, and the mean and standard deviation (SD) were calculated.

Colour analysis

Colour measurement was done on the surface of the macerated meat samples by using Chroma Meter (CR-410, Konica Minolta, Japan). The illuminant D65 (representing typical daylight) was used during analysis. The L* (lightness), a* (redness), b* (yellowness) values of meat samples were measured and calculated. The average value of three meat samples for each maceration duration and concentration (triplicates) were used for statistical analysis (Nadzirah *et al*., 2016).

Microbiological analysis

The meat samples' microbial load after each maceration duration was measured using the Total Plate Count Method (AOAC 966.23). After solidifying the nutrient agar (Merk, Darmstadt, Germany), the plates were inverted and incubated for 48 h at 37°C. The entire colony-forming units (CFU) were counted, including those of pinpoint size. The parameter used to count the colonies: regular plates (25–250 counts), plates with more than 250 colonies for all dilutions (too many to count), and plates with less than 25 colonies for all dilutions (too low to count).

Statistical analysis

All results were expressed as the mean ± SD. The results obtained were analysed with a two-way ANOVA using Minitab version 17 statistical package to determine if there was any significant difference between maceration duration and concentration of the core extract with regard to meat quality. Turkey's method was used to determine which pair is significantly different from each other. Differences were significant when $P < 0.05$.

Results and Discussion

Pineapple core extract characteristics

The proximate analysis of pineapple core extract revealed the moisture content, ash content, protein content, crude fibre, pH, TSS, and enzyme properties (i.e., browning inhibition and bromelain activity) of the Josephine variety of pineapple core extract, as shown in Table 1.

The pH of macerated broiler breast meat

The pH values of the control and macerated meat samples are shown in Table 2. It can be observed that the pH value of the control meat samples was the highest compared to the treated meat samples. The treated meat samples showed a significant decrease in pH value for all concentrations when the maceration duration increased. However, the pH value significantly increased when the concentration of the core extract decreased. It can be suggested that the lowest pH in broiler breast meat

Table 1. Physicochemical properties of pineapple core extract.

Analysis	Josephine pineapple core extract value
Moisture content (%)	89.67 ± 0.24
Ash content (%)	0.75 ± 0.04
Protein content (%)	19.68 ± 0.09
Crude fibre (%)	1.74 ± 0.14
pH	3.83 ± 0.01
Total soluble solid (°Brix)	9.60 ± 0.00
Browning inhibition (%)	4.18 ± 0.25
Bromelain activity (CDU/mL)	152.01 ± 1.54

is influenced by the acidic pH (3.83 ± 0.01) of the core extract. These findings are similar to those of Mohamad Afifi *et al*. (2018), who reported that the lowest pH (5.61) of the beef cut sample is most likely due to the pH of the core extract and maceration time.

According to Ketnawa and Rawduken (2011), pineapple juice, which contains bromelain, will hydrolyse the muscle, thus releasing amino acid to reduce the meat's pH. These findings were supported by Manohar *et al*. (2016) who reported that an increase in the pineapple extract concentration decreases the treated boneless meat samples' pH, thus becoming more acidic. Maryana *et al*. (2018) reported that any pH range treatments from 4 to 5 could decrease meat texture's hardness. Any pH between the isoelectric point of myofibrillar protein reduced the capacity to bind water. Burke and Monahan (2003) also reported a significant reduction in pH from 5.7 to 3.1 of bovine muscle strips marinated with citrus juice compared to the untreated samples. Thus, the meat's acidity can be used as an indicator to detect the soft meat texture. The lower the pH value, the greater the meat tenderisation effect (Manohar *et al*., 2016). The broiler breast meat macerated in 100% concentration of Josephine pineapple core extract for 35 min had the lowest pH value and significant tenderness compared to other treatments.

Bromelain content of the macerated broiler breast meat

The bromelain activity of the diluted core extract and the macerated meat's bromelain activity are shown in Table 3. It can be observed that when the concentration of the core extract decreased from 100% to 30%, the bromelain activity also decreased from 151.06 CDU/mL to 56.87 GDU/mL. It can be suggested that the bromelain activity was affected by the percentage of the concentrated core extract. Pineapple core, which has been regarded as a significant waste from pineapple production, was reported to have more bromelain content than other residue parts (Banerjee *et al*., 2020). These findings agreed with the findings of this study where the higher the concentrations of the pineapple core extract in the macerated meat, the higher the bromelain activity. Hence, with the increased maceration duration, higher tenderisation affects the meat, as shown in Table 4. The bromelain intervention has been proven by its potential to disrupt the muscle microstructure and cause myofibril protein degradation (Bhat *et al*., 2018).

Table 2. pH value of macerated broiler breast meat at different concentrations and durations.

Treatments (%)	Maceration duration (min)		
	15 min	25 min	35 min
Control (DW)	5.87 ± 0.02^{Aa}	5.87 ± 0.02^{Aa}	5.87 ± 0.02^{Aa}
Josephine (30)	5.65 ± 0.01^{ABa}	5.50 ± 0.01^{Bb}	5.54 ± 0.01^{Bb}
Josephine (50)	5.33 ± 0.01^{Ba}	5.20 ± 0.02^{Cb}	5.12 ± 0.01^{Cc}
Josephine (100)	5.30 ± 0.01^{Ba}	5.16 ± 0.01^{Cb}	4.99 ± 0.01^{Dc}

Values are expressed as mean ± standard deviation (n = 3).
Mean with different superscript capital letters within column are significantly different (P < 0.05).
Mean with different superscript lower case letters within row are significantly different (P < 0.05).
Notes: 100%, 50%, and 30%, concentration of the core extract; DW, distilled water; 15, 25, and 35 min, maceration duration.

Texture profile analysis

Texture profile analysis measured hardness and chewiness properties in meat to reflect the effect of bromelain enzyme as a natural meat tenderiser. The macerated meat's hardness and chewiness had significantly reduced (P < 0.05) with the extract's increased duration and concentration (Table 4). The longer maceration duration in meat reduced the hardness (3766.50 to 1044.20 N) and chewiness (4012.95 to 726.65 N) of the macerated meat. These findings align with the study carried out by Ketnawa and Rawdkuen (2011). They reported that by increasing the concentration of the bromelain extracted from the pineapple peel, a continuous decrease of hardness was found in marinated beef, chicken, and squid samples. A previous study by Daniela *et al*. (2012) observed that an increase in the meat treatments' action time leads to a significant increase in rigidity index value, reflecting the degree of tenderness of the meat. Based on the results, chicken meat macerated with 100% Josephine pineapple core extract for 35 min was significantly (P < 0.05) softer in texture than chicken meat subjected to other treatment concentrations and maceration durations. It shows the lowest value of hardness and chewiness compared to the other treatments.

Ketnawa and Rawdkuen (2011) reported that the increase in treated meat's tenderness was due to proteolysis enzyme action on myofibrillar protein by bromelain. The myofibrillar protein breakdown generates small peptides or protein with low molecular weight, thus increasing the meat samples' tenderness. Bille and Taapopi (2008) also found that bromelain's action in denaturing the protein and breaking down the collagen, muscle fibre, and tissue resulted in increased meat tenderness in their study samples of goat meat (back, ribs, and rear limbs). The samples were marinated with bromelain extract powder and citric marinade to tenderise for 10 min at room temperature. Rawdkuen and Benjakul (2012) also reported that the enzymes increased the collagen solubility, and this

Table 3. Bromelain content of the diluted pineapple core extract, macerated broiler breast meat at different concentrations and durations.

Concentration (%)	Bromelain activity (CDU/mL)			
	Diluted pineapple extract	Maceration duration (min)		
		15 min	25 min	35 min
Control (DW)	NA	0.00 ± 0.00^{Aa}	0.00 ± 0.00^{Aa}	0.00 ± 0.00^{Aa}
Josephine (30)	56.87 ± 1.26^{A}	8.95 ± 0.01^{Ba}	12.93 ± 0.01^{Bb}	17.58 ± 0.01^{Bbc}
Josephine (50)	79.29 ± 1.01^{B}	12.28 ± 0.01^{Ca}	20.67 ± 0.02^{Cb}	29.49 ± 0.01^{Cc}
Josephine (100)	151.06 ± 1.11^{C}	18.30 ± 0.01^{Da}	26.47 ± 0.01^{Db}	39.19 ± 0.01^{Dc}

Values are expressed as mean ± standard deviation (n = 3).
Mean with different superscript capital letters within column are significantly different ($P < 0.05$).
Mean with different superscript lower case letters within row are significantly different ($P < 0.05$).
Notes: 100%, 50%, and 30%, concentration of the core extract; DW, distilled water; 15 , 25 , and 35 min, maceration duration; NA, not available.

promoted the structural alteration through the process of collagens cross-link.

Meat colour analysis

The control and treated meat samples' colour parameters for 15, 25, and 35 min are shown in Table 5 (L*, a*, and b*value). The results show that the maceration process significantly affected the L* and b* values of the broiler breast samples. The lightness (L*value) increased as the maceration duration increased but decreased when the core extract concentration decreased compared to the control. According to Kim *et al.* (2012), the meat colour influenced meat quality; hence, they were affected by marination.

The colour of the meat is related to muscle pigments, myoglobin, and haemoglobin. However, meat's discolouration is affected by pigment conditions (amount and chemical state). The entire breast muscle, commonly discoloured as breast muscle, comprises a large portion of the weight (~5%), so it is more sensitive, contributing to discolouration and the meat's light appearance.

Therefore, small changes in colour on the breast part is more noticeable than in other parts. Serdaroglu *et al.* (2007) reported that the increase in lightness is due to the swell of the muscle protein and light reflection altered at low pH and ionic strength, thus forming the lighter colour. According to Wismer-Pedersen (1959), it is widely accepted that variations in muscle structure may affect light reflectance or light scattering. The extent of denaturation of the muscle proteins differs in ordinary and pale coloured meat. The b*value decreased with increased maceration duration. However, when the concentration of the core extract decreased, the b*value increased. Meanwhile, the a*value of the control and treated meat samples shows no significant difference at all concentrations used during the first 15 min. A similar pattern of a*value was also reported by Serdaroglu *et al.* (2007) in which the turkey breast was marinated in grapefruit juice (50% and 100%) and citric acid (0.05 M, 0.1 M, and 0.2 M). The a*value (redness) is related to the concentration of myoglobin and myoglobin denaturation level (Francis and Clydesdale, 2008; Vaudagna *et al.*, 2008). The acid treatment appeared to enhance myoglobin's conversion to metmyoglobin, which results in lower colour intensity. Table 7 shows the colour difference (ΔE*) of macerated meat in different core extract concentrations at 15, 25, and 35 min. The highest colour difference was found in meat samples macerated in 100% concentration of Josephine core extracts for 35 min. According to Francis and Clydesdale (2008), when colour differences (ΔE*) exceed the value of 3, the meat's colour change is detectable to the human eye.

Microbiological analysis of the macerated broiler breast meat

According to Table 6, the total microbial count decreased as the maceration duration increased for all treatments. However, when the concentration of the core extract decreased, the total microbial count increased. In this study, the total microbial count was below 7 Log CFU/g after 35 min of maceration. In contrast, the highest microbial counts were observed as early as 15 min of maceration using 30% concentration of core extract (4.34 Log CFU/g) regardless of the control sample. According to Hong *et al.* (2013), this might be due to the sample's initial microbial contamination because bacterial counts in fresh meat are generally less than 3 Log CFU/g.

Jeong *et al.* (2018) also reported that citrus juice such as pineapple juice has an antimicrobial function, causes denaturation of microorganisms, and affects the water-holding capacity. The pH reduction caused by this

Table 4. Hardness and chewiness value of the macerated broiler breast meat at different concentrations and durations.

Treatments (%)	Texture profile analysis (TPA)					
	Hardness (*N*)			Chewiness (*N*)		
	15 min	25 min	35 min	15 min	25 min	35 min
Control (DW)	7292.30 ± 99.48^{Aa}	7292.30 ± 99.48^{Aa}	7292.30 ± 99.48^{Aa}	4012.95 ± 96.75^{Aa}	4012.95 ± 96.75^{Aa}	4012.95 ± 96.75^{Aa}
Josephine (30)	3766.50 ± 84.40^{Ba}	2755.60 ± 104.47^{Bb}	2741.80 ± 91.78^{Bb}	1711.87 ± 103.79^{Ba}	1281.10 ± 85.94^{Bb}	800.15 ± 96.87^{Bc}
Josephine (50)	2552.40 ± 92.25^{Ca}	2272.40 ± 91.97^{Cb}	1707.90 ± 85.78^{Cc}	1594.06 ± 87.25^{Ca}	1146.83 ± 101.79^{Cb}	733.46 ± 97.18^{BCc}
Josephine (100)	2224.90 ± 94.57^{Da}	1806.10 ± 89.05^{Db}	1044.20 ± 106.95^{Dc}	1107.22 ± 87.79^{Da}	1074.90 ± 91.82^{CDab}	726.65 ± 94.85^{Cb}

Values are expressed as mean ± standard deviation (n = 3).
Mean with different superscript capital letters within column are significantly different (P < 0.05).
Mean with different superscript lower case letters within the row are significantly different (P < 0.05).
Notes: 100%, 50%, and 30%, concentration of the core extract; DW, distilled water; 15, 25 and 35 min, maceration duration.

Table 5. Colour (L*, a*, b*value) of macerated broiler breast meat at different concentrations and durations.

Treatments (%)	Colour Analysis								
	L*value (lightness)			a*value (redness)			b*value (yellowness)		
	15 min	25 min	35 min	15 min	25 min	35 min	15 min	25 min	35 min
Control (DW)	40.49 ± 0.40^{Aa}	40.49 ± 0.40^{Aa}	40.49 ± 0.40^{Aa}	8.08 ± 0.30^{Aa}	8.08 ± 0.30^{Aa}	8.08 ± 0.30^{Aa}	12.59 ± 0.25^{Aa}	12.59 ± 0.25^{Aa}	12.59 ± 0.25^{Aa}
Josephine (30)	43.44 ± 0.35^{Aa}	50.61 ± 0.94^{Bb}	51.98 ± 0.49^{Bbc}	8.05 ± 0.17^{Aa}	8.01 ± 0.09^{Aa}	7.95 ± 0.30^{Bb}	12.47 ± 0.11^{Aa}	11.73 ± 0.42^{Ba}	11.64 ± 0.17^{Bb}
Josephine (50)	46.67 ± 0.81^{Ba}	52.60 ± 0.30^{Cb}	55.11 ± 0.28^{Cbc}	8.05 ± 0.04^{Aa}	7.31 ± 0.08^{Bb}	7.25 ± 0.12^{Cb}	12.31 ± 0.15^{Aa}	11.52 ± 0.07^{Bab}	10.87 ± 0.24^{Cb}
Josephine (100)	50.01 ± 0.73^{Ca}	54.99 ± 0.41^{Db}	58.35 ± 0.25^{Dc}	7.32 ± 0.08^{Ba}	6.75 ± 0.16^{Cb}	6.64 ± 0.07^{Dc}	12.05 ± 0.51^{Ba}	11.52 ± 0.31^{Bab}	10.33 ± 0.32^{CDb}

Values are expressed as mean ± standard deviation (n = 3). Mean with different superscript capital letters within column and superscript lower case letters within row are significantly different (P < 0.05).

Table 6. Total microbial count of macerated broiler breast meat at different concentrations and durations.

Concentration (%)	Microbiological load (total microbial count log CFU/g)		
	maceration duration (min)		
	15 min	25 min	35 min
Control (DW)	4.35 ± 0.03	4.35 ± 0.03	4.35 ± 0.03
Josephine (30)	4.34 ± 0.06	4.18 ± 0.02	4.10 ± 0.02
Josephine (50)	4.26 ± 0.04	4.16 ± 0.03	4.03 ± 0.05
Josephine (100)	4.07 ± 0.02	4.03 ± 0.06	3.98 ± 0.03

Values are expressed as mean ± standard deviation (n = 3).
Notes: 100%, 50%, and 30%, concentration of the core extract; DW, distilled water; 15, 25 and 35 min, maceration duration.

citrus extract was the primary factor that affected the reduction of microorganisms. According to Alvarado and Mckee (2017), most microorganisms slowed their growth in an acidic environment. This statement is also supported by Kotzekidou *et al*. (2008), which stated that pineapple extract could suppress the growth of Escherichia coli O157:H7 EDL-933. The pineapple extract contains active substances such as terpenoids and phenolic compounds, and these compounds attach to the bacterial membrane and deplete the metabolic energy of bacteria. Our study found that samples macerated in 100% concentration of the core extract for 35 min had the lowest microbial count (3.98 Log CFU/g).

Conclusions

The maceration technique using 100% concentration of the core extract (Josephine variety) for 35 min shows the most significant meat tenderisation effect compared to other concentrations and durations used in this study. The hardness and chewiness of the broiler breast meat were reduced. Pineapple core extract is applicable as a meat tenderiser in the food industry, which may increase the demand for local pineapple core.

Acknowledgements

The authors would like to thank the faculty and the personnel of Food Science and Technology, Universiti Putra Malaysia (UPM), for their assistance in completing the study.

Author Contributions Statement

C.H.W. conducted the experiment, C.H.W. and N. H. analysed the findings, and C.H.W., N. H., and N. S.M. wrote and edited the manuscript.

Additional information

The authors declare no conflict of interest.

References

Abdullah & Hanafi, M. (2008). Characterization of Solid Waste and Liquid Pineapple Waste. Reaktor, 12(1), 48–52.

Alvarado, C. and McKee, S., 2017. Marination to improve functional properties and safety of poultry meat. Journal of Applied Poultry Research 16(1): 113. https://doi.org/10.1093/japr/16.1.113

AOAC, 2006. Official methods of analysis. 20th ed. Arlington, TX: The Association of the Official Analytical Chemist.

Banerjee, S., Arora, A., Vijayaraghavan, R. and Patti, A.F., 2020. Extraction and crosslinking of bromelain aggregates for improved stability and reusability from pineapple processing waste. International Journal of Biological Macromolecules 158: 318. https://doi.org/10.1016/j.ijbiomac.2020.04.220

Bhaskar, N., Sachindra, N., Modi, V., Sakhare, P. and Mahendrakar, N., 2006. Preparation of proteolytic activity rich ginger powder and evaluation of its tenderising effect on spent-hen muscles. Journal of Muscle Foods 17: 174. https://doi.org/10.1111/j.1745-4573.2006.00043.x

Bhat, Z.F., Morton, J.D., Mason, S.L. and Bekhit, A.E.D.A., 2018. Applied and emerging methods for meat tenderisation: a comparative perspective. Comprehensive Reviews in Food Science and Food Safety 17(4): 841. https://doi.org/10.1111/1541-4337.12356

Bhattacharyya, B.K., 2008. Bromelain: an overview. Natural Product Radiance 7: 359.

Bille, P.G. and Taapopi, M.S., 2008. Effects of two commercial meat tenderisers on different cuts of goat's meat In Namibia. African Journal of Food Agriculture Nutrition and Development 8(4): 417. https://doi.org/10.4314/ajfand.v8i4.19202

Burke, R.M. and Monahan, F.J., 2003. The tenderisation of shin beef using a citrus juice marinade. Meat Science 63: 161. https://doi.org/10.1016/S0309-1740(02)00062-1

Christner, J., Pfleiderer, E., Taeger, T. and Bernschein, U., 1992. Methods for leather processing including liquid enzyme formulation. US Patent No. 5,102,422.

Daniela, I., Camelia, V., Felicia, D. and Rodica, D., 2012. Effect of marination with proteolytic enzyme on quality of beef muscle. Scientific Study and Research 13(1): 81.

Debora, C.F.D.S., Alex, M.V.D.A. and Alex, A.G., 2017. Quality characteristics of broiler chicken meat from free-range and industrial poultry system for the consumers. Journal Food Science Technology 54(7): 1818. https://doi.org/10.1007/s13197-017-2612-x

Edmund, O.B. and Isaac, W.O., 2018. Bromelain activity of waste parts of two pineapple varieties. Journal of Sustainable Food Production 2: 21. https://doi.org/10.18052/www.scipress.com/SFP.2.21

Francis, F.J. and Clydesdale, F.M., 1975. Food colorimetry: theory and applications. Westport, CT: AVI Publishing.

Frank, N.J.E. and Schulze, R., 2010. Protease for wound conditioning and skin care. European Patent No. EP 2226382. Munich, Germany: European Patent Office.

Gok, V. and Bor, Y., 2016. Effect of marination with fruit and vegetable juice on the some quality characteristics of Turkey breast meat. Brazilian Journal of Poultry Science 18(3): 481. https://doi.org/10.1590/1806-9061-2016-0225

Han, J., Morton, J.D., Bekhit, A.E.D. and Sedcole, J.R., 2009. Pre-rigor infusion with kiwifruit juice improves lamb tenderness. Meat Science 82: 324. https://doi.org/10.1016/j.meatsci.2009.02.003

Hong, K.W., Kim, S.H., Park, W.P., Lee, J.H., Jo, Y.B. and Lee, J.H., 2013. Food hygienics. Seoul, Korea: Dae Wang Press.

Janhvi, M., Gayathri, R., & Vishnupriya, V. (2016). Tenderization of Meat Using Bromelain from Pineapple Extract. Institute. Journal. Phramaceutical. Science. Review. Reources, 39(1), 81–85.

Jeong, K.J., Hyeonbin, O., So, Y.S. and Young, S.K., 2018. Effect of different marination condition on quality, microbiology properties, and sensory characteristic of Pork Ham Cooked By The Sous-vide Method. Korean Journal for Food Science of Animal Resource 38(3): 506.

Ketnawa, S. and Rawdkuen, S., 2011. Application of bromelain extract for muscle foods tenderisation. Food Nutrition Sciences 2: 393. https://doi.org/10.4236/fns.2011.25055

Kim, D.J., Lee, D.H., Lee, Y.G., Park, D.W., Kim, G.D., Jung, E.Y., et al., 2012. The relationship between carcass ColorGrade and instrumental values. Journal of Agriculture Life Scienc 46: 133.

Kim, M.J., Kim, C.Y., & Park, I. (2005). Prevention of Enzymatic Browning of Pear by Onion Extract. Food Chemistry, 89(2), 181–184.

Kotzekidou, P., Giannakidis, P. and Boulamatsis, A., 2008. Antimicrobial activity of some plant extracts and essential oils against Foodborne pathogens in vitro and on the fate of inoculated pathogens in chocolate. LWT-Food Science Technology 41: 119. https://doi.org/10.1016/j.lwt.2007.01.016

Manohar, J., Gayathri, R. and Vishnupriya, V., 2016. Tenderisation of meat using bromelain from pineapple extract. International Journal of Pharmaceutical Science Review and Research 39(17): 81.

Maryana, M.N., Lukman, I., Siti, N.H. and Ikhmal, H.A.H., 2018. Evaluation of tendering effect from date seed extract (*P. dactalytera*) in Knuckle part meat. Journal of Tropical Resource and Sustainable Science 6: 23. https://doi.org/10.47253/jtrss.v6i1.722

Mohamad Afifi, I., Chong, G.H., & Mohammad Rashedi, I.F. (2018). Potential Effect of *Averrhoa bilimbi* (belimbing buluh) Marinades on Tenderizing the Buffalo Meat Compared to *Actinidia chinenesis* (kiwifruit), *Citrus limon* (lemon) and Commercial Bromelain. Journal of Science and Technology, 10(2), 77–84.

Nadzirah, K.Z., Zainal, S., Noriham, A. and Normah, I., 2016. Application of bromelain powder produced from pineapple crowns in tenderising beef round cuts. International Food Research Journal 23(4): 1590.

Nor Mazila, A.R., 2020. Pineapple waste commercialisation. UMP News. Available from: http://news.ump.edu.my/experts/pineapple-waste-commercialisation. Accessed 26 October 2020.

Rawdkuen, S. and Benjakul, S., 2012. Biochemical and microstructural characteristics of meat samples treated with different plant proteases. African Journal of Biotechnology 11(76): 14088. https://doi.org/10.5897/AJB12.1587

Serdaroglu, M., Abdraimov, K. and Onenc, A., 2007. The effects of marinating with citric acid solutions and grapefruit juice on cooking and eating quality of Turkey breast. Journal of Muscle Foods. 18: 162. https://doi.org/10.1111/j.1745-4573.2007.00074.x

Vaudagna, S.R., Pazos, A.A., Guidi, S.M., Sanchez, G., Carp, D.J. and Gonzalez, C.B., 2008. Effect of salt addition on sous vide cooked whole beef muscles from Argentina. Meat Science 79: 470. https://doi.org/10.1016/j.meatsci.2007.11.001

Wismer-Pedersen, J., 1959. Quality of pork in relation to rate of pH change post mortem. Food Resource 24: 711. https://doi.org/10.1111/j.1365-2621.1959.tb17325.x

Yuris, A. and Lee, F.S., 2014. A comparative study of the antioxidant properties of three pineapple (*Ananas comosus* L.) varieties. Journal of Food Studies 3: 1–11. https://doi.org/10.5296/jfs.v3i1.4995

Italian Journal of Food Science, 2022; 34 (1): 132–139

Two cases of black human breast milk not related to minocycline. A sphingolipidomic approach

Laura Cerquiglini[1], Stefania Troiani[1], Chiara Gizzi[1], Michele Dei Cas[2], Rita Paroni[2], Paola Signorelli[2], Antonella Mencacci[3], Maurizio Radicioni[1], Stefano Pasquino[4], Maria Cristina De Lio[5], Lina Cossignani[6], Giuseppa Verducci[6], Carmela Conte[6], Tommaso Beccari[6],Samuela Cataldi,[6] Elisabetta Albi[6]*

[1]Struttura Complessa di Neonatologia e Terapia Intensiva Neonatale, Azienda Ospedaliera di Perugia – Santa Maria della Misericordia, Perugia, Italy; [2]Department of Health Sciences, Università degli Studi di Milano, Milan, Italy; [3]Medical Microbiology, Department of Medicine and Surgery, University of Perugia, Perugia, Italy; [4]Department of Cardiac Surgery, Azienda Ospedaliera di Perugia – Santa Maria della Misericordia, Perugia, Italy; [5]Igiene e Organizzazione dei Servizi Ospedalieri, Azienda Ospedaliera di Perugia – Santa Maria della Misericordia, Perugia, Italy; [6]Department of Pharmaceutical Sciences, University of Perugia, Perugia, Italy

***Corresponding Author:** Elisabetta Albi, Department of Pharmaceutical Sciences, University of Perugia, Perugia 06126, Italy. Email: elisabetta.albi@unipg.it

Received: 19 January 2022; Accepted: 13 February 2022; Published: 4 March 2022

OPINION PAPER

Abstract

Different colors of human breast milk (HBM) are reported in literature, and black milk is produced only during minocycline therapy. We herein report two cases of black/dark gray color HBM without minocycline involvement. We analyzed both milk samples and compared the data with two control HBM samples taken from two mothers who had the same dietary behaviors and took the same supplements (iron) as done by the mothers under study. Results indicated that the black color was not due to iron intake, disease or infection. With Sudan III stain, specific for lipids, dark precipitates were evident. Antioxidant power was much higher in studied milk samples than in control samples. As antioxidants at high levels become pro-oxidants, our data suggested possible lipid oxidation. Sphingolipid profile of black milk samples demonstrated accumulation of sphingomyelin and ceramide, which could be a sign of impaired lipid metabolism. It was concluded that iron supplementation was not responsible for HBM pigmentation, but altered biochemical mechanisms in the mammary gland could be implicated. In our experience, dark color HBM did not represent an absolute indication for discontinuation of breastfeeding.

Keywords: black milk, breast milk, ceramide, fatty acids, human milk, sphingomyelin

Introduction

Human breast milk (HBM) is universally recognized as the preferred source of neonatal nutrition. It is an extremely complex biological fluid. Some components vary with the maternal diet, while others are independent of this and depend on metabolic activity of the mammary gland (Dei Cas *et al.*, 2020). Thus, breast milk is species-specific and reflects the requirement of infants (Tripaldi *et al.,* 2021). In fact, HBM protects infants from diseases as they wait for their immune systems to mature (Hanson and Korotkova, 2002), from dysfunctional lipid metabolism and gut dysbiosis (Norris *et al.*, 2019). Moreover, HBM has good antioxidant properties (Codini *et al.*, 2020) and it is essential for the cognitive maturation (Skinner and Narchi, 2021).

Throughout lactation, HBM undergoes a gradual biochemical modification in lipid and protein concentration so that the milk is commonly classified into colostrum,

ISSN 1120-1770 online, DOI 10.15586/ijfs.v34i1.2173

transitional milk and mature milk (Jenness, 1979). Colostrum, the first milk produced after parturition, is rich in proteins and growth factors and has high concentrations of secretory immunoglobulin, thus indicating its immunological function (Castellote *et al.*, 2011). Transitional milk is produced around the third–fifth day after childbirth until 20 days–1 month of child birth. After this, mature milk is produced and it lasts for the duration of breastfeeding. Transitional milk has high contents of fat and carbohydrates and is low in minerals and proteins. Mature milk is truly abundant in fats and carbohydrates and has an optimal protein and minerals intake in relation to the increased nutritional needs of the newborn (Riordan and Wambach, 2014).

The color of HBM changes with lactation. If sometimes, the colostrum appears clear, thin and watery, at other times it is often yellow or orange, thanks to the presence of high levels of beta-carotene (Patton *et al.*, 1990). Transitional milk typically changes from yellow to white, and mature milk is first clear or bluish and afterwards white or yellow in color (Riordan and Wambach, 2014).

Milk color may vary physiologically depending on diet, nutritional supplements and medications. HBM can appear pink, red and orange with fruit drinks or green with green color beverages, green vegetables, vitamins or mineral supplements in diet (Yazgan *et al.*, 2012) or intake of blue-green algae (Naor *et al.*, 2019). However, the color of HBM may change for different reasons, as pink color is described in colonization of *Serratia marcescens* (Ayuzo del Valle and Treviño Salinas, 2014; Jones *et al.*, 2014; Quinn *et al.*, 2018). Moreover, green color is reported after administration of propofol (Birkholz *et al.*, 2009; Rainone *et al.*, 2018). However, black HBM is reported only in relation to minocycline therapy (Basler, *et al.*, 1985; Hunt *et al.*, 1996; Lawrence, 1985).

Although different observations have been reported on the colors of HBM, possible modifications in lipid components have not been studied yet. Since the sphingomyelin (SM) present in breast milk is important for the maturation of child's nervous system (Jiang *et al.*, 2021), we particularly focused on sphingolipidomic study.

We report two cases of black HBM produced during early lactation by two mothers not under antibiotic therapy but both taking iron for anemia. Iron intake and breastfeeding were discontinued. Milk color in both cases turned white within a few days of iron discontinuation and mothers restarted breastfeeding without any incident. As a control (CRT), two clear/white milk samples from two mothers on iron supplementation were examined. We investigated and reported microbiological, cytological and biochemical aspects of both samples.

Materials and Methods

Population and sample collection procedure

BLUD in Perugia, Italy (Banca del Latte Umano Donato, Struttura Complessa di Neonatologia e Terapia Intensiva Neonatale—Azienda Ospedaliera Santa Maria della Misericordia—Perugia, Italy) provided human milk samples. Two black milk samples under investigation and two CRT white milk samples collected from healthy iron-supplemented mothers were examined for the study. All procedures were performed according to the indications of Bioethics Committee, and the women signed informed consent. Mothers were invited to answer questions about: (1) age; (2) cigarette use; (3) use of medical products containing nicotine; (4) alcohol use; (5) use of restrictive or specific diets; and (6) medical therapy. Immediately after harvesting, milk sample was kept for microbiological analysis and the remaining amount was submitted for Holder pasteurization (HoP) by heating it to 62.5°C (145°F) for 30 min, and then cooling it back to 4–10°C; it is a globally used method to ensure distribution of microbiologically safe milk to infants (Codini *et al.*, 2020). After pasteurization, microbiological analysis was performed again and the milk samples were stored at –20°C in a freezer before analysis.

Materials

Anhydrous sodium sulfate, chloroform, hexane, methanol and potassium hydroxide were purchased from Carlo Erba Reagents (Milan, Italy). Sudan III, codex S-4131, was obtained from Sigma Chemical Co. (St. Louis, MO, USA). Supelco™ 37-component fatty acid methyl esters (FAME) mix, containing methyl esters of 37 fatty acids, was supplied by Supelco (Bellefonte, PA, USA). Lipids standards were purchased from Avanti Polar Lipids (Alabaster, AL, USA). Chemicals, all analytical grade, were purchased from Sigma-Aldrich (St. Louis, MO, USA). All aqueous solutions were prepared using purified water of Milli-Q grade (Burlington, MA, USA).

Microbiological analysis

Milk samples were collected aseptically by using breast pump and an aliquot was taken for Gram staining and culture. Quantitative culture was performed onto chocolate, blood supplemented with colistin and nalidixic acid, McConkey, mannitol salt and Sabouraud agar plates (all media were acquired from Becton Dickinson, East Rutherford, NJ, USA). Plates were incubated in CO_2 or air-incubators and were read for development of colonies after being kept overnight and 48-h incubation.

Microbial load in milk samples was measured as colony forming units/mL. Colonies were identified using the Bruker MALDI Biotyper instrument (Bruker Daltonik GmbH, Bremen, Germany), and antimicrobial susceptibility testing was performed with the BD Phoenix automatic system (Becton Dickinson).

Sudan III staining

Saturated Sudan III was prepared by diluting 0.5-g powder in 100-mL 99% isopropanol. The solution was allowed to set for 2 days before using the supernatant. Working Sudan III stain was obtained by diluting 6 mL of saturated Sudan III dye in 4 mL of distilled water, and letting it stand for 10 min and filtering the solution before use. Each sample, 50 µL, was dispersed on polarized slides and allowed to air-dry for 24 h. The samples were stained with working Sudan III, left at room temperature for 10 min, washed with distilled water, and allowed to air-dry. The stained slides were examined with Euromex-Holland FE 2915 microscope (BD Arnhem, The Netherlands) equipped with a DC5000 CMEX-5.0 pixel digital USB camera system and analyzed at 40× magnification.

Antioxidant assay by Oxygen Radical Absorbance Capacity (ORAC)

The antioxidant capacity of human milk samples was determined using the ORAC method as reported by Ceccarini *et al.* (2016). We used ORAC method because it is a robust and reliable method. In fact, the ORAC assay, with other common measures of antioxidant capacity, including ferric ion-reducing antioxidant power and trolox equivalence antioxidant capacity assays, is regarded as a preferable method because of its biological relevance (Codini *et al*., 2015). A duplicate extraction was performed for each sample and used to evaluate lipophilic ORACFL (L-ORACFL) and hydrophilic ORACFL (H-ORACFL) values. Evaluations of lipophilic and hydrophilic ORACFL values in the samples were performed separately, and the total antioxidant capacity was calculated by adding L-ORACFL and H-ORACFL values. ORACFL assays were conducted on a FLUOstar OPTIMA microplate fluorescence reader (BMG Labtech, Offenburg, Germany) at an excitation wavelength of 485 nm and an emission wavelength of 520 nm. 2,20-Azobis (2-methylpropionamide) dihydrochloride was used as a peroxyl radical generator; trolox was used as a reference antioxidant standard; and fluorescein was used as a fluorescent probe. The data were expressed as micromoles of trolox equivalents (TE) per gram of sample (µmol TE/g).

Gas chromatographic analysis of fatty acids

Milk lipid fraction was extracted using a chloroform–methanol mixture (2:1, v/v), following the procedure reported previously (Codini *et al.*, 2020). The FAME of total lipids was prepared by transmethylation with methanolic KOH and analyzed using high-resolution gas chromatography. A DANI 1000DPC gas-chromatograph (Norwalk, CT, USA), equipped with a split–splitless injector and a flame ionization detector, was used. The FAME separation was performed with a CP-select CB for FAME-fused silica capillary column (50 m × 0.25 mm I.D., 0.25-µm F.T.; Varian, Superchrom, Milan, Italy). The injector and detector temperatures were 250°C. The oven temperature was 60°C, held for 5 min, then raised to 225°C at a rate of 3°C/min; the final temperature was held for 10 min. The chromatograms were acquired and processed using the Clarity Integration software (DataApex Ltd., Prague, Czech Republic). A standard solution containing 37 FAME was used to identify individual fatty acids. High resolution gas chromatography analysis was conducted in triplicate.

Liquid chromatography with tandem mass spectrometry

Sphingolipid (Sph) extraction and liquid chromatography coupled with tandem mass spectrometry (LC–MS/MS) analyses were performed as described by Dei Cas *et al.* (2020). Sphingolipids were extracted from three independent 25-µL aliquots of HBM using monophasic solvent extraction (chloroform:methanol:water—30:60:10, v/v/v). These were analyzed with liquid chromatography (Dionex 3000 UltiMate, ThermoFisher Scientific, Waltham, MA, USA) coupled with tandem mass spectrometer (AB Sciex 3200 QTRAP, Sciex, Vaughn, ON, Canada). The separation was achieved by a reversed-phase analytical column (Acquity BEH C8 100 × 2.1 mm × 1.7 µm; Waters, Milford, MA, USA) through a linear gradient between eluent A (0.2% formic acid, 2-mM ammonium formate in water solution) and eluent B (0.2% formic acid, 1-mM ammonium formate in methanol). Quantitative analysis was performed interpolating each peak area of analyte/area internal standards with a calibration curve for each sphingolipid.

Statistical analysis

Statistical analysis of lipidomic study was performed with GraphPad Prism 7.0 (GraphPad Software Inc, La Jolla, CA, USA). Statistical differences of fatty acids and sphingolipidomic study were investigated by unpaired *t*-test. Graphs were represented as mean ± SD, and statistical significance was set as $p < 0.05$.

Results

Mothers

Two women, A: 26-year-old, and B: 43-year-old , were examined for the study. The women were enrolled because of the dark color of their colostrum. It emerged from the analysis of their questionnaires that both mothers neither smoked nor used alcohol and followed a Mediterranean diet without restrictions. Mother A was under iron supplementation due to physiological anemic condition during pregnancy. Mother B took iron for anemia as well and methyldopa for hypertension arising during pregnancy. Moreover, she supplemented the diet with folic acid and docosahexaenoic acid (DHA). In order to address possible bias because of the suspected role of iron, we also included in the study two healthy mothers, aged 26 and 43 years, taking iron but producing light color milk, as CRT samples. The selected mothers were neither affected by any chronic pathology nor had received any recent transfusion; they were only anemic and followed a Mediterranean diet.

Characteristics of human breast black milk samples

Microbiology was aspecific. Milk samples of control as well as A and B mothers were positive to culture test for bacteria but negative to culture test for yeasts. Organisms identified in the milk of control 1 mother were *Staphylococcus epidermidis* (20.000 colony-forming units [CFU]/mL), *Acinetobacter junii* (>100.000 CFU/mL), *Acinetobacter ursingii* (3.000 CFU/mL) and *Staphylococcus aureus* (<3.000 CFU/mL). Organisms identified in the milk of control 2 mother were *Staphylococcus epidermidis* (10.000 CFU/mL) and *Staphylococcus haemolyticus* (1.000 CFU/mL). Organisms identified in the milk sample of mother A were *Staphylococcus lugdunenesis* (20.000 CFU/mL) and *Staphylococcus aureus* (5.000 CFU/mL). Organisms identified in the milk sample of mother B were *Staphylococcus epidermidis* (10.000 CFU/mL), *Staphylococcus lugdunensis* (800 CFU/mL) and *Pseudomonas fluorescens* (800 CFU/mL). After pasteurization, all microbiological tests were negative in all milk samples and the black color of milk samples A and B remained unchanged. Therefore, we decided to investigate the lipid component of black milk samples and compared them with the light milk samples. First, we performed milk staining with Sudan III. Figure 1 shows the presence of fat globules of different sizes in the two CRT samples with physiological orange color. In the two samples of black milk, black precipitations appeared in the central or peripheral part of fat globules.

The analysis of antioxidant capacity demonstrated that samples A and B had very high antioxidant capacity (Figure 2). ORAC value in CRT samples was

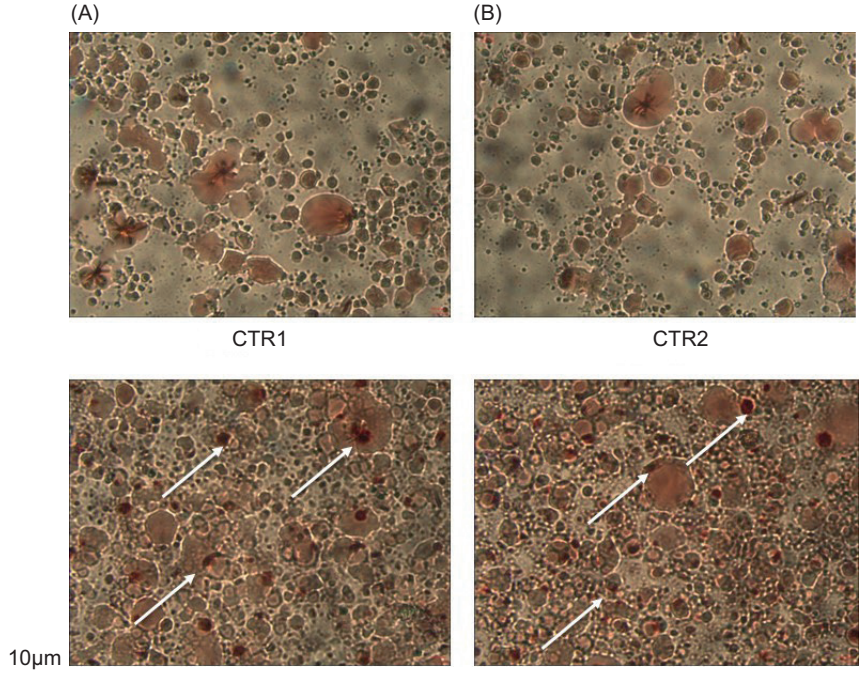

Figure 1. Image of milk samples stained with Sudan III. The arrows indicate black precipitates in fatty granules. Magnification 20×.

632.97 + 19.24 µmolTE/mL. In black milk sample A, the value was 1826.09 + 46.95 µmolTE/mL and in black milk sample B, it was 122.49 + 37.34 µmolTE/mL.

Lipid composition of human breast black milk samples

First, we measured fatty acids (FA) in HBM. Results of black milk samples A and B were compared with those of white milk CRT samples. We analyzed the general similarity and difference of total saturated fatty acids (sFA) and unsaturated fatty acids (uFA). Black milk sample A contained more uFA but black milk sample B had less sFA than CTR milk samples (Figure 3A). Interestingly, the sFA:uFA ratio was similar in black milk samples A and B and it was lower than that of CRT milk samples (Figure 3B).

If each species of FA was examined, it became evident that in both black milk samples A and B, C16:1n-9, C18:3n-3, C20:1, C20:4, C22:5 and C22:6 were higher than in CRT milk samples (Figure 4). Moreover, milk sample A was particularly rich in C12:0 and C18:1n-9 content whereas milk sample B was deficient in C14:0 and C16:0 contents (Figure 4).

We investigated possible changes in the composition of sphingolipids in black milk samples in comparison to CTR milk samples. The results highlight a higher level of sphingomyelin content in both black milk samples A and B (Figure 5A) but a higher level of ceramide (Cer) content in black milk sample A (Figure 5B).

In Figure 6, each sphingolipid species was reported. Of note, all sphingomyelin species were increased in milk samples A and B except 24:0 SM compared to CRT milk samples. 14:0 Cer, 16:0 Cer, 18:0 Cer, 18:1 Cer and 20:0 Cer were increased in milk sample A but only 10:0 Cer was enhanced in milk sample B. Dihydroceramide (DhCer) species was present only in milk sample A.

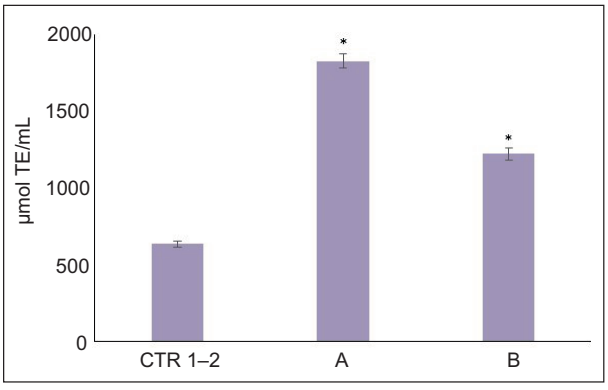

Figure 2. Antioxidant potential of human breast milk. CRT: control milk sample; A and B: black milk samples. Data are expressed as mean ± SD calculated as reported in 'Statistical analysis'. Significance of A and B versus CTR 1–2; *$p < 0.05$.

Discussion

Previous studies have demonstrated that color of HBM may vary physiologically, in relation to diet, nutritional supplements, infections and medications, from pink to orange, red and green (Ayuzo del Valle and Treviño Salinas, 2014; Jones *et al.*, 2014; Naor *et al.*, 2019; Quinn *et al.*, 2018; Yazgan *et al.*, 2012). The black color of HBM is reported only during minocycline treatment (Basler and Lynch, 1985; Hunt *et al.*, 1996; Lawrence, 1985). However, here we report for the first time the case of two mothers who neither suffered from any pathology nor had minocycline therapy but had a black/deep dark color HBM. The only clinical aspect they had in common was iron supplementation. Mothers who had dark color milk as well as control mothers who had white color normal milk were using iron for anemia, suggesting that mineral intake was not responsible for milk's color, and

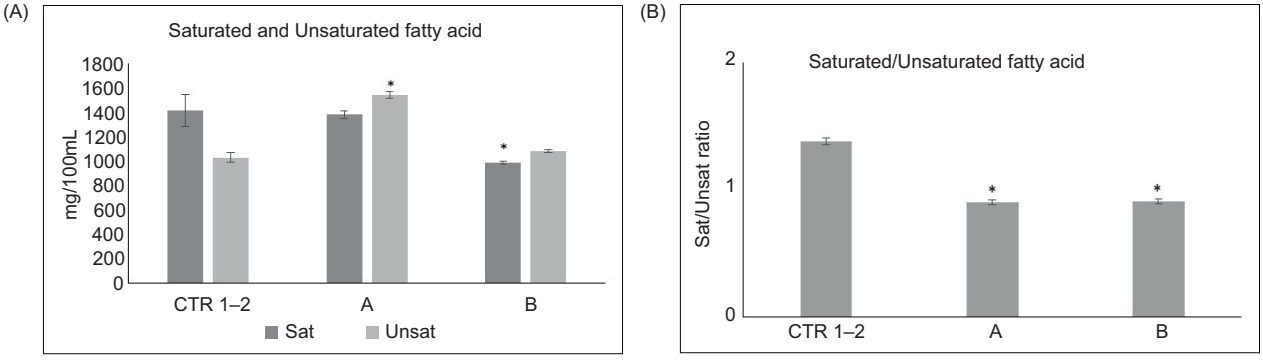

Figure 3. Composition of fatty acids in human breast milk. (A) Total saturated and total unsaturated fatty acids. (B) Ratio of saturated and unsaturated fatty acids. CRT: control milk samples; A and B: black milk samples. Data are expressed as mean ± SD calculated as reported in 'Statistical analysis'. Significance of A and B versus CTR 1–2; *$p < 0.05$.

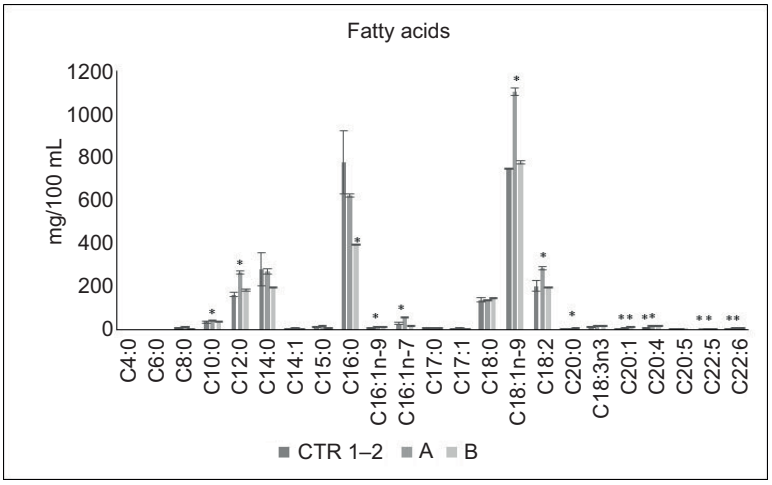

Figure 4. Fatty acid species in human breast milk. CRT: control milk samples; A and B: black milk samples. Data are expressed as mean ± SD calculated as reported in 'Statistical analysis'. Significance of A and B versus CTR 1–2; *$p < 0.05$.

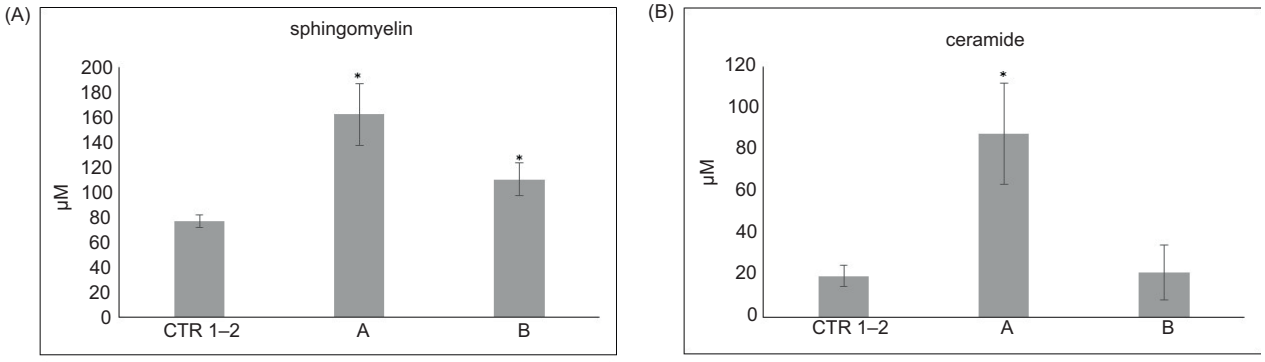

Figure 5. Total sphingomyelins and ceramides in human breast milk. CRT: control milk samples; A and B: black milk samples. Data are expressed as mean ± SD calculated as reported in 'Statistical analysis'. Significance of A and B versus CTR 1–2; *$p < 0.05$.

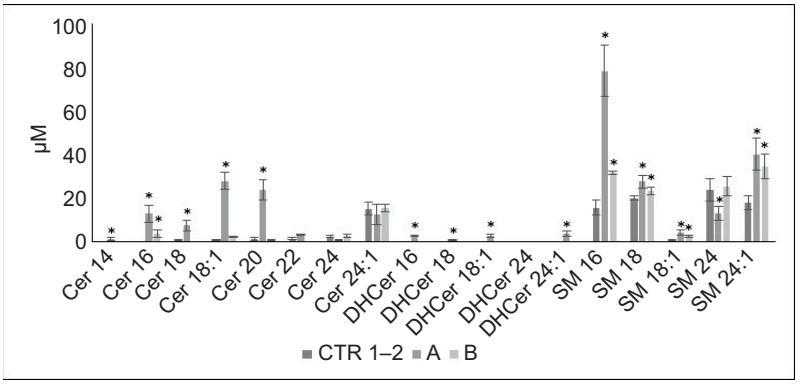

Figure 6. Species of sphingomyelins, ceramides and dihydroceramides in human breast milk. CRT: control milk samples; A and B: black milk samples. Data are expressed as mean ± SD calculated as reported in 'Statistical analysis'. Significance of A and B versus CTR 1–2; *$p < 0.05$.

it could just be an incidental finding of dark color HBM reported by both mothers A and B. As a matter of fact, these are the only two cases of black color HBM among a large number of pregnant/brestfeeding mothers taking this mineral globally. On discontinuation of iron intake and breastfeeding, milk in both cases again became white after a few days and both mothers restarted breastfeeding without any incident. In our experience, dark color of breast milk is not an absolute indication for discontinuation of breastfeeding.

Microbiology was aspecific. Staining with Sudan III, specific for lipids, revealed the presence of dark formations inside fat granules, which were absent in CRT milk samples. It was difficult to exactly articulate these formations, but the possibility that they were altered lipids cannot be excluded. We assumed that these could be partially oxidized lipids that precipitated as lipofuscins, which stained with Sudan III (Marani and Lazarov, 2017).

The analysis of antioxidant properties revealed that dark milk samples had a much higher antioxidant power compared to CRT milk samples. For analysis, we have chosen ORAC method was chosen because it is a robust and reliable method. In fact, the ORAC assay, other common measures of antioxidant capacity include ferric ion reducing antioxidant power and trolox equivalence antioxidant capacity assays and therefore is considered to be a preferable method because of its biologic relevance (Codini *et al.*, 2015). A high antioxidant power is generally considered positive for the quality of a food. However, if a food has very high antioxidant properties, it becomes pro-oxidant (Mendes-da-Silva *et al.*, 2014). In addition, it has been demonstrated that in a large number of women milk has medium level of antioxidant properties (Codini *et al.*, 2020), similar to that we observed in two CRT milk samples. In addition, CRT milk samples had a higher sFA content than uFA, as demonstrated by Codini *et al.* (2020). This is a characteristic of HBM that differentiates it from formula milk, which is particularly enriched in polyunsaturated fatty acids (Codini *et al.*, 2020). We assumed that a higher value of uFA in black milk samples predisposed them to easier oxidation.

We demonstrated that HBM of mothers who followed a Mediterranean diet had richer sphingomyelin contents than found in infant formulas (Dei Cas *et al.*, 2021). In the present case also, we discovered similar sphingomyelin content in CRT milk samples as reported by Dei Cas *et al.* (2021). However, in dark milk samples, higher content values of sphingomyelin, dihydroceramide and ceramide were evident, compared to CRT milk samples. The composition between the two dark milks is different indicating a high variability in the samples. At the same time, it was possible to hypothesize that sphingolipid metabolism was altered in dark milk samples.

Conclusions

To the best of our knowledge, we reported the first two cases of black/dark gray color breast milk of women not related to minocycline therapy but having iron supplementation in common. Iron intake does not seem responsible for black milk pigmentation. The dark color of milk could be due to an alteration in antioxidant properties that become pro-oxidant. This induces a biochemical modification in lipid components in terms of fatty acids and sphingolipids. However, it was not possible to determine whether this was due to a change in the metabolic activity of the mammary gland. In summary, our data highlights that it is possible to have black/dark color milk from a healthy mother having a normal diet, and this finding does not represent an absolute indication for discontinuation of breastfeeding.

References

Ayuzo del Valle C. and Treviño Salinas E. 2014. Pink breast milk: *Serratia marcescens* colonization. AJP Rep. 4(2): e101–e104. https://doi.org/10.1055/s-0034-1387934

Birkholz T., Eckardt G., Renner S., Irouschek A. and Schmidt J. 2009. Green breast milk after propofol administration. Anesthesiology. 111(5): 1168–1169. https://doi.org/10.1097/ALN.0b013e3181bbc4b1

Basler R.S. and Lynch P.J. 1985. Black galactorrhea as a consequence of minocycline and phenothiazine therapy. Case Rep Arch Dermatol. 121(3): 417–478. https://doi.org/10.1001/archderm.1985.01660030139039

Castellote C., Casillas R., Ramirez-Santana C., Perez-Cano F.J., Castell M., Moretones M.G., et al. 2011. Premature delivery influences the immunological composition of colostrum and transitional and mature human milk. J Nutr. 141(6): 1181–1187. https://doi.org/10.3945/jn.110.133652

Ceccarini M.R., Codini M., Cataldi S., Vannini S., Lazzarini A., Floridi A., et al. 2016. Acid sphingomyelinase as target of Lycium Chinense: promising new action for cell health. Lipids Health Dis. 15(1): 183. https://doi.org/10.1186/s12944-016-0351-z

Codini M., Cataldi S., Ambesi-Impiombato F.S., Lazzarini A., Floridi A., Lazzarini R., et al. 2015. Gentamicin arrests cancer cell growth: the intriguing involvement of nuclear sphingomyelin metabolism. E Int J Mol Sci. 16: 2307–2319. https://doi.org/10.3390/ijms16022307

Codini M., Tringaniello C., Cossignani L., Boccuto A., Mirarchi A., Cerquiglini L., et al. 2020. Relationship between fatty acids composition/antioxidant potential of breast milk and maternal diet: comparison with infant formulas. Molecules. 25: E2910. https://doi.org/10.3390/molecules25122910

Dei Cas M., Paroni R., Signorelli P., Mirarchi A., Cerquiglini L., Troiani S., et al. 2020. Human breast milk as source of sphingo lipids for newborns: comparison with infant formulas and commercial cow's milk. J Transl Med. 18: 481–494. https://doi.org/10.1186/s12967-020-02641-0

Hanson L.A. and Korotkova M. 2002. The role of breastfeeding in prevention of neonatal infection. Semin Neonat. 7(4): 275–281. https://doi.org/10.1053/siny.2002.0124

Hunt M.J., Salisbury E.L., Grace J. and Armati R.1996. Black breast milk due to minocycline therapy. Br J Dermatol. 134(5): 943–944. https://doi.org/10.1111/j.1365-2133.1996.tb06332.x

Jenness R. 1979. The composition of human milk. Semin Perinatol. 3(3): 225–239.

Jiang C., Cheong L.Z., Zhang X., Ali A.H., Jin Q., Wei W., et al. 2021. Dietary sphingomyelin metabolism and roles in gut health and cognitive development. Adv Nutr. nmab117. https://doi.org/10.1093/advances/nmab117

Jones J., Crete J. and Neumeier R. 2014. A case report of pink breast milk. J Obstet Gynecol Neonatal Nurs. 43(5): 625–630. https://doi.org/10.1111/1552-6909.12492

Lawrence R.A. 1985. Black galactorrhea as a consequence of minocycline and phenothiazine therapy. Case Rep Arch Dermatol. 121(3): 417–418. https://doi.org/10.1001/archderm.121.3.417

Marani E. and Lazarov N. 2017. Lipofuscin an lipofuscinosis. In: Reference Module in Neuroscience and Biobehavioral Psychology. Elsevier, Cambridge, MA. https://doi.org/10.1016/B978-0-12-809324-5.02594-3

Mendes-da-Silva R.F., Lopes-de-Morais A.A., Bandim-daSilva M.E., Cavalcanti G.A., Rodrigues, A.R., Andrade-da-Costa B.L., et al. 2014. Prooxidant versus antioxidant brain action of ascorbic acid in well-nourished and malnourished rats as a function of dose: a cortical spreading depression and malondialdehyde analysis. Neuropharmacology. 86: 155–160. https://doi.org/10.1016/j.neuropharm.2014.06.027

Naor N., Fridman E., Kouadio F., Merlob P. and Linder N. 2019. green breast milk following ingestion of blue-green algae: a case report. Breastfeed Med. 14(3): 203–204. https://doi.org/10.1089/bfm.2018.0184

Norris G.H., Milard M., Michalski M.C. and Blesso C.N. 2019. Protective properties of milk sphingomyelin against dysfunctional lipid metabolism, gut dysbiosis, and infammation. J Nutr Biochem. 73: 108224. https://doi.org/10.1016/j.jnutbio.2019.108224

Patton S., Canfield L.M., Huston G.E., Ferris A.M. and Jensen R.G. 1990. Carotenoids of human colostrum. Lipids. 25(3): 159–165. https://doi.org/10.1007/BF02544331

Quinn L., Ailsworth M., Matthews E., Kellams A. and Shirley DA. 2018. Serratia marcescens colonization causing pink breast milk and pink diapers: a case report and literature review. Breastfeed Med. 13(5): 388–394. https://doi.org/10.1089/bfm.2018.0002

Rainone A., Delucilla L., Elofer S., Bensimon L. and Abittan G. 2018. Propofol-induced green breast milk: a case report. Can J Hosp Pharm. 71(6): 389–391. https://doi.org/10.4212/cjhp.v71i6.2856

Riordan J. and Wambach K. 2014. Breastfeeding and Human Lactation, 4th ed. Jones and Bartlett Learning, Burlington, MA.

Skinner AM and Narchi H. 2021. Preterm nutrition and neurodevelopmental outcomes. World J Methodol. 20;11(6): 278–293. https://doi.org/10.5662/wjm.v11.i6.278

Tripaldi C., Palocci G., Di Giovanni S., Iacurto M., Steri R., Campagna M.C., et al. 2021. Effects of the drying method for flowers of Cynara cardunculus var. Altilis on milk coagulating properties. Ital J Food Sci. 33(4): 57–66. https://doi.org/10.15586/ijfs.v33i4.2026

Yazgan H., Demirdöven M., Yazgan Z., Toraman A.R. and Gürel A. 2012. A mother with green breast milk due to multivitamin and mineral intake: a case report. Breastfeed Med. 7: 310–312. https://doi.org/10.1089/bfm.2011.0048

Italian Journal of Food Science, 2022; 34 (1): 140–148

Is coffee powder extract a possible functional ingredient useful in food and nutraceutical industries?

Ancuta Nartea[1], Paolo Lucci[2], Monica Rosa Loizzo[3]*, Rosa Tundis[3], Mariarosaria Leporini[3], Luigia Gervasi[3], Benedetta Fanesi[1], Oscar Núñez[4], Natale Giuseppe Frega[1], Dennis Fiorini[5], Deborah Pacetti[1]

[1]Dipartimento di Scienze Agrarie, Alimentari e Ambientali, Università Politecnica delle Marche, Ancona, Italy; [2]Department of Agri-Food, Animal and Environmental Sciences, University of Udine, Udine, Italy; [3]Department of Pharmacy, Health and Nutritional Sciences, University of Calabria, Rende, Italy; [4]Department of Chemical Engineering and Analytical Chemistry, University of Barcelona, Barcelona, Spain; [5]Chemistry Division, School of Science and Technology, University of Camerino, Camerino, Italy

***Corresponding Author:** Monica Rosa Loizzo, Department of Pharmacy, Health and Nutritional Sciences, University of Calabria, 87036 Rende (CS), Italy. Email: monica_rosa.loizzo@unical.it

Received: 12 January 2022; Accepted: 21 February 2022; Published: 8 March 2022

PAPER

Abstract

The present study aimed to assess the phytochemical content and *in vitro* bioactivity of ethanolic extracts of Arabica (A) and/or Robusta (R) coffee powder having different geographical origins. For this purpose, total phenols (TPC) and flavonoids (TFC) content as well as α- and β-tocopherol were quantified. The antioxidant activity was assessed by using a multi-target approach in which the radical scavenging potential, the protection from lipid peroxidation, and the involvement of the iron-reducing mechanism were applied. The carbohydrate hydrolyzing enzymes' (α-amylase and α-glucosidase) inhibitory activities were also assessed. Arabica coffee sample (C2-A) showed the highest TPC, TFC, and α-tocopherol content with values of 63.1 mg chlorogenic acid equivalents (CAE)/g dry powder, 16.2 mg of quercetin (QE) equivalents/g dry powder, and 5.6 mg/100 g dry powder, respectively. Relative Antioxidant Capacity Index (RACI), used to statistically integrate results from 2,2′-azino-bis(3-ethylbenzothiazoline-6-sulfonic acid) diammonium salt (ABTS), 2,2-diphenyl-1-picrylhydrazyl (DPPH), ferric reducing ability power (FRAP), and protection of lipid peroxidation assays, evidenced that sample C4-R derived from Robusta from Guatemala showed the highest antioxidant potential with a value of –0.61. Arabica from Puerto Rico was the most active against α-amylase, whereas the blend Arabica/Robusta sample (C5-$A_{60}R_{40}$) showed the highest inhibitory activity against α-glucosidase with IC_{50} values of 120.2 and 134.6 mg/mL, respectively. The results show how the qualitative-quantitative composition of the extracts is strongly associated not only with the variety but also with the geographical origin of the samples.

Keywords: antioxidant activity; coffee; ethanolic extract; hypoglycemic effect; phenols; tocopherols

Introduction

Coffee is consumed worldwide with a total production of 16,868 million of 60-kg bags in 2019/2020. The two commercially produced coffee species are *Coffea Arabica* Linn. (known as Arabica) and *Coffea canephora* Pierre *ex* Froehner (known as Arabica). More than 70 countries produce coffee, but most of the global output comes from the top five producers: Brazil, Vietnam, Colombia, Indonesia, and Ethiopia. Arabica coffee is mainly cultivated in Colombia, whereas Robusta is mainly cultivated in Vietnam and Ethiopia. Brazil cultivates

 ISSN 1120-1770 online, DOI 10.15586/ijfs.v34i1.2171

copious amounts of both species (International Coffee Organization, 2019). Roasted coffee contains many bioactive compounds that have beneficial effects on human health. Most investigations have so far focused on the potential therapeutic effect of caffeine (Farah and de Paula Lima, 2019). Cafestol and kahweol, present in the coffee unsaponifiable matter, have positive effects against cancer and diabetes. Other secondary metabolites of coffee beans, such as tocopherols and polar phenolic compounds, have well-known antioxidant abilities. Among them, chlorogenic, ferulic, cinnamic, and caffeic acids are the most frequently investigated (Dórea and da Costa, 2005). Furthermore, the presence of tyrosol in spent espresso coffee grounds in rather high concentration, from 0.83 to 11.85 mg/100 g of dry spent powder, was recently reported (Balzano *et al*., 2020). According to different studies, tyrosol demonstrates a wide spectrum of biological effects on physiological processes. Based on the most recent epidemiological and research data, consumption of coffee is associated with a lower risk of developing type II diabetes in healthy individuals, probably requiring a series of mechanisms of action involving the antioxidant activity and interventions on glucose homeostasis (Osama *et al*., 2021). Diabetes mellitus (DM) will reach pandemic proportions in the next 20 years. The International Diabetes Federation estimated that in 2025, 371 million people will be affected by DM (IDF, 2019). Chronic hyperglycemia, insulin resistance in target tissues, and a relative deficiency of insulin secretion from pancreatic b-cells are the major features of type 2 DM (T2DM). The strict linkage between ROS and metabolic disorder was recently demonstrated (Carrier, 2017). Nutritional stress, caused by excess of carbohydrate and/or high-fat diets, promotes oxidative stress and results in decreased antioxidant status. Oxidative stress, in fact, may contribute to the long-term deterioration of pancreatic islet β-cell by affecting mitochondrial ATP production, which is necessary for insulin secretion. The consequent mitochondrial dysfunction influenced insulin sensitivity within muscle, liver, and adipose tissue. To reduce sugar intestinal absorption, treatment of T2DM patients with carbohydrate-hydrolyzing enzymes (α-amylase and α-glucosidase) inhibitors has been reported (Loizzo *et al*., 2017). Regarding chronic diseases, including hyperglycemia, the market of nutraceutical ingredients, as phytochemical and plant extracts, is projected to reach a compound annual growth rate of 7.5%. Due to the rising global demand for nutraceuticals made up of natural ingredients (Global Nutraceutical Statistics, 2019), the formulation of new natural extracts and the study of their bioactivities and their content of bioactive molecules become a fundamental task. From this point of view and considering the safety and acceptability for the human use of ethanol compared to other solvents, the coffee powder ethanol extracts could represent suitable ingredients in formulations of nutraceutical/functional foods rich in antioxidant compounds. Anyway, the standardization of raw material for their preparation is quite a challenge. In fact, it is known that the overall composition of bioactive substances of roasted coffee, as well as their functional activity, is heavily influenced by agronomical and technological factors (Kròl *et al*., 2020). The genetic background (species and variety), geographical origin, and roasting conditions of the coffee beans play a pivot role in defining the final bioactivity of the derived coffee products. Within this frame, the present study aimed to assess the phytochemical content, in terms of total phenols, total flavonoids, α- and β-tochopherol, and *in vitro* antioxidant activity evaluated by ABTS, DPPH, FRAP, and β-carotene bleaching test of ethanol extracts obtained from roasted *Coffea Arabica* and *C. Robusta* beans. These samples are characterized by different geographical origins (Brazil, Colombia, Vietnam, India, Ethiopia, Guatemala, Puerto Rico, and Costa Rica) and commercial coffee blend (Arabica/Robusta) powders. Furthermore, the hypoglycemic effect of the ethanol extracts was assessed by testing the inhibition of carbohydrate-hydrolyzing enzymes against α-amylase and α-glucosidase.

Materials and Methods

Reagents and standard

All chemicals and reagents used in this study were purchased from Sigma-Aldrich Chemical Co. Ltd (Milan, Italy) and VWR International (Milan, Italy) and, unless specified otherwise, were of analytical grade or higher.

Coffee samples and preparation of ethanolic extract

The roasted coffee powder from *Coffea Arabica*, *C. canephora* var. Robusta, and roasted coffee blends were supplied by a local industrial coffee roaster (Caffè del Faro, Robin S.r.l., Montegranaro, Italy) able to confirm their botanical and geographical origin, as well as the general type of postharvest processing (dry/wet process). Both Arabica and Robusta coffees had different geographic origins. All samples were roasted under the same conditions (175°C, 15 min). The compositional features of coffee samples investigated are reported in Table 1.

Seven grams of coffee powder were added to 30 mL of anhydrous ethanol and the mixture was magnetically stirred in the dark, at 25°C for 12 h. Then, the top phase was filtered and dried in a rotary evaporator. For each coffee sample, the ethanol extraction procedure was repeated in triplicate.

Table 1. Composition and geographical origin of coffee blend powders used for preparing ethanol extracts.

Sample code	Coffee blend composition
C1-A	Arabica 100% (Puerto Rico)
C2-A	Arabica 100% (50% Brazil, 20% Colombia, 20% Guatemala, 10% Ethiopia)
C3-A	Arabica 100% (Colombia)
C4-R	Robusta 100% (Guatemala)
C5-$A_{60}R_{40}$	60% Arabica (20% Brazil, 20% Colombia, 10% Guatemala, 10% Costa Rica)/40% Robusta (15% Vietnam, 25% India)
C6-$A_{10}R_{90}$	10% Arabica (Brazil)/90% Robusta (20% India, 70% Vietnam)
C7-$A_{75}R_{25}$	Decaffeinated coffee blend Arabica 75% (Unknown)/Robusta 25% (Unknown)

Bioactive phytochemicals content in coffee powder ethanol extracts

Total phenol (TPC) and flavonoid (TFC) contents were quantified using the spectrophotometric methods already published elsewhere (Loizzo *et al*., 2019). Coffee extract at a concentration of 1.5 mg/mL (0.1 mL) was mixed with a solution of Folin–Ciocalteu reagent (0.5 mL) and water (1 mL). After 1 min of incubation, 1.5 mL of 20% sodium carbonate was added, and the mixture was incubated at room temperature. The absorbance was measured at 765 nm using a UV-Vis Jenway 6003 spectrophotometer (Carlo Erba, Milan, Italy). The total phenol content was expressed as milligrams of chlorogenic acid equivalents (CAE)/g dry powder. In the total flavonoid content (TFC) determination, coffee extract was mixed with aluminum chloride solution (2%) in a 1:1 *ratio* and incubated at room temperature for 15 min. The absorbance was measured using a UV-Vis Jenway 6003 spectrophotometer (Carlo Erba, Milan, Italy) at 510 nm. The TFC was expressed as milligrams of quercetin equivalents (QE)/g dry powder.

Tocopherols' profile was determined following the procedure reported by Giardinieri *et al*. (2019). Coffee ethanolic extract was dissolved in acetonitrile and analyzed by means of ultra-high performance liquid chromatography-fluorescence (UHPLC-FLD) using Ascentis® Express C18 (75 × 4.6 mm, 2.7 µm, from Supelco, Milan, Italy) as the analytical column. The mobile phase was acetonitrile/methanol (90:10, v/v), at a flow rate of 0.45 mL/min. The injection volume was 1 µL. FLD was set with an excitation wavelength of 290 nm and an emission wavelength of 330 nm. Calibration curves (25–250 µg/mL) were prepared for quantitative analysis with R^2 higher than 0.996 for both tocopherols.

In vitro antioxidant assays

ABTS and DPPH radicals scavenging tests were performed following the procedures reported by Loizzo *et al*. (2019), to investigate the radical scavenging potential of coffee powder samples.

For the ABTS test, a solution of ABTS radical cation was prepared by mixing 7 mM ABTS solution with 2.45 mM potassium persulfate and stored at room temperature. After 12 h, the solution was diluted with ethanol to an absorbance of 0.70 at 734 nm using a UV-Vis Jenway 6003 spectrophotometer. Dilution of extracts in ethanol was added to 2 mL of diluted $ABTS^+$ solution in order to test the following concentrations from 400 to 1 µg/mL. After 6 min, the absorbance was read at 734 nm by using an UV-Vis Jenway 6003 spectrophotometer (Carlo Erba, Milan, Italy).

In the DPPH test, an aliquot of 1.5 mL of 0.25 mM DPPH radical (DPPH·) in ethanol was mixed with 12 µL of coffee extract to test concentrations ranging from 1000 to 1 µg/mL. The mixture was shaken and allowed to reach a steady state at 25°C for 30 min. After that, the absorbance was read at 517 nm by using the UV-Vis Jenway 6003 spectrophotometer (Carlo Erba, Milan, Italy). Ascorbic acid was used as positive control in both tests, and IC_{50} values are reported in Table 4.

Protective effect on lipid peroxidation was assessed by using the previously described β-carotene bleaching test (Loizzo *et al*., 2019). One milliliter of β-carotene (0.2 mg/mL in chloroform) was mixed with linoleic acid (20 µL) and 100% Tween 20 (200 µL). After evaporation of the solvent and dilution with water, the emulsion (288 µL) was added to a 96-well microplate containing 12 µL of coffee extract in ethanol (concentrations ranging from 100 to 2.5 µg/mL). The plate was shaken and placed in a water bath at 45°C for 30 and 60 min of incubation. The absorbance was measured at 470 nm by using UV-Vis Jenway 6003 spectrophotometer (Carlo Erba, Milan, Italy). Propyl gallate was used as positive control, and IC_{50} is reported in Table 4.

The ***FRAP test*** was performed following the procedure previously described by Loizzo *et al*. (2019). The FRAP value represents the ratio between the slope of the linear plot for reducing Fe^{3+}-TPTZ reagent by different coffee powder ethanol extracts, compared to the slope of the plot obtained for $FeSO_4$. Butylated hydroxytoluene (BHT) was used as positive control. For the preparation of the FRAP reagent, a mixture of 2.5 mL of 10 mM tripyridyltriazine (TPTZ) solution, 40 mM HCl, 2.5 mL of 20 mM FeCl3, and 25 mL of 0.3 M acetate buffer (pH 3.6) was prepared. Sample at a concentration of 2.5 mg/mL in ethanol (100 µL) was mixed with 2.0 mL of FRAP reagent

and 900 mL of water; the absorbance was measured at 595 nm by using the UV-Vis Jenway 6003 spectrophotometer (Carlo Erba, Milan, Italy) after 30 min of incubation at room temperature.

Carbohydrate hydrolysis enzymes inhibition

The hypoglycemic potential of coffee powder extracts was assessed by using the α-amylase and α-glucosidase inhibitory tests (Loizzo *et al*., 2019). The enzyme solution was prepared by adding 0.0253 g of enzyme in 100 mL of cold water, and the starch solution was prepared by stirring (at 65°C for 15 min) 0.125 g of potato starch in 25 mL of sodium phosphate buffer (20 mM) and sodium chloride (6.7 mM). Samples were dissolved in ethanol at concentrations ranging from 1000 to 25 μg/mL, added to starch solution, and left to react with the enzyme at 25°C for 5 min. The absorbance was read at 540 nm by using the UV-Vis Jenway 6003 spectrophotometer (Carlo Erba, Milan, Italy).

In the α-glucosidase inhibitory test, a maltose solution was prepared by dissolving 12 g of maltose in 300 mL of 50 mM sodium acetate buffer; α-glucosidase (EC 3.2.1.20) solution was prepared by adding 1 mg of enzyme (10 units/mg) in 10 mL of ice-cold distilled water; and O-dianisidine (DIAN) solution was prepared by dissolving 1 tablet in 25 mL of distilled water [15]. The peroxidase/glucose oxidase (PGO) system-color reagent solution was obtained by dissolving one capsule in 100 mL of ice-cold distilled water. A mixture of 5 μL of the sample (at concentrations ranging from 1000 to 25 μg/mL), 250 μL maltose solution, and 5 μL enzyme was left to incubate at 37°C for 30 min. Then, 50 μL of perchloric acid was added, and the mixture was centrifuged. The supernatant was collected and mixed with 5 μL of DIAN and 300 μL of PGO and left to incubate at 37°C for 30 min. The absorbance was read at 500 nm by using the UV-Vis Jenway 6003 spectrophotometer (Carlo Erba, Milan, Italy). Acarbose was the positive control in both tests, and IC_{50} is reported in Table 5.

In the α-glucosidase inhibitory activity test, Acarbose was used as a positive control in both tests.

Statistical analysis

Data were expressed as means ± standard deviation (S.D.) (n = 3). Differences of polar phenolic substances and tocopherol content among samples were calculated using one-way analysis of variance (ANOVA) with Tukey's *post hoc* procedure ($P < 0.05$). The inhibitory concentration of 50% (IC_{50}) was calculated by nonlinear regression with the use of Prism Graph Pad Prism version 4.0 for Windows (Graph Pad Software, San Diego, CA, USA). Differences within and between groups were evaluated by one-way analysis of variance test (ANOVA) followed by a multicomparison Dunnett's test compared with the positive control at a significance level of $P < 0.001$. *Pearson*'s correlation coefficient (r) and linear regression, assessment of repeatability, calculation of average and relative standard deviation were performed using Microsoft Excel 2010 software. The Relative Antioxidant Capacity Index (RACI) was used as a statistical approach to compare the antioxidant activity of coffee powder ethanol extracts obtained by different applied tests (Loizzo *et al*., 2019).

Results and Discussion

Ethanol extraction yield

Ethanol was chosen as the extraction solvent because it complies with the legislation on extraction solvents to be used in the production of foodstuffs and food ingredients (Directive 2009/32/EC, 2009), and also considering the effectiveness toward the extraction of bioactive substances, the toxicity, and environmental impact (Socaci *et al*., 2018). The investigated coffee powders provided an ethanol extract yield ranging from 43.5 to 111.0 g/kg dry powder. Generally, Arabica coffee powders gave higher extraction yields than Robusta samples, with the blends containing higher percentage of Robusta (40 and 60%) giving lower yields. Results are similar to those obtained from spent ground coffee, reported by Balzano *et al*. (2020), where samples of spent ground coffee extracted in the same experimental conditions gave a range of 58 to 112 g/kg of dry powder.

Bioactive phytochemicals in coffee ethanolic powder

Table 2 shows the average values of TPC and TFC in coffee powder ethanolic extracts. TPC content ranged from 11.0 to 63.1 mg CAE/g dry powder, whereas TFC varied from 4.5 to 16.2 mg QE/g dry powder. Generally, samples obtained from the Arabica variety had higher TPC and TFC than Robusta or Arabica/Robusta mixtures. These results are in agreement with those previously reported by other researchers. In particular, Bobková *et al*. (2020) investigated the effect of roasting process on the TPC of Arabica and Robusta coffee beans from different geographical origins. TPC values ranged from 49.19 to 74.05 mg CAE/g dry powder. Water coffee extracts showed the highest levels of TPC in green and light roasted coffees where values ranged from 49.19 to 74.05 g GAE/kg for Vietnam Queen and Ethiopia Sidamo, respectively, and from 38.34 to 59.79 g GAE/kg for India Monsooned Malabar and Ethiopia Sidamo, respectively. Interestingly,

the roasting process led to a reduction in TPC values from the green to dark roasting stage. This evidence confirmed that the coffee-growing region has probably an important influence on the development of this class of phytochemicals in coffee. The impact of the roasting process was the object of investigation by Sulaiman *et al.* (2011) that evidenced how TPC decreased linearly over the roasting temperature from 63.51 mg CAE/g coffee beans (roasted at 200°C) to 42.56 mg CAE/g coffee beans (roasted at 240°C). Similarly, Kròl *et al.* (2020) demonstrated that coffees roasted in light and medium roasting conditions are richer in TPC in comparison to dark roast coffee. Furthermore, organic coffee beans showed higher TPC and TFC content than conventional coffee beans (8.95 *vs* 8.28 mg/g and 1.35 *vs* 0.94 mg/g, respectively). The same observation was done by Acidri *et al.* (2020) that found a decline in TPC from 146.8 to 87 mg GAE/g DW in Indonesian Arabica coffee after the roasting process. The great variability of TPC found in literature confirmed that the content of these phytochemicals may be related to the varieties, the cultivation method, as well as to the coffee origin.

Tocopherol content

Tocopherols are very important molecules effectively inhibiting lipid oxidation in foods and the biological system. In coffee beans, the tocopherol content is approximately 3–10 mg/100 g (Górnaś *et al.*, 2014). To investigate the relation between the overall antioxidant activity of the coffee extracts and their main chemical contributors, tocopherol composition and content were determined by means of RP-UPLC-FLD. As a result, α- and β- were the tocopherols largely predominant in the ethanol coffee extract samples investigated, with a certain variability of the total content, ranging, in the dry powder form, between 3 and 27 mg/100 g (in the decaffeinated sample C7-$A_{75}R_{25}$ and in the sample C1-A from Puerto Rico, respectively). The values referred to the ethanol extract range between 36 and 362 mg/100 g (Table 3). β-Tocopherol is predominant, and the ratio β-tocopherol/α-tocopherol varies from 1.6 to 4.0. The overall results are in agreement with several studies (Alves *et al.*, 2009; González *et al.*, 2001; Górnaś *et al.*, 2014). Górnaś *et al.* (2014) found an average total tocopherol content in roasted Robusta of 11.54 mg/100 g, and 28.8 mg/100 g in roasted Arabica, and an average ratio β-/α-tocopherol of 1.2 in roasted Robusta and 3.1 in roasted Arabica. Alves *et al.* (2009) reported an average total value of a- and β-tocopherol of 9.7 mg/100 g in roasted Arabica and 3.1 mg/100 g in roasted Robusta, with a ratio β-/α-tocopherol of 3.0 and 1.0 for Arabica and Robusta, respectively. González *et al.* (2001), found a total value of α- and β-tocopherol ranging from 1.9 to 4.6 mg/100 g in roasted Robusta and from 11.5 to 19.3 mg/100 g in roasted Arabica, with a ratio β-/α-tocopherol ranging from 2.1 to 6.1 and from 3.5 and 6.0 in roasted Arabica and Robusta, respectively. The variability found in the investigated samples did not allow to highlight any statistical relationships between the tocopherol content and the Arabica/Robusta composition of the powder. A similar situation was observed also by Górnaś *et al.* (2014) and Alves *et al.* (2009).

Coffee powder ethanolic extract bioactivity

Antioxidant effects

Oxidative stress in humans arises from an imbalance between radical oxygen species (ROS) and endogenous defense enzymes such as superoxide dismutase, catalase, glutathione peroxidase, etc. Besides these defenses, consumption of dietary antioxidants is fundamental to prevent the development of several diseases. By using different *in vitro* tests, we have checked the ability of

Table 2. Total phenols content (TPC) and flavonoids content (TFC) in coffee powder ethanol extracts.

Sample	TPC°	TFC^
C1-A	51.5 ± 0.9^{b}	15.6 ± 0.5^{b}
C2-A	63.1 ± 1.1^{a}	16.2 ± 0.7^{a}
C3-A	25.9 ± 0.4^{e}	13.3 ± 0.4^{c}
C4-R	11.0 ± 0.3^{g}	4.5 ± 0.0^{g}
C5-$A_{60}R_{40}$	35.5 ± 0.5^{d}	11.0 ± 0.2^{d}
C6-$A_{10}R_{90}$	19.9 ± 0.4^{f}	10.0 ± 0.2^{e}
C7-$A_{75}R_{25}$	38.6 ± 0.6^{c}	9.5 ± 0.1^{f}

Data are expressed as mean ± standard deviation (n = 3). °mg chlorogenic acid equivalents (CAE)/g dry powder; ^mg of quercetin (QE) equivalents/g dry powder; and values in the same column with different superscript letters are significantly different (P < 0.05).

Table 3. Content of α- and β-tocopherols in coffee ethanol extracts.

Sample	α – tocopherol§	β – tocopherol§
C1-A	5.4 ± 0.5^{b}	21.3 ± 0.2^{a}
C2-A	5.6 ± 0.5^{a}	10.6 ± 0.2^{c}
C3-A	4.1 ± 0.0^{c}	13.9 ± 0.5^{b}
C4-R	4.1 ± 1.1^{c}	10.5 ± 0.5^{c}
C5-$A_{60}R_{40}$	2.3 ± 0.0^{d}	4.9 ± 0.1^{b}
C6-$A_{10}R_{90}$	5.4 ± 1.1^{b}	10.8 ± 0.4^{c}
C7-$A_{75}R_{25}$	1.0 ± 0.0^{e}	1.6 ± 0.0^{d}

Data are expressed as mean ± standard deviation (n = 3). §mg/100 g dry powder. Values in the same column with different superscript letters are significantly different (P < 0.05).

coffee powder ethanolic extract to act as an antiradical or antioxidant agent. The approach with multiple tests is recommended for measuring antioxidant properties of food matrix to better reflect their potential protective effects. The antiradical activity characterizes the ability of phytocomplex to react with free radicals, while the antioxidant activity represents the ability to inhibit the oxidation process, which usually occurs through different reactions (Tirzitis and Bartosz, 2010). Generally, a concentration-effect relationship was found in all the tests except in the FRAP assay (Table 4).

The extract obtained from the Robusta sample (C4-R) showed the highest radical scavenging potential with IC_{50} values of 1.1 and 9.2 mg/mL for ABTS and DPPH assay, respectively. A promising radical scavenging activity was also observed in the decaffeinated sample C7-$A_{75}R_{25}$ (IC_{50} values of 8.6 and 16.4 mg/mL for ABTS and DPPH assay, respectively). Both samples are also able to react as reductants in the FRAP assay (FRAP values of 56.8 and 56.9 mM Fe (II)/g at 2.5 mg/mL). These values are quite lower than that reported for the positive control BHT (63.2 mM Fe (II)/g at 2.5 mg/mL). The antioxidant activity of coffee samples was also tested, using the b-carotene bleaching method. This assay evaluated the ability of the phytocomplex to protect against lipid peroxidation. Since no high temperatures are required, the antioxidant activity of thermosensitive phytochemicals may be determined and quantitatively evaluated. The sample C4-R showed a promising protection against lipid peroxidation with IC_{50} values of 5.3 and 5.9 mg/mL at 30 and 60 min of incubation, respectively. A promising activity was also observed with decaffeinated coffee powder extract (C7-$A_{75}R_{25}$), followed by the blend C5-$A_{60}R_{40}$. RACI was calculated to evaluate and create a ranking clustering of the antioxidant capacity of different samples. Based on this parameter, the following antioxidant ranking could be evidenced: C4-R>C5-$A_{60}R_{40}$>C7-$A_{75}R_{25}$>C6$A_{10}R_{90}$>C2-A>C1-A>C3-A (Figure 1).

A positive *Pearson's* correlation coefficient was found between TFC and DPPH (r = 0.70) and b-tocopherol and both DPPH and ABTS tests (r = 0.87 and 0.76, respectively). A significant positive correlation coefficient was also observed for TFC and b-carotene bleaching test after 30 and 60 min of incubation (r = 0.61 and 0.79, respectively). Based on RACI statistical approach C4-R, richest in phenols and b-tocopherol resulted the most active as antioxidant. Tocopherols are able not only to react toward free radicals and hydroperoxides but also with many other possible side reactions which are affected by tocopherol concentrations, type of substrate, and by other chemical species acting as pro-oxidants and synergists in the system.

Carbohydrate hydrolysis enzymes' inhibitory effect by coffee powder extracts

The inhibition of carbohydrate hydrolyzing enzymes, α-amylase and α-glucosidase, given by coffee powder extract was concentration-dependent (Table 5). Generally, α-amylase enzyme was the most sensitive to the action of the extracts (see selectivity index, SI).

Table 4. ***In vitro*** **antioxidant activity of coffee powder ethanol extracts from Arabica and Robusta varieties and their blend.**

Sample	DPPH test IC_{50} (μg/mL)	ABTS test IC_{50} (μg/mL)	FRAP# test μM Fe (II)/g	β-Carotene bleaching test IC_{50} (μg/mL)	
				30 min	60 min
C1-A	809.5 ± 2.9****	411.3 ± 3.8****	16.9 ± 1.3****	34.6 ± 0.7****	38.9 ± 1.4****
C2-A	212.6 ± 2.4****	101.2 ± 3.7****	6.8 ± 0.7****	20.5 ± 0.8****	94.1 ± 1.9****
C3-A	460.4 ± 3.5****	445.5 ± 3.1****	13.5 ± 0.7****	52.1 ± 0.7****	59.6 ± 1.7****
C4-R	9.2 ± 0.8**	1.1 ± 0.4^{ns}	56.8 ± 2.7**	5.3 ± 0.6*	5.9 ± 0.9*
C5-$A_{60}R_{40}$	138.5 ± 2.6****	83.6 ± 1.2****	2.4 ± 0.6****	11.0 ± 0.2***	18.3 ± 1.2****
C6-$A_{10}R_{90}$	178.9 ± 3.5****	52.8 ± 1.3****	15.0 ± 0.6****	50.9 ± 1.6****	43.9 ± 1.6****
C7-$A_{75}R_{25}$	16.4 ± 1.1***	8.6 ± 0.9***	57.9 ± 1.8**	10.9 ± 1.4***	16.8 ± 1.7****
Positive controls					
Ascorbic acid	5.0 ± 0.8	1.7 ± 0.06	–	–	–
BHT	–	–	63.2 ± 4.3	–	–
Propyl gallate	–	–	–	1.0 ± 0.04	0.09 ± 0.004

Data are given as media ± S.D. (n = 3); #at 2.5 mg/mL; DPPH Radical Scavenging Activity Assay; Antioxidant Capacity Determined by Radical Cation ($ABTS^+$). β-Carotene bleaching test. Ferric ion reducing antioxidant power (FRAP); Ascorbic acid. BHT and Propyl gallate were used as positive controls in antioxidant tests. Differences within and between groups were evaluated by One-way ANOVA followed by a multicomparison Dunnett's test (α = 0.01): ****P < 0.0001, ***P < 0.001, **P < 0.01, *P < 0.1 compared to the positive controls.

C1-A extract showed the best activity with IC_{50} value of 120.2 mg/mL followed by Guatemalan Robusta extract (C4-R) and decaffeinated sample (C7-$A_{75}R_{25}$) with IC_{50} values of 122.4 and 130.9 mg/mL, respectively. Except sample C5-$A_{60}R_{40}$ that showed IC_{50}value of 134.6 mg/mL against α-glucosidase, all other samples are less active (IC_{50} values in the range 320.4–472.4 mg/mL). Sample C1-A showed the highest TPC content. Among phytochemicals able to interfere with carbohydrate hydrolyzing enzymes, phenols represent the main studied compounds (Loizzo *et al*., 2017). Several studies pointed out that CGAs, that are reported as the most abundant phytochemicals in coffee extract (Jeon *et al*., 2019; Jeszka-Skowron *et al*., 2016), inhibited both α-amylase and α-glucosidase with IC_{50} values of 25 and 26.07 M, respectively (Oboh *et al*., 2015). CGAs also stimulate glucose uptake in skeletal muscle and suppression of hepatic glucose production by AMPK activation (Ong *et al*., 2013). In addition, it has been found that CGAs could modulate glucose in both genetically and healthy metabolic related disorders including DM (Naveed *et al*., 2018). Differently Nyambe-Silavwe and Williamson (2018) demonstrated that both CGAs are only weak inhibitors of human salivary α-amylase despite several publications claiming otherwise. In fact, more recently, Herawati *et al*. (2019) demonstrated that Robusta coffee beans extract obtained after roasting, grinding, and brewing process was able to inhibit α-glucosidase activity up to 69% and exerted anti-glycation activity.

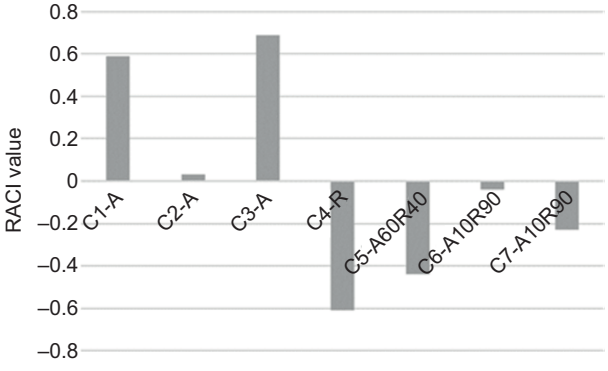

Figure 1. Relative Antioxidant Capacity Index (RACI) of coffee powder ethanol extracts from Arabica and Robusta varieties.

Conclusion

The present work investigated the bioactive phytochemicals content, in vitro antioxidant activity, and hypoglycemic potential of ethanol extracts deriving from Arabica and Robusta coffee powders, as well as their mixture, from different geographical origins. A great variability in terms of total phenol, flavonoid, and tocopherol content was observed, and this evidence strongly influenced the bioactivity although it is not possible to identify any relationship with the coffee variety and blend composition. Our findings strongly emphasize that coffee ethanol extracts should be used as a value-added ingredient for formulations of nutraceutical or functional products useful for the prevention of disease associated with oxidative stress and hyperglycemic condition.

Declarations

Funding

This work was supported by Università Politecnica delle Marche (Ricerca di Ateneo 2019).

Table 5. Carbohydrates hydrolyzing enzymes inhibition by coffee powder ethanol extracts from Arabica and Robusta varieties and their blend.

Sample	α-Amylase IC_{50} (μg/mL)	α-Glucosidase IC_{50} (μg/mL)	SI α-Amylase/ α-Glucosidase
C1-A	120.2 ± 3.1****	412.5 ± 6.1****	0.3
C2-A	880.3 ± 7.4****	362.2 ± 6.3****	2.4
C3-A	132.6 ± 5.2****	445.3 ± 8.1****	0.3
C4-R	122.4 ± 5.0****	320.4 ± 7.2****	0.4
C5-$A_{60}R_{40}$	800.3 ± 8.3****	134.6 ± 2.8****	5.9
C6-$A_{10}R_{90}$	970.5 ± 8.9****	244.7 ± 3.5****	4.0
C7-$A_{75}R_{25}$	130.9 ± 2.8****	472.4 ± 8.6****	0.3
Positive control			
Acarbose	52.4 ± 3.9	35.3 ± 3.7	1.5

Data are expressed as mean ± S.D. (n = 3). One-way ANOVA ****P < 0.0001 followed by a multicomparison Dunnett's test: ****P < 0.0001 compared with acarbose.

Conflicts of Interest

The authors have no conflicts of interest to disclose with the present submission.

Availability of Data and Material

The data sets supporting the results of this article are available from the corresponding author (M.R.L.) upon reasonable request.

Code Availability

Not applicable.

Author Contributions

D.P. conceptualized and supervised the study; M.R.L. prepared the original draft; A.N., M.L., L.G., and B.F. did the formal analysis; R.T., P.L., and D.F. performed data curation; O.N., P.L., and D.F. edited the manuscript; N.G.F and D.P. were concerned with funding acquisition. All authors have read and agreed to the published version of the manuscript.

Ethics Approval

Not applicable. Ethical experiments were not involved in this article.

Consent to Participate

All authors consented to participate.

Consent for Publication

All the authors have read the manuscript and approved it for possible publication.

References

Acidri, R., Sawai, Y., Sugimoto, Y., Handa, T., Sasagawa, D., Masunaga, T., et al. 2020. Phytochemical profile and antioxidant capacity of coffee plant organs compared to green and roasted coffee beans. Antioxidants 9: 93–111. https://doi.org/10.3390/antiox9020093

Alves, R.C., Casal, S., Alves, M.R. and Oliveira, M.B., 2009. Discrimination between Arabica and Robusta coffee species on the basis of their tocopherol profiles. Food Chemistry 114: 295–299. https://doi.org/10.1016/j.foodchem.2008.08.093

Balzano, M., Loizzo, M.R., Tundis, R., Lucci, P., Nunez, O., Fiorini, D., et al. 2020. Spent Espresso coffee grounds as a source of anti-proliferative and antioxidant compounds. Innovative Food Science and Emerging Technologies 59: 102254. https://doi.org/10.1016/j.ifset.2019.102254

Bobková, A., Hudáček, M., Jakabová, S., Belej, Ľ., Capcarová, M., Čurlej, J., et al. 2020. The effect of roasting on the total polyphenols and antioxidant activity of coffee. Journal of Environmental Science and Health 55: 495–500. https://doi.org/10.1080/03601234.2020.1724660

Carrier, A., 2017. Metabolic syndrome and oxidative stress: a complex relationship. Antioxidants Redox Signaling 26: 429–431. https://doi.org/10.1089/ars.2016.6929

Directive 2009/32/EC of the European Parliament and of the Council of 23 April 2009 on the approximation of the laws of the Member States on extraction solvents used in the production of foodstuffs and food ingredients. Official Journal of the European Union 141/3-11. Access January 2019.

Dórea, J.G. and da Costa, T.H., 2005. Is coffee a functional food? British Journal of Nutrition 93: 773–782. https://doi.org/10.1079/bjn20051370

Farah, A. and de Paula Lima, J., 2019. Consumption of chlorogenic acids through coffee and health implications. Beverages 5: 11–40. https://doi.org/10.3390/beverages5010011

Giardinieri, A., Schicchi, R., Geraci, A., Rosselli, S., Maggi, F., Fiorini, D., et al. 2019. Fixed oil from seeds of narrow-leaved ash (*F. angustifolia* subsp. *angustifolia*): chemical profile, antioxidant and antiproliferative activities. Food Research International 119: 369–377. https://doi.org/10.1016/j.foodres.2019.02.013

Global Nutraceuticals Market Size, Analysis, Trends, Industry Statistics (2019–2024). Available at: https://www.mordorintelligence.com/industry-reports/global-nutraceuticals-market-industry

González, A.G., Pablos, F., Martín, M.J., León-Camacho, M. and Valdenebro, M.S., 2001. HPLC analysis of tocopherols and triglycerides in coffee and their use as authentication parameters. Food Chemistry 73: 93–101. https://doi.org/10.1016/S0308-8146(00)00282-X

Górnaś, P., Siger, A., Pugajeva, I., Czubinski, J., Waśkiewicz, A. and Polewski, K., 2014. New insights regarding tocopherols in Arabica and Robusta species coffee beans: RP-UPLC-ESI/MSn and NP-HPLC/FLD study. Journal of Food Composition and Analysis 36: 117–123. https://doi.org/10.1016/j.jfca.2014.08.005

Herawati, D., Giriwono, P., Dewi, F., Kashiwagi, T. and Andarwulan, N., 2019. Antioxidant, anti-α-glucosidase and anti-glycation activities of coffee brew from Robusta coffee beans roasted at different levels. International Food Research Journal 26: 1305–1313.

International Coffee Organization, 2019. Growing for prosperity. Economic viability as the catalyst for a sustainable coffee sector, coffee development report 2019. Available at: https://www.internationalcoffeecouncil.org/media/coffeeDevelopmentReport.pdf Coffee market report 2021. Accessed 11 May 2021.

International Diabetes Federation, 2019. IDF diabetes atlas. 9th ed. pp. 1–176, Brussels, Belgium.

Jeon, J.S., Kim, H.T., Jeong, I.H., Hong, S.R., Oh, M.S., Yoon, M.H., et al. 2019. Contents of chlorogenic acids and caffeine in various coffee-related products. Journal of Advanced Research 17: 85–94. https://doi.org/10.1016/j.jare.2019.01.002

Jeszka-Skowron, M., Sentkowska, A., Pyrzyńska, K. and De Peña, M.P., 2016. Chlorogenic acids, caffeine content and antioxidant properties of green coffee extracts: influence of green coffee bean preparation. European Food Research and Technology 242: 1403–1409. https://doi.org/10.1007/s00217-016-2643-y

Kròl, K., Gantner, M., Tatarak, A. and Hallmann, E., 2020. The content of polyphenols in coffee beans as roasting, origin and storage effect. European Food Research and Technology 246: 33–39. https://doi.org/10.1007/s00217-019-03388-9

Loizzo, M.R., Bonesi, M., Nabavi, S.M., Sobarzo-Sánchez, E., Rastrelli, L. and Tundis, R., 2017. Hypoglycaemic effects of plants food constituents via inhibition of carbohydrate-hydrolysing enzymes: from chemistry to future applications. In: Natural Products Targeting Clinically Relevant Enzymes. Wiley-VCH Verlag GmbH & Co. KgaA, Weinheim, pp. 135–161. https://doi.org/10.1002/9783527805921.ch6

Loizzo, M.R., Sicari, V., Tundis, R., Leporini, M., Falco, T. and Calabrò, V., 2019. The influence of ultrafiltration of *Citrus Limon* L. Burm. cv Femminello comune juice on its chemical composition and antioxidant and hypoglycemic properties. Antioxidants 8: 23. https://doi.org/10.3390/antiox8010023

Naveed, M., Hejazi, V., Abbas, M., Kamboh, A.A., Khan, G.J., Shumzaid, M., et al. 2018. Chlorogenic acid (CGA): a pharmacological review and call for further research. Biomedicine & Pharmacotherapy 97: 67–74. https://doi.org/10.1016/j.biopha.2017.10.064

Nyambe-Silavwe, H. and Williamson, G., 2018. Chlorogenic and phenolic acids are only very weak inhibitors of human salivary α-amylase and rat intestinal maltase activities. Food Research International 113: 452–455. https://doi.org/10.1016/j.foodres.2018.07.038

Oboh, G., Agunloye, O.M., Adefegha, S.A., Akinyemi, A.J. and Ademiluyi, A.O., 2015. Caffeic and chlorogenic acids inhibit key enzymes linked to type 2 diabetes (*in vitro*): a comparative study. Journal of Basic and Clinical Physiology and Pharmacology 26: 165–170. https://doi.org/10.1515/jbcpp-2013-0141

Ong, K.W., Hsu, A. and Tan, B.K.H., 2013. Anti-diabetic and anti-lipidemic effects of chlorogenic acid are mediated by AMPK Activation. Biochemical Pharmacology 85: 1341–1351. https://doi.org/10.1016/j.bcp.2013.02.008

Osama, H., Abdelrahman, M.A., Madney, Y.M., Harb, H.S., Saeed, H. and Abdelrahim, M.E.A., 2021. Coffee and type 2 diabetes risk: is the association mediated by adiponectin, leptin, C-reactive protein or interleukin-6? A systematic review and meta-analysis. International Journal of Clinical Practice 75: e13983. https://doi.org/10.1111/ijcp.13983

Socaci, S., Fărcaş, A., Diaconeasa, Z., Vodnar, D.C., Rusu, B. and Tofana, M., 2018. Influence of the extraction solvent on phenolic content, antioxidant, antimicrobial and antimutagenic activities of brewers' spent grain. Journal of Cereal Science 80: 180–187. https://doi.org/10.1016/j.jcs.2018.03.006

Sulaiman, S.F., Moon, J.K. and Shibamoto, T., 2011. Investigation of optimum roasting conditions to obtain possible health benefit supplement, antioxidants from coffee beans. Journal of Dietary Supplements 8: 293–310. https://doi.org/10.3109/19390211.2011.593618

Tirzitis, G. and Bartosz, G., 2010. Determination of antiradical and antioxidant activity: basic principles and new insights. Acta Biochimica Polonica 57: 139–142. https://doi.org/10.18388/abp.2010_2386